Technische Universität München
TUM School of Engineering and Design

Development and characterization of bio-based epoxy thermosets and composites

Nikita Reinhardt

Vollständiger Abdruck der von der TUM School of Engineering and Design der Technischen Universität München zur Erlangung eines

Doktors der Ingenieurwissenschaften (Dr. Ing.)

genehmigten Dissertation.

Vorsitz: Prof. Dr.-Ing. Karsten Stahl

Prüfende der Dissertation:

1. Prof. Dr.-Ing. Klaus Drechsler
2. Prof. Dr. Thomas Brück

Die Dissertation wurde am 11.02.2025 bei der Technischen Universität München eingereicht und durch die TUM School of Engineering and Design am 27.06.2025 angenommen.

Technische Universität München
TUM School of Engineering and Design
Lehrstuhl für Carbon Composites
Boltzmannstraße 15
D-85748 Garching bei München

Tel.: +49 (0) 89 / 289 – 15092
Fax.: +49 (0) 89 / 289 – 15097
Email: info@lcc.mw.tum.de
Web: www.lcc.mw.tum.de

ACKNOWLEDGEMENTS

First of all, I would like to express my gratitude to my supervisor Prof. Dr.-Ing. Klaus Drechsler for giving me the opportunity to work at the Chair of Carbon Composites. I would also like to thank my supervisor David Colin for his guidance throughout my thesis.

A special thanks goes to Jonas Martin Breitsameter for the great collaboration and for the help with the chemical side of this thesis. Thanks also to Walter Alabiso for taking his time when I had questions regarding the chemistry behind vitrimer materials.

I am grateful to my LCC colleagues and for the good times spent together. Special thanks to Reiner Rauch for his easy-going attitude and his expertise for everything regarding the workshop, tools and machinery.

Last but certainly not least, I would like to thank all the students which I supervised throughout my years at LCC, who helped a lot with the investigation of the various materials and the comprehension of their characteristics.

KURZFASSUNG

Epoxidharze spielen eine entscheidende Rolle auf dem Markt für duroplastische Kunststoffe und Verbundwerkstoffe, wobei das prognostizierte Wachstum auf ihren außergewöhnlichen Eigenschaften und vielseitigen Anwendungen in verschiedenen Branchen beruht. Allerdings werfen die Abhängigkeit von fossilen Ressourcen, die Notwendigkeit von Bisphenol A (BPA) und Epichlorhydrin (ECH) für die Synthese, die Umweltbelastung durch die Herstellung von Epoxid- und epoxidbasierten Carbonfaser (CF)-Verbundwerkstoffen sowie deren schwierige Recyclingfähigkeit Fragen zur Nachhaltigkeit auf. Diese Studie untersucht die Entwicklung von BPA- und ECH-freien Epoxidsystemen, die vollständig oder teilweise biobasiert sind und für eine Recyclingfähigkeit ausgelegt wurden. Dabei werden natürliche und verfügbare Ressourcen genutzt, um eine Kreislaufwirtschaft zu fördern. Die mechanischen und thermischen Eigenschaften der entwickelten Materialien werden charakterisiert und mit Literaturwerten sowie konventionellen Epoxidsystemen verglichen.

Die Untersuchung des vollständig biobasierten Epoxidharzes auf Basis von epoxidiertem Leinöl (ELO) und Tanninsäure (TA) zeigte für ein pflanzenölbasiertes Epoxid starke mechanische und thermische Eigenschaften. Verschiedene Herstellungsverfahren wurden angewendet, um CF-Verbundwerkstoffe mit TA/ELO-Epoxid herzustellen, und die Ergebnisse der Charakterisierung wurden mit CF-Verbundwerkstoffen verglichen, die mit einem leistungsstarken erdölbasierten Epoxidsystem gefertigt wurden. Zudem wird die Möglichkeit des mechanischen Recyclings von TA/ELO und TA/ELO-CF-Verbundwerkstoffen sowie die Rückgewinnung sauberer Carbonfasern durch Solvolyse mit handelsüblichen Chemikalien untersucht.

Im weiteren Verlauf werden die thermischen, mechanischen und Recycling-Eigenschaften einer neuartigen multifunktionalen Epoxidverbindung (EGCHC) mit einem hohen biobasierten Anteil von 68.4 %, die aus hochverfügbaren Ressourcen wie Sorbinsäure, Maleinsäureanhydrid und Allylalkohol gewonnen wird, untersucht. Die Ergebnisse werden mit dem bekanntesten Epoxidsystem auf dem Markt, Bisphenol A Diglycidylether (DGEBA), verglichen. Die Resultate zeigen vergleichbare Eigenschaften zu DGEBA, während gleichzeitig eine mechanisches Recycling des Materials und eine Rückgewinnung von Carbonfasern mit geringem technischen und energetischen Aufwand möglich ist.

Die Vorteile der entwickelten Epoxidsysteme im Bereich der CF-Verbundwerkstoffindustrie werden diskutiert, ebenso wie die Herausforderungen, darunter eine hohe Wasseraufnahme und die schwierige Verarbeitung der Verbundstoffe. Zudem werden Verbesserungspotenziale für eine industrielle Umsetzung erörtert.

ABSTRACT

Epoxy thermosets play a vital role in the thermosetting and composite market, with projected growth driven by their exceptional properties and versatile applications across various industries. However, the reliance on fossil resources, the need for Bisphenol A (BPA) and Epichlorohydrin (ECH) for synthesis, the environmental impact associated with epoxy and epoxy-based carbon fibers (CF) composites production, and their challenging recyclability raise sustainability concerns. This study explores the development of BPA- and ECH-free epoxy systems that are fully or partially bio-based and designed for recyclability, using natural and available resources to foster a circular economy mindset. The mechanical and thermal properties of the developed materials are characterized and compared with literature and conventional epoxy systems.

The investigation of the fully bio-based epoxy thermoset based on epoxidized linseed oil (ELO) and tannic acid (TA) showed strong mechanical and thermal properties for a vegetable-oil-based epoxy. Different manufacturing methods were employed to manufacture CF composites with TA/ELO epoxy, and the characterization results are compared with CF composites made with a high-performance petroleum-based epoxy system. The possibility of mechanically recycling TA/ELO, TA/ELO CF composites, and recovering clean carbon fibers through solvolysis with commodity chemicals is investigated.

Later on, the thermal, mechanical, and recyclability properties of a novel multi-functional epoxy compound (EGCHC) with a significant bio-based content of 68.4 % and derived from highly available resources such as sorbic acid, maleic anhydride, and allyl alcohol are investigated and compared with the most well-known epoxy system on the market: Bisphenol A diglycidyl ether (DGEBA). The results show comparable properties to DGEBA while offering the possibility of mechanically recycling the material and recovering carbon fibers with low technical efforts and energy.

The advantages of the developed epoxy systems are discussed in the realm of CF composites industry, and the drawbacks such as high-water absorption and challenging composites manufacturing are highlighted. Improvement possibilities for industrial viability are also discussed.

Contents

Nomenclature

Formula symbol	Unit	Description
D50	µm	Median particle size distribution
E’	MPa	Storage Modulus
E’’	MPa	Loss Modulus
GWP	kg CO_2e/kg	Global Warming Potential
L	mm	Span length
rpm	-	Revolutions per Minute
T	°C	Temperature
$T_{5\%}$	°C	Temperature of 5 % weight-loss
t	1000 kg	Ton
tan δ	-	Loss factor
V_f	%	Fiber volume fraction
τ	s	Relaxation time
σ	N/mm²	Shear stress
σ (t)	N/mm²	Shear stress at time t
σ (0)	N/mm²	Initial shear stress
ρ	g/cm³	Density
w_{bb}	-	Bio-based content

List of abbreviations

Abbreviation	Description
ACN	Acrylonitrile
AHIBC	Allyl-7-methyl-1,3-dioxo-1,3,3a,4,7,7a-hexahydroisobenzofuran-4-carboxylate
ATR-FTIR	Attenuated Total Reflection Fourier Transformed Infrared Spectroscopy
BPA	Bisphenol A
CAGR	Compound Annual Growth Rate
CAN	Covalent Adaptable Network
CF	Carbon fibers
CO_2e	Carbon dioxide equivalent
DSC	Differential Scanning Calorimetry
DGEBA	Bisphenol A diglycidyl ether
DMA	Dynamic Mechanical Analysis
ECH	Epichlorohydrin
EE	Embodied Energy
EEW	Epoxy Equivalent Weight
EGCHC	1,2-Epoxy-6-methyl-triglycidyl-3,4,5-cyclohexanetricarboxylate
EKO	Epoxidized Karanja Oil
ELO	Epoxidized Linseed Oil
ESO	Epoxidized Soybean Oil
EU	European Union
EVO	Epoxidized Vegetable Oil

Abbreviation	Description
FRPC	Fiber Reinforced Polymer Composites
GWP	Global Warming Potential
IPD	Isophorone diamine
LCA	Life Cycle Assessment
*m*CPBA	meta-Chloroperoxybenzoic acid
N2	Nitrogen
NaOH	Sodium hydroxide
PAN	Polyacrylonitrile
RT	Room Temperature
RTM	Resin Transfer Molding
SEM	Scanning Electron Microscope
SGL Tow	Sigrafil Tow C T50-4.4/255-E100 (SGL Carbon)
T403 Jeffamine	Polyoxypropylenetriamine
TA	Tannic acid
TA/ELO	Tannic acid/Epoxidized Linseed Oil
TACHC	Triallyl-6-methylcyclohex-4-ene-1,2,3-tricarboxylate
Tg	Glass transition temperature
Tg∞	Glass transition temperature of the fully cured material
TGA	Thermogravimetric analysis
Tm	Melting point
Tv	Topology freezing transition temperature
UD	Unidirectional
UD SGL	SIGRATEX® C U170-0/ST-E214/10g (SGL Carbon)

Abbreviation	Description
UD Twill 3/1	UD Twill 3/1 UTS 50 (Teijin)
USD	US Dollar
VARI	Vacuum Assisted Resin Infusion
V_f	Fiber volume fraction

List of figures

List of tables

1 Introduction

1.1 Motivation

Epoxy thermosets represent a prominent place in the thermosetting market. In 2020, epoxy resins accounted for over 30 % of the thermoset market and they are expected to witness further growth in the forecast period of 2023–2028, growing at a Compound Annual Growth rate (CAGR) of 6.4 % [1]. Due to its outstanding properties, epoxy is a well-suited matrix for the production of composite materials. Thanks to their excellent mechanical properties, chemical resistance, remarkable strength-to-weight ratio and versatility, epoxy-based composites find applications across various industries including aerospace, automotive, wind energy, construction, marine and sports. The size of the global composite market was USD 90 billion in 2019 and is expected to rise with a growth rate of 7.6 %, reaching USD 160 billion by 2027 [2]. To date, most produced epoxies, common reinforcing fibers like carbon fibers, and hence epoxy-based composites are derived from fossil resources. Additionally, bisphenol A (BPA) and epichlorohydrin (ECH), both needed for the production of standard epoxy thermosets are known to cause adverse effects on living organisms and ecosystems [3–5]. With the depletion of fossil resources, the development of bio-based materials from renewable feedstocks has become a necessity.

Furthermore, epoxy and epoxy-based composites are energy intensive materials with a high global warming potential (GWP) and therefore ideal possible candidates for recycling. Indeed, epoxy systems can represent a GWP of up to 14.1 kg CO_2e per kg. The reinforcement fibers used to produce high-performance epoxy composites also represent a high GWP (carbon fibers 25 kg CO_2e per kg and glass fibers 1.64 kg CO_2e per kg) [6,7]. However, at the same time, epoxy materials are challenging to recycle. In fact, epoxies are thermosets with a permanent cross-linked structure after cure and possess properties that render them highly sought-after in the production of composites materials for high-performance applications, but these same properties (such as high chemical and heat resistance) as well as its thermoset nature impose constraints on their recyclability and the recovery of the reinforcement fibers [8,9]. Current methods for disposing epoxy and epoxy-based composite still involve landfilling. In fact, due to different waste related legislation existing in the individual countries of the European Union, some countries implemented a ban for landfilling, while others have not [10,11]. The practice of landfilling, when it comes to composites, represents a significant wastage of valuable materials and the energy invested in their production [2,10]. However, according to the EU's waste hierarchy, landfilling is the least preferable option and should be limited to

the necessary minimum and the implementation of the EU Directive on Landfill of Waste (Directive 99/31/EC) will lead to a decrease in the quantity of organic waste being disposed of in landfills [10,12]. Incineration is another disposal method for epoxy and its composites which causes significant negative impacts on whole ecosystems. The waste treatment policy in the European Union (EU) prioritizes the waste prevention, reuse, and recycling of the materials over incineration and landfilling [8,9,13].

Consequently, there is a pressing requirement for innovative approaches to develop epoxy thermosets from renewable feedstocks and manage the disposal of epoxy and epoxy composites at the end of their life cycle to foster a circular economy mindset. The 12 principles of Green Chemistry, postulated in 1998 by Anastas and Warner are the most important reference for a sustainable chemical synthesis. The principles of Green Chemistry advocate for the adoption of renewable resources to address the depletion of fossil resources and the associated challenges. Additionally, they emphasize the need to minimize or eliminate the use and production of hazardous substances, as well as the prevention of waste generation [14,15].

Therefore, finding bio-based epoxies that are recyclable can strongly contribute to the principles of Green Chemistry and the circular economy by promoting the use of renewable resources and reducing waste generation as they can be a part of a closed-loop system where materials are recycled at the end of their life cycle, minimizing waste and promoting resource efficiency.

1.2 Objectives

The aim of this doctoral thesis is to develop innovative bio-based epoxy thermosets that can be used for the production of CF composites and that adhere to the principles of Green Chemistry by meeting the following criteria:

- Partially or fully bio-based. Various renewable resources will be used as raw materials in order to provide several solutions to address the depletion of fossil resources.
- Free from BPA and ECH to mitigate possible adverse effects on living organisms and ecosystems.
- Designed for recyclability to promote a circular economy.

The developed bio-based epoxy thermosets will be characterized in order to understand the relationship between molecule structure and properties. Additionally, their performance and potential as substitutes for conventional petroleum-based epoxy thermosets will also be evaluated. Furthermore, their recycling ability will be demonstrated. Conventional composite processing techniques will be utilized to produce bio-based CF composites and their performance will be assessed. Later on, the recycling of the developed composites will be investigated.

1.3 Outline

This thesis is divided into 7 chapters:

Chapter 1 introduces the motivation of this doctoral thesis and presents the objectives of this work.

Chapter 2 outlines the state of the art relevant to the objectives of this research and helps highlight the need for bio-based epoxy thermosets with recycling ability. It begins by addressing the challenges associated with the use of conventional epoxy thermosets and composites. Subsequently, it offers an overview of both commercially available and ongoing research in the field of bio-based epoxies and curing agents, as well as their advantages and limitations. Furthermore, the concept of epoxy thermosets with dynamic covalent chemistry which enables mechanical recyclability and facilitates the recovery of CF is presented and its advantages for the composite industry are discussed. Finally, the characteristics and importance of CF for the industry are discussed and the standard CF production and alternative and more sustainable production methods are presented.

Chapter 3 describes the materials and methods used to produce and characterize the various bio-based thermosets and composites in this dissertation.

Chapter 4 focuses on the development and characterization of a fully bio-based, BPA- and ECH-free epoxy thermoset made from available bio-based resources. Epoxidized linseed oil (ELO) and the hardener tannic acid (TA) are mixed together with various contents and cured at different temperatures to understand the impact of the mixing ratio

and curing temperature on the mechanical, thermal, and thermo-mechanical properties of the thermoset. The results are compared with literature and with a commercially available high-performance epoxy system to evaluate the performance of the fully bio-based epoxy thermoset. Further on, the recycling ability of TA/ELO epoxy thermoset is demonstrated and mechanical recycling and solvolysis are investigated.

Chapter 5 describes methods for producing CF composites with the fully bio-based thermoset TA/ELO developed in chapter 4. Various conventional composites manufacturing techniques are explored, and the produced composites are characterized and compared to CF composites made with a conventional high-performance petroleum-based epoxy system. The advantages of the recycling ability of TA/ELO are shown in the realm of the composite industry by studying mechanical recycling and the recovery of CF through solvolysis. Later on, CF composite parts (a longboard and a pipe) are produced with TA/ELO and CF to demonstrate the feasibility of using bio-based epoxy for composite production.

Chapter 6 characterizes the properties of a novel multi-functional, BPA- and ECH- free epoxy resin (EGCHC) with a significant bio-based content cured with two conventional curing agents (T403 and IPD). The characterization results are compared with the most-used petroleum-based epoxy resin (DGEBA) to demonstrate the ability of EGCHC to serve as greener alternative to DGEBA. Furthermore, the recycling ability of EGCHC is demonstrated, and scenarios for increasing the bio-based content of EGCHC are discussed with an ecological assessment.

Chapter 7 summarizes the advantages of the developed bio-based epoxy thermosets and CF composites for the composite industry. The limitations and drawbacks of the developed materials are also highlighted, and improvement possibilities for industrial viability are also discussed.

2 State of the art

2.1 Epoxy thermosets and epoxy composites

2.1.1 Definition and properties

Epoxy resins are classified as thermoset polymers. Before curing, epoxy resin is a chemical compound containing two or more epoxide groups per monomer. A hardener/curing agent is required in the curing process of epoxy. During polymerization, the curing agent opens the epoxide groups and the bonds are rearranged to join the monomers into a three-dimensional network of crosslinked chain-like molecules [16].

Epoxy resins are one of the most versatile classes of thermosets. After curing, the glass transition temperature of the epoxy can vary in the broad range of 60 °C up to 250 °C, depending on the choice of constituents, as the performance of epoxy thermosets greatly varies depending on the resin and curing agent utilized [17]. Tensile strength values can be among the highest achievable in thermosets. In some cases, they exceed 80 MPa. The compressive strength can double this value. In addition to the high mechanical strength, epoxy can exhibit high stiffness. They also exhibit excellent adhesive strength, high thermostability, high corrosion and chemical resistance. In addition, they experience little to no shrinkage after they are cured [18,19].

Thanks to these attributes, epoxy thermosets are well-established in a large variety of applications, including electronic encapsulation, paints, coatings, adhesives and sealants (Figure 1). Its easy processability and good wettability to fibers makes it also a popular matrix for composite materials. When reinforced with glass or carbon fibers, epoxy-based composite materials are widely used in load-bearing high-performance applications such as automotive, aerospace, construction, marine and wind turbine industries [20]. As an example, 50 % of the composition of the Boeing Dreamliner 787 launched in 2011 was made up of carbon fibre-reinforced epoxy resin composite [21]. In 2020, epoxy resins dominated the thermoset market, securing a substantial share of over 30 %, primarily attributable to its outstanding features [22].

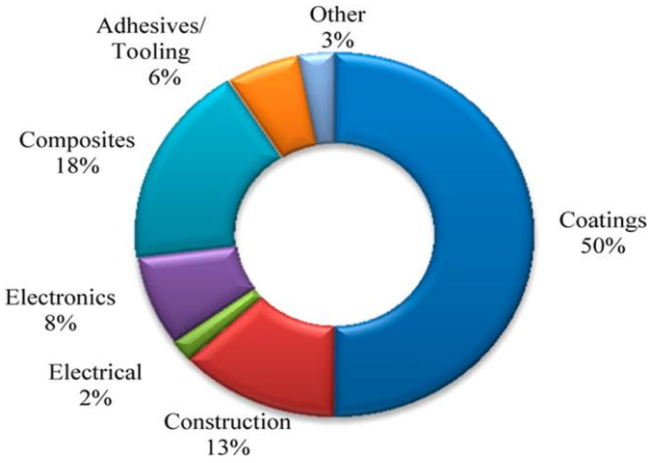

Figure 1: Global epoxy demand by sector. From [23]**.**

About 90% of the global epoxy thermoset demand is derived from diglycidyl ether of bisphenol A (DGEBA). The presence of bisphenol A core in DGEBA imparts outstanding mechanical and thermal properties to the polymer network, along with exceptional chemical resistance (Figure 2). Furthermore, DGEBA-based epoxy resins with low molecular weight are usually liquids at room temperature, which is a great advantage regarding processability [3,24–26].

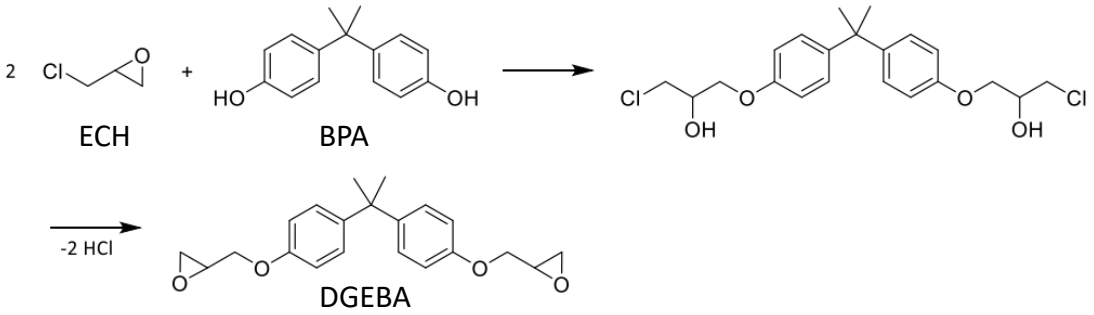

Figure 2: Synthesis of DGEBA from BPA and ECH. Adapted from [14]**.**

2.1.2 Limitations associated with epoxy thermosets and epoxy-based composites

2.1.2.1 Composition

Concerns have been raised regarding the use of DGEBA, the most well-known epoxy resin. Firstly, the raw materials needed for the production of DGEBA, namely bisphenol A (BPA) and epichlorohydrin (ECH), are petroleum-based (Figure 2). With the depletion of fossil resources, the development of materials from renewable feedstocks has become a necessity. Secondly, BPA and ECH are known to cause adverse effects on living organisms and ecosystems. BPA in particular is kept under watch. According to the CLP (Classification, Labelling and Packaging) Regulation, in 2016, BPA was categorized as toxic to reproduction category 1B, specifically labeled as "may impair

fertility". In 2017, it was identified as a substance of very high concern (SVHC) by the European Chemicals Agency (ECHA) due to its endocrine disruptor nature for the environment and human health. Since June 2011, the use of BPA has been prohibited in infant feeding bottles throughout the EU. Furthermore, starting from September 2018, it has also been banned in plastic bottles and packaging intended for food for babies and children under three years of age. Since March 2018, BPA has been subject to restrictions both as a standalone substance and as part of mixtures intended for consumer use within the EU. Additionally, its utilization in thermal paper has been restricted since January 2020 [3–5]. BPA is, however, still used for the production of DGEBA.

Furthermore, certain frequently employed curing agents, including polyamine, polyamide, and anhydride hardeners, exhibit toxicity prior to curing. Therefore, even after curing, there is a possibility of toxicity in the cured epoxy materials if the curing agents are not fully consumed [27,28].

Thus, for environmental and health reasons, there is a need to develop BPA- and ECH-free bio-based epoxies that can compete with DGEBA-based epoxy thermosets.

2.1.2.2 Composite waste generation

The amount of composite waste generated by various industries (building & construction, electrical & electronics, transportation, marine, production waste, aeronautics, tanks & pipes and wind sectors) across Europe is expected to grow drastically in the upcoming decades. Figure 3 shows the forecasted amount of composite waste in Europe for 2025 and 2040. The rapid composite waste growth is anticipated as an increased amount of composite-based structures will reach their end-of-life in the next decade. As an example, in the aeronautics sector, about 22 % of the aircraft currently in operation will enter their end-of-life phase within the next decade [29]. Regarding the wind sector, WindEurope expects blade waste to reach about 25 000 tons per year by 2025 and up to 52 000 tons per year by 2030. Epoxy and epoxy composites are materials that demand a significant amount of energy for their production (carbon fibers 183–704 MJ/kg, glass fibers 13–54 MJ/kg and epoxy resins 76–80 MJ/kg), contributing to a notable global warming potential [30]. Consequently, they present themselves as promising and suitable contenders for recycling efforts. Indeed, epoxy systems can represent a global warming potential of up to 14.1 kg CO_2e per kg, carbon fibers 25 kg CO_2e per kg and glass fibers 1.64 kg CO_2e per kg [6,7]. In addition, CF is an expensive fiber reinforcement for the production of CFRP, and the demand for CF recovery from recycled composite to reduce production costs and environmental impact is growing [26].

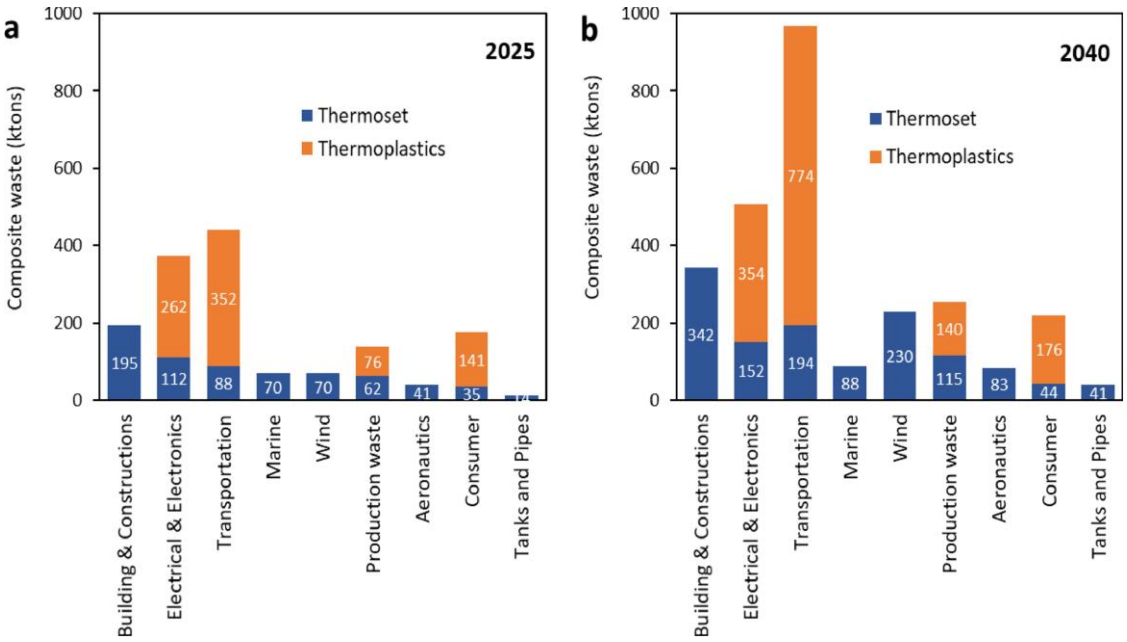

Figure 3: Estimated composite waste per sector (ktons). From [30]**.**

Due to its thermoset nature and permanent crosslinked structure, epoxy cannot be reprocessed and reformed like thermoplastics. Also, its decomposition requires harsh reaction conditions such as high temperatures, high pressures and/or strong acids. Therefore, the recycling of epoxy thermosets and the recovery of the reinforcement fibers from epoxy-based composite is a real challenge. As a consequence, landfilling and incineration are disposal methods for epoxy and epoxy-based composites that are still in practice. Landfilling as a disposal method results in substantial wastage of valuable materials and the energy invested in their production. Incineration is the most common disposal route. The heat generated from the incineration is used to create electricity. Nevertheless, problems arise due to the possible emission of hazardous gases. Moreover, due to the elevated inorganic content of the composites, a high amount of the scrap remains as ash after the incineration process. The incineration ash has the potential to be polluting and is usually landfilled. Last but not least, the efficiency when converting the heat to electricity is low when incinerating Carbon Fiber-Reinforced Plastics (CFRP) [26,31–34].

Directives and political drivers however are helping landfilling to gradually phase out of the European union countries. According to the European Composites Industry Association (EuCIA), there is a growing trend towards stricter regulations and prohibitions on conventional disposal methods like landfills and incineration. Consequently, companies in the composites industry, as well as their customers, are actively seeking more sustainable alternatives. Moreover, directives, such as the EU End-of-life Vehicle (ELV) directive states that by no later than January 1, 2015, a minimum of 95 % of the weight of each end-of-life vehicle should be subject to re-use and recovery. Additionally, within the same timeframe, a minimum of 85 % of the weight of each vehicle should be targeted for re-use and recycling. Additionally, the Landfill Directive 1999/31/EC aids the European Union's shift towards a circular economy by designating landfilling as the least

favorable choice in the EU's waste hierarchy (Figure 4). It also introduces restrictions on landfilling of all waste that is suitable for recycling or other material or energy recovery from 2030. Subsequently, Germany, as an example, banned the landfilling of composite waste in 2009 and other countries are expected to follow [35–37].

Figure 4: **The foundation of EU waste management is the five-step "waste hierarchy", established in the Waste Framework Directive. From:** [12]**.**

2.1.2.3 Recycling of epoxy and epoxy-based composites

Consequently, there is a heightened emphasis on composite recycling. Conventional methods for recycling epoxy-based composites and thermoset-based composites in general include mechanical recycling, pyrolysis and solvolysis:

- **<u>Mechanical recycling</u>**

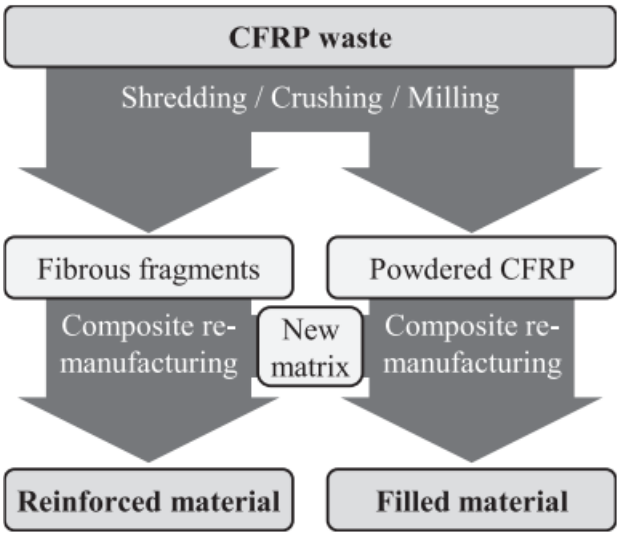

Figure 5: **Mechanical recycling of CFRP. From:** [38]**.**

Mechanical recycling involves the fragmenting of the composite through actions like shredding, crushing, milling, or comparable mechanical techniques. The resultant scrap fragments can subsequently be sorted using sieving methods into powdered materials (abundant in resin) and fibrous materials (abundant in fibers) (Figure 5). This recycling approach offers the benefit of straightforward implementation and minimal energy requirements in contrast to alternative recycling techniques. Mechanically recycled composites find common use in various applications, such as being reintroduced into new composites as fillers or reinforcement, as well as in the construction industry, where they serve purposes like enhancing artificial woods or asphalt, or acting as mineral sources for cement. Nevertheless, it's worth noting that these applications are considered to have relatively lower value, as the unstructured, coarse and non-consistent fiber architecture of mechanically recycled composites results in a significant loss of mechanical properties. A range of applications have been investigated for the use of recyclates in the production of new composites. The powdered material (rich in resin) can effectively replace calcium carbonate filler in new Sheet Molding Compounds (SMC) or Bulk Molding Compounds (BMC). At loading levels of approximately 10 %, the decreases in mechanical properties are within acceptable limits. Noticeable declines in mechanical properties are observed at higher loadings. The use of the fibrous recyclate (rich in fibers) in the production of new composites is generally described as more challenging, as a decrease in strength and toughness is observed already when introduced in small amounts. This is attributed to the low bonding between the matrix resin and the recyclate, its unstructured architecture and its non-consistent arrangement in the matrix. Furthermore, the larger particles of the recyclate act as a stress raiser [10,38–42].

- **Pyrolysis**

Pyrolysis is a thermal process which involves the thermal breakdown of organic molecules in an inert atmosphere (e.g., N2) and stands as one of the most widely utilized recycling techniques for CFRP. In this process, CFRP is subjected to temperatures ranging from 350 °C to 700 °C, with oxygen nearly absent. During this phase, the polymeric matrix undergoes degradation and produces an oil, gaseous and solid products (fillers, char), while the carbon fibers remain inert and can be reclaimed. Both the oil and gas products produced can serve as valuable chemical feedstock as the oil has a calorific value similar to fuel and the gas can be regenerated into the pyrolysis reactor (Figure 6). However, the fiber surfaces are contaminated with solid char that affects the mechanical characteristics of the recovered fibers. A post-pyrolysis treatment, involving oxidation for example is necessary for the obtention of clean fibers. Pyrolysis is an effective method to preserve the properties of carbon fibers. Nevertheless, treatment conditions have a great impact on the resulting fiber properties. Pimenta et al. [43] reported a decrease in the original tensile strength, which ranged from 2 % to as much as 85 %, depending on the treatment conditions applied. Glass fibers tend to suffer more from the temperatures than carbon fibers which results in a significant loss of their mechanical

properties. Pyrolysis stands out as the most extensively studied thermal recycling technique and is one of the most widespread recycling processes for CFRP. Recycled carbon fibers obtained with the pyrolysis process are already available on an industrial scale. As an example, the Milled Carbon Group from the UK started developing a pyrolysis process for CFRP in a pilot-plant in 2003. This operation later evolved into what is now recognized as "the world's first commercial scale continuous recycled carbon fibre operation" leading to the establishment of Recycled Carbon Fibre Ltd. (RCFL) in 2009. [34,38,44–47]

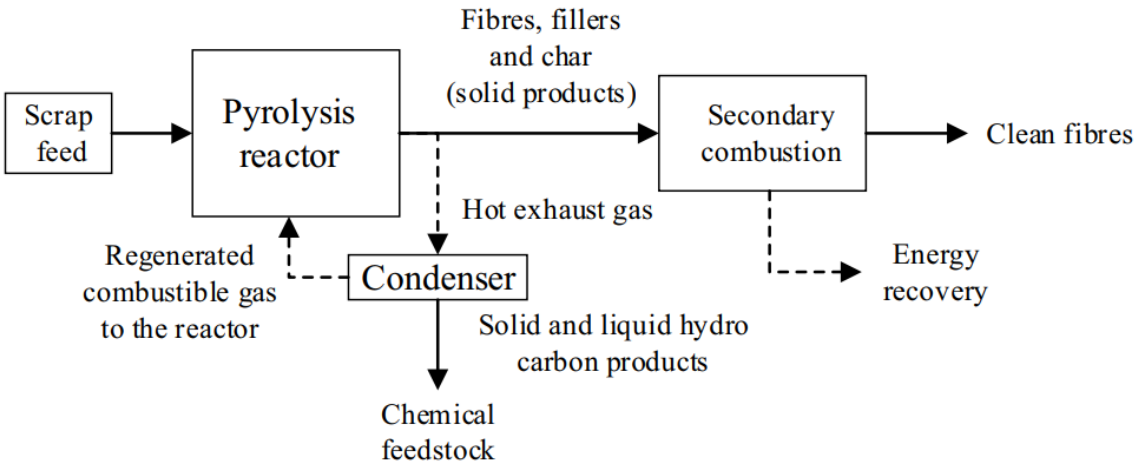

Figure 6: Pyrolysis process. From: [34].

- **Solvolysis**

Solvolysis is a chemical recycling method using a nucleophilic solvent to degrade the matrix. It offers flexibility in terms of solvent choice, temperature, pressure, and catalysts. Unlike pyrolysis, it generally operates at lower temperatures (typically < 350 °C). After the dissolution of the polymer matrix, a washing process is employed to eliminate any minor surface residues from the recycled fibers. Solvolysis is known in general to have a smaller impact on the mechanical properties of carbon fibers and glass fibers than pyrolysis. However, challenges arise with the elevated expenses associated with reagents, the release of harmful gases as well as the safe use and disposal of strong solvents (such as strong acids). Hence, environmentally friendly options such as supercritical water or alcohol are often used to replace highly concentrated and hazardous chemicals. Nonetheless, the use of water at supercritical condition involves the need of reactors that can incur high costs because they must endure elevated temperature and pressures which hinders the scalability of the process on an industrial level, along with potential corrosion due to modified properties of the solvent. Another drawback frequently encountered is the diminished adhesion observed between the recycled fiber and the new resin.

Because of the reduced temperatures used, life cycle assessments (LCAs) documented in literature favored chemical recycling over pyrolysis as the energy footprint and

greenhouse gas emissions of chemical recycling were lower for chemical recycling. [34,47–49]

Fig.A- 1 illustrates the performance of composite fibers following different recycling methods [50]. Solvolysis is identified as the process that retains the highest fiber performance.

Tab. 1: Advantages and drawbacks of the recycling processes.

Recycling Process	Advantages	Drawbacks
Mechanical	• Recovery of both fibers and resin [38] • No use of hazardous materials [38] • Easy to implement [50] • Low costs [50]	• Significant loss of mechanical properties [38] • Unstructured, coarse and non-consistent fiber architecture [38]
Pyrolysis	• High retention of mechanical properties [38] • No use of chemical solvent [38] • Potential to recover chemical feedstock [38]	• Possible deposition of char on fiber surface [38] • Sensitivity of properties of recycled fibers to processing parameters [38] • Environmentally hazardous off-gases [38] • High Embodied Energy (EE) [51]
Solvolysis	• Very high retention of mechanical properties [38] • High potential for material recovery from resin [38] • Very high retention of fiber length [38]	• Common reduced adhesion to polymeric resins [38] • Reduced scalability of most methods [38] • Possible environmental impact if hazardous solvents are used [38] • High costs [50] • Very High EE [51]

Tab. 1 presents the advantages and drawbacks of each recycling technique. All in all, every epoxy-based recycling process has its advantages and disadvantages. Due to the existence of the covalent cross-link bonding network in the epoxy matrix and its superior heat and chemical resistance, epoxy and epoxy-based composites are challenging to recycle at their end-of-life [23]. Mechanical recycling is an easy to implement and low-cost method. However, only low value applications can be targeted as a significant loss of mechanical properties is experienced. Pyrolysis and solvolysis can be performed to recover fibers with high to very high mechanical properties but they involve a higher technical effort, as well as a high energy consumption [50]. Pyrolysis and chemical

recycling methods have already been successfully adapted to the specific challenges of composite recycling by several companies, enabling the recovery of high-quality fibers. For example, Recycled Carbon Fibre Ltd. operates a pyrolysis commercial-scale plant with a processing capacity of 2000 tons/year. Adherent Technologies Inc. has a pilot-scale plant capable of chemically recycling 1000 tons/year. [38]. Given the anticipated increase in composite waste in the coming decade (Figure 3), it is evident that companies are still far from being able to recycle the entirety of the expected waste generation.

The study on the composite recycling published in 2023 presented by AVK ("Industrievereinigung Verstärkte Kunststoffe") and IKK ("Institut für Kunststoff und Kreislaufwirtschaft der Leibniz-Universität Hannover") effectively summarizes the issue. Currently, there is no technology available that enables efficient and cost-effective recycling of composite materials while preserving their original properties [50]. Given the growing amount of composite waste in the coming years, and the need to foster the circular economy, further efforts are still needed.

2.2 Bio-based epoxy thermosets

Alternatives to petroleum-based epoxies do exist. This chapter presents the current bio-based epoxy systems on the market as well as possible natural resources that can be used for producing bio-based epoxies. The advantages and limitations will also be highlighted.

2.2.1 Commercially available bio-based epoxies

Traditionally, DGEBA epoxy resins are obtained from BPA and ECH, both derived from fossil resources (Figure 2). However, glycerol, a by-product of the production of biofuels, can be used for the production of ECH (Figure 7). Epicerol, based on glycerol is an already commercially available bio-based drop-in for ECH. Using Epicerol to produce the standard DGEBA resin is a common way adopted by companies such as Sicomin, Cardolite, Entropy Resins, Resoltech to produce a performance epoxy resin with bio-based content. Studies demonstrated that bio-based epoxy systems produced by these companies showed good mechanical and thermal properties, as well as very good potential for use in composite materials [52,53].

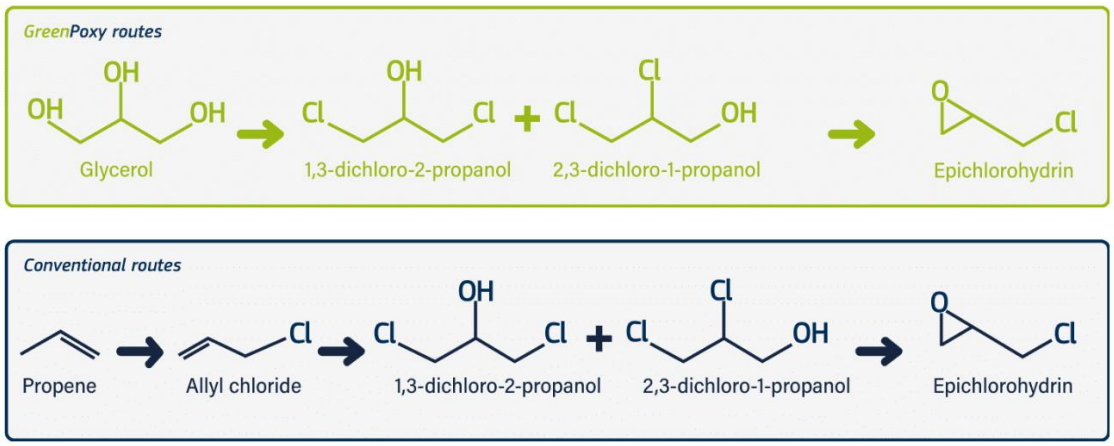

Figure 7: Use of glycerol to produce ECH (Epicerol) vs use of fossil resources to produce ECH from propene. From: [54]**.**

Yet, this approach has its limitations. By using Epicerol to produce DGEBA-based epoxies, only a limited amount of bio-content can be introduced in the final product. Assuming that all ECH used in standard DGEBA were replaced with Epicerol, 6 out of 21 carbon atoms in each molecule would be derived from bio-based sources. In a mixture with a resin-to-hardener ratio of 100:33 and no bio-based content in the hardener, this results in a system with a bio-based content of 21.5 % by weight [52]. The incorporation of a bio-based reactive diluent into the resin made with Epicerol allows an increase of the bio-based content but can be detrimental to the thermal and mechanical properties of the system. Using reactive amine curing agents with low amine hydrogen equivalent weight (AHEW) to reduce the amount of curing agent needed to cure DGEBA can also help increasing the percentage of the bio-based content in the epoxy thermoset. Reactive amine curing agents are however often linked with high toxicity. In general, the use of Epicerol to produce DGEBA-based resins evidently ensures the production of a performance epoxy thermoset containing a certain bio-based content and helps diminish the carbon footprint. Nevertheless, the health hazards linked with the use of BPA and ECH remain unchanged. Furthermore, the production of BPA (needed for the obtention of DGEBA) and the curing agents used by these companies (needed for curing DGEBA), still rely on fossil resources. [28,52,53,55]

2.2.2 Bio-based epoxies from alternative feedstocks

In order to avoid the usage of DGEBA due to problems and limitations already mentioned above and find a bio-based alternative, research focused on discovering bio-based substances that can serve as building blocks for epoxy resins. This led to the identification of various biomolecules that can potentially be used as precursors. Among the most promising candidates are phenolic structures such as eugenol, cinnamic acid, vanillin, and lignin fragments [56–65] (Figure 8). These molecules are particularly attractive due to their structural resemblance to BPA and their high aromaticity which imparts high mechanical and thermal properties. These molecules are reacted with ECH in order to

introduce epoxy groups in their structures [66]. Vanillin especially showed to be a great candidate to produce bio-based epoxies that can compete with DGEBA-based thermosets. Su and al. [56] synthetized a vanillin-based epoxy resin which was cured with a conventional amine hardener (D230) and compared the mechanical and thermal properties with DGEBA cured with the same hardener. The results showed superior tensile strength, and glass transition temperature for the vanillin-based epoxy.

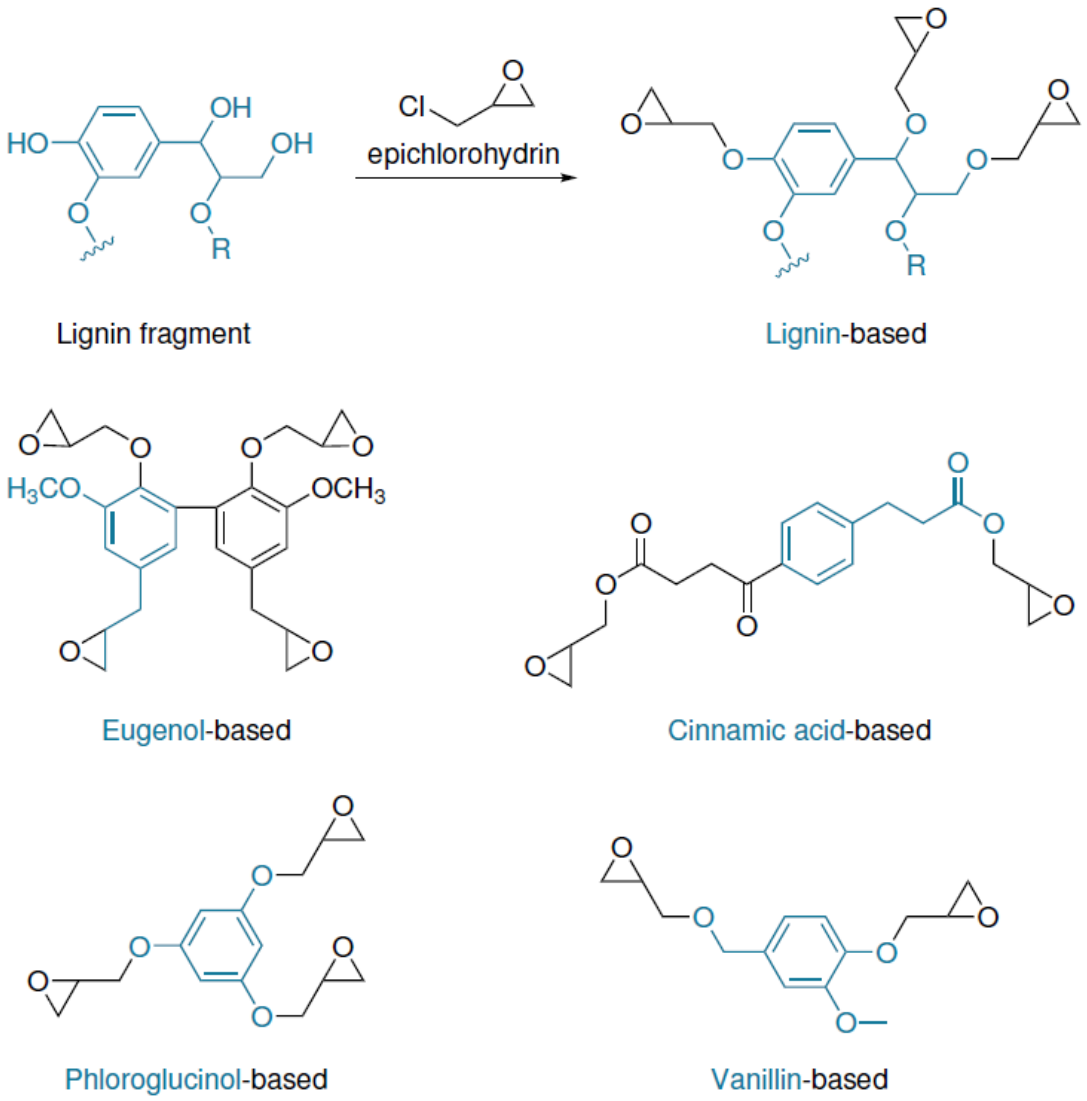

Figure 8: **Exemplary reaction for the introduction of epoxide groups with ECH as reagent. Structures of some phenolic bio-based developments. In blue: fundamental biomolecule. From:** [66].

However, limitations exist. The processes of extracting and purifying aromatic molecules to obtain homogeneous fractions have been found to impose a substantial environmental burden. As an example, the extraction and purification of vanillin typically require the use of hazardous and toxic solvents, such as benzene and toluene [67,68]. Another drawback is the need of ECH, which is known to cause adverse effects on living

organisms and ecosystems, to introduce the epoxy groups in these biomolecules [53,69]. Additionally, it is crucial for the substances to be readily accessible, and the cost of the bio-based feedstock must be competitive with fossil fuel resources for the large-scale production of bio-based epoxies to be viable. For instance, vanillin sources still face the challenge of higher costs compared to fossil fuel sources [70].

2.2.3 Bio-based epoxies from epoxidized vegetable oils

Vegetable oils are composed of triglycerides, which are composed of three fatty acid chains linked to a glycerol backbone through the carboxyl group (Figure 9). The amount of double bonds on these fatty acid chains greatly varies with the nature of the vegetable oil (Tab. 2). Thanks to a chemical reaction which usually involves the use of peracids and that takes place at the double bonds, the vegetable oils can be epoxidized and hence, epoxidized vegetable oils (EVO) can be used as a renewable feedstock to produce epoxy resins [71,72].

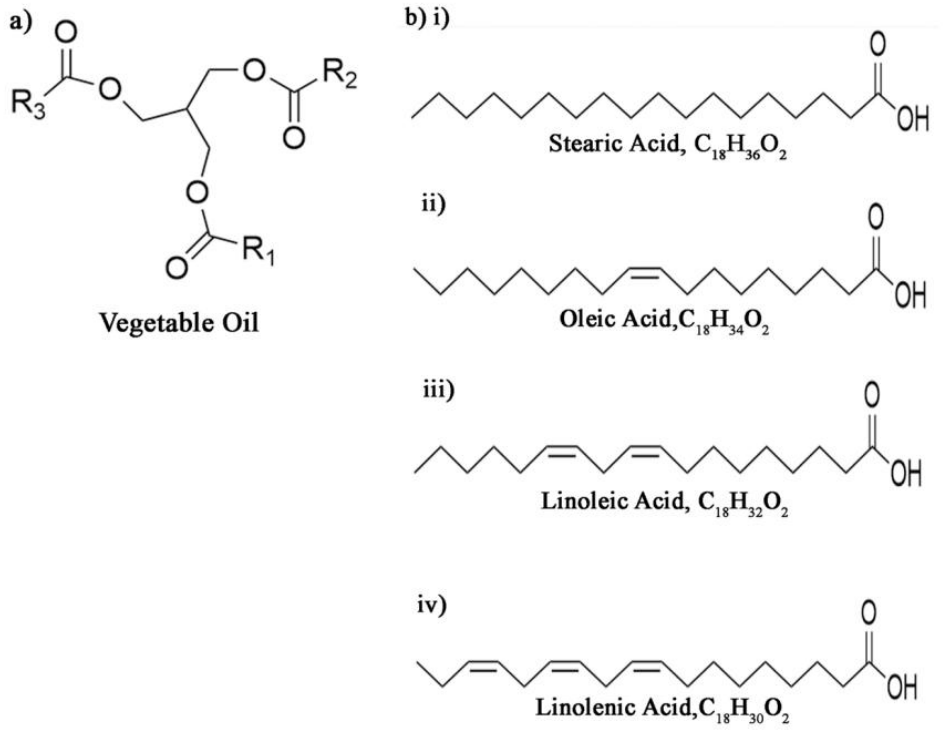

Figure 9: **a) General chemical structure of vegetable oil with R1, R2, R3, represent three fatty acid chains. b) Chemical structure of common fatty acids in vegetable oils: i) stearic acid. ii) oleic acid. iii) linoleic acid. iv) linolenic acid. From:** [73]**.**

In the last decade, EVO such as epoxidized linseed oil (ELO), epoxidized soybean oil (ESO), epoxidized karanja oil (EKO) or epoxidized canola oil have attracted great attention as an epoxy resin substitute (Figure 10).

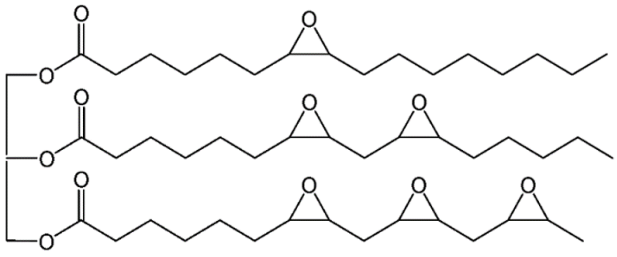

Figure 10: Chemical structure of ELO

In fact, vegetable oils are unharmful and abundant renewable resources that are available in the whole world at low cost. Therefore, many scientific publications investigating the potential use of EVO to produce bio-based epoxy thermosets emerged. Soybean oil, canola oil and linseed oil stand as prime candidates to produce bio-based epoxy thermosets as they have a high double bonds content which can be turned into epoxy groups (Tab. 2). However, EVO are known to have drawbacks. Indeed, the long aliphatic chains present in their chemical structure and the lack of aromatic structures impart flexibility. Also, the oxirane groups in EVO are located in non-terminal positions (Figure 10). When compared to DGEBA resins, EVO are known to be less reactive and less stiff. These characteristics strongly limit the practical use of EVO in the composite industry and structural applications [66,74–76].

Tab. 2: Fatty acid composition in wt% (X:Y, where X is the number of carbon atoms and Y is the number of double bonds) of different vegetable oils. Adapted from [70].

Vegetable oil	Palmitic (C16:0)	Stearic (C18:0)	Oleic (C18:1)	Linoleic (C18:2)	Linolenic (C18:3)
Soybean	11	4	23.4	53.3	7.8
Rape-seed/canola	4.1	1.8	60.9	21	8.8
Sunflower	5.2	2.7	37.2	53.8	1
Coconut	9.8	3	6.9	2.2	-
Linseed	5.5	3.5	19.1	15.3	56.6
Palm	42.8	4.2	40.5	10.1	-

In fact, the mechanical properties found in the literature for the different EVO are quite poor, especially in regard to stiffness. Tab. 3 depicts flexural modulus and tensile modulus reported in literature for EVO-based epoxies. As a comparison, SikaBiresin CR80, a DGEBA-based epoxy resin from the company SIKA, presents a tensile modulus of 3000 MPa and a flexural modulus of 2900 MPa when cured with the curing agent CH80-

10. SikaBiresin CR80 is a suitable epoxy resin for high-performance composites applications in the marine and wind energy [77]. Such a high stiffness is needed for structural applications.

Tab. 3: Tensile modulus and flexural modulus values reported for various EVO in the literature.

Resin	Curing agent	Tensile Modulus (MPa)	Flexural Modulus (MPa)
EKO	citric acid	2.65 [78]	/
ELO	citric acid	1140 [79]	/
ELO	dicarboxylic acids	22 [80]	/
ESO	terpene-based anhydrides	< 800 [81]	/
ESO	maleic anhydride	/	432 [82]
ELO	mixture of phtalic and maleic anhydride	/	622.8 [83]
ELO	methyl nadic anhydride	/	1772 [84]
ELO	sebacic acid	7.1 [85]	/
ESO	phtalic anhydride	648 [86]	775.4 [86]
CR80 (DGEBA-based)	CH80-10	3000 [77]	2900 [77]

EVO-based epoxies are also often associated with a low glass transition temperature due to their aliphatic and flexible structure. When used as a matrix material in composites, the resin state is desired to be rigid/glassy at temperatures of utilization and therefore, a high Tg is desired [76]. Wang et al. [87] found a Tg around 40 °C for ESO cured with MHHPA (methylhexahydrophthalic anhydride). Necolau et al. [88] found a Tg of 41 °C for ELO cured with citric acid and 29 °C for ELO cured with Jeffamine D230. A Tg of 9.7 °C was found for ELO cured with sebacic acid by Schwaiger et al. [85].

Nevertheless, some high Tg values for EVO based epoxies, especially for ELO, were reported. Pin et al. [89] found a Tg of 134 °C for ELO cured with MHHPA. Todorovic

et al. [90] found a Tg of 145 °C for ELO cured with MTHPA (methyltetrahydrophthalic anhydride). However, when measuring the glass transition temperature (Tg) of EVO based epoxies using Dynamic Mechanical Analysis (DMA), a highly sensitive machine designed for Tg measurement [91,92], it becomes apparent that the glass transition is broad. This broad glass transition results in a rapid loss of stiffness, as seen in the storage modulus (E') curve, that occurs before reaching the Tg (identified as the maximum of the tan δ peak). This greatly limits the use of EVO at elevated temperatures in structural applications as high stiffness is needed. Figure 11 illustrates an example of broad glass transitions and the rapid loss of stiffness observed in vegetable oil-based thermosets and composites. A broad glass transition can be the result of a heterogeneous polymer structure. In the case of EVO, the oxirane groups are statistically distributed across the aliphatic triglyceride backbone, which results in a complex crosslinked structure and broadens the glass transition [76,93–95].

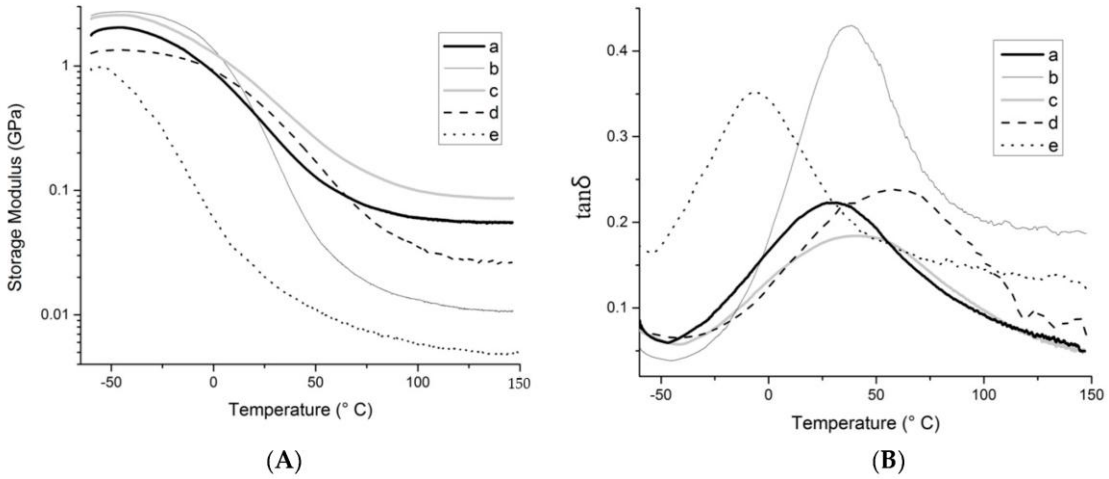

Figure 11: (A) Storage modulus (E') vs. temperature and (B) tan δ curves for (a) a resin prepared with tung oil, (b) a resin prepared with fatty acids, (c) a composite prepared with tung oil, (d) a composite prepared with fatty acids, and (e) a composite prepared with methyl esters. From: [96]**.**

Due to the rather poor mechanical and thermal properties of EVO, there is a rising tendency to mix EVO with petroleum-based polymer resin. In fact, the use of EVO as a toughening agent in conventional petroleum-based epoxies, such as DGEBA, is extensively studied in literature [75,87,97,98]. Highly crosslinked and stiff petroleum-based epoxies may experience issues such as brittleness and low toughness. The inherent flexible structure of EVOs can be of great interest when used as toughening agent. In fact, their ability to form heterogeneous phases when mixed with DGEBA-based epoxies has been found to yield advantageous effects, such as enhancing the impact strength and fracture toughness of the epoxy. However, when added in high quantity (for example at a quantity higher than 50 %), a significant loss in thermal and mechanical properties is

observed. Thus, EVOs can only be incorporated into petroleum-based epoxies in small amount, which greatly limits the overall bio-based content of the system [75,76].

2.2.4 Bio-based curing agents: tannic acid

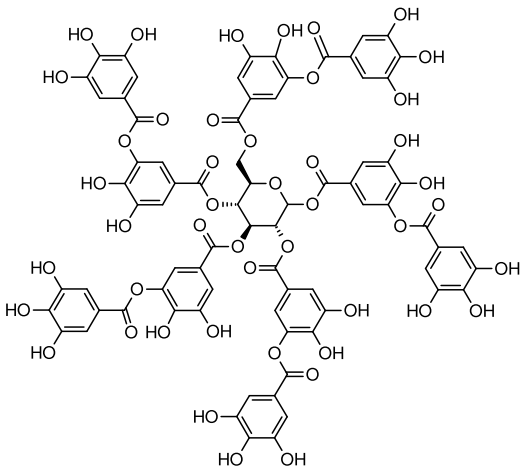

Figure 12: Chemical structure of Tannic acid. From: [99]**.**

Extensive global research efforts have been dedicated to the development of safer and bio-based and/or sustainable epoxy resins. Nonetheless, it is equally vital to create environmentally safe and sustainable curing agents, given that many industrially used curing agents, such as isophorone diamine (IPD) and various petroleum-derived polyamines, polyamides, and anhydrides, pose toxicity concerns prior to the curing process [27,28,100]. Various biologically derived compounds have been investigated as potential replacements to petroleum-based curing agents. Grapeseed, cardanol, and furans functionalized with amine groups have been explored as alternatives to amine curing agents. Anhydride-functionalized terpene has been researched as a potential substitute for common anhydride hardeners. The potential of unmodified compounds like cardanol, amino acids, citric acid and rosins as crosslinker has also been researched. However, bio-based curing agents are often linked with poor performance as the Tg values are rather low. Moreover, the complexity of their synthesis and isolation processes frequently hinders the commercialization of these biologically derived compounds [28,101,102].

Nevertheless, some bio-based curing agents, like tannic acid (TA) showed great potential as a biologically sourced hardener for epoxy resins. TA is a polyphenolic compound that can be found in nuts, galls, seeds, and tree bark. The typical chemical formula for TA is $C_{76}H_{52}O_{46}$, although it commonly consists of a blend of related compounds primarily centered around the glucose ester of gallic acid (Figure 12). TA is nontoxic and is generally recognized as safe (GRAS). TA has a high potential of crosslinking as it can

occur at the 25 galloyl hydroxyl groups [3,103,104]. The high crosslinking capability, its unharmful nature and its rigid structure make TA an interesting candidate for curing epoxy resins. Furthermore, TA has the advantage of being already industrially isolated. Its potential as a bio-based hardener has been widely studied for curing epoxy resins. Particular interesting results were found when TA was used as a hardener to cure a DGEBA resin as a Tg > 200 °C could be found [101], which is within the range of high-Tg epoxies available on the market. Feng et al. [105] found an outstanding tensile strength of 98.4 MPa when curing DGEBA with TA. TA as a curing agent for EVO has also been studied. Qi et al. [106] and Shibata et al. [107] used TA to cure ESO. Nevertheless, the stiffness of the cured material was quite poor as the tensile moduli were below 500 MPa. However, the publications were confronted with the low compatibility of TA with the resin and ethanol was used to dissolve TA in ESO to achieve homogeneous mixtures. Using solvents in epoxy thermosets comes with disadvantages, primarily because the solvent removal process is time-consuming and labor-intensive, thus complicating material processing. Furthermore, solvent residues within the material can adversely affect the epoxy's final properties [108,109].

2.3 Epoxy with dynamic covalent chemistry: vitrimers

Epoxies due to their thermoset nature are known to be challenging to recycle. Turning an epoxy thermoset into a vitrimer or vitrimer-like material can help make epoxies more sustainable by facilitating their recycling. The definition, characteristics and chemistry of vitrimers will be presented in this chapter. Later on, their benefits for the composite industry will be discussed.

2.3.1 Definition and characteristics

Thermosets in general are known for their outstanding mechanical properties and chemical and heat resistance. However, unlike thermoplastics, they cannot be reprocessed at their end of life, hindering therefore their recyclability. A ground-breaking novelty was found in 2011 as Leibler’s group reported a new class of Covalent Adaptable Networks (CAN), which they named vitrimer due to their silica-like viscosity-temperature relationship, which follows an Arrhenius-like dependence. Vitrimers are associative CANs, with their crosslinks being broken only when new bonds are formed. Hence, the number of chemical bonds remains constant throughout the reprocessing, thus maintaining the cross-link density [110–112] (Figure 13).

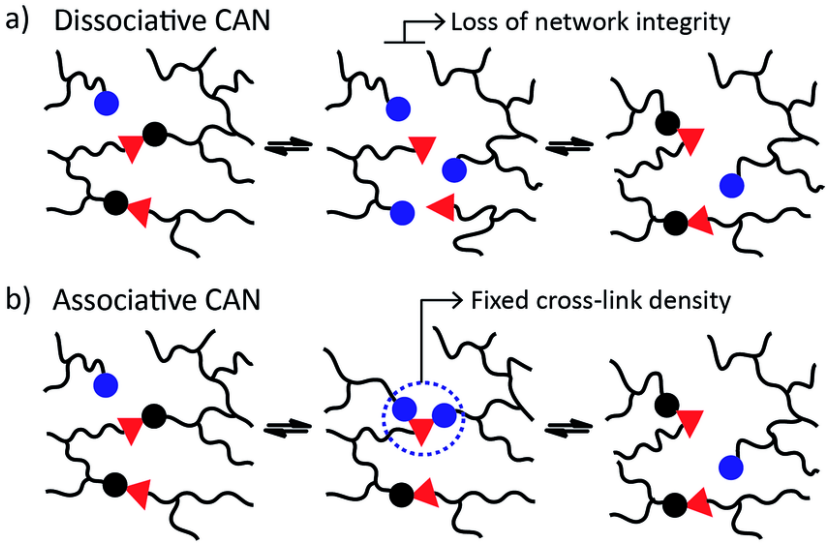

Figure 13: Illustration of the modification of network topology in CAN, depending on the type of dynamic linkages: (a) dissociative CAN, with a decrease in network connectivity, and (b) associative CAN, also called vitrimer, with a constant crosslink density. From: [113].

Vitrimers exhibit a characteristic temperature known as the "topology freezing transition temperature," denoted as Tv. Above this temperature, the viscosity follows an Arrhenius trend which allows the vitrimer to flow like a silica-based glass. This unique attribute allows vitrimers to function as a thermoset below Tv and as a viscoelastic fluid that can be reshaped and reprocessed (Figure 14) when heated above Tv [111].

Figure 14: Reshaping and recycling of a vitrimer. From: [114].

Therefore, vitrimers are considered as a bridging material between thermoplastics and thermosets (Figure 15).

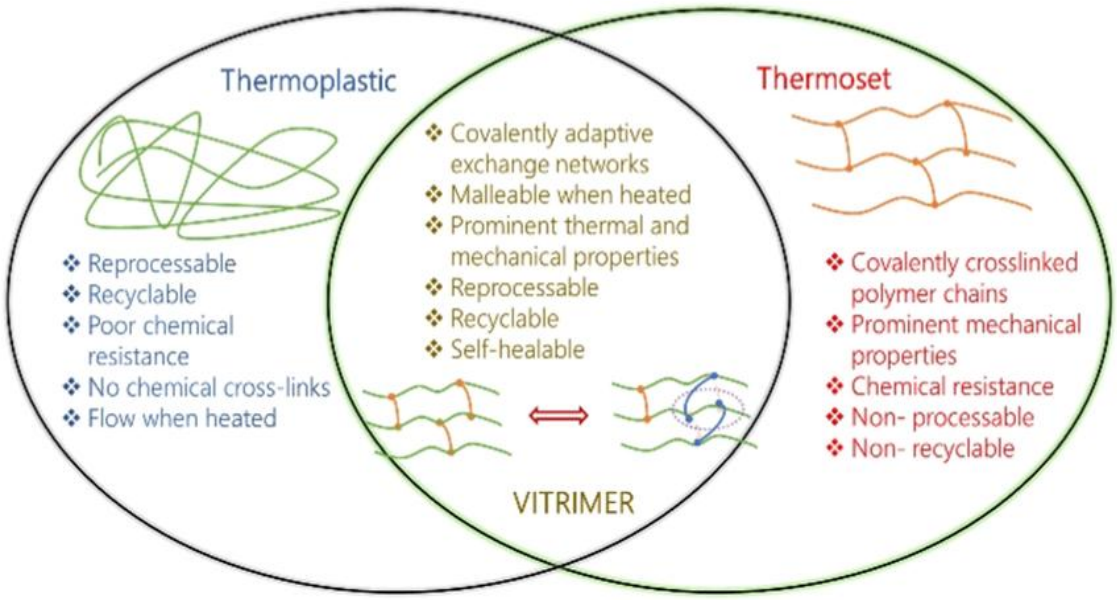

Figure 15: Schematic representation of vitrimers' properties/advantages, compared with thermoplastic and thermoset. From: [115].

Tv marks the point at which dynamic molecular rearrangement through cross-link exchange reactions becomes notably significant. Commonly, for vitrimers, Tg is below Tv. Figure 16a shows a typical case where Tg is below Tv. The material first undergoes a transformation from a rigid to a rubbery state. As the temperature continues to rise, the viscosity reaches a level of 10^{12} Pa·s, a value identified by Leibler et al. [116] as the point at which topological rearrangement begins, as stated in their initial research. Ultimately, the viscosity exhibit an exponential decay [111,116]. Some cases were reported with astoundingly low activation energy for the exchange reaction. Then, Tg becomes the limiting factor for viscoelastic fluidity [111] (Figure 16b).

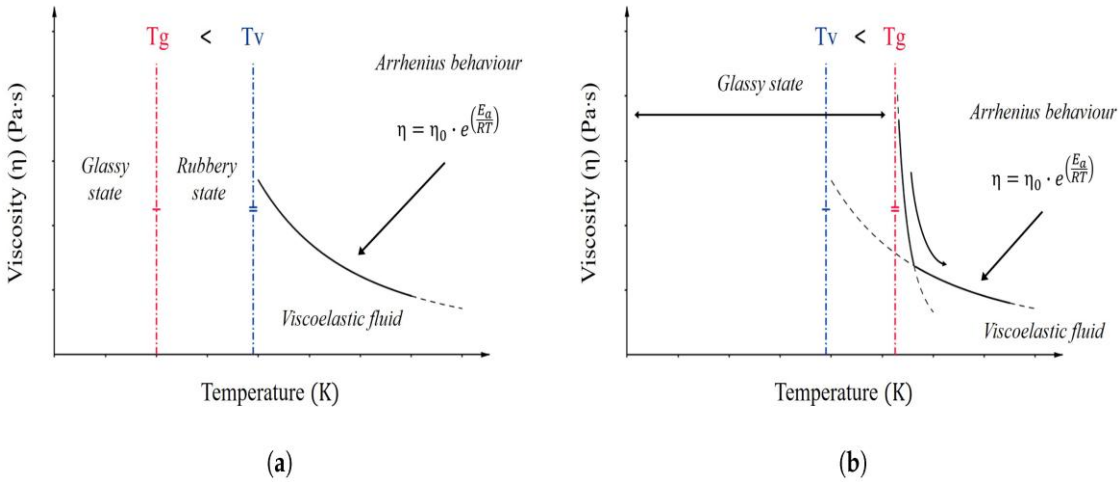

Figure 16: a) Case with Tg lower than Tv. b) Case with Tv lower than Tg. From: [111].

Unlike the case of Tg, there is no consensus regarding a standardized protocol or experimental arrangement for evaluating Tv [111]. Various definitions of Tv have been

proposed based on different measurement methods such as the value identified by Leibler et al. [116] and mentioned above: the point where the effective viscosity crosses a value of 10^{12} Pa.s. Typically, the determination of Tv is obtained by fitting stress relaxation experiments conducted at temperatures above Tv. Alternatively, it can be derived from dilatometry, which involves measuring the elongational expansion over time under specific heating rates and low stress conditions [115].

As another feature, vitrimers exhibit great stress relaxation above Tv. Stress relaxation tests are also performed to assess the bond exchange rate as a rapid stress relaxation would mean an accelerating exchange rate (Figure 17). The relaxation time τ is typically defined as the time when the stress normalized by the initial stress decays to 1/e. When plotting the logarithmic relaxation time as a function of inverse temperature, one can see the Arrhenius relationship of τ [117] (Figure 17). Some reported systems in the literature showed extremely fast stress relaxation. In the work of Chen et al. [118], a τ of 1.5 seconds could be reached at 200 °C for their epoxy vitrimer.

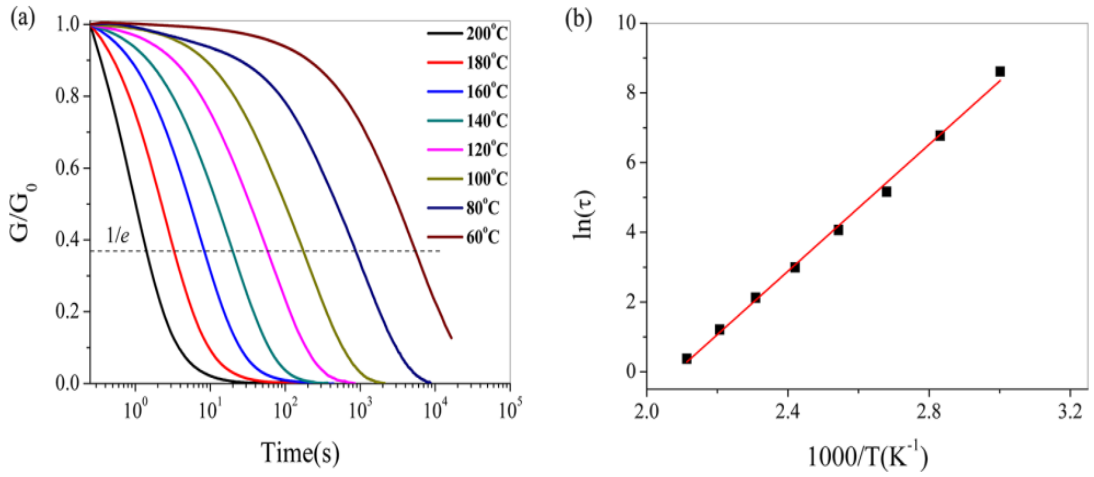

Figure 17: (a) Normalized stress relaxation curves of the dual dynamic vitrimer. (b) Plots of ln (τ) vs 1000/T and a linear fit to extract the activation energy. From: [118].

As a summary, vitrimers can be defined by the following criteria according to Dennissin et al. [119]:

- covalently bonded chains forming an organic network
- the network can change its topology through associative exchange reactions (dynamic covalent network) triggered by heat
- above Tv, vitrimers' viscosity is primarily governed by chemical exchange reactions, and the decrease of viscosity follows an Arrhenius behavior similar to inorganic silica materials
- vitrimers maintain permanent crosslinking density at all temperatures (excluding degradation)
- vitrimers swell but do not dissolve in chemically inert solvents, even when heated.

However, the insolubility requirement may be open to debate as vitrimers that could fully dissolve in tetrahydrofuran after 120 h were designed by Breuillac et al. [120]. This demonstrates that if the conditions promote dynamic bond exchanges, an extended exposure to a suitable solvent can eventually result in the dissolution of a vitrimer [111].

2.3.2 Transesterification reaction

Different exchange reactions can be used to obtain vitrimers and vitrimer-like materials including transesterification, transamination of vinylogous acyls (urea/urethanes), disulfide exchange, imine-exchange and siloxane-silanol exchange (Fig.A- 2). Only the transesterification reaction will be described in this chapter.

The transesterification reaction is a widely recognized chemical reaction in which the organic group of an ester is substituted with the group of an alcohol. Organo-metallic complexes and organic bases can be used to catalyze the reaction [111] (Figure 18).

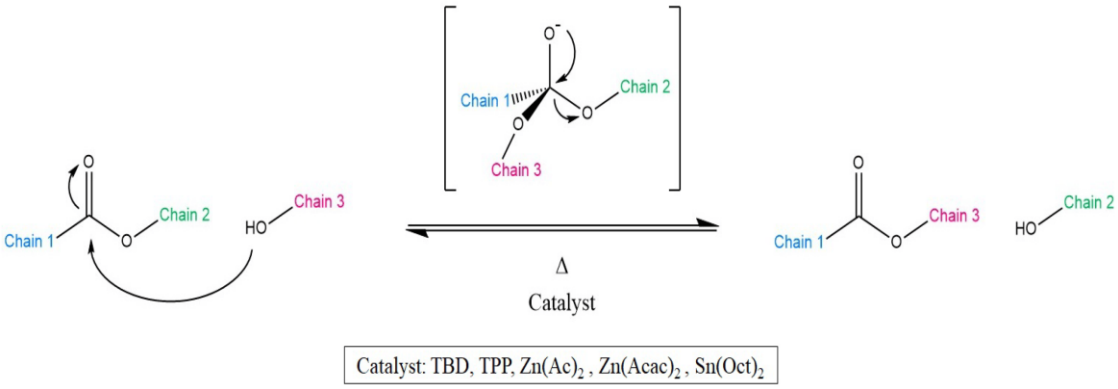

Figure 18: Representation of the Transesterification (TE) mechanism together with the most common catalysts. As a result, Chains 2 and 3 exchange positions, yet yielding again an alcohol and an ester. From: [111].

In 2011, Leibler and his team pioneered the development of vitrimers by employing the transesterification reaction with a standard DGEBA epoxy resin. They used a mixture of fatty tricarboxylic and dicarboxylic acids as a curing agent along with $ZnAc_2$ as a catalyst. Figure 19 illustrates examples of transesterification reactions permitted in this system [116].

The transesterification reaction is a commonly employed method to transform standard epoxy thermosets into vitrimers by introducing dynamic covalent bonds, and it can be applied in both Epoxy/Anhydride and Epoxy/acid systems [111]. In Epoxy/Anhydride systems, commercial applications often maintain epoxy/anhydride ratios ranging from 1:0.8 to 1:1 to ensure strong mechanical and thermal properties of the epoxy material. However, in the context of creating vitrimers, ratios as low as 1:0.5 are required to ensure an adequate supply of free -OH groups for the transesterification reaction. Notably, some of the commonly used anhydrides for forming vitrimeric networks include succinic anhydride, glutaric anhydride, methylhexahydrophthalic anhydride (MHHPA), and phthalic anhydride. Epoxy/acid represents the classic vitrimeric system, as first explored

in the pioneering work of Leibler. When carboxylic acid groups are introduced to epoxy rings under stoichiometric conditions, β-hydroxy esters with free -OH groups are formed, which is essential for transesterification. The curing agent Pripol 1040 which is a mixture of di- and tri-carboxylic fatty acids is often used in combination with DGEBA in literature to form vitrimers [110,111,121,122].

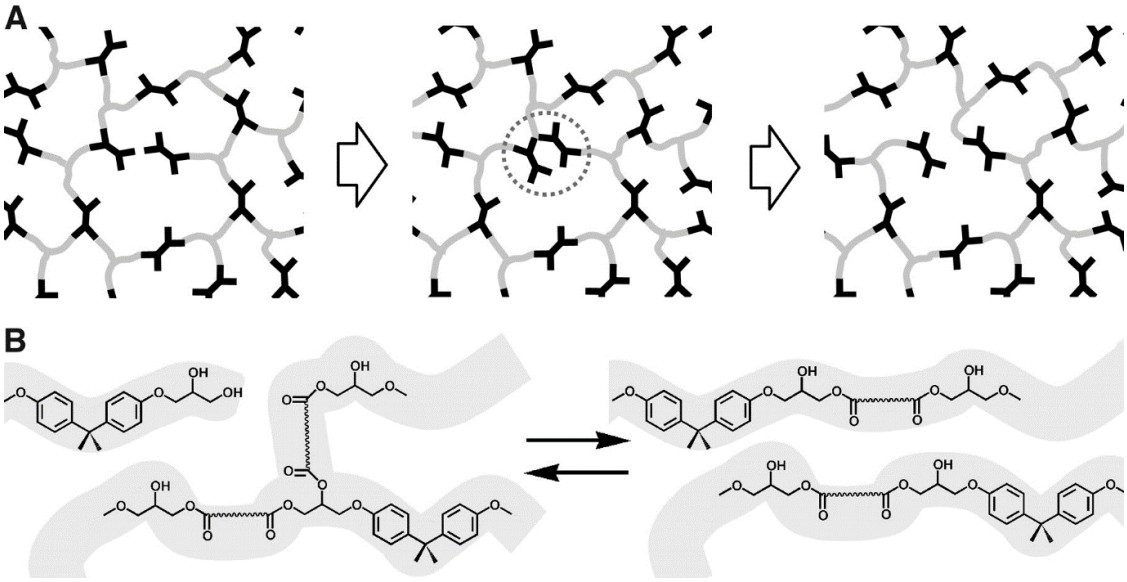

Figure 19: Topological rearrangements via exchange reactions preserving the network integrity. (A) Schematic view of a network with exchange processes that preserve the total-number of links and average functionality of cross-links. The middle image illustrates that the exchange does not require depolymerization in the intermediate step. (B) Exchange process via transesterification in hydroxy-ester networks. From: [116]**.**

2.3.3 Outstanding properties for the production of sustainable and recyclable composites

The greatest advantage of using a vitrimer as a matrix for composites over an epoxy thermoset matrix is surely its ability to be recycled. Two main recycling strategies for vitrimers exist and are well researched in the literature: the physical (mechanical) and chemical recycling of vitrimers.

2.3.3.1 Mechanical recycling

Unlike epoxy thermosets, vitrimers possess the ability of being reprocessable when a rapid rearrangement of the topology of the network ($T \geq Tv$) occurs, which makes a physical (mechanical) recycling of material scraps possible.

Physical recycling methods primarily encompass processes such as hot pressing, injection molding and extrusion molding [123] (Figure 20), where vitrimer powder or broken pieces are recycled into new samples by applying heat and/or pressure. Recycled epoxy vitrimer specimens with mechanical properties similar to the pristine material could be achieved. Zhou et al. [124] demonstrated that their dynamic polyurea/epoxy (DPE)

vitrimer had a similar strength after the recycling process. The repeatability of the recycling process has also been demonstrated in literature. As the polymer chains in vitrimers undergo only exchange and aren't consumed during recycling, it is possible to achieve several recycling cycles [125]. In fact, in the work of Zhou et al. [124], the DPE vitrimer could undergo 6 recycling process without showing any significant loss in the tensile strength.

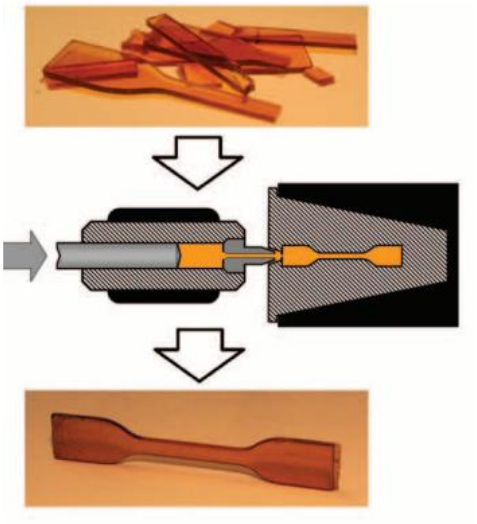

Figure 20: A cross-linked sample broken into pieces is reprocessed in an injection machine to recover its initial aspect and properties. From: [116]**.**

This feature could particularly be interesting for the epoxy and composite industry as processing techniques can result in a lot of unused resin. Mechanically recycling the resin leftovers would help prevent resin waste.

The mechanical recycling of vitrimers has been investigated in depth as a large amount of publications on this topic emerged in the past years. Even if it has been shown that mechanically recycled epoxy vitrimers can exhibit mechanical properties similar to the pristine material [124], many publications studying the recycling of vitrimers reported a significant decrease in mechanical properties after the recycling process, as can be seen from Tab. 4. The possible reasons for this decrease were:

- transesterification occurred only locally and not on all areas [105]
- recycled samples exhibited a lower crosslink density [126]
- unadapted recycling parameters led to thermal degradation [127]
- irreversible destruction of C-C bonds occurred during the recycling process [128]
- oxidation process occurred throughout the recycling process [129]
- destruction of partial permanent bonds during the recycling process [130].

Interestingly, Tab. 4 also reveals significant variations in the parameters (temperature, time, pressure) applied during the recycling process from one publication to another. This suggests a lack of a defined consensus method for the mechanical recycling of

vitrimers and emphasizes the complexity of the recycling process, underscoring the importance of the parameters involved.

Tab. 4: Overview on the mechanical recycling of vitrimers and vitrimers-like materials based on the transesterification reaction. Modulus and strength values of the vitrimers after and before recycling and parameters used for the recycling process.

Resin/curing agent	Modulus (pristine material/recycled material/recycling efficiency)	Strength (pristine material/recycled material/recycling efficiency)	Parameters for the recycling process (T / time / pressure)
ESO / Glycyrrhizic acid [130]	2483 MPa / 2366 MPa / 95 %	3.1 MPa / 1.4 MPa / 45 %	200 °C / 135 min / 200 kg/cm²
ESO / fumaropimaric acid [131]	-	16 MPa / 13 MPa / 81 %	160 °C / 1h / 10 MPa
Palm oil-based methyl methacrylate / citric acid [132]	-	28.9 MPa/ 9.5 MPa/ 33 %	170 °C / 12 min / 10 MPa
ESO / camphoric acid [133]	2.4 MPa / 1.8 MPa / 75 %	0.56 MPa / 0.46 MPa / 82 %	200 °C / - / 10 t
DGEBA / TA [105]	-	98.4 MPa / 35 MPa / 36 %	180 & 210 °C / 2 & 4h / 14 MPa
DGEBA / phtalic anhydride [134]	-	41,2 MPa / 4,7 – 36,3 MPa / 11,4 – 88,1 %	90 – 210 °C / 1 – 10 h / 3 – 12 MPa
DGEBA / tung oil-based tetrafunctional carboxylic acid [135]	2.55 GPa / 2.43 GPa / 95 %	64.62 MPa / 62.81 MPa / 97 %	180 °C / 2 h / 20 MPa

If the mechanical recycling of vitrimers has already been investigated in depth, astonishingly, the mechanical recycling of fiber-reinforced vitrimers has not. De Luzuriaga et al. [136] highlighted the possibility of mechanically recycling vitrimer composites scraps with compression molding as a recycled plate could be manufactured (Figure 21). However, no mechanical testing has been performed to evaluate the performance of the recycled composite. A clear loss of performance is expected through the mechanical

recycling process as the fibers are shortened, leading to a downgrading and a possible use only for non-structural applications. This expected loss of property and downcycling might be the reason for the lack of interest shown in literature for the mechanical recycling of vitrimer composites. However, the idea of fabricating composites from process-leftovers (leftover resin and fibers) or composite waste has not been considered and should be investigated, as transforming remnants into valuable products constitutes a form of upcycling.

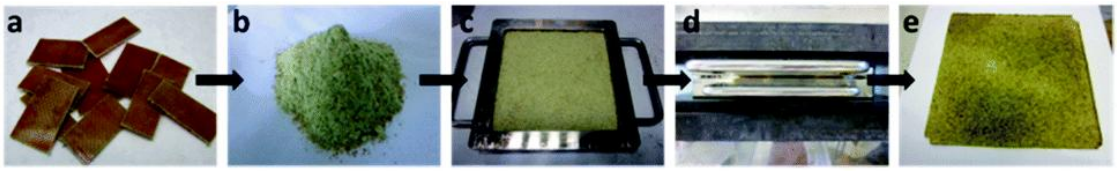

Figure 21: Mechanical recycling of dynamic epoxy composites. FRPC scraps (a) were grinded to fine powder (b), which was then transferred to a square mold (c) and submitted to 200 bars and 210 °C in a hot press (d) to obtain a 2nd generation composite sheet (e). From: [136]**.**

2.3.3.2 Chemical recycling

Given their thermoset nature and permanent crosslinked structure, the decomposition of epoxy requires extreme reaction conditions. As a result, extracting reinforcement fibers from epoxy-based composites at their end-of-life poses significant challenges. As seen in chapter 2.1.2.3, chemical recycling such as solvolysis can be performed for fiber recovery in epoxy composites but this process typically involves strong and environmentally unfriendly chemical solvents, coupled with high temperatures and pressures. This not only poses environmental concerns but also makes the scalability of the process challenging [34,47–49].

Chemical recycling is a process well-described in literature for the recovery of fibers in vitrimer-composites systems. Chemical solvents or monomers are used to break down vitrimers into oligomers [123]. The presence of dynamic covalent bonds in vitrimers, allowing their networks to be broken and reformed using a triggered stimulus, makes the vitrimers suitable for chemical recycling. When exposed to the appropriate chemical agents, the dynamic covalent bonds in vitrimers can be cleaved, allowing the material to be depolymerized [137]. Vitrimers based on the transesterification reaction are especially prone to chemical recycling as the ester bonds can undergo hydrolysis [138].

Very mild conditions were applied in the literature to chemically recycle vitrimers and recover the fibers. Si et al. [139] could recover the carbon fibers of an epoxy-vitrimer composite under an hour by immersing the composite in diluted dithiothreitol (DTT) at 90 °C. Zhou et al. [124] could fully recover the carbon fibers of a polyurea/epoxy vitrimer composite in a 1-dodecanethiol / dimethylformamide (DDT/DMF) solvent after stirring 24 h at room temperature (Figure 22). The fibers were reused and impregnated with the vitrimer to form recycled CFRP. The tensile strength of the recycled CFRP was similar to the pristine CFRP. Liu et al. [140] could dissolve their vitrimer epoxy matrix in a

0.1 mol/L ethylenediamine (EDA) solution (solvent: DMF) after 2 h at 50 °C. Following the ethanol washing and drying process, the recycled fibers were utilized in the production of composites, demonstrating no decline in mechanical properties when compared to the original material. The prospect of breaking down vitrimers under mild conditions (low temperatures and no pressure) to recover CF is of high interest. This approach could facilitate a more straightforward scalability of the solvolysis process, thanks to reduced technical demands compared to standard thermoset solvolysis.

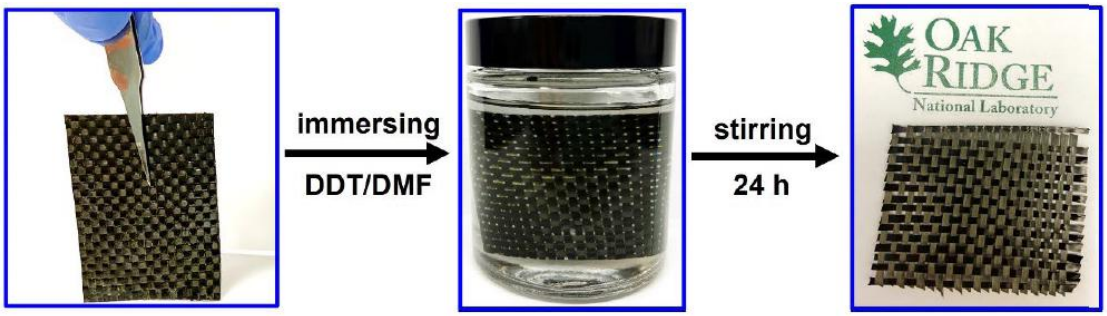

Figure 22: Recovery of the CF from a vitrimer-composite using DDT/DMF as a chemical solvent after stirring 24 h at RT. From: [124]**.**

Moreover, the possibility of reusing the degraded vitrimer matrix after chemical recycling to synthesize a new vitrimer has also been demonstrated in literature [141].

2.3.4 Bio-based epoxy vitrimers

The recycling abilities of vitrimers represent a significant step towards sustainability, as carbon fibers can be recovered at the end-of-life of the vitrimer composite, and resin leftovers can be reused and reprocessed. An additional step towards sustainability would involve using bio-based raw materials to produce the vitrimer resin. Since epoxy resins can be manufactured from natural resources, they are well-suited for the development of bio-based and recyclable vitrimer resins for the composite industry.

Literature reports vitrimer resins based on bio-based aromatic precursors found in lignins, phenolic building blocks, and bio-based aliphatic precursors such as vegetable oils and polysaccharides diacids. Epoxidized vegetable oils as a raw material for the production of vitrimers attracted a lot of attention due to their relatively low price and high availability [113]. Taking inspiration from Leibler's discovery, researchers explored the creation of EVO-based vitrimers through transesterification reactions in the presence of a catalyst. Yang et al. [131] produced a fully bio-based vitrimer using ESO and a rosin derivative-fumaropimaric acid (FPA), employing zinc acetylacetonate as the catalyst. While catalyst-driven reactions typically facilitate bond exchange in vitrimers, some catalysts can impact material properties. Consequently, some researchers opted to synthesize EVO-based vitrimers without an external catalyst. Altuna et al. [142] achieved the synthesis of a vitrimer epoxy resin by utilizing ESO and an aqueous solution of citric acid monohydrate (CA). The integration of dynamic covalent networks into the

epoxidized vegetable oil-based materials impart new functionality like recyclability and reprocessability, however their relatively low mechanical properties remain an issue [73]. As an example, the vitrimer based on ESO produced in the work of Liu et al. [143], showed excellent reprocessability but poor mechanical properties as a maximum Young modulus of 3.46 MPa and a tensile strength of 3.49 MPa were found.

Vanillin showed to be a promising bio-based precursor for the production of high-performance vitrimers as very good mechanical properties are reported in the literature [70]. Wang et al. [144] synthesized a vanillin-modified epoxy vitrimer that showed better mechanical properties than the heavily used high-performance reference DGEBA epoxy thermoset. However, limitations impede the utilization of vanillin as a bio-based raw material to replace fuel resources for the development of vitrimers. Issues include the higher cost and limited scale of production, collection, and storage of vanillin compared to fossil fuel sources, as well as the challenging synthesis pathway for vanillin-based vitrimers [70].

2.4 Carbon fibers

In this chapter, the properties and importance of CF for the composite industry will be presented. Additionally, the standard methods of CF production and alternative feedstocks for CF production will be discussed.

2.4.1 Properties

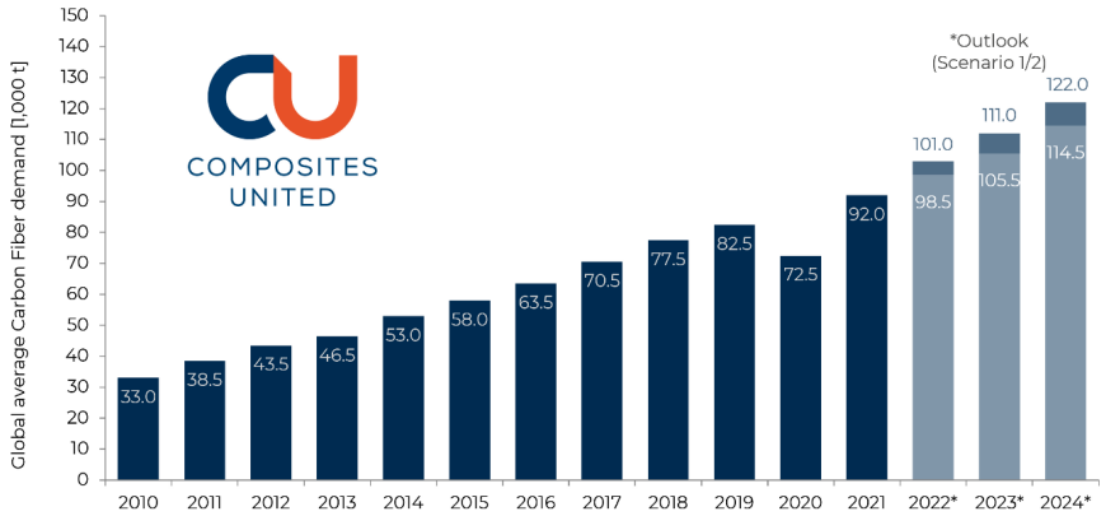

Figure 23: Development of the global average CF demand from 2010 to 2024 (*estimations; 03/2022). From: [145].

Carbon fiber is a type of fiber that must contain a minimum of 92 wt. % carbon, with fibers consisting of at least 99 wt. % carbon commonly referred to as graphite fibers. These fibers offer numerous advantages, including high tensile strength, elevated stiffness, a low weight-to-strength ratio, tolerance to high temperatures, low thermal

expansion, and resistance to chemicals. The mechanical properties of carbon fibers are heavily influenced by the treatment and manufacturing processes involving organic precursors and specific conditions. Tab. 5 presents the tensile modulus and tensile strength of different classes of carbon fibers. Typically ranging from 5 to 10 µm in diameter, carbon fibers find widespread application in various forms such as woven textiles, prepregs, continuous fibers/rovings, and chopped fibers within composites. Compared to glass, aramid and natural fibers, carbon fibers offer superior strength and modulus, making it a prime reinforcement fiber for the production of high-performance composites (Tab. 6) [146,147].

Tab. 5: Types of carbon fibers by mechanical properties.

Classification	Tensile Modulus (GPa)	Tensile Strength (MPa)
Ultra-high elastic modulus (UHM)	≥ 600 [148]	≥ 2500 [148]
High elastic modulus (HM)	350 - 600 [148]	≥ 2500 [148]
Intermediate elastic modulus (IM)	280 - 350 [148]	≥ 3500 [148]
Standard elastic Modulus (HT)	200 - 280 [148]	≥ 2500 [148]
Low elastic Modulus (LM)	≤ 200 [148]	≤ 3500 [148]

Due to their outstanding properties, over the past few years, the carbon fiber industry has experienced a consistent expansion (Figure 23) to fulfill the increasing demand from various sectors, including aerospace, turbine blades, construction, pressure vessels, automotive, sporting goods, and more [146,147].

Tab. 6: Tensile strength and tensile modulus of various fibers.

Fiber art	Tensile Modulus (GPa)	Tensile Strength (Mpa)
Flax	27,6 [149]	345-1035 [149]
Hemp	70 [149]	690 [149]
E-Glass	70 [149]	2000-3500 [149]
Aramid	63 - 67[149]	3000 -3150[149]
IM Carbon	280 - 350 [148]	≥ 3500 [148]
UHM Carbon	≥ 600 [148]	≥ 2500 [148]

2.4.2 Production

Historically, carbon fibers were manufactured using rayon as the precursor material. However, nowadays, commercially available carbon fibers are mainly manufactured using polyacrylonitrile (PAN), with petroleum pitch-based fibers constituting only a minor portion [66]. PAN is a synthetic, semicrystalline organic polymer resin derived from petroleum. It stands as the predominant choice for carbon fiber production due to its capacity to yield carbon fibers characterized by high strength and a high elastic modulus. Nevertheless, the primary drawback associated with PAN-based carbon fibers is the elevated processing cost. Initially, carbon fibers derived from PAN undergo a stretching process ranging from 500 % to 1300 %. Subsequently, they are subjected to thermostabilizing in an oxygen atmosphere, conducted under tension within the temperature range of 200 to 300 °C. Following this, the fibers undergo carbonization through heat treatment under an inert atmosphere, with temperatures ranging from 1000 to 1700 °C. Subsequently, the process involves graphitization (optional step), achieved through heat treatment within the temperature range of 2500 to 3000 °C. Parameters during the carbonization and graphitization process such as temperatures and heating rates strongly influence the mechanical properties of the CF. Finally, after undergoing surface treatment and epoxy sizing, the carbon fibers are prepared for use [146,147,150,151]. The CF production steps using PAN precursor are depicted in Figure 24.

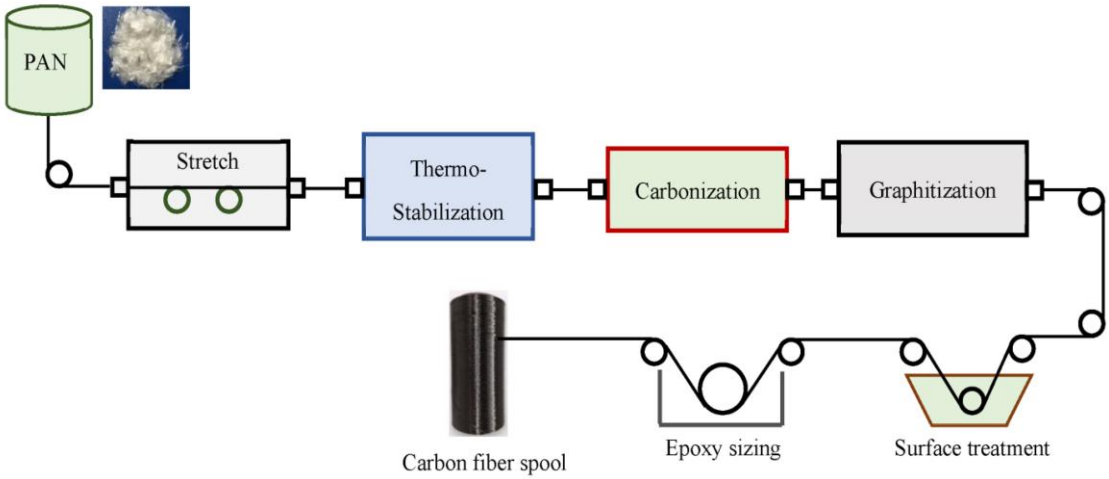

Figure 24: Carbon fiber production using PAN precursor. From: [147].

Petroleum pitch is a viscoelastic polymer. The production of pitch-based carbon fibers employs identical processes to those used in PAN-based fiber production, but without the need of the expensive stretching process. Pitch-based carbon fibers exhibit a lower tensile strength and a higher elastic modulus compared to PAN-based carbon fibers (Tab. 7) but demonstrate enhanced thermal and electrical properties in comparison to PAN-based carbon fibers. Rayon-based carbon fibers have limited applications in the commercial market due to their inferior performance and productivity [147,152].

2.4.3 Alternative feedstocks for carbon fibers production

More than 90% of the carbon fibers commercially accessible on the market are derived from PAN. Additionally, the Sohio Acrylonitrile Process, responsible for converting fossil-based propene into acrylonitrile (ACN) through catalytic ammoxidation, supplies 90 % of the globally used ACN [66]. To make the production of CF more sustainable, efforts are being made to identify alternative methods for producing ACN. In the past, carbon fibers were manufactured using rayon, derived from natural cellulose-based materials like wood pulp and cotton linters. Another potential biopolymer for carbon fiber production is lignin, the second-most abundant natural polymer and a plentiful waste material in the paper industry. Nevertheless, both rayon and lignin-based carbon fibers exhibit inferior mechanical properties when compared to PAN-based carbon fibers, as illustrated in Tab. 7 [147,153].

Tab. 7: Tensile Modulus and Tensile Strength of different Carbon fibers.

Carbon Fiber	Tensile Modulus (GPa)	Tensile Strength (MPa)
PAN-based CF	200 – 500 [147]	3500 – 6300 [147]
Pitch-based CF	150 – 900 [147]	1300 – 3100 [147]
Lignin-based CF	40 [147]	388 – 1060 [147]
Rayon-based CF	40 – 100 [147]	500 – 1200 [147]

Therefore, ongoing research is focused on bio-based molecules capable of being converted into acrylonitrile (ACN), with glycerol emerging as a promising candidate for ACN production. This glycerol-derived ACN can then undergo polymerization and spinning processes to yield polyacrylonitrile (PAN). Originally obtained primarily from petroleum through synthetic methods, glycerol is now readily accessible from plants as a byproduct of various industrial processes, including biodiesel production. Despite the abundant availability of resources, investigations into glycerol-to-ACN pathways have been limited, and studies suggest that the current economic viability of ACN production from glycerol is unfavorable. An alternative approach to ACN production involves the utilization of lignocellulosic sugars which are biomass-derived sugars derived from the cellulose and hemicellulose fractions of biomass. Laboratory studies have shown that this method has the potential to serve as a direct substitute for traditional ACN production, offering mechanical properties comparable to the conventional process. With the exception of carbon fiber production from rayon, most of the technologies mentioned previously are currently at relatively early stages of technology readiness, having been demonstrated only at the laboratory bench or pilot scale [153].

Econitrile from the company AnQore is an already commercially available sustainable ACN. Indeed, Econitrile supports the production of both bio-methane to bio-ammonia and of bio- and circular-naphtha into sustainable propene and helps CF manufactures to enhance the sustainability of their product [154]. Figure 25 summarizes the alternative sustainable route described above to produce CF.

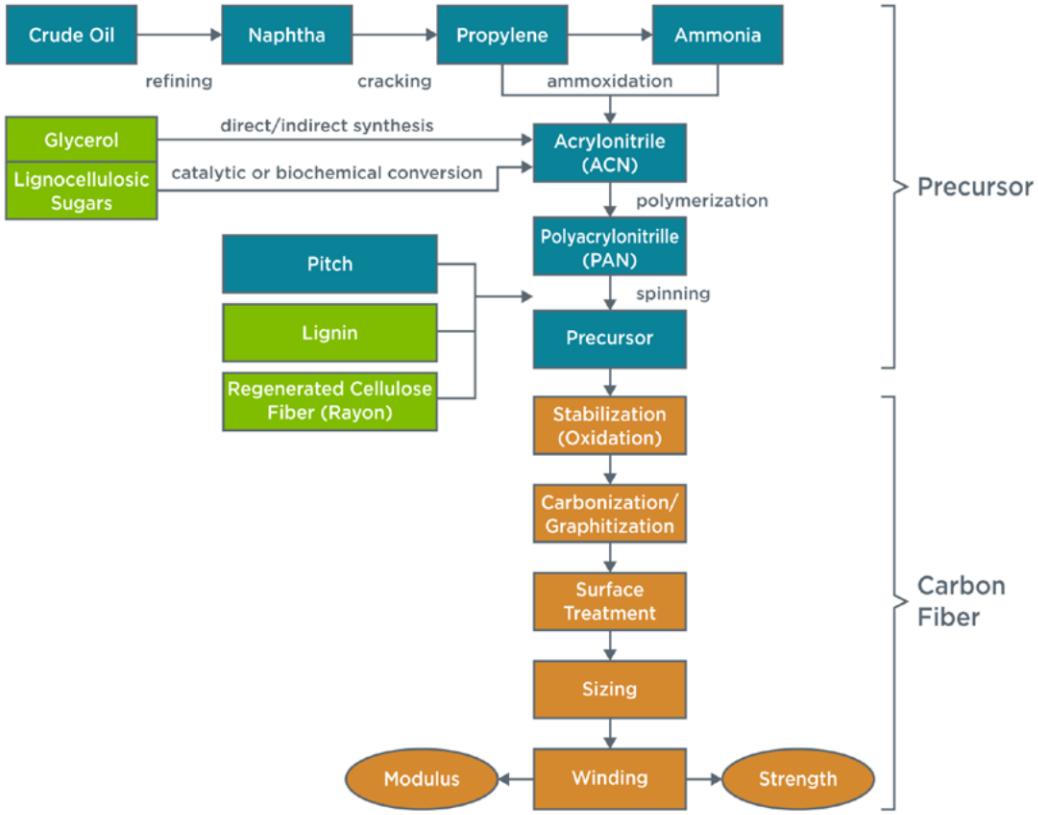

Figure 25: Carbon fiber manufacturing process from various precursors. From: [153].

An important parameter to assess the sustainability of an alternative route is to measure the global warming potential (GWP) in kg of CO_2 per kg of CF produced. Figure 26 from the Fraunhofer IGCV compares the global warming potential of the classic production of CF with the alternative routes, considering the state-of-the-art technology (SotA) and the best-case scenario (electricity from hydropower, thermal energy/steam from biogas and the use of Power-to-Chemical technologies). The classic PAN production from crude-oil via ACN, stabilization and carbonization is an energy-intensive process, which exhibits a GWP of 25 kg CO_2/kg CF. Using renewable energy sources and energy-efficient technologies in stabilization and carbonization can lead to significant reduction as a GWP of 8 kg CO_2/kg CF can be reached. Interestingly, using bio-glycerol for producing ACN doesn't lead to a significant reduction compared to the classic fossil route. A striking reduction is only observed when using renewable energy. With the use of the commercially available Econitrile made from bio-naphtha to produce CF, a GWP reduction of 22 % compared to the classic route is possible. By using renewable energies and energy-efficient technologies, an approximative GWP of 2.3 kg CO_2/kg CF can be

reached. The use of lignocellulosic sugars to produce CF leads to a significant potential savings of 25 % to approximately 19 kg CO_2/kg CF.

The global warming potentials for producing CF, even with alternative routes are still massive. Considerable reductions can be achieved through the adoption of renewable energies and energy-efficient technologies. However, realizing these benefits would likely necessitate substantial investments in the scale-up evaluation and testing of these technologies to transition them from their current state to a commercial facility. Considering the high cost of CF and the high global warming potential associated with its production, there is an increasing imperative to prioritize the recycling and reuse of CF. This highlights the importance of matrix materials that facilitate the straightforward recovery of CF once a CF-reinforced composite reaches the end of its lifecycle.

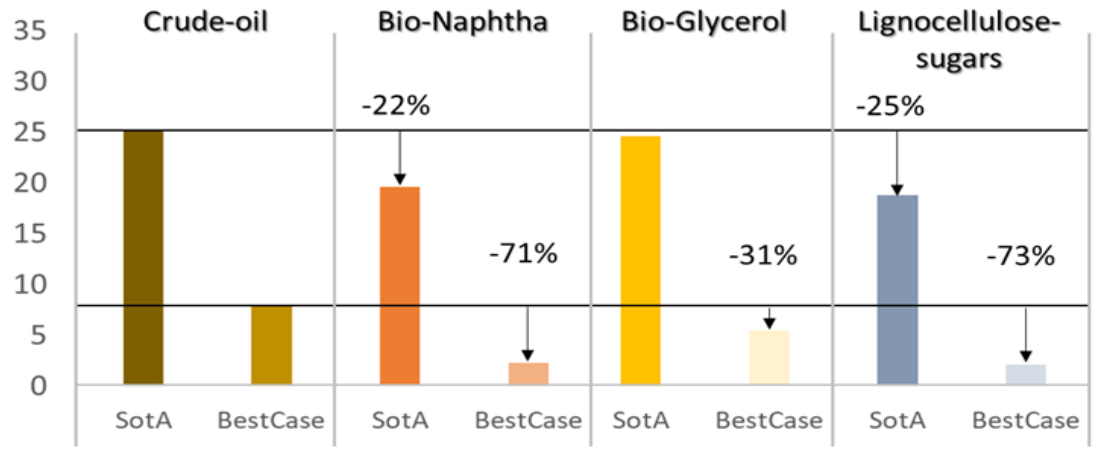

Figure 26: Global warming potential of carbon fiber production kg CO_2e per kg CF (production site EU-28). Adapted from: [6].

2.5 Conclusion of the state of the art

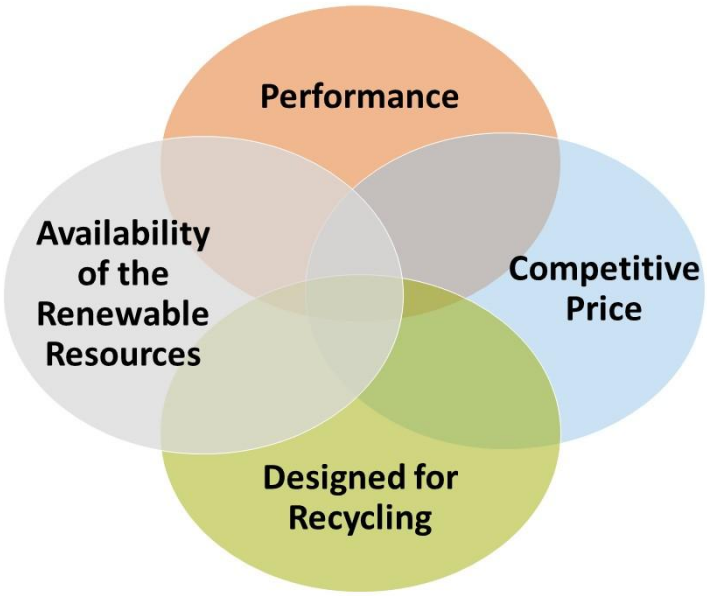

Figure 27: Characteristics of the ideal bio-based and sustainable epoxy for composites applications.

Epoxy thermosets, particularly DGEBA-based epoxies, stand out as excellent matrix materials for composites and are suited for high-performance applications, especially when reinforced with CF. However, challenges such as the depletion of fossil resources, concerns over the use of BPA and ECH in DGEBA production, the significant global warming potential of epoxies and CF, and the complexities associated with recycling composites at the end of their life create an urgent need for a sustainable and bio-based epoxy system designed for recyclability.

Addressing these challenges in the realm of bio-based epoxies is complex. To be a viable alternative to DGEBA-based epoxies, the bio-based epoxy must compete effectively in terms of thermal and mechanical properties. Additionally, the resources used in its development must be environmentally and human-friendly, abundantly available to meet market demand, and priced competitively in comparison to established commercial systems. The recyclability of the epoxy system is also a crucial consideration for fostering a circular economy. This would enable the reuse of carbon fibers as well as waste and process leftovers, thereby promoting a circular economy. Figure 27 illustrates the four essential characteristics that a sustainable and bio-based epoxy must possess to be an ideal replacement for conventional systems.

3 Material and methods

Section 3.1 describes the materials used in this work. Section 3.2 explains the synthesis of the thermosets and the production of thermoset samples, composite samples, and recycled samples. Section 3.3 outlines the various tests performed on the materials, along with the parameters used.

3.1 Materials

The curing agent TA with a molecular weight of 1701.20 $g.mol^{-1}$ was purchased from Sigma–Aldrich (Taufkirchen, Germany), along with formic acid and hydrogen peroxide (35%). The bio-based air release additive Epinal EL 12.42 was bought from bto epoxy GmbH (Amstetten, Austria). In chapter 4, linseed oil was purchased from a local commercial source and used for the synthesis of epoxidized linseed oil without further purification. The oil was cold-pressed, unprocessed, and of food-grade quality. The acid number was determined by the procedure of ISO 660.2009 to be 0.93 mg KOH per gram and the iodine value 186 $g(I_2)$ per 100 g (ISO 3961.2018). In Chapter 5, epoxidized linseed oil with an EEW of 182 was directly purchased from the company Bio-Composites and More GmbH (Germany).

LOCTITE® FREKOTE 700-NC from Henkel was used as a release agent.

Following chemicals were purchased from Sigma–Aldrich unless otherwise noted and were used as received: Sorbic acid (⩾ 99.0 %), allyl alcohol (⩾ 98.5 %), maleic anhydride (⩾ 99.0 %), sulfuric acid (ACS reagent, 95.0–98.0 %), toluene (ACS reagent, ⩾ 99.5 %), diethyl ether (⩾ 99.9 %, suitable for HPLC, inhibitor free) 3-chloroperbenzoic acid (*m*CPBA, ⩾ 77 %), oxone (>4.0 % active oxygen basis), methylene chloride (suitable for HPLC, ⩾ 99.8 %, contains 40–150 ppm amylene as stabilizer), potassium carbonate (Grüssing, K_2CO_3, ⩾ 99.5 %), sodium sulfate (Grüssing, Na_2SO_4, 99 %, anhydrous), sodium bicarbonate (Grüssing, $NaHCO_3$, ⩾ 99.5 %), sodium hydroxide (Fischer scientific, NaOH, ⩾ 98.0 % Baker analyzed), bisphenol A-diglycidyl-ether (DGEBA) with an epoxide equivalent weight 172-176, Jeffamine T403 (Huntsman Holland B.V.), isophoron diamine (mixed isomers, ⩾ 99 %).

Following UD carbon fibers fabrics were used to produce composites plates: SIGRAFIL® Tow C T50-4.4/255-E100 (referred as SGL Tow) from SGL Carbon, UD Twill 3/1 UTS 50 (referred as UD Twill 3/1) from Teijin, SIGRATEX® C U170-0/ST-E214/10g (referred as UD SGL) from SGL Carbon and T700/50C 24k Tows from Toray. SikaBiresin® CR80 (with the curing agent CH80-10) from SIKA was used as a reference resin.

Milled CF (CF powder) with an average fiber length of 0.2 mm were purchased from R&G Faserverbundwerkstoffe (Germany) and used as short fibers reinforcement for the recycled composites samples in chapter 5.2.1.1. Hand-cut fibers SIGRAFIL® Tow C T50-4.4/255-E100 with an approximate length of 5 mm were used as long fibers reinforcements for the recycled composites samples in chapter 5.2.1.2.

3.2 Experimental procedures

3.2.1 Synthesis of epoxidized linseed oil

The synthesis of epoxidized linseed oil was performed by Jonas Martin Breitsameter and is described in [3]. The epoxidation of linseed oil was carried out by the in-situ generation of performic acid from formic acid and hydrogen peroxide. A ratio of linseed oil to formic acid to hydrogen peroxide of 1.0:1.0:10 was used. As a reaction vessel, a double-wall 2 L glass reactor connected to a thermostat for cooling or heating, respectively was used. The linseed oil (422 g, 0.479 mol) was loaded into the reactor. Hydrogen peroxide (411.8 mL, 4.79 mol, 35 %) was added, and the mixture was stirred with a glass overhead stirrer (400 rpm), and the reactor was cooled to 10 °C. Then, 18.60 mL of formic acid (22.04 g, 0.479 mol) was added dropwise throughout 30 min. The temperature was raised to 50 °C and stirred for 48 h. The epoxidation progress can be followed by ^{1}H-NMR spectroscopy (Fig.A- 3). The reaction mixture was neutralized by addition of a saturated sodium bicarbonate solution (200 mL) after cooling to room temperature and diluted with diethyl ether (200 mL). After washing with a saturated sodium chloride solution, the solvent was removed in vacuo. The EEW was estimated to be 140.6 g mol^{-1} resulting from the molecular weight of linseed oil (878 g mol^{-1}) and approximately 6.2 double bonds per triglyceride determined by ^{1}H-NMR analysis (Fig.A- 4).

3.2.2 Milling of tannic acid

TA was milled with aluminum oxide (Al_2O_3) balls in a two-step milling process. First, TA was dried in a vacuum oven at 105 °C for 2 h. One hundred grams of dried TA, together with 40 Al_2O_3 balls with a diameter of 10 mm and 40 Al_2O_3 balls with a diameter of 5 mm, were placed inside an aluminum container of 1000 mL. The container was placed inside a speed mixer DAC-3000 HP (Hauschild GmbH & Co. KG, Germany), and a pre-milling was performed at a rotation speed of 650 rpm for 3 min. Four grinding cycles were applied. TA was cooled down to room temperature for 15 min between every grinding cycle. The gained powder was then dried again at 105 °C under vacuum for 2 h to remove the released water, cooled down to room temperature, and four more grinding cycles were applied. As a second step, the pre-milled TA powder, together with the Al_2O_3 balls, was put inside a 3D shaker mixer by Willy A. Bachofen AG (Switzerland). Milling at a speed of 50 rpm was then performed for 16 h. At last, the fine TA powder was separated from the grinding balls by a coarse meshed stainless-steel sieve

and dried under vacuum at 105 °C for 4 h. The size of the TA particles after milling is shown in Figure 28.

Particle size before milling: D50 = 50.2 µm; after milling: D50 = 6.6 µm.

A less time-consuming milling process offering the same TA particles quality can be performed with a planetary ball mill machine (Pulverisette 6, Fritsch), which is particularly convenient for producing TA/ELO composites as more TA powder is needed. The grinding bowl is filled with 50 balls with a diameter of 10 mm. 50g of dried TA was ground per cycle. TA is ground in 3 passes of 3 min each at 500 rpm. After each pass, the grinding bowl was opened and TA powder had to be detached from the grinding bowl. From here, the ground TA was filtered using a sieve machine Haver & Boecker TS EML 200. The sieves with mesh sizes of 5.6 mm, 180 µm, and 90 µm were stacked in descending order. The sieved material was collected without further processing. The overflow from the sieve was ground again for 5 min at 500 rpm and sieved again. Finally, the obtained TA powder is dried under vacuum at 105 °C for 4 h.

3.2.3 TA/ELO epoxy sample preparation

TA/ELO epoxy samples with a molar ratio -OH/epoxide of 0.85, 1.0, 1.15, 1.25, 1.5, 1.75, and 2.0 were prepared to examine how the molar ratio affects the thermal and mechanical properties of the resulting thermoset. The samples were prepared as follows: 50 g of ELO and the corresponding amount of the finely milled and dried TA powder and 0.5 wt.% of the air release additive (Epinal EL 12.42 bto epoxy GmbH) were placed in a 500 mL aluminum container. The mixing ratios are given in Tab. 8. Epinal EL 12.42 is a surface active polyether siloxane with a certified biobased-carbon content that facilitates the removal of air inclusion and does not participate in the curing reaction. The container was placed inside a speed mixer DAC-3000 HP (Hauschild GmbH & Co. KG, Germany) and sealed with a vacuum. Mixing of the components was performed at a rotation speed of 600 rpm for 10 min. The mixture was then poured into the cavities of an aluminum mold. The cavities had the dimensions 60 × 6 × 2 mm (for DMA, the samples are then cut lengthwise in two to have the dimensions 30 x 6 x 2 mm) and 80 × 10 × 4 mm (for flexural testing). Teflon tape was applied inside the cavities to ensure easy removal of the samples after curing. The mold was placed in a vacuum oven to remove air inclusions with a temperature of 80 °C and a pressure of 1 mbar for 2 h. Finally, the mold was placed in a standard oven for curing. The TA/ELO samples listed in Tab. 8 were prepared once with the curing condition C1: 16 h at 90 °C + 3 h at 140 °C and once with the curing condition C2: 16 h at 120 °C + 3 h at 140 °C. After curing, the edges of the samples were wet-polished with sandpaper (grit size 500) for a smooth finish.

3.2.4 Preparation of mechanically recycled TA/ELO thermoset samples and mechanically recycled TA/ELO composite samples

Preparation of TA/ELO recyclate

TA/ELO 1.5 and 2.0 samples cured with C2 were first cut into small pieces using a lever shear. Subsequently, the pieces are pulverized in the planetary ball mill (Pulverisette 6, Fritsch). Each time, 75 g of TA/ELO and four Al_2O_3 balls with a diameter of 2 cm are placed into the milling vessel and ground at 500 rpm for 5 minutes to initially coarse grind the material. In the next step, 50 g of the already coarsely ground material, along with two Al_2O_3 balls (diameter of 2 cm) and 48 small Al_2O_3 balls (diameter 1 cm), are placed into the milling vessel each time and ground at 500 rpm for 5 min. This procedure is repeated until every TA/ELO particle can be sieved through a sieve with a mesh size of 355 µm.

Preparation of recycled TA/ELO samples

The obtained recycle powder was hot-pressed with a stamp-die system made of aluminum constructed by Florian Gehringer in [S15] (Fig.A- 5) with cavities with the dimensions 80 x 10 x 10 mm in a Polystat 200 T press (Servitec). An even amount of TA/ELO 1.5 or TA/ELO 2.0 powder (4.2 g) was placed inside each cavity to ensure that every sample is compacted the same way. With an increasing hot-pressing temperature, the pressure had to be reduced as otherwise, only damaged samples could be obtained. Following hot-pressing parameters combinations (temperature/pressure on each sample/time) were applied to manufacture homogeneous recycled TA/ELO samples:

- 130 °C/10.4 MPa/1 h
- 145 °C/5.2 MPa/1 h
- 160 °C/pressure during closing/1h
- 115 °C/10.4 MPa/2 h
- 130 °C/10.4 MPa/2 h
- 145 °C/5.2 MPa/2 h
- 160 °C/pressure during closing/2 h

When hot-pressed at 160 °C, only the hydraulic pressure during the closing of the hot press was applied. After 1 or 2 h, the pressure is released, the hot-press is opened, and the stamp-die system is immediately removed and the specimens are removed from underneath using tweezers. The specimens are placed between two metal sheets with a mass to prevent deformation during cooling. After hot-pressing, the samples had an approximate thickness of 4 mm. If needed, the edges were sanded with a sandpaper (grit 400) for a smooth finish.

Preparation of recycled TA/ELO composites samples

For the preparation of recycled TA/ELO composites, TA/ELO recyclate powder (TA/ELO 1.5 or TA/ELO 2.0) was mixed either with 5 or 10 wt. % of milled CF (average fiber length of 0.2 mm) or with 10 wt. % hand-cut CF with an average length of 5 mm from the roving C T50-4.4/255 (SGL Carbon) in a metal can and mixed in a speedmixer for 2 min at 1000 rpm. Since the short fibers are heavily clumped together, they are pressed through a kitchen sieve with the help of a spoon during addition to loosen the clumps. The mixtures were hot-pressed with the stamp-die system in a Polystat 200 T press (Servitec) with following parameters (temperature/pressure on each sample/time):

- 130 °C/10.4 MPa/2 h
- 160 °C/pressure during closing/2 h

3.2.5 Preparation of TA/ELO composites

Various UD CF fabrics (SIGRATEX® C U170-0/ST-E214/10g, UD Twill 3/1 UTS 50, T700/50C 24k) were analyzed to determine whether the nature of the UD fiber fabric significantly influences the mechanical properties of UD TA/ELO composites. Towpreg and manually laminated CF fabrics were used to assess the impact of an automated fiber pre-impregnation process on TA/ELO composite performance. Finally, different composite manufacturing processes were investigated to evaluate the suitability of TA/ELO as a resin for different composite processes.

3.2.5.1 Preparation of TA/ELO towpreg

Towpregs with T700/50C 24k CF tows from Toray and the mixture TA/ELO 1.5 were manufactured using the TLM 2.4 Towpreg machine from Roth Composite Machinery GmbH. Following process parameters were used:

- Speed: 20 m/min
- Tension: 30 N
- Spread unit temperature (before impregnation): 100 °C
- Impregnation temperature: 30 °C
- Impregnation gap: 1 mm
- Fulling rollers temperature: 60 °C
- Calender temperature: 60 °C
- Calender gap: 0.37 mm
- Cooled rollers temperature: 10 °C

Approximately 500 g of the mixture TA/ELO 1.5 was used for towpreg production.

3.2.5.2 Hand-lamination

The resins TA/ELO 1.5, TA/ELO 1.75, and CR80 (mixed with the curing agent CH80-10) were prepared and degassed for an hour with a vacuum of 2 mbar. CF fabrics were laminated on both sides with the various resins using a sponge roller and then stacked together. Lamination with TA/ELO 2.0 was found to be extremely complicated as TA had the tendency to agglomerate on the sponge roller and on the fibers (Fig.A- 6). Therefore, the focus was placed on the mixtures 1.5 and 1.75. CR80 was used as a reference. The amount of CF layers used to manufacture the bio-based and reference composites plates can be seen in Tab. A- 1.

3.2.5.3 Hot-pressing

In the hot-pressing process, composites plates were manufactured with UD Twill 3/1 UTS 50 (referred as UD Twill 3/1) from Teijin (Fig.A- 7). The CF fabrics were cut into squares of approximately 20 x 20 cm and manually laminated with TA/ELO 1.5, TA/ELO 1.75 or CR80 (for reference) following the procedure described above. Fig.A- 8 shows an example of CF layers hand-laminated prior to hot-pressing. Various layers of CF fabric were stacked together in order to obtain composite plates with various fiber volume fractions and placed on an aluminum sheet of dimensions 25 x 25 cm with a thickness of 0.5 cm covered with Teflon tape. An aluminum spacer with a thickness of 2 mm was placed on the edges and an aluminum sheet 25 cm x 25 cm x 0.5 cm covered with Teflon tape was placed on top. After pre-heating the press at 140 °C the aluminum sheets were placed in the press (Polystat 200 T, Servitec). and a hydraulic pressure of 100 bar was applied for 90 min. The plates were then cured for 12 h without pressure at 120 °C.

The hot-pressing temperature was chosen based on preliminary investigations. Two different hot-pressing temperatures were investigated. Plates hot-pressed at 120 °C exhibited a tendency to become sticky on the surface. This can be attributed to a high concentration of ELO and low TA content on the surface, resulting in a poorly reacted material with an oily texture (Fig.A- 9). Due to the pressure applied and the decrease of ELO's viscosity at 120 °C, the fibers must have acted as barrier filtering ELO from TA and a lot of ELO seem to escape the plate and inherently lead to fibers poorly coated with ELO. When hot-pressing at 140 °C, this phenomenon decreased as the formulation is more reactive and TA/ELO sets more rapidly and has less time to escape the plate. TA/ELO is known to be extremely brittle when cured at 140 °C according to chapter 4.4.1. Therefore, samples were only hot-pressed at 140 °C for 90 min and cured afterwards at 120 °C.

Reference composite plates were manufactured with the resin CR80 from SIKA. The reference plates were hot-pressed at 80 °C for 60 min with 100 bar and post-cured without pressure for 3 additional hours at 80 °C. Another reference plate with CR80 was manufactured with the CF fibers Sigrafil Tow C T50-4.4/255-E100 (referred as SGL

Tow) from SGL Carbon. The fibers tows (width approximately 15 mm) were manually cut, laminated with CR80, placed next to each other and hot-pressed 2 h at 80 °C with 100 bar and post-cured without pressure at 80 °C for 2 h.

The amount of CF layers used to manufacture the bio-based and reference composites plates can be seen in Tab. A- 1.

3.2.5.4 Vacuum bagging

The CF fabric SIGRATEX® C U170-0/ST/1511/01G (referred as UD SGL, Fig.A- 10) and towpregs (manufactured as described in chapter 3.2.5.1) were used for producing composite plates via vacuum bagging. TA/ELO 1.5 and 1.75 were used as resins. Towpregs or hand-laminated UD SGL fabrics (following the procedure described in chapter 3.2.5.2) were stacked together and placed on a glass plate coated with release agent. A perforated release film was placed on top of the CF layers along with a breathing fabric to soak up excess resin. The entire setup was sealed with vacuum foil and tacky tape. An outlet was placed inside the setup and connected to a vacuum pump. A vacuum of 400 or 600 mbar respectively was applied, and curing was performed at 90 °C for 1 hour followed by 16 hours at 120 °C. After removing the composite plates, a post-curing at 140 °C for 2 hours was performed.

The amount of CF layers used to manufacture the bio-based composites plates can be seen in Tab. A- 1.

3.2.5.5 Vacuum Assisted Resin Infusion (VARI)

Various layers (1 to 5) of UD SGL fabrics or UD Twill 3/1 were stacked on top of each other on a glass plate coated with a release agent. A peel ply and a flow promoter were placed on top of the fabrics. The entire setup was sealed with tacky tape and a vacuum foil. Inlet and outlet were positioned on opposite sides. The inlet was connected to the resin, and the outlet was connected to the vacuum pump. A vacuum of 2 mbar was applied for resin infusion. The resins TA/ELO 1.0, 1.25, 1.5 and 1.75 were investigated. The resin was pre-heated to 80 °C to reduce its viscosity. However, full impregnation could not be achieved with VARI as TA particles agglomerated in the fabrics close to the inlet and saturated the infusion process. No composite plates could be manufactured with VARI.

3.2.5.6 Resin Transfer Molding (RTM)

An RTM mold was designed using a 1 cm aluminum block with a 2 mm cavity for fiber placement, two grooves and an inlet. Release agent was applied on the aluminum block and various layers (2 to 7) of UD SGL fabrics or UD Twill 3/1 were stacked on top of each other. Two Silicone rings were placed in the grooves. Another aluminum block, 1 cm thick with an outlet, was placed on top and screwed to seal it. The inlet was connected to the resin, which was placed in a pressure pot, and the outlet was connected to a

vacuum pump. The resins TA/ELO 1.0, 1.25, 1.5, and 1.75 were preheated to 80 °C to reduce their viscosity. Vacuum was initially applied to remove air from the cavity. Then, the resin was injected with a pressure of 3 bar. After injection, the RTM form was heated to 120 °C for curing. The fibers acted as a filter, with the first fiber layer being rich in TA and the subsequent layers rich in ELO. No composite plates could be manufactured with the RTM process.

This finding supports the observations made by Todorovic et al. [155], as they also found that no composites could be manufactured using VARI or RTM with a citric acid (CA)/ELO resin, where CA, is also a solid curing agent like TA.

3.2.6 Synthesis of EGCHC epoxy monomer

The synthesis of the epoxy monomer 1,2-epoxy-6-methyl-triglycidyl-3,4,5-cyclohexanetricarboxylate EGCHC was performed by Jonas Martin Breitsameter and this chapter is described in [53].

3.2.6.1 Allyl Sorbate

Sorbic acid (50 g, 445.9 mmol) was dissolved in allyl alcohol (200 mL). After the addition of a catalytic amount of H_2SO_4 (0.5 vol.%, 1.0 mL) the mixture was stirred under reflux for 24 h. After the reaction had cooled to room temperature it was neutralized by the addition of saturated sodium bicarbonate solution and the product was extracted with diethyl ether (3 × 200 mL). The combined organic layers were washed with saturated sodium chloride (200 mL) and dried with anhydrous sodium sulfate. After filtration, the solvent was removed in vacuo and the crude product was purified by distillation (82 °C, 8 mbar). The product allyl sorbate was obtained in the form of a colorless liquid (55.6 g, 82 %).

^{1}H-NMR (400 MHz, chloroform-d): δ [ppm] = 7.27 (m, H4), 6.17 (m, H3), 5.95 (m, H8), 5.80 (d, J = 15.4 Hz, H2), 5.27 (m, H5/H9), 4.65 (m, H7), 1.86 (d, J = 5.7 Hz, H1).

^{13}C-NMR (100 MHz, chloroform-d) : δ [ppm] = 167.00 (C6), 145.46 (C4), 139.65 (C2), 132.54 (C8), 129.88 (C3), 118.37 (C5), 118.07 (C9), 64.99 (C7), 18.75 (C1).

3.2.6.2 Allyl-7-methyl-1,3-dioxo-1,3,3a,4,7,7a-hexahydroisobenzofuran-4-carboxylate (AHIBC)

Maleic anhydride (26.3 g, 268.08 mmol, 1.02 eq.) was dissolved in toluene (26 mL, 10 M solution) and heated to reflux. Allyl sorbate (40 g, 262.82 mmol, 1.0 eq.) was added under vigorous stirring. Since the reaction was strongly exothermal, heating of the mixture was interrupted for several minutes when exceeding 140 °C in the vessel. Reaction progress was monitored by 1H-NMR and stopped after full conversion which was reached within 2.5 h. The crude product crystallizes by cooling down the reaction mixture to 0 °C and the solid was washed with cold methanol. After drying in vacuo, the

product allyl 7-methyl-1,3-dioxo-1,3,3a,4,7,7a-hexahydroisobenzofuran-4-carboxylate (AHIBC) was obtained as a white, crystalline solid (56.4 g, 84 %).

^{1}H-NMR (400 MHz, chloroform-d): δ [ppm] = 6.47 (1H, dt, *J* = 9.49, 3.32 Hz, H3), 5.98 (1H, m, *J* = 16.61, 10.38, 5.98 Hz, H12), 5.86 (1H, dt, *J* = 9.40, 3.24 Hz, H2), 5.4 – 5.2 (2H, m, H13), 4.76 (2H, dt, *J* = 6.09, 1.32 Hz, H11), 4.02 (1H, dd, *J* = 9.78, 5.55 Hz, H5), 3.39 (1H, dd, *J* = 9.79, 7.82 Hz, H6), 3.19 (1H, m, H4), 2.47 (1H, m, H1), 1.43 (3H, d, *J* = 7.34 Hz, H9).

^{13}C-NMR (100 MHz, chloroform-d) : δ [ppm] = 171.3 (C7), 170.3 (C8), 169.2 (C10), 134.8 (C2), 131.7 (C12), 127.0 (C3), 119.1 (C13), 66.4 (C11), 44.6 and 44.5 (C5 and C6), 40.1 (C4), 30.8 (C3), 16.4 (C9).

ATR-IR ν̃max 2975, 2938, 2881, 1846, 1768, 1716, 1648, 1455, 1426, 1391, 1363, 1329, 1302, 1260, 1227, 1196, 1141, 1084, 1066, 1052, 1030, 950, 922, 904, 884, 817, 781, 747, 712 cm^{-1}.

EA Found: C, 62.08; H, 5.63. $C_{13}H_{14}O_5$ requires C, 62.39; H, 5.64 %.

HRMS (ESI) calculated $C_{13}H_{15}O_5$ [M + H^+] 251.0914, found 251.0912.

Tm = 88.6 °C.

3.2.6.3 Triallyl-6-methylcyclohex-4-ene-1,2,3-tricarboxylate (TACHC)

AHIBC (40 g, 159.84 mmol) was dissolved in allyl alcohol (190 mL). After the addition of a catalytic amount of H_2SO_4 (0.5 vol.%, 0.9 mL), the mixture was stirred under reflux and the reaction progress was monitored by ^{1}H-NMR. The reaction was usually complete within 24 h. After the mixture had cooled to room temperature it was neutralized by the addition of a saturated sodium bicarbonate solution and the product was extracted with diethyl ether (3 × 200 mL). The combined organic layers were washed with saturated sodium chloride (200 mL) and dried over anhydrous sodium sulfate. After filtration, the solvent was removed *in vacuo*. The crude product was purified by column chromatography (1:6 EtOAc/hexanes). The product triallyl-6-methylcyclohex-4-ene-1,2,3-tricarboxylate (TACHC) was obtained as a colorless oil (45.2 g, 81 %).

^{1}H-NMR (400 MHz, chloroform-d): δ [ppm] = 6.09 (1H, m, H3), 5.90 (3H, m, H12, H12', H12″), 5.65 (1H, m, H2), 5.38 – 5.16 (6H, m, H13, H13', H13″), 4.58 (6H, m, H11, H11', H11″), 3.55 (1H, m, H5), 3.45 (1H, m, H6), 3.11 (1H, m, H4), 2.64 (1H, m, H1), 1.06 (3H, d, *J* = 7.36 Hz, H9).

^{13}C-NMR (100 MHz, chloroform-d) : δ [ppm] = 171.8, 171.4 and 170.73 (C10, C7 and C8), 132.5, 132.4, 132.1, 132.0 (C12, C12', C12″ and C2), 122.9 (C3), 118.5, 118.4 and 118.4 (C13, C13', C13″), 65.8, 65.7 and 65.3 (C11, C11', C11″), 43.5 (C6), 42.3 and 42.1 (C4, C5), 32.2 (C1), 17.2 (C9).

ATR-IR ν̃max 3455, 2940, 2882, 1730, 1649, 1454, 1379, 1310, 1169, 1094, 1061, 911, 927, 833, 720 cm^{-1}.

EA Found: C, 65.22; H, 6.88. $C_{19}H_{24}O_6$ requires C, 65.50; H, 6.94 %.

HRMS (ESI) calculated $C_{19}H_{24}O_6Na$ [M + Na^+] 371.1471, found 371.1451.

3.2.6.4 1,2-Epoxy-6-methyl-triglycidyl-3,4,5-cyclohexanetricarboxylate (EGCHC)

Epoxidation with mCPBA. 40 g (114.81 mmol, 1.0 eq.) of the TACHC was reacted with 158.50 g *m*CPBA (918.5 mmol, 8 eq.) in DCM (500 mL) at room temperature. Reaction progress was monitored by ^{1}H-NMR and was usually completed within 48 h. The reaction mixture was then stirred over K_2CO_3 (200 g) to deactivate residual *m*CPBA and the resulting *m*-chlorobenzoic acid was separated by filtration. The organic phase was then washed with a sodium thiosulfate solution (300 mL, 10 wt.%), H_2O (200 mL), and brine (200 mL). After drying over sodium sulfate and removing the solvent *in vacuo* 1,2-epoxy-6-methyl-triglycidyl-3,4,5-cyclohexanetricarboxylate (EGCHC) was obtained as a colorless viscous oil (36.9 g, 78 %).

^{1}H-NMR (400 MHz, chloroform-d): δ [ppm] = 4.45 - 4.0 (3H, m, H11, H11', H11″), 3.93 (1H, m, H3), 3.76 (3H, m, H11, H11', H11″), 3.35 (1H, m, H4), 3.28 (1H, m, H5), 3.13 (3H, m, H12, H12', H12″), 2.97 (1H, m, H2), 2.93 (1H, m, H6), 2.80 - 2.73 (3H, m, H13, H13', H13″), 2.60 – 2.54 (3H, m, H13, H13', H13″), 2.38 (1H, q, H1), 1.06 (3H, m, H9).

^{13}C-NMR (100 MHz, chloroform-d): δ [ppm] = 172.6, 172.0 and 169.8 (C10, C7 and C8), 65.9 (C11, C11', C11″), 56.8 (C3), 53.6 (C2), 49.2 – 48.9 (C12, C12', C12″), 44.8 – 44.5 (C13, C13', C13″), 41.5 (C4), 40.9 (C6), 39.6 (C5), 30.9 (C1), 14.8 (C9).

ATR-IR ν̃max 2950, 1729, 1434, 1385, 1348, 1304, 1256, 1199, 1179, 1078, 1045, 1012, 940, 905, 840, 762, 738 cm^{-1}.

EA Found: C, 55.12; H, 8.87. $C_{19}H_{24}O_{10}$ requires C, 55.12; H, 8.83 %.

HRMS (ESI) calculated $C_{19}H_{24}O_{10}Na$ [M + Na^+] 435.1267, found 435.1249.

Epoxidation with Oxone®. 0.943 g (2.71 mmol, 1.0 eq.) of TACHC was dissolved in acetone (200 mL). Sodium bicarbonate (37.5 g, 446.0 mmol, 165 eq.) was added suspended in 90 mL of water and added to the acetone-solution. The mixture was cooled in an ice bath and oxone (50.0 g, 81.2 mmol, 30 eq.) in H_2O (170 mL) was added drop wise over a period of 30 min. The reaction mixture was then stirred for three days at room temperature. After extraction with ethyl acetate (3 × 100 mL) the combined organic phases were washed with a saturated sodium chloride solution, dried over sodium sulfate, and the solvent was removed *in vacuo*. EGCHC was obtained as a colorless viscous oil (0.338 g, 30.2 %). Spectral data as described for the epoxidation with *m*CPBA. The

EEW was determined to be 107.7 g mol^{-1} by titration following the procedure of EN ISO 3001 : 9000.

3.2.7 Preparation of EGCHC and DGEBA epoxy samples

EGCHC and DGEBA-based epoxy samples were prepared as follows: 2 g of EGCHC or DGEBA and the corresponding amount of curing agent (Tab. A- 5) were mixed in 20 mL screw cap vials with a septum using a Classic Advanced Vortex Mixer (Velp Scientifica, Italy) at a speed of 30000 rpm for 1 min. The mixtures were degassed with vacuum for 3 min to remove air inclusions. The EGCHC-IPD mixture was degassed for 30 s only as it already sets after 4 min at room temperature. Then, the mixture was poured into the cavities of a silicone mold. For Dynamic Mechanical Analysis (DMA), the silicone mold had cavities with the dimensions 30 × 5 × 1 mm. For tensile testing, the silicone mold had cavities with the dimensions of the dogbone sample geometry 1BB from ISO 527-2 with a thickness of 1 mm and a total length of 30 mm. A glass plate coated with release agent was put on the silicone mold in order to ensure a flat surface of the epoxy samples. Finally, the mold was placed in an oven for curing (Tab. 14). After curing, the edges of the samples were wet-polished with sandpaper (grid size 500) for a smooth finish.

3.2.8 Preparation of mechanically recycled EGCHC samples

Broken EGCHC samples from tensile testing were milled using the same method as described in chapter 3.2.4. Powders of EGCHC+T403 or EGCHC+IPD were placed in an aluminum mold with cavities of the dimensions 30 x 5 x 1 mm (Fig.A- 31) previously coated with release agent and hot-pressed with 50 bar for 1 h at 130 °C for EGCHC+T403 and 110 °C for EGCHC+IPD in a Polystat 200 T press (Servitec). After, the hot-press is opened and the samples are cooled down at RT before removal.

3.2.9 Solvolysis

Broken EGCHC samples after tensile testing, TA/ELO 1.5 and 2.0 cured with C2 with the dimensions 30 x 5 x 1 mm and TA/ELO 1.5 CF composite with the dimensions 80 x 10 x 2 mm were weighed and placed in a NaOH solution (1 mol/L). The solution was heated at a defined temperature (RT, 30 °C, 40 °C or 80 °C) and stirred regularly. Samples were taken out of the NaOH solution, dried and weighed at different immersion times to assess the residual weight.

3.3 Devices and analysis

Flexural testing

As epoxy thermosets commonly experience flexural loading in typical applications, flexural testing becomes a pertinent mechanical evaluation method, providing insights into key flexural properties such as flexural strength, flexural modulus, and bending elongation at break. The three-point bending configuration is an easy to set up configuration and widely used to examine flexural properties of polymers, while the four-point bending configuration is better suited for stiffer structures such as unidirectional composites.

TA/ELO thermoset

TA/ELO samples of dimensions 80 x 10 x 4 mm were first dried for 3 days in a vacuum chamber with silica balls before testing. Three-point bending flexural testing was performed with a universal testing machine Inspekt 250 (Hegewald & Peschke, Germany) according to DIN EN ISO 178. The force was measured using a 500 N load cell. The tests were performed at a constant loading speed of 2 mm min^{-1} with a span L = (16 ± 1) x thickness. A videoextensometer was used to measure the deflection of the sample and stress/strain curves were recorded. The flexural modulus was evaluated from the stress/strain curve in the elongation range between 0.05 and 0.25 %. Flexural strength and elongation at break were also evaluated. Five specimens were tested for each TA/ELO sample cured with curing conditions C1 and C2 (Tab. 9).

Recycled TA/ELO thermoset and recycled TA/ELO composites

Samples with the dimensions 80 x 10 x 4 mm were dried and tested with the same setup described above. However, deflection of the sample was assessed using a deflection gage from Hegewald & Peschke instead of a videoextensometer for practical reasons. At least 6 samples were tested per configuration.

TA/ELO composite

Unidirectional composites samples with dimensions 100 x 15 x 2 mm were cut out from CF composites plates using a diamond saw with water cooling. Samples were dried out in a vacumm oven (2mbar) at 45 °C for 3 days. Four-point bending flexural testing was performed with a universal testing machine Inspekt 250 (Hegewald & Peschke, Germany) according to DIN EN ISO 14125. The tests were performed at a constant loading speed of 5 mm min^{-1}. A deflection gage from Hegewald & Peschke was used to assess the deflection of the samples. The force was measured using a 2.5 kN load cell. At least 5 samples were tested per configuration.

Optical microscopy

Analyses with the optical microscopy were performed to analyze the morphology of the cured TA/ELO thermosets and composites. Microscopic images were acquired using a BX41M-LED optical microscope (Olympus) or the stereomicroscope SZX10 (Olympus). Cured TA/ELO thermosets and TA/ELO composites specimens were embedded in

Sika CR80 epoxy resin in a cylindrical mold. Curing of Sika CR80 was performed at 55 °C for 16 h. The specimens were then polished with a polishing machine Struers Tegra and the surface morphology was observed under the microscope.

Gel content determination

To assess the degree of cross-linking of cured epoxy samples, the gel content was determined by Soxleth extraction using methanol (for TA/ELO samples) or acetone (for EGCHC samples) as solvent. After one day of extraction time, the samples were dried in a vacuum oven at 100 °C for 24 h and the mass loss was determined. Soxleth extraction was performed by Jonas Breitsameter.

Differential Scanning Calorimetry (DSC)

To investigate the curing mechanisms of the different epoxy thermosets, DSC tests were performed.

For TA/ELO samples:

DSC was performed on unreacted ELO/TA mixtures with a Q200 Differential Scanning Calorimeter (TA Instruments, USA). Five grams of ELO and the corresponding amount of milled TA were put inside small plastic containers of 50 mL and mixed for 3 min inside a speed mixer DAC 150 SP by Hauschild Engineering (Germany) at a rotation speed of 1500 rpm. 5-7 mg of the TA/ELO mixture were loaded inside a TZero aluminum pan and sealed with a TZero Hermetic lid from TA Instruments. Thermograms of the various TA/ELO formulations were recorded between 23 and 320 °C under a nitrogen atmosphere (gas flow = 50 mL min^{-1}). The applied heating rate was 10 K min^{-1}. The temperature of the peak of the curing enthalpy was determined with the software Universal Analysis. Three thermograms were recorded for each TA/ELO formulation. Thermograms of the neat, milled, and dried TA were also recorded.

For EGCHC and DGEBA samples:

DSC measurements were conducted with a TA Instruments Q200 differential scanning calorimeter under 25 mL min^{-1} helium flow. 5 to 9 mg of of the hand-mixed resin/curing agent mixtures were loaded inside a TZero aluminum pan from TA Instruments. Samples were cooled down at -50 °C and subjected to a heating rate of 10 K min^{-1}. The onset temperature of the curing enthalpy and the temperature of the maximum of the exothermic peak were determined with the software Universal Analysis.

Thermogravimetric Analysis (TGA)

TGA Q5000, (TA Instruments, US) was used to conduct thermogravimetric analyses on TA/ELO samples cured 16 h at 120 °C + 3 h at 140 °C, on neat TA and ELO and on EGCHC and DGEBA samples. 1-2 mg of each sample is heated from 23 to 1000 °C with a heating rate of 10 K min^{-1} under an argon atmosphere. Analysis of the mass loss as a function of temperature is performed using TA universal software. The temperature $T_{5\%}$ at a weight loss of 5 % of the various samples was determined.

Dynamic Mechanical Analysis (DMA)

DMA is a very sensitive technique to measure the glass transition temperature and evaluate the stiffness of a sample. DMA measurements were performed using a DMA Q800 (TA Instruments, US) under a nitrogen atmosphere. For TA/ELO specimens, a 20 mm 3-point bending clamp was used. For EGCHC, recycled EGCHC and DGEBA specimens, a film tension clamp was used. The sample geometry and testing clamp was specifically chosen to possess a geometry factor and stiffness that fall within the operational limits of the DMA machine (30 x 6 x 2 mm for TA/ELO specimens and 30 x 5 x 1 mm for EGCHC and DGEBA specimens). After conducting initial frequency and amplitude sweep tests, specific frequency and amplitude values were selected to ensure that the sample would not incur any damage during testing. Samples were subjected to a static pre-load of 0.01 N, a force profile of 125 % and the selected amplitude and frequency. During loading, the samples were first equilibrated at the starting temperature for 10 min, then a temperature ramp of 2K min^{-1} or 1K min^{-1} was applied. The glass transition temperature Tg was identified as the temperature of the peak of the tan δ curve using the software Universal Analysis.

Tensile Testing

EGCHC and DGEBA dogbone samples with the geometry 1BB from ISO 527-2 with a thickness of 1 mm and a total length of 30 mm were painted using an airbrush and a matte acrylic-based paint. A white base coat was applied to the region of interest and then a black speckle pattern was sprayed on top. The amount of paint applied was carefully minimized in order not to smear the underlying stress field. Tensile testing was performed with a universal testing machine Inspekt 100 (Hegewald & Peschke, Germany) equipped with screw clamps. The force was measured using a 500 N load cell. The Dogbones samples were tested at a constant loading speed of 0.125 mm min^{-1}. Five specimens were tested for each epoxy system (Tab. 14). The average laboratory temperature and humidity during testing were 21.8 °C and 33 %. A VCXU-124M camera (Baumer, Germany) mounted on a telecentric lens VS-TCM1-130/S (VS Technology, Japan) captured the deformation on the specimens' surface during testing. The recorded pictures were transferred to the software GOM Correlate Professional 2020 and the tensile modulus was evaluated from the stress/strain curves in the elongation range between 0.05 and 0.25 %. Tensile strength was also evaluated.

Attenuated Total Reflection Fourier Transformed Infrared Spectroscopy (ATR-FTIR)

ATR-FTIR measurements were performed on a Bruker Vertex70v ATR-IR spectrometer at room temperature in absorption mode. If needed, spectra were converted from absorbance to transmittance. ATR-FTIR measurements were performed by Jonas Martin Breitsameter.

Particle Size Analysis

The particle size distribution of the milled and unmilled TA was determined by an LS 13 320 laser diffraction particle size analyzer (Beckman Coulter, US) using the Tornado dry powder system and the Mie optical model. The particle size analysis was performed by Jonas Martin Breitsameter.

Water uptake

TA/ELO thermoset

TA/ELO plates were manufactured by using ELO and milled TA. The mixtures were poured on a aluminum plate coated with release agent and the edges were sealed with tacky tape. Curing was performed at 120 °C for 16 h. Samples with the dimensions 50 x 50 x 1 mm were cut out with a diamond saw with water cooling.

After drying in a vacuum oven (2 mbar) for 2 weeks at 40 °C, the samples were weighed and then immersed in distilled water for a period of 84 days. At different time intervals, the samples were taken out of the water, dried out with a towel and weighed to calculate the water uptake.

EGCHC

Pieces of EGCHC after tensile testing were dried in a vacuum oven (2 mbar) for 2 weeks at 40 °C, weighed, and immersed in distilled water for a period of 72 h. At different time intervals, the samples were taken out of water, dried out with a towel and weighed to calculate the water uptake.

Determination of the fiber volume fraction (V_f %)

When using following formula:

$$Vf = \frac{Vfiber}{Vcomposite} = \frac{\frac{m\ fiber}{\rho\ fiber}}{Vcomposite}$$

V_f could be determined by weighing the fibers before the production of the composite plates or by weighing the fibers after solvolysis of the composites in NaOH (1 mol/L), washing in water and drying. ρ of the CF fabrics used was 1.8 g/cm³.

Scanning electron microscope (SEM)

SEM pictures were taken using a JCM-7000 (JEOL GmbH, Germany).

Stress relaxation

TA/ELO 1.5 samples with a thickness of 1 mm and a diameter of 30 mm were placed in a plate-plate rheometer (MCR 302, Anton Paar). The testing procedure was as follows: first, the samples were heated for 15 min to the testing temperature (160, 170 or 180 °C). Then, a force of 5 N was applied to the samples for 5 min while holding the temperature constant. Finally, a constant shear deformation of 1 % was applied while maintaining a

constant temperature. The changes over time of shear stress and relaxation modulus were recorded.

Nuclear Magnetic Resonance (NMR) Spectroscopy

^{1}H-NMR spectra of natural linseed oil and ELO were recorded on a Bruker Ascend 400 MHz spectrometer. All spectra are referenced on the proton signal of $CDCl_3$ (7.26 ppm).

^{1}H (400 MHz) and ^{13}C (100 MHz) nuclear magnetic resonance experiments were conducted on a *Bruker* AV400 instrument in deuterated chloroform (Sigma–Aldrich, $CDCl_3$, 99.8 atom% D) or methylene chloride (Sigma–Aldrich, CD_2Cl_2, 99.9 atom% D) as the solvent at a temperature of 294 K. Chemical shifts were referenced to the solvent proton resonance ($CDCl_3$: 7.26 ppm for ^{1}H-NMR, 77.2 ppm for ^{13}C-NMR; CD_2Cl_2: 5.32 ppm for ^{1}H-NMR, 53.84 ppm for ^{13}C-NMR).

NMR spectroscopy was performed by Jonas Martin Breitsameter.

4 Development and characterization of a sustainable and fully bio-based epoxy thermoset based on linseed oil and tannic acid

Parts of this chapter were published in the Journal Macromolecular Materials and Engineering with the article entitled "Fully Bio-Based Epoxy Thermoset Based on Epoxidized Linseed Oil and Tannic Acid" [3] . The publication was developed in cooperation with the Wacker-Chair of Macromolecular Chemistry (TU Munich) within the framework of the project "Green Carbon" funded by the German Federal Ministry of Education and Research (FKZ: 03SF0577A). The ELO resin used in this chapter was synthesized by Jonas Martin Breitsameter, who also did the NMR spectroscopy analysis, particle size analysis, gel content measurements, ATR-FTIR measurements and parts of the DSC measurements. The contributors are listed in the reference:

Reinhardt, N.*, Breitsameter, J.M.*, Drechsler, K. and Rieger, B., Fully Bio-Based Epoxy Thermoset Based on Epoxidized Linseed Oil and Tannic Acid, Macromolecular Materials and Engineering, 2022, 307, 12, 2200455. *These authors contributed equally.

Parts of the results of this chapter were obtained in the theses of Linder [S3], Herold [S9] and Gehringer [S15]. The Stamp-die system (Fig.A- 5) used for hot-pressing recycled TA/ELO samples was constructed by Florian Gehringer [S15].

4.1 Objectives and goal

Vegetable oils, being both unharmful and readily available as cost-effective renewable resources, have garnered significant interest as potential substitutes for epoxy resins, as evidenced by numerous scientific studies exploring their application. Despite this attention, EVO faces challenges when compared to DGEBA-based epoxies, as their mechanical properties are inferior due to the presence of long aliphatic chains in their chemical structure [66,74–76].

To face this inherent problem, ELO was chosen due to its high amount of epoxy groups in its linolenic acid chain (Tab. 2). Linseed oil is a highly available resource as it is one of the world’s largest oil crops with an approximate yearly production of 2.4 million tons [156]. A hardener with a rigid structure is also needed to counter the flexibility of the aliphatic chains of ELO and impart high stiffness [90]. Bio-based curing agents are often associated with poor mechanical properties. However, TA is a bio-based compound that can be commercially extracted from chinese gallnuts, aleppo gallnuts, sumac leaves and tara pods [157,158], and it possesses a rigid gallic structure that suggests the formation of highly crosslinked networks (chapter 2.2.4). TA has the advantage of being

already industrially isolated. Therefore, TA was selected as the crosslinking agent. Moreover, owing to the inherent ester and hydroxy groups in TA, coupled with the hydroxyl group formed during curing with ELO, a transesterification reaction should be able to occur. This reaction is expected to confer vitrimer-like properties to the TA/ELO thermoset, thereby enabling the material to be mechanically recycled. Furthermore, TA/ELO is likely to undergo chemical recycling under mild conditions. This is due to the susceptibility of ester groups to hydrolysis. This characteristic is particularly noteworthy when utilizing TA/ELO for composites, as it facilitates the recovery of fibers.

The goal of this chapter is to develop a fully bio-based epoxy that is designed for recyclability using non-harmful and available resources. A particular focus is given to the thermal and mechanical properties of TA/ELO as the goal is to obtain similar properties to a standard DGEBA-based epoxy. To maintain the fully bio-based composition of the TA/ELO epoxy, the use of solvents and catalysts was deliberately avoided.

4.2 Milling of TA

Unlike typical curing agents, TA is a solid hardener [101,102]. When mixed as bought with ELO, a highly heterogeneous material was obtained after curing (Fig.A- 11). To avoid the use of solvents and yet still properly disperse TA in ELO to obtain a homogenous material, a milling procedure was adopted to reduce the particle size of TA. Achieving a good distribution of tannic acid (TA) within ELO is essential to ensure the uniform curing of the epoxy thermoset and optimize both thermal and mechanical properties.

TA was first dried and then milled with Al_2O_3 balls in a two-step milling process. The two-step milling process led to a notable reduction in the particle size of TA, as illustrated in Figure 28. A similar procedure was adopted by Anusic et al. [79], who milled the solid citric acid (CA) to obtain a homogeneous CA/ELO mixture.

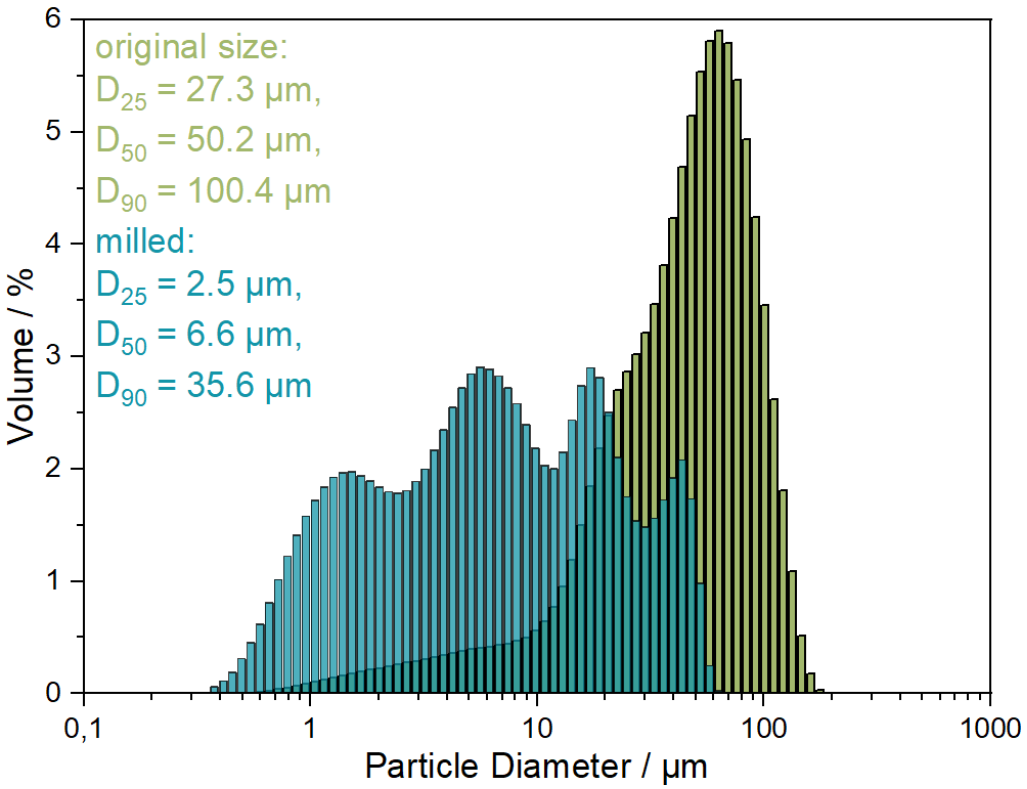

Figure 28: Particle size distribution of original size TA (as bought) and milled TA. From: [5].

Microscopic images reveal that the purchased TA particles are relatively large and exhibit a bubble-shaped morphology, possibly resulting from an industrial drying process (Figure 29A). This bubble-like structure may impede a uniform curing process, as air could be trapped in the center, and the interior might be inadequately accessible during the curing reaction. Following the milling process, the particle size significantly decreases, as observed in the particle size determination (Figure 28). Dispersion analyses of both the original-sized and milled TA in ELO demonstrate a much more homogeneous distribution of the milled product (Figure 29C and Figure 29D).

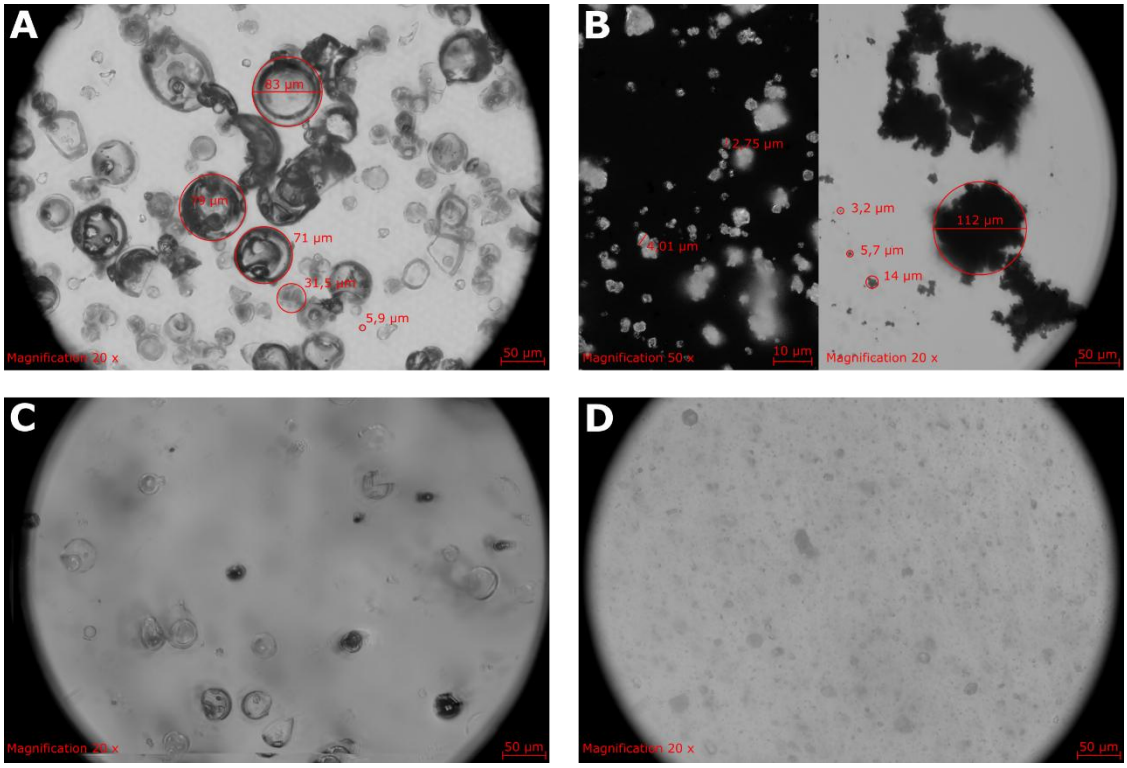

Figure 29: Microscope pictures of A) TA original size (as bought), B) TA milled, C) TA original size dispersed in ELO, D) TA milled dispersed in ELO. From: [5].

4.3 Curing mechanism of TA/ELO

Tannic acid given formula is $C_{76}H_{52}O_{46}$ with a molecular weight of 1701.2 g/mol although its structure still remains unclear [159]. TA has potentially 25 galloyl hydroxyl groups capable of cross-linking. Due to steric hindrance effects during the curing process and low reactivity of the galloyl groups, the participation of every single hydroxyl functionality in the curing reaction is very unlikely, making the calculation of the optimal TA/ELO mixing ratio complicated and the curing process complex.

The curing reaction adheres to a ring-opening mechanism of the oxirane group, as elucidated by Qi et al. [106] through a zwitterionic pathway. In this process, the alcohol group coordinates with the epoxide, establishing a hydrogen-bridge linkage (depicted in Figure 30a). This coordination enables the nucleophilic attack of the alcohol oxygen on an epoxide carbon, resulting in the formation of a zwitterionic species and subsequent ring-opening, leading to the creation of an ether bond. The schematic representation of the network formed is illustrated in Figure 30b.

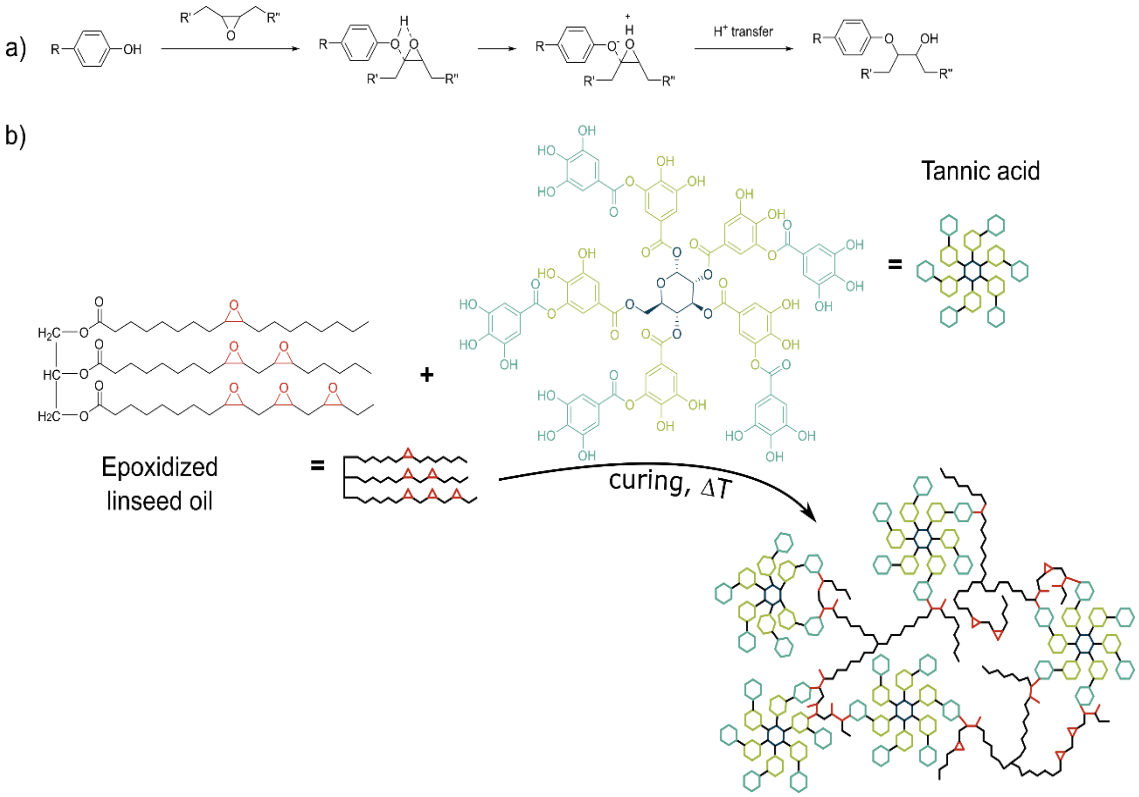

Figure 30: a) Curing mechanism following a zwitterionic ring-opening reaction exemplary shown on a phenol group according to Qi et al. [106]**. b) Schematic formation of a 3D network during the curing reaction. From: [5].**

Various TA/ELO mixing ratios (Tab. 8) were investigated in the DSC to better understand the curing mechanism. Figure 31a illustrates a representative DSC heating scan of TA/ELO 1.75. All conducted DSC scans display similar patterns, revealing three distinct regions:

- Firstly, there is an endothermic peak observed within the temperature range of approximately 25 to 100 °C, corresponding to the evaporation of hydrated water. The persistence of water, despite the drying process, is confirmed by examining the DSC and TGA scans of the neat, milled, and dried TA. The TGA scan demonstrates a 1.7 % mass loss at 120 °C (Figure 31d), while the DSC scan indicates an endothermic process occurring from 25 to 120 °C (Figure 31c). Following a one-day exposure to laboratory atmosphere (at 55 % humidity and 25 °C), the repeated TGA measurement reveals a 9.1 % mass loss at 120 °C, emphasizing the hygroscopic characteristics of TA (Figure 31d).

- Next, an exothermic peak is observed, indicating the reaction between phenolic -OH groups and epoxides, commencing around ≈ 100 °C and concluding at ≈ 250 °C (Figure 31a). This observation is consistent with existing literature, which suggests that the reaction between phenolic -OH groups and epoxy rings can initiate at 100 °C [101,160,161]. As the quantity of TA increases, the temperature at which the maximum of the exothermic peak occurs shifts to lower

temperatures (Figure 31b). Consequently, in the presence of an excess of TA, the maximum curing reaction speed is achieved at lower temperatures, thereby enhancing curing efficiency. This phenomenon can be elucidated by considering the elevated molar mass and significant steric hindrance associated with TA. Following the formation of a few ether bonds in the initial curing stage, the fundamental structure of the epoxy network is already established. Consequently, a substantial proportion of potential hydroxy linking positions does not actively contribute to network linking. Consequently, augmenting the quantity of TA increases the likelihood of galloyl groups accessing areas with unreacted oxiranes, thereby amplifying the overall degree of cross-linking.

- Lastly, an additional feature in the DSC scan appears as a shoulder at temperatures exceeding 250 °C (Figure 31a). This is connected to the degradation of TA, a connection supported by the TGA scan of pure TA (Figure 31d). The distinctiveness of the shoulder increases with an excess of TA, indicating that a greater quantity of TA particles is unable to engage in the curing reaction and establish cross-links with ELO and thus commence the degradation process (Fig.A- 12).

Tab. 8: Mixing ratios used for the preparation TA/ELO thermoset. Adapted from: [5]

Samples	ELO [g]: TA [g]	Molar ratio R [-OH/epoxide]
TA/ELO 0.85	100:41.14	0.85
TA/ELO 1.0	100:48.40	1.0
TA/ELO 1.15	100:50.66	1.15
TA/ELO 1.25	100:60.50	1.25
TA/ELO 1.5	100:72.60	1.5
TA/ELO 1.75	100:84.70	1.75
TA/ELO 2.0	100:96.80	2.0

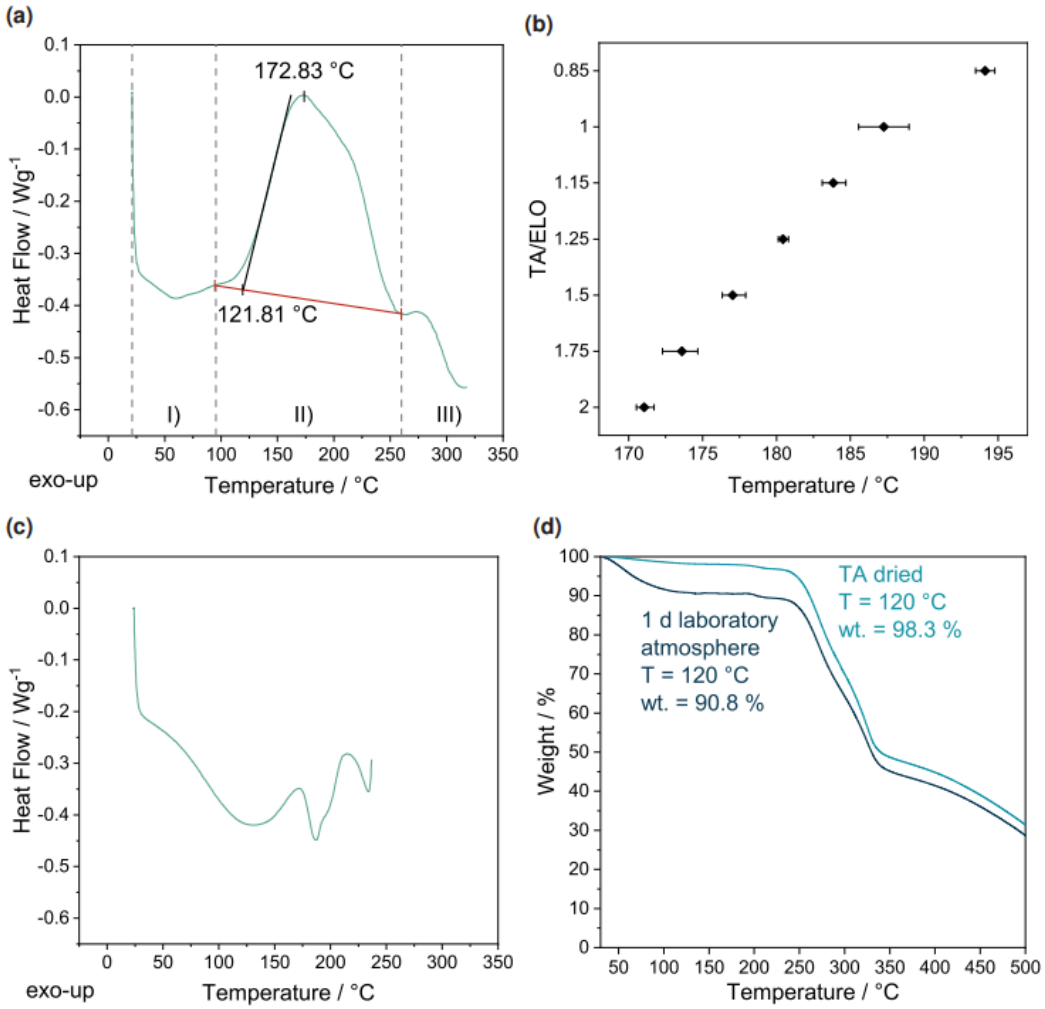

Figure 31: **a) DSC-scan of the sample TA/ELO 1.75 with onset temperature of the curing enthalpy (121.81 °C) and temperature of the peak of the curing enthalpy of 172.83 °C, b) Average temperature of the peak of the curing enthalpy for the different TA/ELO mixtures, c) DSC-scan of pure milled and dried TA, d) TGA-measurements of dried TA and TA after being exposed one day to the laboratory atmosphere. Adapted from** [3]**.**

4.4 Thermal and mechanical properties

4.4.1 Investigated TA/ELO formulations and curing temperatures

Samples of TA/ELO epoxy with molar ratios of -OH/epoxide of 0.85, 1.0, 1.15, 1.25, 1.5, 1.75, and 2.0 were prepared to examine how the molar ratio affects the thermal and mechanical properties of the resulting thermoset (Tab. 8). The curing process for all specimens took place under two distinct conditions, denoted as C1 and C2 (Tab. 9). The curing temperature of 120 °C was selected based on the approximate onset temperature of the curing enthalpy for TA/ELO (Figure 31a). Specimens subjected to a higher curing

temperature exhibited increased stiffness. Nevertheless, these samples demonstrated extreme brittleness, with significantly lower flexural strength and elongation at break (Tab. A- 2). Consequently, the curing temperature was set to 120 °C. Opting for a lower curing temperature results in energy savings and also facilitates easier processing. The choice of a curing temperature of 90 °C was also made to investigate the possibility of attaining favorable mechanical and thermal properties under these conditions. Typically, a post-curing step is necessary to optimize the thermal and mechanical characteristics of epoxy thermosets, with the post-curing temperature commonly being higher than the preceding precuring temperature [162]. Through DMA tests, it was observed that a post-curing temperature of 140 °C contributed to an enhancement in the stiffness and glass transition temperature (Tg) of the TA/ELO thermoset.

Tab. 9: Curing conditions for the TA/ELO samples. Adapted from: [3]**.**

Curing condition	Curing time + temperature	Post-curing time + temperature
C1	16 h at 90 °C	3 h at 140 °C
C2	16 h at 120 °C	3 h at 140 °C

4.4.2 Thermo-mechanical properties

The glass transition temperature (Tg) is a crucial indicator for epoxy thermosets. Indeed, it establishes the temperature range within which epoxy thermosets can be effectively employed in high-performance structural applications. Beyond Tg, epoxies are viscoelastic and soft materials. The Tg of the various TA/ELO samples were assessed using Dynamic Mechanical Analysis (DMA), a highly sensitive technique renowned for its precision in measuring Tg [91,92]. Figure 32 shows an example of a DMA curve obtained for TA/ELO. It can be observed that the tan δ peak is very broad. This broad tan δ peak was observed for all the samples tested. As previously outlined in chapter 2.2.3, a broad tan δ peak can be the characteristic of the relaxation of a heterogeneous network [94,95]. Yet, in the context of TA/ELO, the emergence of a wide tan δ is attributed to the complex crosslinked structure formed. In contrast to conventional epoxy compounds like DGEBA, where oxirane groups have fixed positions, the cross-linking process in ELO is more complex. Specifically, the oxirane groups in ELO are statistically distributed across the aliphatic triglyceride backbone [93]. Additionally, TA, with its high molecular weight, exhibits varying reactivity among its 25 hydroxy groups, a reactivity that changes throughout the curing reaction due to steric and electronic effects [101]. Consequently, the cross-linking between ELO and TA results in a complex and unpredictable network structure, contributing to the broadening of the glass transition.

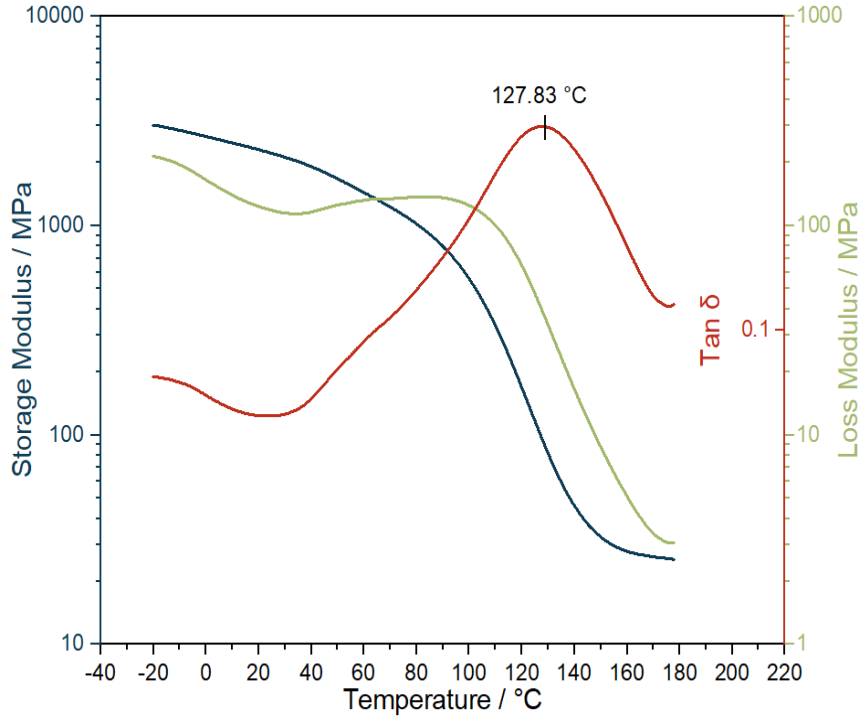

Figure 32: Storage modulus, loss modulus and tan δ variations versus temperature for the sample TA/ELO 1.75 cured with C1. Tg of 127.83 °C. From: [3]**.**

Figure 33 compiles the Tg acquired for the various TA/ELO samples cured with C1 and C2. A distinct pattern is evident as the Tg for all samples experiences a notable elevation when subjected to a curing temperature of 120 °C (curing condition C2), as opposed to 90 °C (condition C1). Hence, the specimens cured using C1 did not achieve their complete cross-linking capacity. This observation is supported by gel content measurements, revealing a lower Soxhlet degree of cross-linking in the C1-cured samples compared to those cured with C2 (Fig.A- 13). As the curing process occurs at a temperature below the Tg of the fully cured resin (Tg∞), the system vitrifies, and the reaction becomes diffusion controlled [163]. Owing to vitrification and the inherent low reactivity of polyphenol groups in TA, coupled with the steric hindrance caused by the epoxy groups along the fatty chains of ELO, an elevated curing temperature promotes increased cross-linking of the polymer chains.

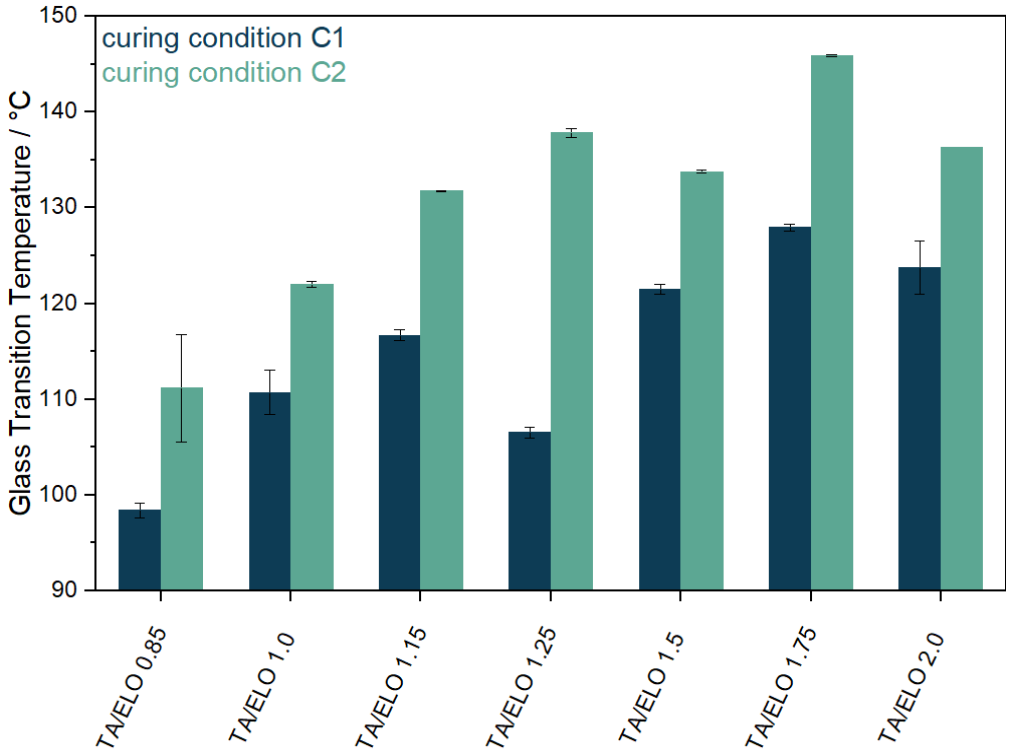

Figure 33: Tg obtained from DMA for the different TA/ELO samples cured with curing conditions C1 and C2. From: [3].

It can also be noticed from Figure 33 that higher Tg are obtained when the TA molar ratio exceeds 1.0. As previously observed in the DSC analysis, an abundance of TA facilitates a more effective curing process, a phenomenon that is also evident in ATR-FTIR (Fig.A- 14 and Fig.A- 15). In the TA/ELO 0.85 sample, a residual signal of the C-O epoxide vibration at 820 cm^{-1} is evident showing that not all epoxide groups participated in the curing reaction. In contrast, this signal is not observed in samples with an excess of TA.

For TA/ELO, a maximum Tg of 146 °C was obtained for TA/ELO 1.75 cured with C2. Figure 33 also illustrates that the Tg shows minimal variation among samples TA/ELO 1.15, 1.25, 1.5, 1.75, and 2.0 cured with C2. This behavior is likely a consequence of the complex crosslinked structure formed, leading to a broadened glass transition. Moreover, the foundational network is established within a few reactions. Various equations in the literature, such as DiBenedetto's equation linking Tg and epoxy cross-linking, provide insight into these phenomena [164,165]. With an excess of TA, all oxiranes can engage with a galloyl-group, resulting in limited variations in cross-linking.

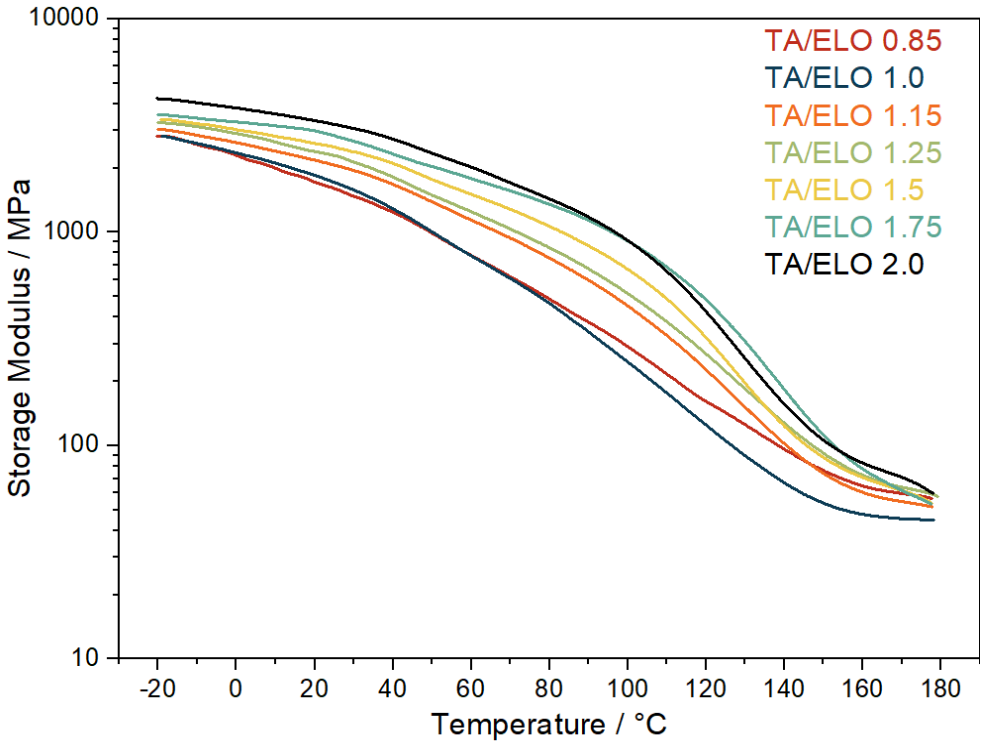

Figure 34: Comparison of the storage modulus curves (E') for the different TA/ELO samples cured with C2. From: [3]**.**

The storage modulus (E') serves as a measure of the sample's elastic behavior and is a characteristic value of stiffness [166]. Analyzing the variation of E' with temperature provides an effective means to compare the stiffness of different samples across different temperature ranges. Figure 34 illustrates the temperature-dependent changes in E' for various TA/ELO samples cured with C2. As anticipated, the stiffness of the TA/ELO thermoset increases proportionally with the TA content, reflecting the formation of a highly crosslinked structure. TA/ELO 2.0 cured with C2 exhibited the highest average storage modulus, reaching 3218 MPa at ambient temperature (25 °C) (Fig.A- 16).

The Tg values and storage modulus values at ambient temperature obtained for TA/ELO are high for EVO cured with bio-based curing agents as literature often reports lower values. Anusic et al. [79] for example found a maximum storage modulus of 1380 MPa at 25 °C and a Tg of 82 °C for ELO cured with citric acid. Altuna et al. [142] obtained a glass transition temperature (Tg) of 30 °C for a fully bio-based thermoset derived from epoxidized soybean oil. Qi et al. [106] cured epoxidized soybean oil (ESO) with tannic acid, resulting in a peak glass transition temperature of 77 °C and a storage modulus of 1103 MPa at 25 °C. Some publications reported high Tg values for ELO-based epoxies; for instance, Todorovic et al. [90] reported a Tg of 145 °C. However, this was obtained for ELO cured with methyltetrahydrophthalic anhydride (MTHPA), a petroleum-based curing agent. This emphasizes TA's capability to form a rigid network due to its highly aromatic structure, enabling it to rival conventional petroleum-based hardeners.

Yet, it is important to note that even though high Tg values were achieved, TA/ELO is not suitable for applications demanding high stiffness beyond 80 °C. A notable decline in stiffness is observed above this temperature, as evident from the storage modulus curves (Figure 34).

4.4.3 Flexural properties

As epoxy thermosets commonly experience flexural loading in typical applications, flexural testing becomes a pertinent mechanical evaluation method, providing insights into key flexural properties such as flexural strength, flexural modulus, and bending elongation at break.

The summarized data in Tab. 10 presents the average flexural modulus, flexural strength, and elongation at break for TA/ELO samples cured with C1 and C2. The application of curing condition C2, as opposed to C1, results in an increase in both flexural modulus and flexural strength. This is attributed to the enhanced stiffness and resilience of the material, stemming from a higher cross-linking of the polymer chains.

Tab. 10: **Average Flexural Modulus, Flexural strength, and elongation at break obtained for the different TA/ELO mixtures cured with the curing conditions C1 and C2. Adapted From:** [3].

	Flexural Modulus [MPa]		**Flexural Strength [MPa]**		**Elongation at break [%]**	
Sample↓/ Curing→	C1	C2	C1	C2	C1	C2
TA/ELO 0.85	924 ± 91	1347 ± 94	33 ± 2	46 ± 2	8.2 ± 0.9	7.8 ± 0.8
TA/ELO 1.0	1484 ± 131	1525 ± 105	48 ± 2	50 ± 2	8.4 ± 1.7	5.9 ± 0.3
TA/ELO 1.15	1711 ± 43	2111 ± 98	50 ± 3	67 ± 1	4.9 ± 1.5	4.7 ± 0.3
TA/ELO 1.25	1692 ± 59	1991 ± 27	50 ± 1	65 ± 1	4.9 ± 0.7	4.2 ± 0.5
TA/ELO 1.5	1943 ± 157	2308 ± 99	54 ± 2	72 ± 1	3.7 ± 0.6	3.7 ± 0.1
TA/ELO 1.75	2328 ± 257	2525 ± 187	63 ± 8	67 ± 6	2.8 ± 0.7	3.0 ± 0.3
TA/ELO 2.0	2686 ± 158	2986 ± 42	45 ± 8	66 ± 3	1.8 ± 0.4	2.5 ± 0.1

Similarly to the storage modulus, there is a rise in the flexural modulus with an increasing quantity of TA incorporated into ELO. An epoxy that exhibits high stiffness is required for structural and high-performance applications. The highest flexural modulus of 2986 MPa was reached for the sample TA/ELO 2.0 cured with C2. The fully bio-based TA/ELO 2.0 thermoset showcases a stiffness under flexural load comparable to

that of high-performance commercial petroleum-based epoxy materials. For comparison, the CR80 epoxy system by SIKA is a DGEBA-based epoxy resin system designed for manufacturing high-performance fiber-reinforced composites used in marine, wind turbine, and various industrial composite applications. Once fully cured, CR80 attains a flexural modulus ranging from 2900 to 2950 MPa [77].

The augmentation of stiffness with the -OH/epoxide molar ratio results in a brittle behavior, evidenced by a decrease in the bending elongation at break. It can be noticed that the elongation at break for samples TA/ELO 0.85, 1.0, and 1.15 cured with C1 exhibits a high level of uncertainty. This can be linked to poor curing efficiency that contributed to non-uniform cross-linking and, consequently, non-homogeneous stiffness along the sample, leading to random deflection under flexural load.

The flexural strength of the samples cured with C2 tends to increase with the amount of TA in ELO until reaching a maximum of 72 MPa for TA/ELO 1.5, after which it decreases with further addition of TA.

From Tab. 10, it can be seen that the flexural properties of TA/ELO can me modulated by varying the amount of TA in the thermoset. This feature expands the versatility of the bio-based epoxy, allowing the TA/ELO thermoset to be utilized in diverse applications. It can be converted into a material that is either very stiff and brittle or flexible, exhibiting a high flexural elongation before breakage. Figure 35 highlights this phenomenon by illustrating the variation in flexural strength and elongation at break with the amount of TA in the material. The materials TA/ELO 1.5, 1.75 and 2.0, when cured with C2, are adapted for the obtention of a material with high stiffness and a significant flexural strength.

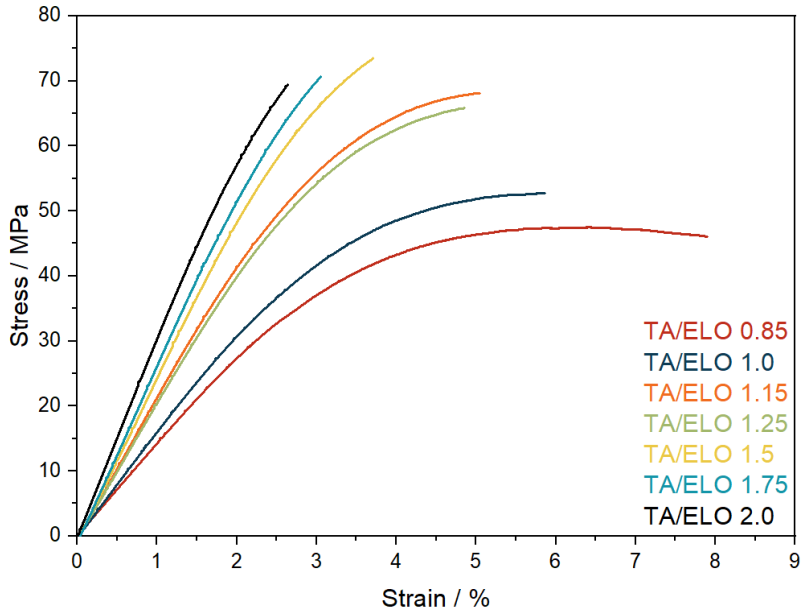

Figure 35: Representative stress-strain curves under flexural load for the different TA/ELO samples cured with C2. From: [3]**.**

It is important to note that the flexural strength values obtained for TA/ELO are significantly lower than those of high-performance commercial petroleum-based epoxy materials. For instance, CR80 demonstrates a flexural strength of 122 to 126 MPa [77].

4.4.4 Thermal stability

The curing process C2, which promotes higher Tg and stiffness, is better suited for achieving a high-performance thermoset. Consequently, only the thermal stabilities under nitrogen of the TA/ELO samples cured with C2 were explored using thermogravimetric analysis (TGA). As anticipated, an excess of TA impacts the thermal stability of the TA/ELO thermoset, particularly evident in TA/ELO 1.75 and 2.0, where a substantial amount of unreacted TA that did not crosslink is present in the matrix (Figure 36). Thus, with an increasing TA content, the $T_{5\%}$ of the thermoset approaches the $T_{5\%}$ of neat TA, approximately at 235 °C.

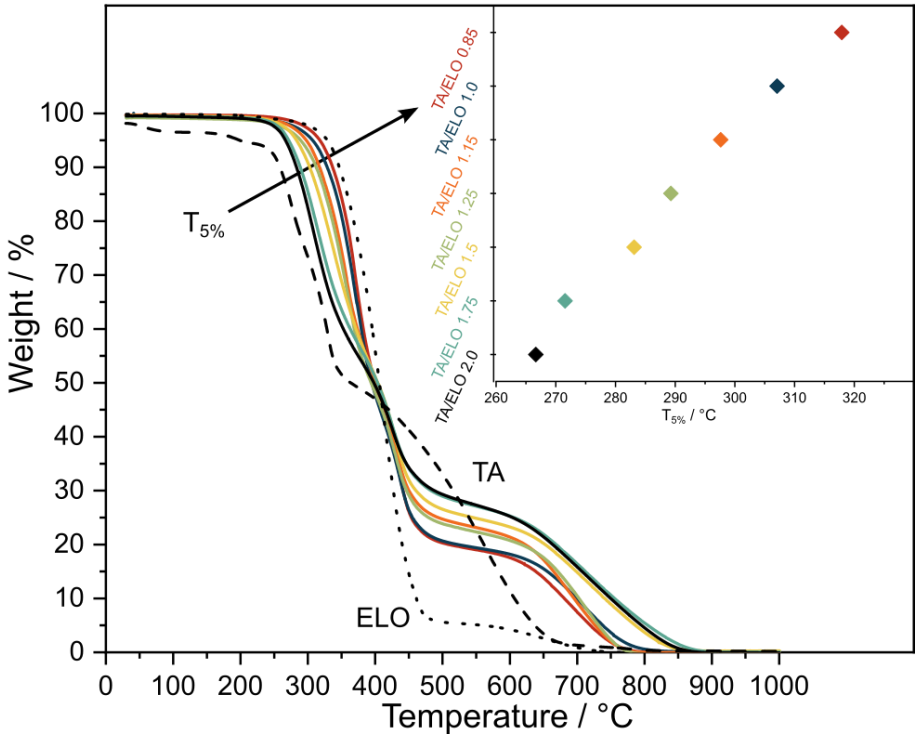

Figure 36: TGA curves of the TA/ELO samples cured with C2 and of pure ELO (dotted) and milled TA (dashed) and respective temperature of 5% weight loss ($T_{5\%}$). From: [3].

Samples with a low TA content, such as TA/ELO 0.85 and 1.0, exhibit TGA curves similar to those of standard commercially available high-performance epoxy. In Fig.A- 17 the TGA curve of TA/ELO 0.85 is compared to the high-performance epoxy CR80 from SIKA. Despite the adverse impact of an increasing amount of TA on the thermal stability of the thermoset, the $T_{5\%}$ of TA/ELO 2.0 at 267 °C remains sufficiently high to prevent material degradation under standard usage applications.

4.5 Sample morphology

Figure 37 displays the morphology of fracture surfaces following flexural testing. Three distinct TA/ELO samples cured with C1 and C2 were selected to assess the influence of curing temperature and TA amount (equimolar amount: TA/ELO 1.0; excess of TA: TA/ELO 1.5; and high excess of TA: TA/ELO 2.0) on the sample morphology.

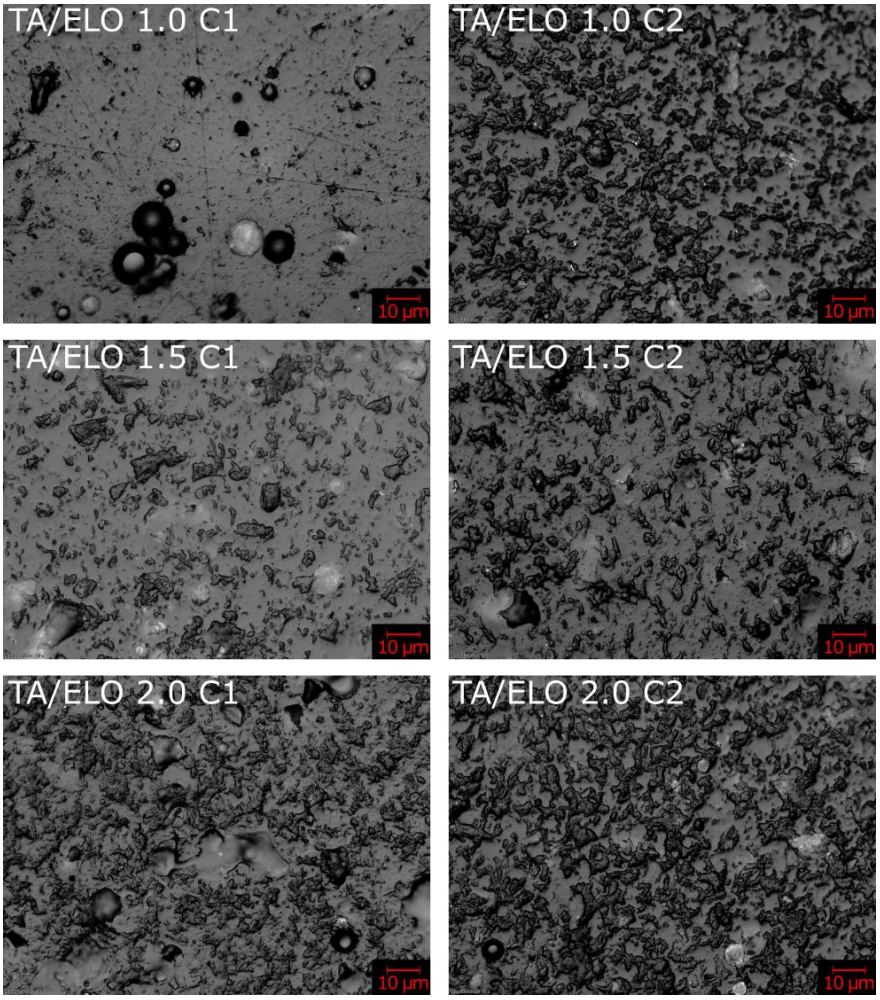

Figure 37: Representative microscope images of the fracture surface of TA/ELO 1.0, 1.5, and 2.0 cured with C1 and C2 after flexural testing. From: [3].

Circular black spots are observable on all examined surfaces. The elevated viscosity of the TA/ELO mixture results in the presence of some voids within the material. The surface of TA/ELO 1.0, cured with C1, appears relatively smooth, while a rough surface is evident under curing condition C2. At a significant TA content (TA/ELO 1.5 and 2.0), a coarse surface is evident even with curing condition C1, and this roughness becomes more pronounced with C2. This rough surface could be attributed to the cross-linking reaction between ELO and TA, primarily occurring with hydroxyl groups on the surface of the milled TA particles, leaving the inner core unreacted.

As previously emphasized, an excess of TA facilitates a higher degree of cross-linking, and the use of C2 for curing enables additional cross-linking. It is evident that, when TA is added excessively, not all TA particles can undergo a reaction with ELO, resulting in a heterogeneous structure, as observed in Figure 37. Despite the surplus of TA contributing to increased cross-linking, the Soxhlet degree of cross-linking diminishes with higher TA concentrations in the material (Fig.A- 13). This indicates a noticeable rise in the quantity of unreacted TA in the material, as illustrated in Fig.A- 12.

4.6 Water absorption

Tannic acid, possessing numerous galloyl groups in its structure is identified as a hydrophilic polyphenolic substance [167]. The microscope images (Figure 37) and Soxhlet extraction results (Fig.A- 13) revealed a composite-like structure as some of the TA cannot react. The high content of unreacted TA in TA/ELO thermoset leads to high-water absorption values as seen in Figure 38. As expected, TA/ELO thermosets containing a significant excess of TA (such as TA/ELO 1.5 and 1.75) are able to absorb more water than TA/ELO thermosets containing less TA. Moreover, TA/ELO 1.5 and TA/ELO 1.75 failed to reach equilibrium even after an extended immersion period (84 days), indicating elevated water uptake with prolonged immersion. When compared to standard epoxy systems reported in the literature, the water absorption of TA/ELO significantly exceeds these values. For instance, the work of Abdelkader et al. that investigated DGEBA with various curing agents and cured at different temperatures, reported a maximum water uptake of 5.6 % at equilibrium [168]. The aerospace industry's reference epoxy resin, RTM6, reaches approximately a water uptake of 2.5 % at equilibrium [169]. The detrimental impact of water absorption on the mechanical properties of epoxy systems is a well-known phenomenon [170,171]. Therefore, common commercial epoxy systems exhibit low water uptake capability.

To reduce the water absorption of TA/ELO thermoset, hydrophobization of the molecules can be considered. As an example, Liu et al. [176] synthesized a hydrophobic TA in their work.

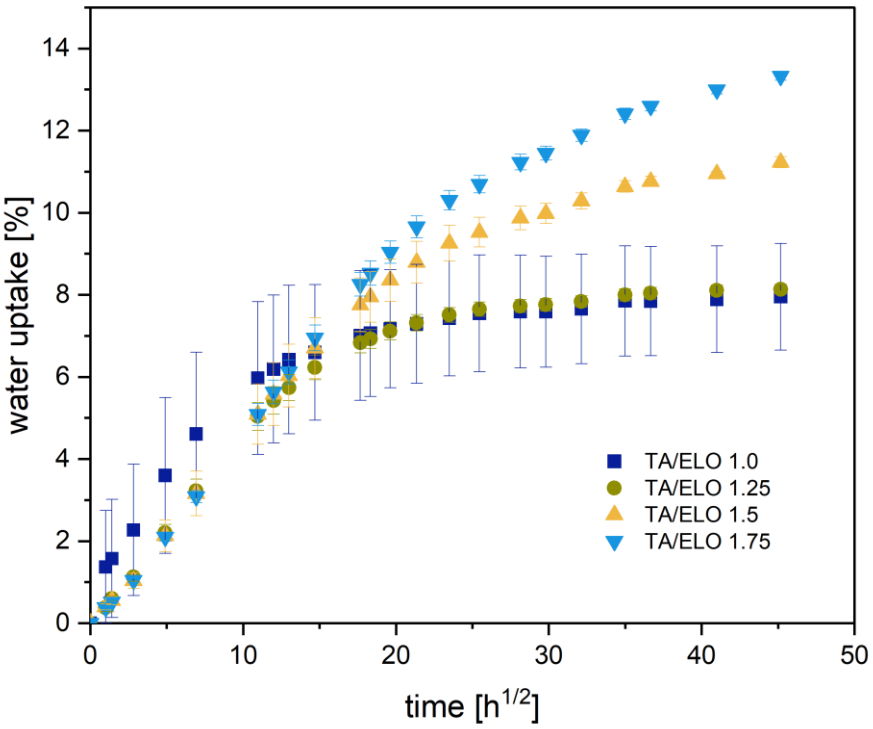

Figure 38: Water uptake of various TA/ELO thermosets.

4.7 Recycling of TA/ELO

4.7.1 Mechanical recycling

4.7.1.1 Preliminary investigation

As already stated in chapter 4.1, the presence of ester bonds and the formed hydroxyl groups after the curing reaction should confer TA/ELO thermoset with recycling capacity through transesterification reaction. To investigate the mechanical recyclability of TA/ELO, cured TA/ELO samples were ground through ball milling. The obtained TA/ELO powder could successfully be hot-pressed to form recycled TA/ELO samples. When looking at the FTIR spectra of the original, ball-milled powder and recycled TA/ELO samples after hot-pressing the powder for 30 min at 160 °C, no striking difference can be observed (Fig.A- 18). The main molecular structure of the thermoset therefore remains unchanged and the ball-milling grinding is adapted to obtain TA/ELO powder prior to recycling without damaging the core structure of the material. The same peaks of ester bonds around 1745 cm^{-1} in the 3 spectras hint on an occurring transesterification reaction during the recycling process [105].

Preliminary tests were performed to assess the parameters needed to successfully hot-press homogeneous recycled TA-ELO samples (chapter 3.2.4).

4.7.1.2 Flexural properties of recycled TA/ELO samples

Various hot-pressing temperatures (115 °C, 130 °C, 145 °C and 160 °C) and hot-pressing time (1 or 2 h) were deliberately chosen to investigate the impact they could have on the mechanical properties of the recycled TA/ELO and to determine the parameters needed to maximize recycling efficiency. This chapter focuses on the recycling of TA/ELO 1.5 and 2.0 as these materials exhibited the most interesting mechanical results in chapter 4.4.3.

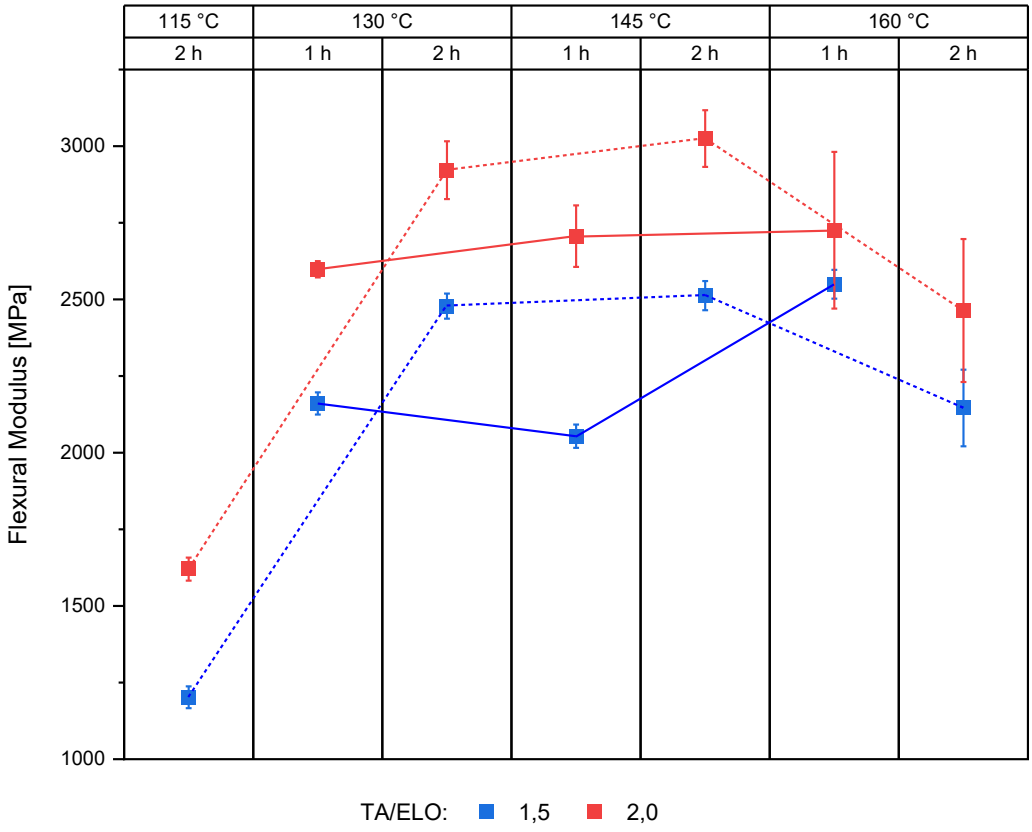

Figure 39: Flexural modulus of TA/ELO 1.5 and 2.0 recycled at various temperatures for 1 (continuous line) and 2 h (dotted line). Adapted from [S15].

Figure 39 shows the evolution of the flexural modulus for TA/ELO 1.5 and 2.0 recycled at various temperatures and times. Similar to the original materials, recycled TA exhibit higher stiffness with a higher TA content.

It can be seen that the pressing time has a great impact on the modulus of the recycled samples. When hot-pressing at 130 °C and 145 °C, the modulus obtained is much higher when hot-pressing the powder for 2 h instead of 1 h. This can be linked to the stiff chemical structure of TA/ELO due to the rigid gallic structure of TA. With the high

amount of phenol groups, molecular motion is difficult and prolonged hot-pressing time is needed for allowing molecular motion and transesterification between the ester and hydroxy groups. However, a clear decline of stiffness for TA/ELO 1.5 and 2.0 is observed when hot-pressing 2 h at 160 °C instead of 1 h. One explanation could be the high oxidation occurring at elevated temperature and at prolonged time. In fact, when looking at Fig.A- 19, recycled samples at 160 °C for 2 h have a very dark color. The highest stiffness values were obtained when hot-pressing at 130 °C or 145 °C for 2 h. When comparing the moduli obtained with the virgin materials (Tab. 11), it can be seen that recycled TA/ELO samples can recover the original stiffness and, in some case, even exceed it. A recycling temperature of 115 °C seems to be too low to have a significant bond-exchange rate as very low moduli were obtained.

Tab. 11: Flexural modulus of TA/ELO 1.5 and 2.0 virgin, and TA/ELO 1.5 and 2.0 recycled 2 h at 130 °C and 2 h at 145 °C

Material	Virgin material [MPa]	Recycled 2 h at 130 °C [MPa]	Recycled 2 h at 145 °C [MPa]
TA/ELO 1.5	2308 ± 99	2478 ± 41	2512 ± 48
TA/ELO 2.0	2986 ± 42	2922 ± 94	3025 ± 93

Figure 40 depicts the flexural strength obtained for the recycled samples. Again, recycling at 115 °C is not recommended, as the tensile strengths obtained are very low. The lowest tensile strengths were observed when recycling for 2 h at 160 °C, which hints at the high oxidation occurring. A prolonged recycling time was found to be beneficial for recycling temperatures of 130 and 145 °C, as the strength increased. The highest flexural strengths obtained for the recycled samples were 33.2 MPa for TA/ELO 1.5 and 31.5 MPa for TA/ELO 2.0, both observed with a recycling of 2 h at 130 °C. If we define recycling efficiency as the ratio between the strength of the recycled sample and the strength of the virgin sample, the maximum recycling efficiency is 46 % for TA/ELO 1.5 and 48 % for TA/ELO 2.0.

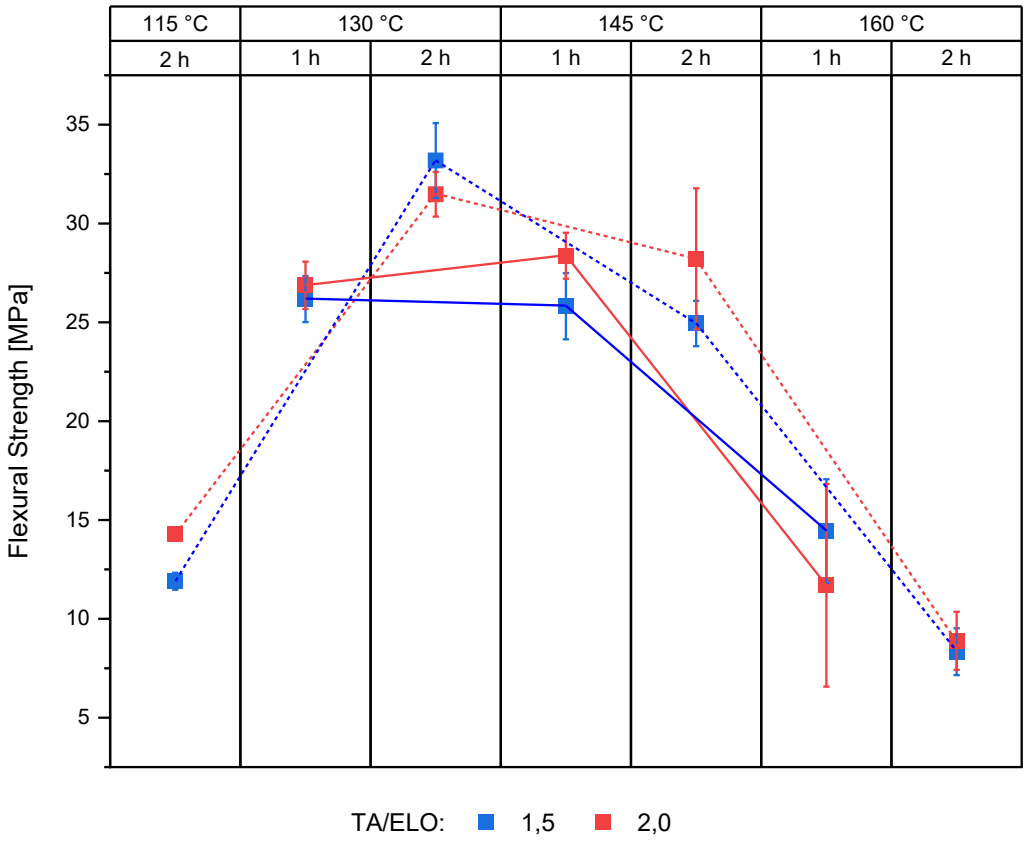

Figure 40: Flexural strength of TA/ELO 1.5 and 2.0 recycled at various temperatures for 1 (continuous line) and 2 h (dotted line). Adapted from [S15].

The reasons for the loss of strength during the recycling process are multiple. First of all, during the recycling process, not all the TA/ELO particles could interact and bind together. This observation is particularly flagrant in Figure 41, where yellowish particles that didn't participate in the bond exchange reaction are still visible inside the material whereas the rest of the material has a rather dark color. The presence of particles that do not bind to the rest of the material creates a stress peak during loading and therefore reduces the strength of the material. Additionally, upon closer inspection of the fracture surface of the recycled samples (Figure 42), some traces of TA/ELO powder remain identifiable. Consequently, the transesterification reaction can only take place at the interface between closely adjacent powders. Hence, transesterification only occurs locally and reduces the recycling efficiency. Furthermore, Zhou et al. [124] showed in their work that the presence of flexible chains in a material helps improve recycling efficiency, as it facilitates chain mobility for bond exchange reaction. The presence of multiple phenol groups in TA/ELO hinders chain mobility, and in addition, no transesterification catalyst was added. Catalysts that promote transesterification have shown to enhance recycling efficiency [172,173]. The particularly slow bond exchange rate in TA/ELO can be deduced from the low stress relaxation observed for TA/ELO even at elevated temperatures (Fig.A- 20).

However, despite the low recycling efficiency observed with TA/ELO, the maximum flexural strengths obtained after recycling are still high, especially when compared with EVO-based thermosets (Tab. 4).

Figure 41: Microscopy image of TA/ELO 2.0 recycled at 145 °C for 2 h. Length of the scale: 2000 µm.

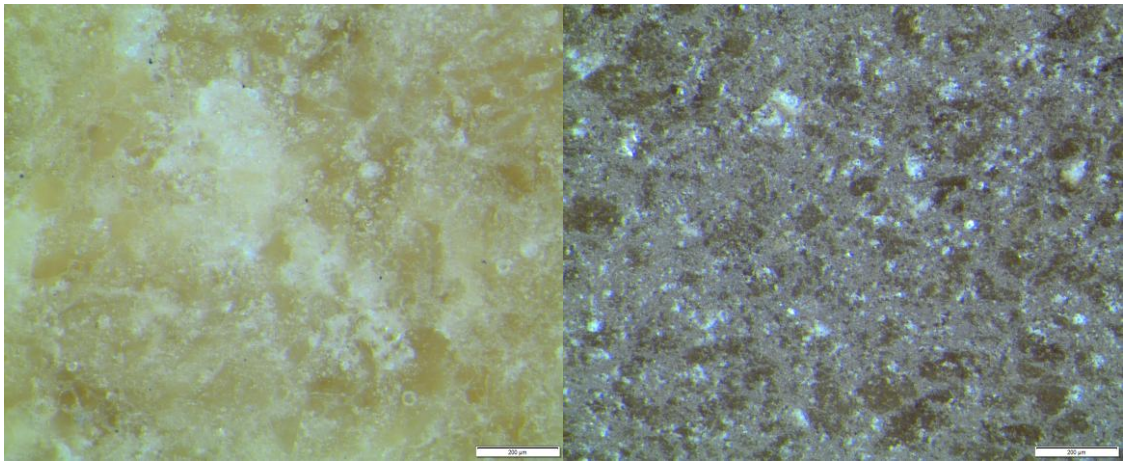

Figure 42: Microscopy images of TA/ELO 1.5 recycled at 130 °C (left) and at 145 °C (right) for 2h. Length of the scale: 200 µm.

4.7.2 Solvolysis

The TA/ELO thermoset, containing a multitude of ester bonds, is prone to solvolysis. In fact, the ester moieties can undergo basic hydrolysis under mild conditions [174]. Figure 43 studies the decomposition of TA/ELO 1.5 in NaOH at different temperatures: room temperature, 40 °C and 60 °C. At 60 °C, TA/ELO 1.5 can be decomposed in under an hour. Decomposition at 40 °C is a bit slower and requires 3 h. TA/ELO 1.5 can also undergo decomposition in a NaOH solution at room temperature, but the process requires 5 h.

The decomposition behavior of TA/ELO 2.0 is quite similar (Fig.A- 21), as the fundamental network is already defined within a few reactions during the initial phase of curing and cannot vary much.

Sodium hydroxide (NaOH) is one of the most common chemicals in the industry. It finds application in various processes for manufacturing a multitude of products, such as plastics, soaps, rayon, and textiles. It also serves purposes like disinfecting, and additionally, it is commonly found in household products like drain and oven cleaners [175]. The ability of being able to break down the TA/ELO under mild conditions, using commodity chemicals such as NaOH, is a great advantage over classic epoxy thermosets and is particularly interesting for CF composite applications as it would allow the recovery of the carbon fibers without high technical efforts and without high embodied energy (EE). Densely crosslinked thermosets such as DGEBA usually require severe conditions such as high temperature and high pressure, which constrain the scalability of a chemical recycling process [38].

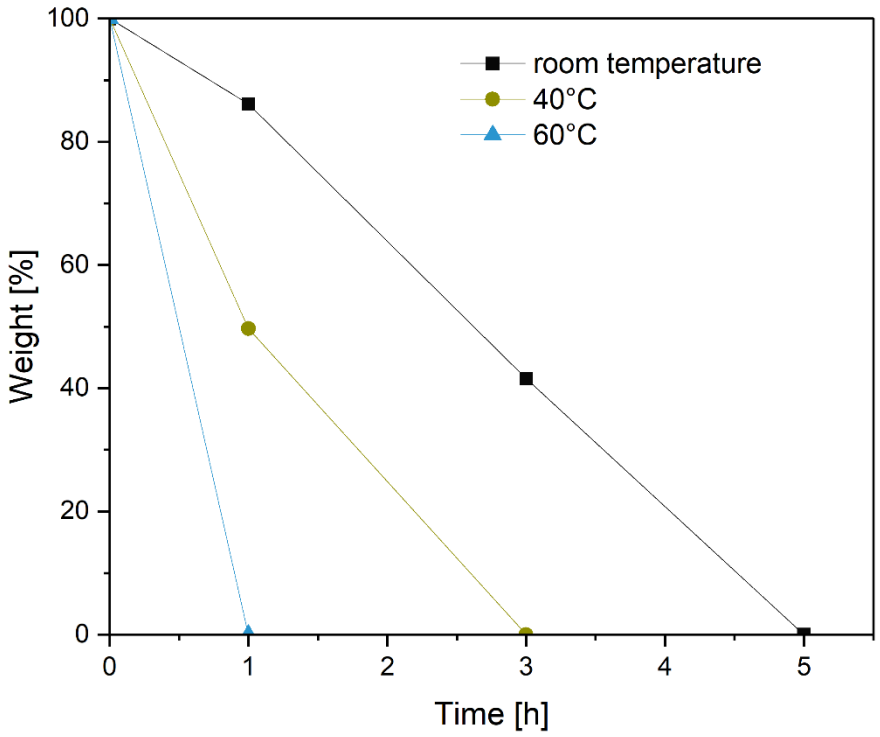

Figure 43: Decomposition of TA/ELO 1.5 in NaOH (1 mol/L) at room temperature, 40 °C and 60 °C.

4.8 Conclusion of chapter 4

EVOs are known to have drawbacks as rather poor mechanical properties can be found in literature. However, this chapter has demonstrated that attractive mechanical and thermal properties can be achieved with ELO cured with the bio-based TA. Despite the poor compatibility of TA with ELO and the absence of a solvent, samples exhibiting strong mechanical properties and high Tg could be obtained by milling TA into a fine powder and facilitating the reaction between the hydroxyl groups of TA and the oxirane groups of ELO by using an excess of hydroxyl groups. It should be noted, however, that while the stiffness can reach values similar to DGEBA-based systems, the strength remains much lower. The mechanical recycling ability of TA/ELO through transesterification and its easy decomposition through solvolysis are great advantages compared to conventional epoxy thermosets.

While this chapter surely demonstrated the potential use of a fully bio-based epoxy thermoset with recycling ability that can be formulated with available resources to obtain a stiff material that outclasses reported mechanical properties for EVO-based epoxies in the literature, the drawbacks also need to be highlighted. The glass transition, due to the complex structure of TA/ELO is very broad and hinders the obtention of a stiff material

at temperatures above 80 °C. Using an excess of TA helped to facilitate the obtention of a dense crosslinked network but will inherently lead to the presence of a lot of unreacted TA particles in the thermoset. Due to the very hydrophilic nature of TA, the water absorption of TA-ELO thermoset is high compared to conventional epoxy systems and constraints its application in humid and wet environments as long term stability and mechanical properties may be affected. The hydrophilicity of plant polyphenols is well-known. To face this problem, hydrophobization of the molecules can be performed. As an example, Liu et al. [176] managed in their work to synthesize a hydrophobic TA. Additionally, there is a need to identify a catalyst capable of significantly accelerating the curing reaction of TA/ELO, thereby reducing the lengthy curing times currently applied and enhancing the attractiveness of the product for industries. A transesterification catalyst might also be considered for improving recycling efficiency.

Finally, vegetable oils are praised in literature for their widespread availability. However, it is crucial to bear in mind that the utilization of edible vegetable oils in the polymer industry may have adverse implications for the long-term security of the food supply chain. To address this concern, a noteworthy study conducted by Fernandes et al. [93] demonstrated that waste cooking oil (used for deep-frying), can be repurposed for epoxy thermoset production. Nevertheless, chemical modifications that would increase the number of double bonds in waste oils to levels comparable to those found in linseed oil would be needed to turn waste products into thermosets with strong mechanical properties.

5 TA/ELO epoxy reinforced with CF for the production of sustainable composites

The potential of TA/ELO to serve as a bio-based replacement to conventional petroleum and BPA-based epoxy resins has been investigated in chapter 4. In order to be utilized in load-bearing applications, the properties of TA/ELO reinforced with fibers must be assessed. This chapter focuses on the manufacturing of TA/ELO CF composites and the characterization of its flexural properties. Later on, the prospects of recycling the manufactured composites through solvolysis to reclaim the carbon fibers and mechanical recycling to reuse composite scraps and leftovers will be presented.

Parts of the results of this chapter were obtained in the thesis of Neumeyer [S6], Frehland [S7], Buchwieser [S12] and Gehringer [S15].

5.1 Flexural properties

As described in chapter 4, TA/ELO, in contrast to conventional epoxy systems, is not a fluid-fluid mixture; instead, it constitutes a homogeneous dispersion of particles (TA) in a fluid medium (ELO). Various standard composite manufacturing processes (VARI, RTM, hot-pressing and vacuum bagging) were explored to produce TA/ELO composites plates using various TA/ELO mixtures and CF fabrics. Due to the uncommon nature of TA/ELO, successful production of composite plates was achieved only through the hot-pressing and vacuum bagging processes. VARI and RTM processes led to unsuccessful attempts and are described in chapters 3.2.5.5 and 3.2.5.6. This chapter focuses on the flexural properties of TA/ELO CF composite plates manufactured using hot-pressing and vacuum bagging (Fig.A- 22 and Fig.A- 23).

5.1.1 Hot-pressing

Figure 45 showcases the results of the flexural testing for the samples manufactured using hot-pressing. TA/ELO 1.5 and TA/ELO 1.75 samples exhibit similar moduli. Among the bio-based samples, a maximum average flexural modulus of 104 GPa was achieved with TA/ELO 1.5 and a V_f of 64.7 %. This value is slightly lower than the maximum stiffness value obtained with CR80: 118 GPa with a V_f of 67.3 %. Even the plate manufactured with CR80 and a V_f of 56.2 % demonstrates higher stiffness than the bio-based samples, with an average modulus of 107 GPa, despite having a lower fiber content. The higher modulus observed with CR80, even with a lower fiber content, can be attributed to the significant number of defects observed in the TA/ELO composites samples. Microscopy images reveal the presence of layers of TA clumps between the CF fabrics and voids in the composite (Figure 44).

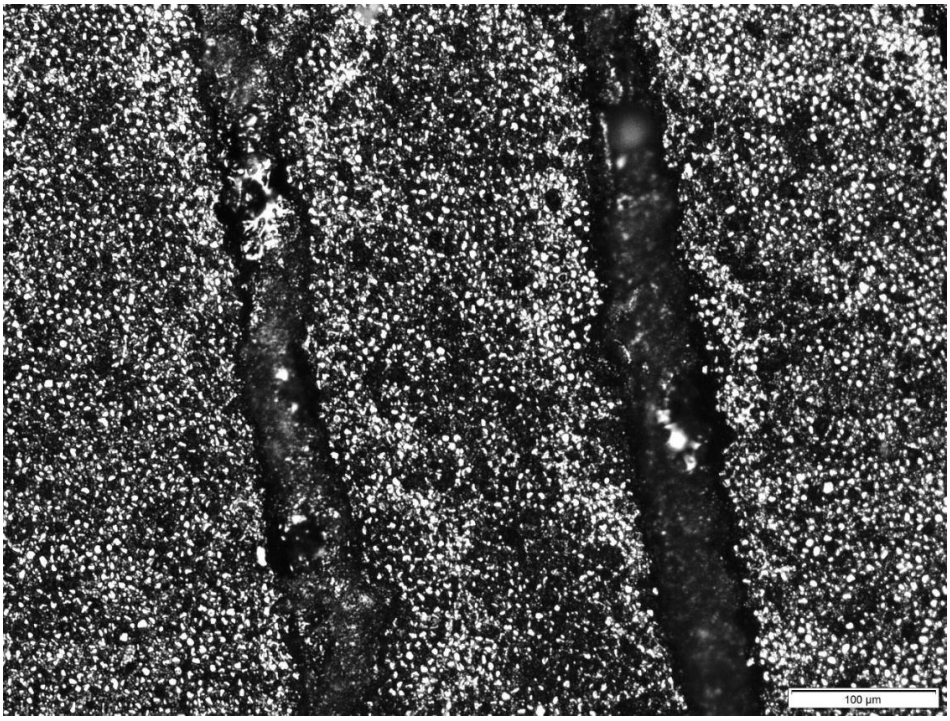

Figure 44: Microscopy image x10 of TA/ELO 1.75 CF composite manufactured with hot-pressing. Length of the scale: 100 µm.

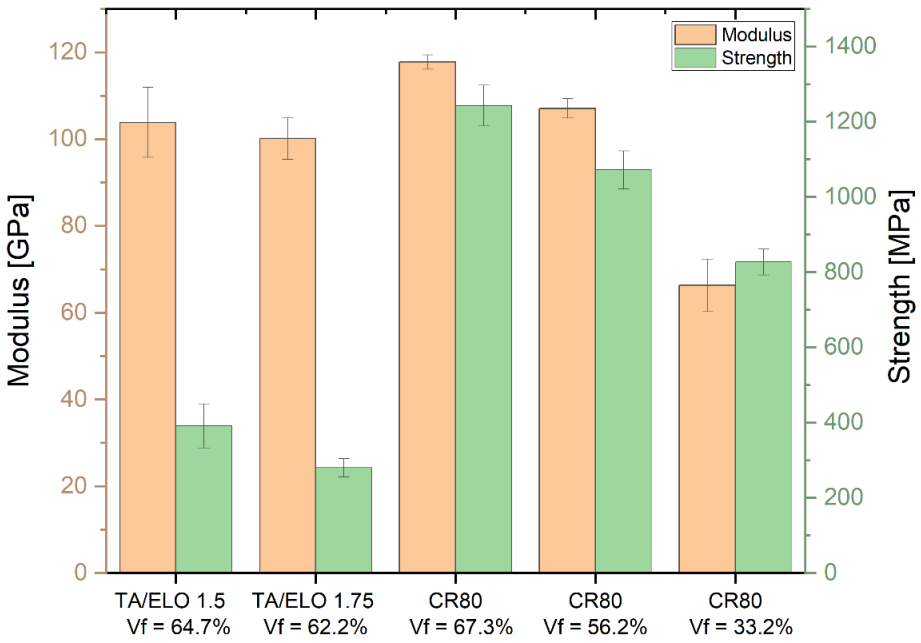

Figure 45: Modulus and strength of the CF-composite plates manufactured with hot-pressing.

Figure 45 also highlights the significant difference in flexural strength observed between samples manufactured with CR80 and TA/ELO. The highest average flexural strength observed for the bio-based samples was 392 MPa (for a V_f of 64.7 %), whereas CR80 achieved a flexural strength of 1243 MPa with a similar fiber content (V_f = 67.3 %). Even a composite plate manufactured with CR80 and a V_f of 33.2 % clearly outperforms the bio-based composites in terms of strength. During flexural testing, delamination of the CF layers was observed (Figure 46), and after testing, spots rich in TA particles in the middle of the CF layers of the composites, along with dry fibers, could be observed (Figure 47).

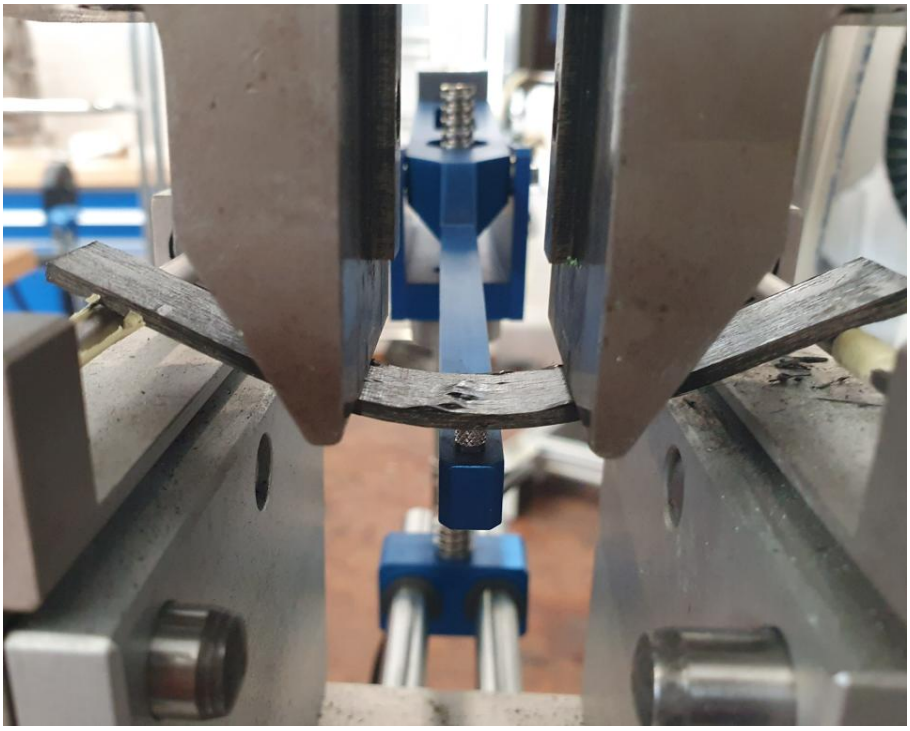

Figure 46: Delamination occurring during flexural testing of the TA/ELO CF composites.

During the hot-pressing process, owing to the abundance of TA particles larger than the gaps between CF fiber, their tendency to agglomerate, and the poor reactivity of TA/ELO, the fibers likely functioned as a filter. This caused the oil to be pressed to the outer layers of the composite, thus leaving the inner core with some dry spots (Figure 47).

Figure 47: TA particles and dry spots in the TA/ELO composites. Sample after flexural testing.

The high amount of defects (such as agglomeration of TA particles, presence of dry fibers, and TA-rich spots) observed in the TA/ELO composites is undoubtedly impacting the mechanical properties of the composites. While relatively high stiffness values can still be observed for TA/ELO composites, with flexural moduli exceeding 100 GPa, the strength is significantly affected. This is due to the failure of the TA/ELO matrix to adequately disperse throughout the composites and fully impregnate all the fibers, consequently limiting the composite's ability to withstand high loads.

5.1.2 Vacuum-bagging

Another composite-processing technique, vacuum-bagging, was investigated to try enhancing the mechanical properties of TA/ELO composites. UD SGL CF fabrics were compacted using the vacuum-bagging technique at either 400 or 600 mbar, as described in chapter 3.2.5.4. The same procedure was repeated using towpregs. Relatively low vacuum values were chosen to attempt to avoid the filtering effect observed in the hot-pressing process and to ensure full impregnation of the fibers.

Figure 48 shows the flexural properties of TA/ELO composites manufactured with UD SGL fabric. It can be observed that the achieved V_f is much lower than with hot-pressing (Figure 45). Despite the lower V_f, slightly higher flexural strengths were observed than in the TA/ELO plates manufactured with hot-pressing. This suggests better fiber impregnation with the vacuum bagging technique. Improved mechanical properties were obtained when applying a vacuum of 400 mbar, as it is expected to result in better compaction between the fiber layers. The best mechanical properties obtained with the UD SGL fabric and vacuum bagging were a modulus of 56 GPa and a flexural strength of

425 MPa achieved with TA/ELO 1.5 and a vacuum of 400 mbar. However, the strength values obtained for TA/ELO CF composites are still much lower than the reference composite plates manufactured with CR80 (Figure 45).

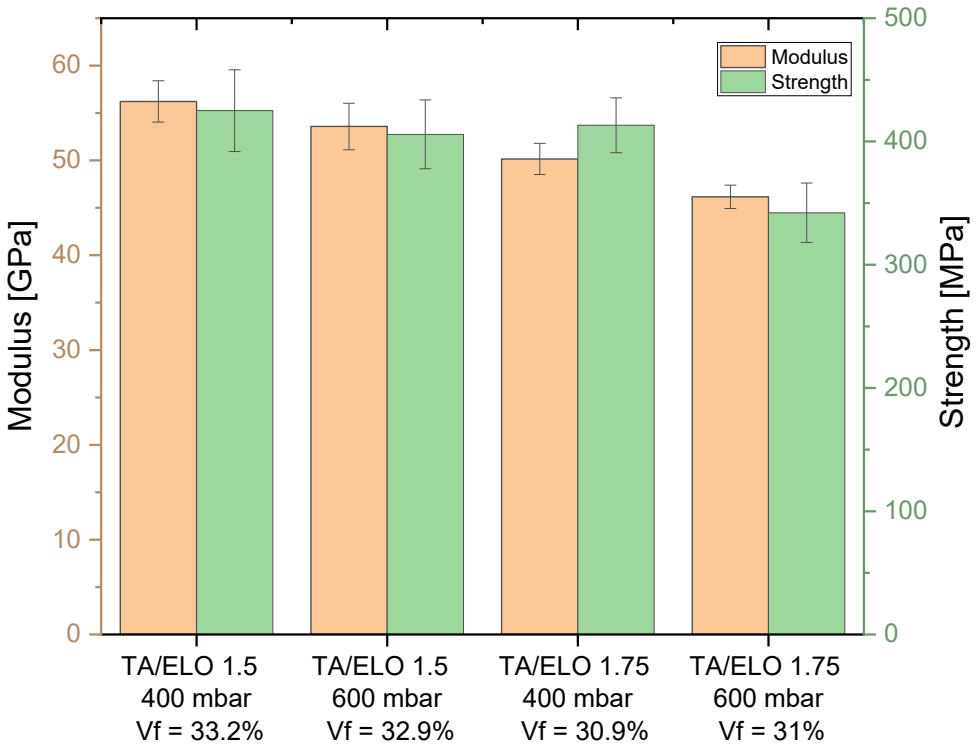

Figure 48: Modulus and strength of the TA/ELO CF-composites plates manufactured with vacuum bagging. CF fabric used: UD SGL.

The composites manufactured with towpregs and the vacuum bagging technique (Figure 51) have the lowest V_f (around 24 %). Again, better mechanical properties were obtained with a vacuum of 400 mbar. TA/ELO 1.5 manufactured with towpregs and 400 mbar shows a flexural strength of 387 MPa (Figure 51), a value close to the maximum flexural strength (425 MPa) obtained with TA/ELO 1.5 and UD SGL fabric with a V_f of 33.2 % (Figure 48). Hence, even with a lower fiber content, TA/ELO composites made with towpregs do not experience a significant loss of strength compared to TA/ELO composites made with UD SGL fabric. Using towpregs to manufacture TA/ELO CF composites seems to be a suitable manufacturing method for obtaining high strength despite a low fiber content.

However, when testing under flexural load, delamination still occurred in the samples made with towpregs or UD SGL fabric, and dry TA particles between the CF layers, similar to those shown in Figure 47, were still visible. Even though better impregnation of the CF fibers is expected with the vacuum bagging technique, the filtering effect caused by a large amount of TA particles, which are larger than the gaps between CF

fibers, cannot be completely avoided. Figure 52 shows an example of TA/ELO composite plates manufactured with the vacuum bagging technique (with UD SGL or towpregs). A high excess of TA/ELO with a sticky consistency (indicating a mixture rich in ELO and poor in TA) absorbed by the breather fabric is visible. This phenomenon was observed for composite plates produced with UD SGL fabrics and towpregs. The applied vacuum seems to be high enough to extract a lot of oil out of the composite plate, leaving some dry spots in the composite. Furthermore, voids and TA agglomerates are still visible in the composites, as seen in Figure 49 and Figure 50.

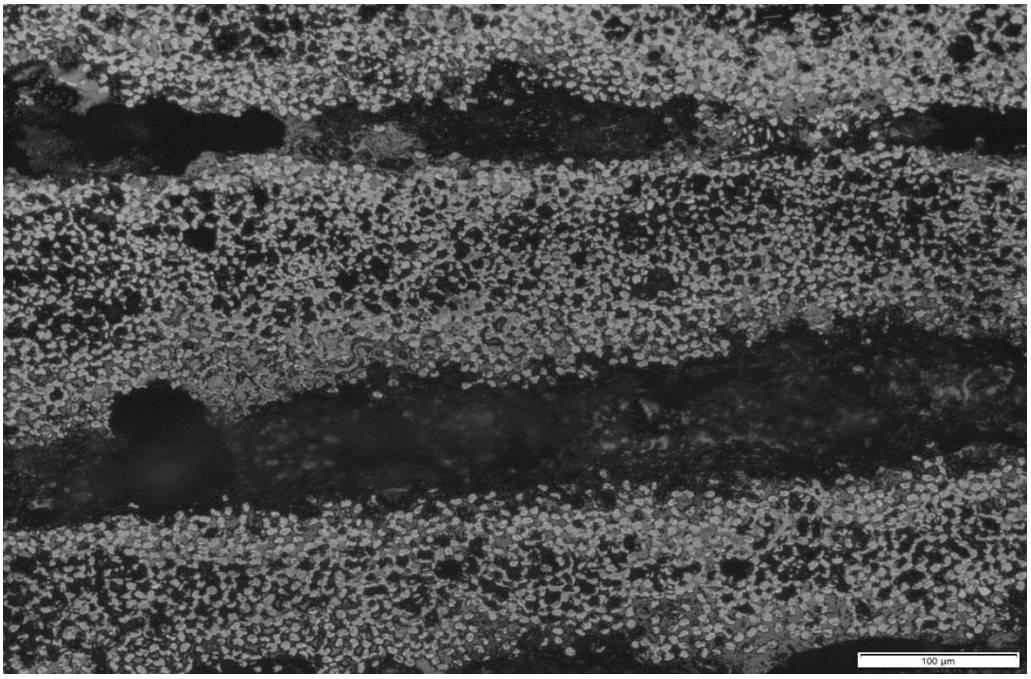

Figure 49: Microscopy image x10 of TA/ELO 1.5 CF composite manufactured with UD SGL fabric and vacuum bagging (600 mbar). Length of the scale: 100 µm.

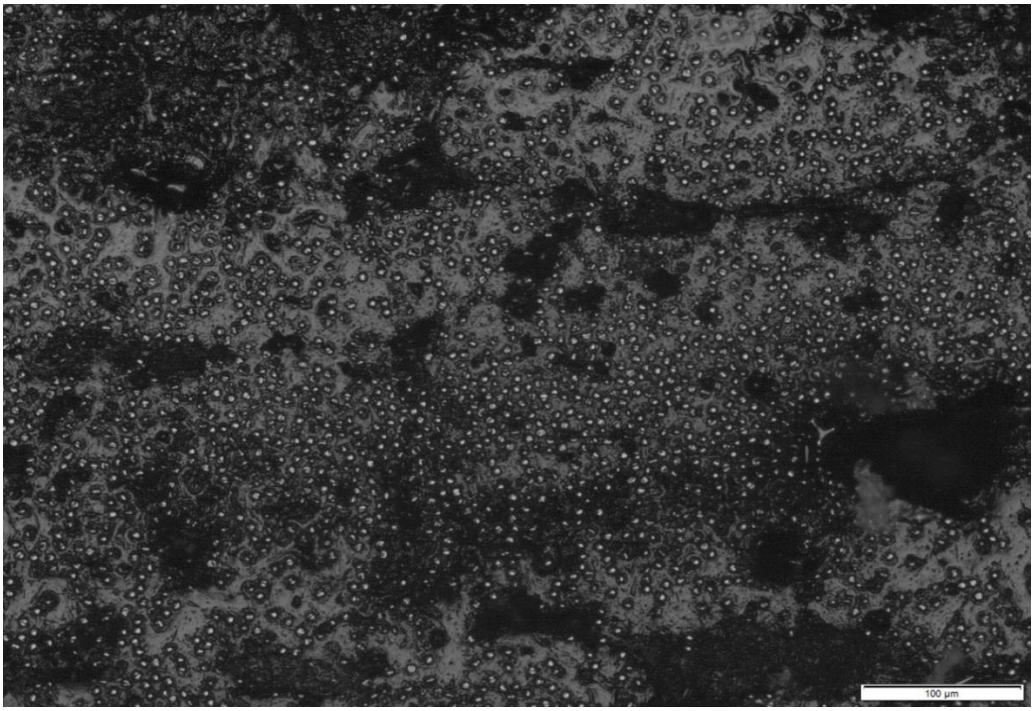

Figure 50: **Microscopy image x10 of TA/ELO 1.5 CF composite manufactured with towpregs and vacuum bagging (400 mbar). Length of the scale: 100 µm.**

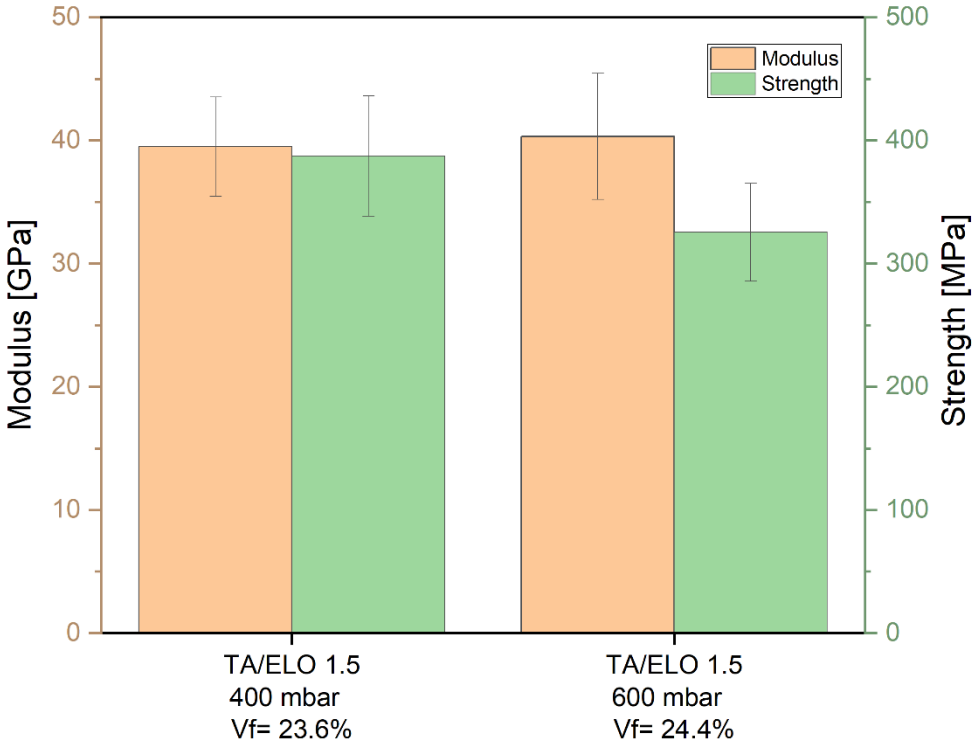

Figure 51: **Modulus and strength of the TA/ELO CF-composites plates manufactured with vacuum bagging and towpregs.**

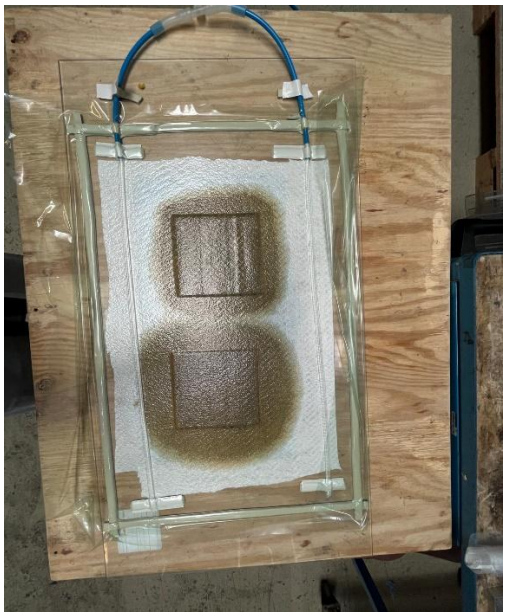

Figure 52: Example of TA/ELO CF composites plates after curing manufactured with UD SGL fabric or towpregs and vacuum bagging technique.

5.2 Recycling of TA/ELO composites

5.2.1 Mechanical recycling

The chapter 4.7.1 demonstrated the mechanical recyclability of TA/ELO, a noteworthy feature for composite applications. In fact, this attribute holds particular interest in the realm of composites, as having a matrix material that can undergo mechanical recycling can strongly help make the composite industry more sustainable as it would open up possibilities such as:

- Constructing new composites from damaged or end-of-life composite scrap. By shredding the composite into a fine powder and utilizing hot-pressing techniques, the production of novel composites becomes feasible.
- Repurposing fibers offcuts and resin leftovers from the composite manufacturing process to manufacture new composite parts. The unused resin can be cured, transformed into a powder, mixed with short or long fibers, and then hot-pressed to produce new composite materials.

These specific points will be the focus of investigation in this chapter. Flexural testing will be used to assess the performance of the recycled samples.

5.2.1.1 Recycling end-of-life composites scraps

To simulate the recycling of damaged or end-of-life CF composite scraps, powdered TA/ELO 1.5 and 2.0 mixed with 5 or 10 wt.% of CF powder were hot-pressed into recycled composites samples according to chapter 3.2.4 at 130 and 160 °C for 2 h.

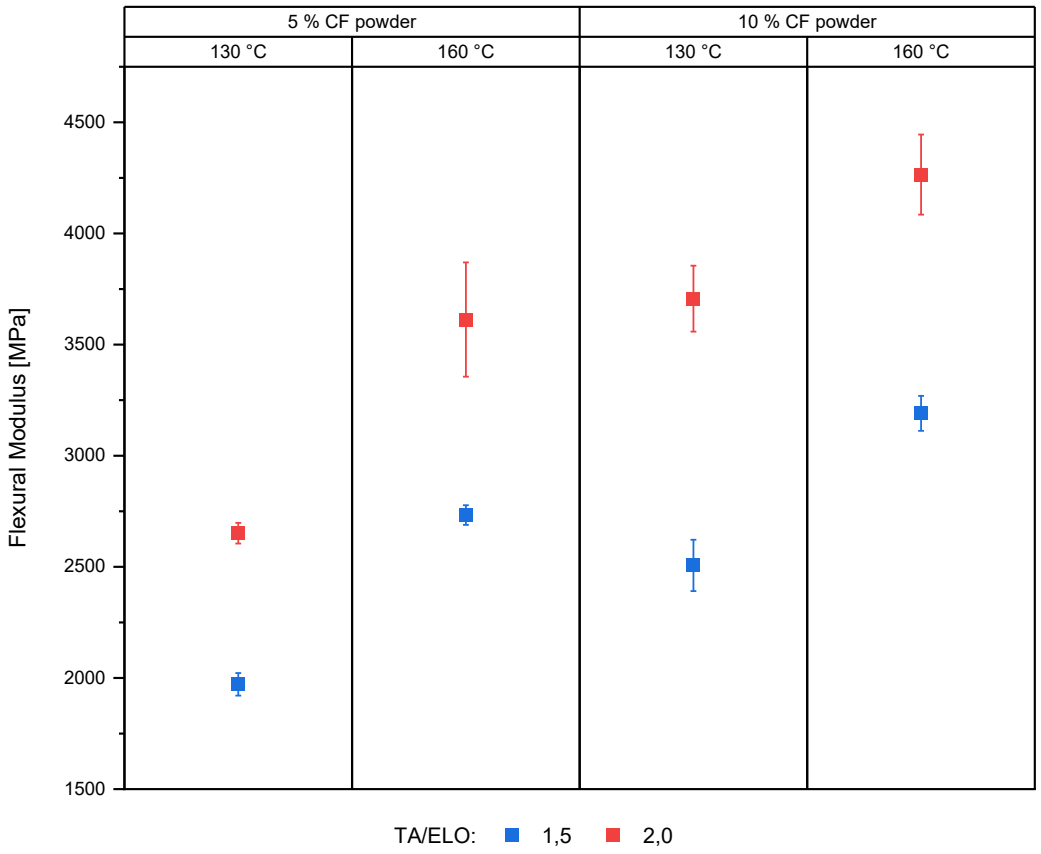

Figure 53: Flexural moduli of recycled TA/ELO 1.5 and 2.0 CF composites with 5 and 10 wt.% CF powder. Samples hot-pressed at 130 and 160 °C for 2 h. Adapted from [S15].

Figure 53 shows the flexural moduli of the recycled composites scraps hot-pressed at 130 and 160 °C. As observed in chapter 4.7.1.2, the stiffness of the samples manufactured with TA/ELO 2.0 is higher than those prepared with TA/ELO 1.5. However, unlike in chapter 4.7.1.2, higher moduli are observed when hot-pressing at 160 °C. Despite the occurring oxidation, a high recycling temperature seems favorable for obtaining a compact recycled composite sample. When comparing the moduli of the recycled TA/ELO composites samples with the recycled TA/ELO samples (Tab. 12 and Tab. A- 3), it can be said that a reinforcing effect is only observed when a hot-pressing temperature of 160 °C is applied as the moduli of the recycled composites increase. A high temperature seems to favor a better flowing of TA/ELO, and hence, a better impregnation of the CF powder.

Tab. 12: Flexural moduli obtained for recycled TA/ELO 1.5 and recycled TA/ELO 1.5 CF composites.

Material	Recycled at 130 °C for 2 h [MPa]	Recycled at 160 °C for 2 h [MPa]
TA/ELO 1.5	2478 ± 41	2146 ± 125
TA/ELO 1.5 + 5 wt.% CF	1972 ± 51	2733 ± 44
TA/ELO 1.5 + 10 wt.% CF	2507 ± 115	3191 ± 79

Likewise, when comparing the flexural strength of the recycled TA/ELO composites samples with the recycled TA/ELO samples (Figure 55, Tab. 13 and Tab. A- 4), higher strength values could only be observed for the recycled composites samples when hot-pressing at 160 °C. When hot-pressing at 130 °C, lower strength values were observed.

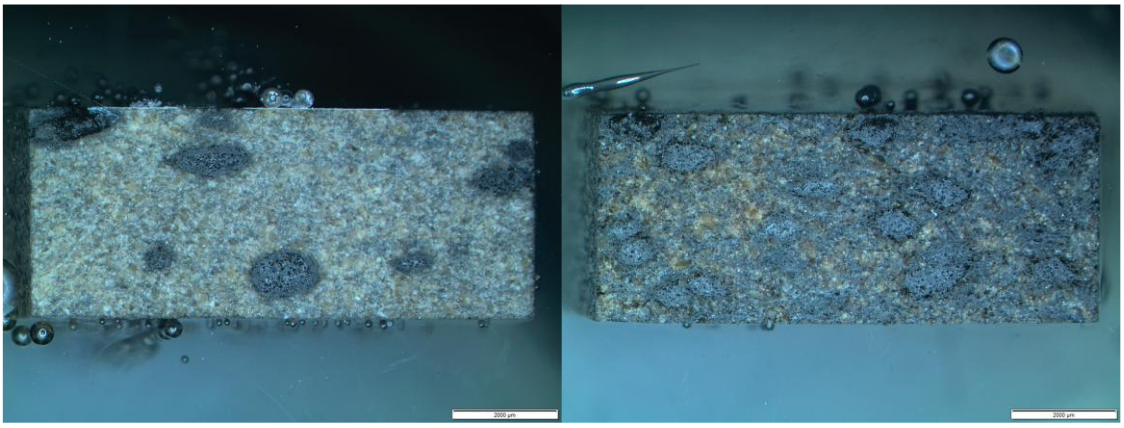

Figure 54: Microscopy image of TA/ELO 1.5 CF composite with 5 (left) and 10 wt.% of CF powder (right) recycled at 130 °C for 2 h. Adapted from [S15]. Length of the scale: 2000 µm.

Interestingly, the higher flexural strength value for all the recycled samples was obtained for recycled TA/ELO 1.5 hot-pressed at 130 °C (33.2 MPa, Figure 40) and not with a recycled TA/ELO composite sample. As can be seen from Figure 54 the CF powder tends to agglomerate and a very bad dispersion of the CF powder is therefore obtained in the samples. This leads to locally reinforced areas and therefore to stress concentrations, affecting the strength of the material.

Tab. 13: Flexural strengths obtained for recycled TA/ELO 1.5 and recycled TA/ELO 1.5 CF composites.

Material	Recycled at 130 °C for 2 h [MPa]	Recycled at 160 °C for 2 h [MPa]
TA/ELO 1.5	33.2 ± 1.9	8.3 ± 1.2
TA/ELO 1.5 + 5% wt. CF	19.8 ± 0.6	20.5 ± 2.0
TA/ELO 1.5 + 10% wt. CF	24 ± 1.4	15.8 ± 0.7

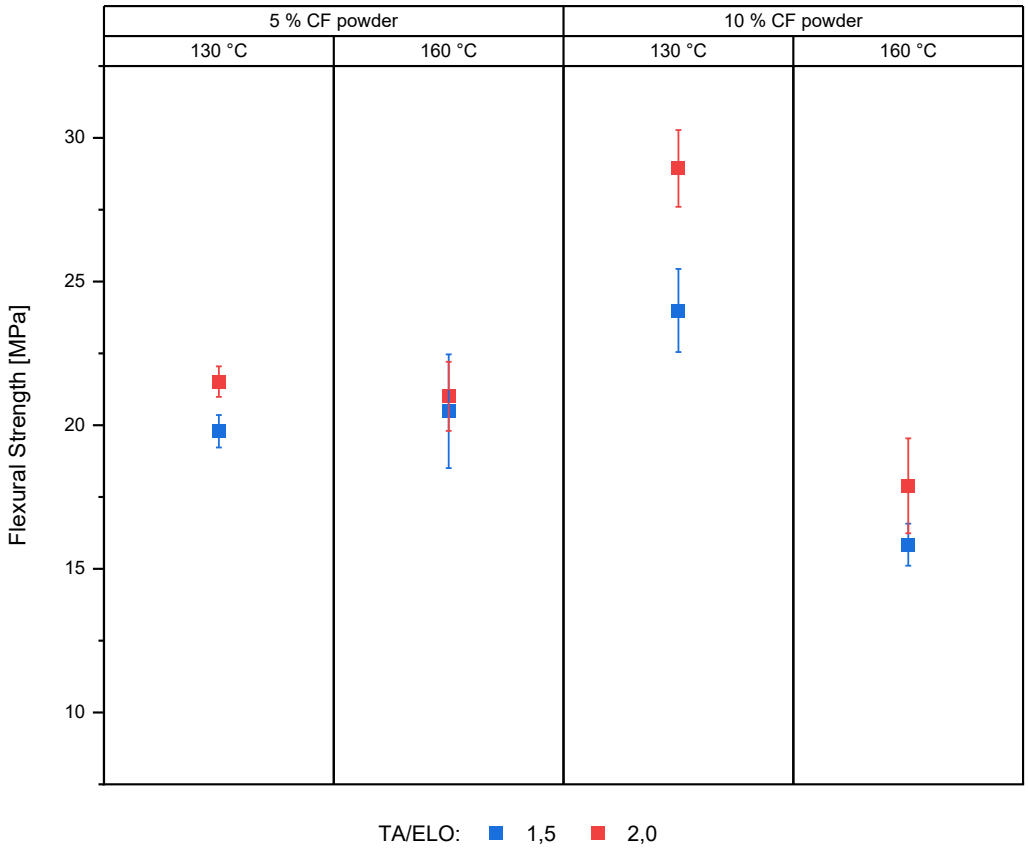

Figure 55: Flexural strengths of recycled TA/ELO 1.5 and 2.0 CF composites with 5 and 10 wt.% of CF powder. Samples hot-pressed at 130 and 160 °C for 2 h. Adapted from [S15].

5.2.1.2 Repurposing resin and fibers leftovers into composites

To simulate the repurposing of fibers offcuts and resin leftovers into new composites, powdered TA/ELO 1.5 and 2.0 were mixed with 10 wt.% hand-cut CF fibers (approximate length of 5 mm) and hot-pressed according to 3.2.4 at 130 and 160 °C for 2 h.

Figure 56 shows an exemplary microscopic image of the inner surface of the recycled composite. Too many dry fibers were present, which hints at a very poor impregnation ability of the TA/ELO powder during hot-pressing. In order to avoid the dispersion of dry fibers in the testing lab and damage to the electronics of the testing machines, these recycled composites samples could not be tested under flexural load.

The tendency of fibers to agglomerate, in addition to the lack of mobility of the TA/ELO chains, seems to hinder a proper impregnation of long fibers during the recycling process, even when a high recycling temperature of 160 °C is applied.

Therefore, the idea of repurposing TA/ELO leftovers with off-cut fibers doesn't seem feasible, and a transesterification catalyst might be a potential solution to accelerate the transesterification reaction and bond-exchanges, facilitating the flowing of TA/ELO and the impregnation of long fibers.

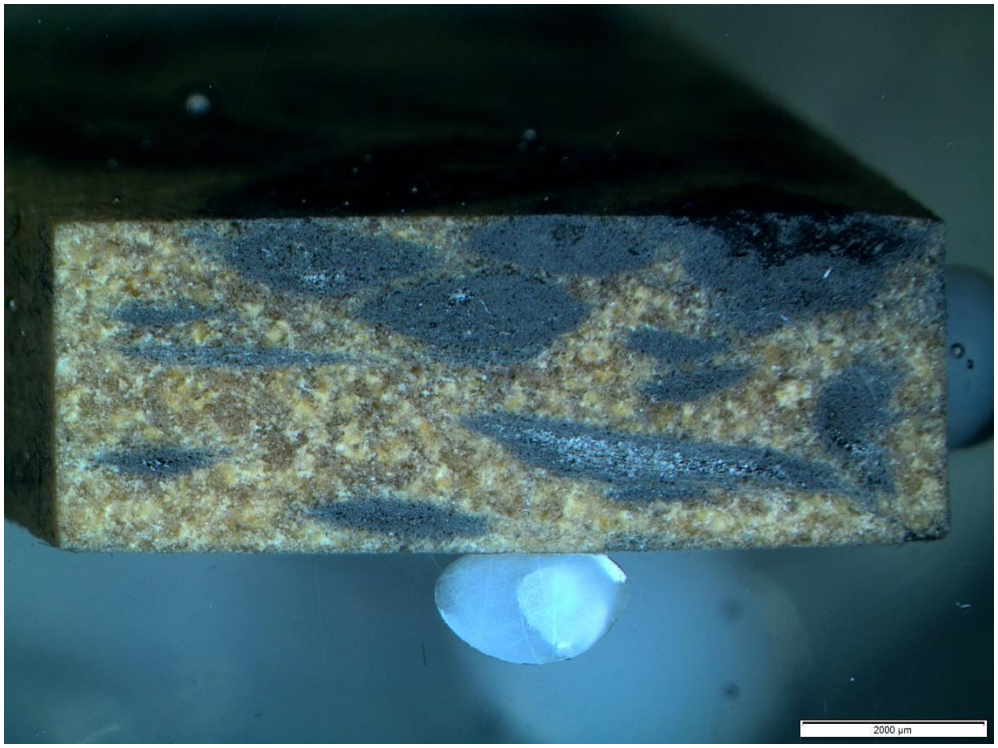

Figure 56: Microscopy image of TA/ELO 2.0 with 10 wt.% of long fibers recycled at 130 °C for 2 h. Adapted from [S15]. Length of the scale: 2000 µm.

5.2.2 Solvolysis: recovery of the CF

CF are known for their expensive production and high energy requirements. A crucial aspect of advancing sustainability in the composite industry is the ability to efficiently recover clean fibers from composites at the end of their life without high technical effort and energy consumption. Thanks to the ability of TA/ELO to break down in NaOH, clean CF could successfully be recovered from TA/ELO composites after immersion in NaOH solution for 1 day at ambient temperature, washing in water and drying, as shown in Figure 57.

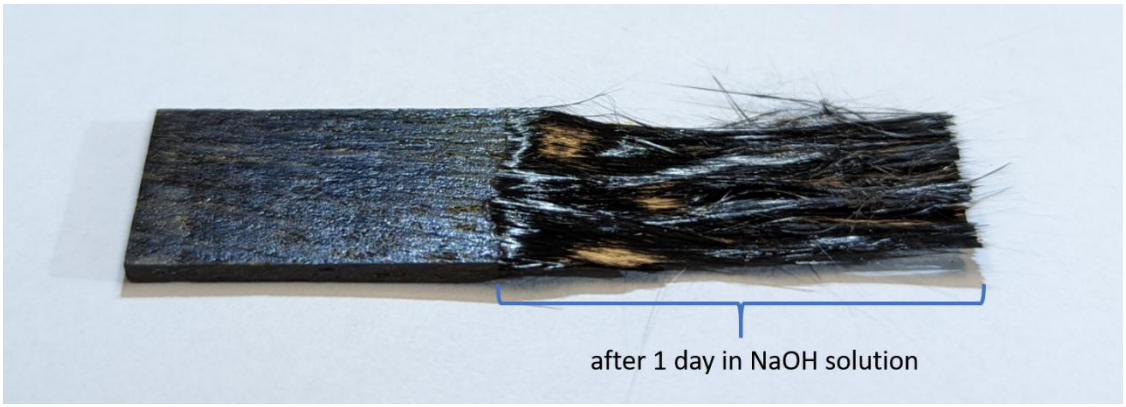

Figure 57: TA/ELO 1.5 composite (80 x 10 x 2 mm) with UD CF dipped in NaOH solution. Recovery of the CF after 1 day at ambient temperature.

The recovered fibers from Figure 57 were analyzed with a SEM. Figure 58 shows clean CF with no signs of TA/ELO residues. The interface between immersed TA/ELO composite in NaOH solution and non-immersed TA/ELO composite is shown in Fig.A- 24. The dissolution of TA/ELO in NaOH is clearly visible. If recovered UD fibers have the tendency to be messy due to the washing process after immersion in NaOH (Figure 57), the organization of the recovered CF remains intact when using a stitched UD CF fabric as seen in Fig.A- 25.

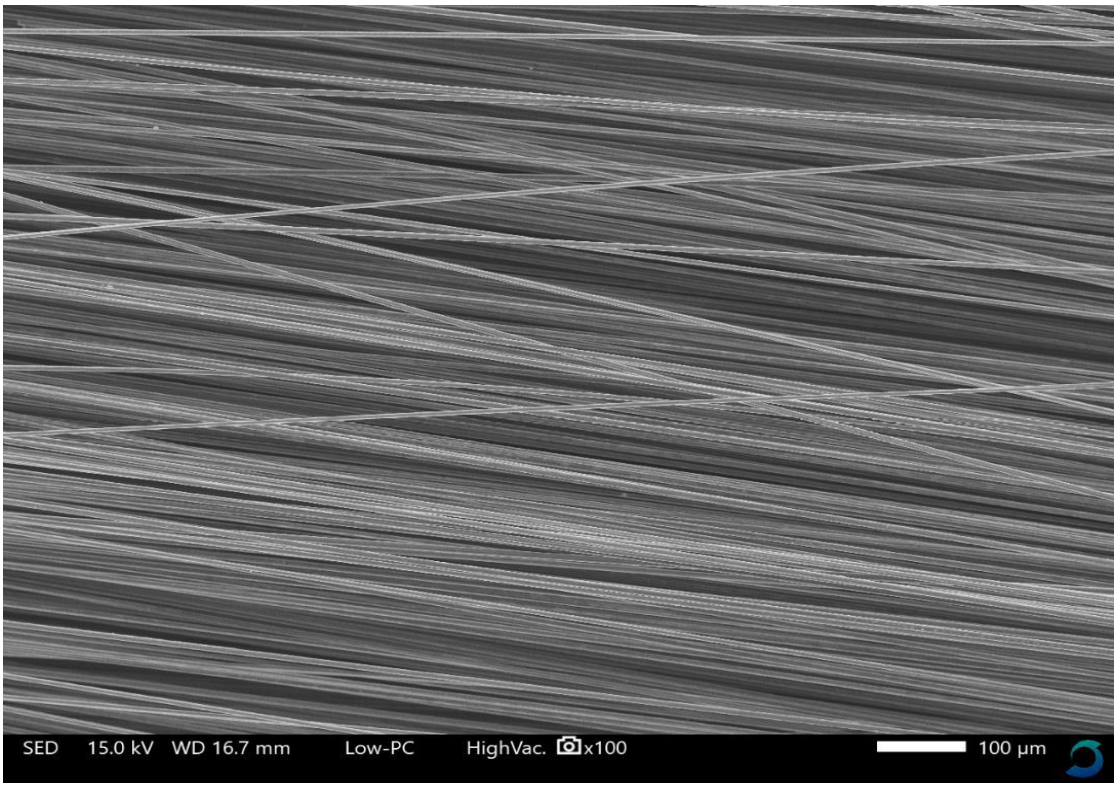

Figure 58: SEM picture of recovered CF after immersion in NaOH solution, washing in water and drying.

5.3 TA/ELO composites demonstrators

The strength of the TA/ELO-CF composites was shown to be inferior to DGEBA-based CF composites. Nevertheless, this chapter demonstrates the capability of TA/ELO to be used as a matrix for carbon fiber-reinforced composites and processed into valuable composite components. A longboard and a pipe were manufactured using TA/ELO and CF as reinforcement fibers.

5.3.1 Longboard

A longboard demonstrator was manufactured using TA/ELO resin, CF fabrics and a plywood core (Figure 59). Two layers of plywood (4 mm thick) were bonded together with TA/ELO 2.0 and cured at 70 °C for 4 h. Clamps were used to apply an even pressure on the 2 layers of plywood during curing. TA/ELO 2.0 exhibits a wood glue-like viscosity and the highest stiffness among the TA/ELO mixtures as shown in chapter 4.4.3. In the next step, two layers of +/- 45° CF fabric (245 g/m²) were applied to the top, and two layers of +/- 45° CF fabric (245 g/m²) plus two layers of unidirectional (UD) fabric (280 g/m²) were applied to the bottom. The CF fabrics were impregnated with the TA/ELO 1.0 mixture using a sponge roller to impart flexibility to the longboard, then coated with a release film. The entire setup was placed in a vacuum bag and cured under 400 mbar at 70 °C for 18 h. Finally, a top layer of TA/ELO 1.5 was applied to the upper side and cured at 90 °C for 18 h. The result is shown in Figure 59.

Low curing temperatures were deliberately chosen for safety reasons to prevent degradation of the plywood during curing. Trucks and wheels were mounted on the longboard and it could successfully be ridden.

Figure 59: Longboard made with a plywood core, CF fabrics and TA/ELO.

5.3.2 Pipe

Towpregs were manufactured with TA/ELO 1.5 and CF tows according to chapter 3.2.5.1. The CF tows passing through the impregnation drum can be seen in Fig.A- 26. The towpregs were then wound in a +/- 45 ° pattern on a metal mandrel (diameter of 20 mm) that was previously coated several times with a release agent.

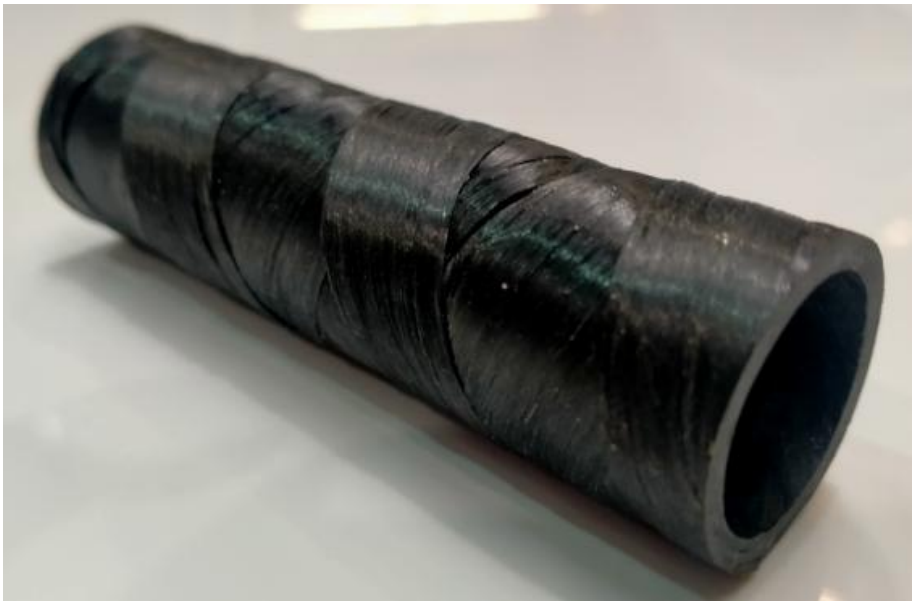

Figure 60: Pipe made with TA/ELO-CF towpregs winded on a metal mandrel.

The wound metal mandrel was covered with a release film and placed in an oven for curing (16 h at 120 °C + 3 h at 140 °C). After curing, the pipe could be removed from the mandrel as shown in Figure 60. Microscopic images of the composite structure in the center part of the pipe were taken and can be seen from Fig.A- 27.

5.4 Conclusion of chapter 5

Various CF fabrics and composites processing techniques were investigated to manufacture TA/ELO CF composites. While VARI and RTM led to unsuccessful attempts, composites plates could be manufactured using hot-pressing and vacuum bagging. However, the size of the TA particles, even after milling, and their tendency to agglomerate still remain issues, as approximately half of the TA particles are still larger (Figure 28) than a CF fiber (~ 10 µm). Dry TA particles and some dry fibers were clearly identified in the manufactured TA/ELO composites. The presence of these defects strongly affects the strength of TA/ELO CF composites and slightly impacts the modulus. Compared to reference CF composites produced with the resin CR80, TA/ELO CF composites clearly underperform in terms of strength. Using towpregs and vacuum bagging appears to be the most suitable configuration for producing TA/ELO CF composites with high strength, despite low fiber content and the presence of a large number of defects.

In order to solve this problem, it seems necessary to have TA powder with a size significantly lower than the size of a fiber in order to allow the TA/ELO resin to properly disperse in the composite fabric and fully impregnate the fibers. Additionally, using a catalyst to enhance the reactivity of TA/ELO might help prevent separation of TA and ELO during curing of the composite plates.

Examples of composites structures made with TA/ELO and CF were manufactured using vacuum bagging for the longboard and towpregs for the pipe, demonstrating the feasibility of these methods for producing bio-based composites. The presence of ester bonds in TA/ELO and the occurrence of transesterification are real advantages in the realm of CF composite materials, as clean CF fibers can be recovered with low technical efforts using commodity chemicals (NaOH). However, relatively poor strength values were obtained with the mechanically recycled samples, indicating the limitations of this method for producing composite parts from composites scraps or leftovers. The use of a transesterification catalyst might be a solution to facilitate bond-exchange reactions and increase the performance of the mechanically recycled composites.

6 Characterization of a sustainable, BPA and ECH-free epoxy thermoset based on sorbic acid – EGCHC

Parts of this chapter were published in the Journal Macromolecular Materials Engineering with the article entitled "Synthesis of a sustainable and bisphenol A-free epoxy resin based on sorbic acid and characterization of the cured thermoset". The publication was developed in cooperation with the Wacker-Chair of Macromolecular Chemistry (Technical University of Munich) and the Chair I of Technical Chemistry (Technical University of Munich) within the framework of the project "Green Carbon" funded by the German Federal Ministry of Education and Research (FKZ: 03SF0577A). The synthesis of EGCHC was performed by Jonas Martin Breitsameter and the ecological assessment was performed by Matthias Feigel. The contributors are listed in the reference:

Breitsameter, J. M.*, Reinhardt, N.*, Feigel, M., Hinrichsen, O., Drechsler, K. and Rieger, B., Synthesis of a sustainable and bisphenol A-free epoxy resin based on sorbic acid and characterization of the cured thermoset, Macromolecular Materials and Engineering, 2023, 2300068. *These authors contributed equally.

6.1 Objectives and goals

As stated in chapter 2.5, one of the most important parameters when developing a bio-based epoxy is the availability of the resources. Indeed, to address the depletion of fossil resources and avoid concentration of production in specific regions, it is important to use readily available chemicals.

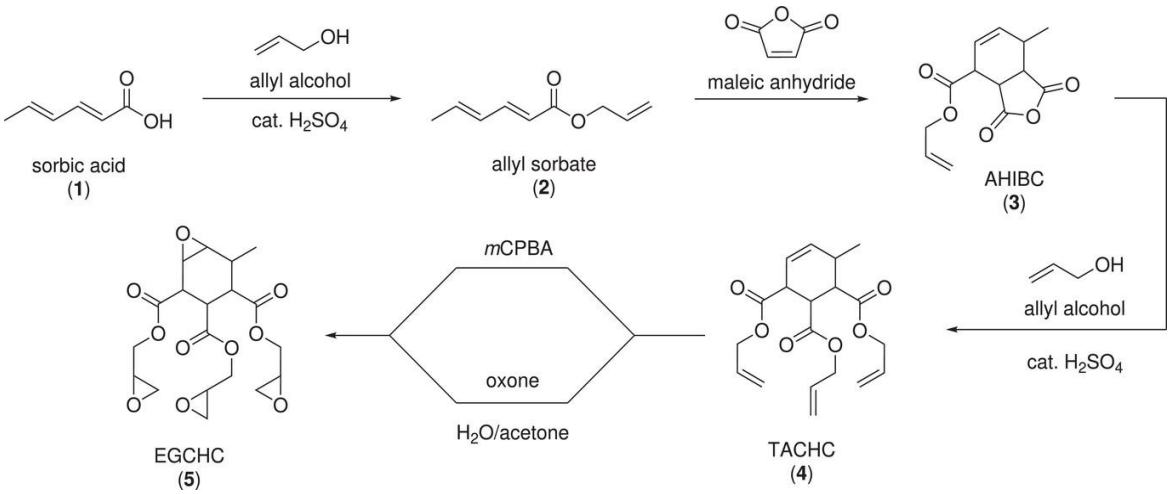

Figure 61: Synthesis toward the epoxy monomer compound EGCHC ((5) starting from the allylation of sorbic acid (1) which is then reacted with maleic anhydride in a Diels–Alder cycloaddition. After the allylation of the anhydride mojety of (4) the double bonds are epoxidized by the use of mCPBA or oxone. From: [53]**.**

Within the framework of the publication "Synthesis of a sustainable and bisphenol A-free epoxy resin based on sorbic acid and characterization of the cured thermoset"[53], a novel epoxy monomer was synthesized. The synthesis of the novel EGCHC epoxy monomer initiates with sorbic acid and requires the use of allyl alcohol and maleic anhydride as feedstocks (Figure 61). These components are classified as commodity chemicals due to their high annual production volume. Sorbic acid and allyl alcohol, key feedstocks, can be sourced with a significant biobased carbon content. For instance, sorbic acid is a biomolecule present in rowan berries and is approved in the EU as a food additive (E200) [177–179]. Allyl alcohol can be derived from biobased glycerol [180]. Maleic anhydride has a great industrial importance and recent publications explored the use of renewable raw materials like furfural and its derivatives that can be obtained from carbohydrates to produce maleic anhydride [181,182].

Due to the presence of numerous ester bonds in its structure, EGCHC, when cured with an amine hardener, should be able to undergo transesterification. Consequently, the mechanical recycling of EGCHC thermoset appears feasible. The abundance of ester groups should also facilitate the degradation of the cured material with chemicals, making solvolysis achievable under mild conditions.

Chapter 6 focuses on the characterization and evaluation of performance of the new multifunctional epoxy resin EGCHC whose components are directly bio-available or can be synthesized from biomolecules. The synthesis being complex, only a few grams of EHCGC material could be synthesized within the framework of the publication. Therefore, characterization tests, sample geometry, and curing agents were carefully chosen to obtain as many relevant material properties as possible for performance evaluation. Once more, the objective is to achieve properties comparable to those of the standard DGEBA-based epoxy.

6.2 Characterization methodology

The investigation of the curing of an epoxy resin is the first important step in order to understand the curing temperatures needed to obtain a highly cross-linked material with desirable properties. Differential Scanning Calorimetry (DSC) is a useful method to comprehend the curing of a thermoset. Non-isothermal tests performed with DSC only require 5-10 mg of material and give insight into the starting temperature of curing and the temperature at the maximum of the exothermic peak, which help to determine the curing temperatures. DSC measurements on cured samples further offer information into the presence or absence of residual curing, confirming the efficacy of specific curing temperatures in achieving a highly cross-linked material.

Moving beyond the curing phase, an understanding of the mechanical properties of the material becomes imperative. Stiffness and strength stand out as the most important and common properties to determine. The sample geometry 1BB from ISO 527-2 allows for the determination of tensile strength and tensile modulus with minimal material usage. A thickness of 1 mm instead of 2 mm and a total length of 30 mm was chosen to minimize the amount of material used.

In order to evaluate the temperature range suitable for utilizing an epoxy resin and, consequently, to identify potential applications for the newly developed thermoset, the evolution of stiffness over temperature, Tg, and degradation temperature are key parameters to define. The evolution of stiffness over temperature and Tg can be effectively determined through Dynamic Mechanical Analysis (DMA). The tensile clamp of the DMA machine is ideal for testing thin samples. The specimen geometry 30 x 5 x 1 mm was chosen for DMA testing. To determine the temperatures at which degradation occurs, Thermogravimetric Analysis (TGA) can be utilized, employing small fractions (5 - 10 mg) of cured samples.

The mechanical and thermal properties of epoxy thermosets are significantly influenced by their chemical structure which, in turn, are shaped by the choice of epoxy resins and curing agents. Two common and commercially available amine-based curing agents, T403 Jeffamine and IPD, were selected to see how the chemical structure of the curing agent impacts the performance of EGCHC thermoset. Their use in common DGEBA-based epoxies is also well-described in the literature. T403, a trifunctional primary amine from Huntsman, finds common use in epoxy formulations for coating, adhesives and composites applications [183]. IPD, a cycloaliphatic diamine, is an industrially standard crosslinker with diverse applications, including rotor blades, pipes, high-performance boats, and automotive parts [184].

The preparation of the samples was also adapted in order to minimize material usage. Small quantities of resin and curing agents were mixed in 20 mL screw cap vials with septum with a Classic Advanced Vortex Mixer. Only mixing ratios resulting in equimolar epoxy to amine groups were studied (Tab. A- 5). For tensile and DMA testing, the

mixture was poured into silicone molds with the desired dimensions to obtain the samples without wastage.

The mechanical and chemical recycling of EGCHC thermoset was investigated using the broken samples obtained after tensile testing. The water absorption of EGCHC thermoset was assessed using samples after DMA testing.

To assess how EGCHC performs compared to commonly used epoxy thermosets, reference samples were prepared using DGEBA cured with T403 and IPD. This allows a direct comparison of the thermo-mechanical properties, mechanical properties and the thermal stability of EGCHC with DGEBA, one of the most used epoxy resins.

6.3 Curing of EGCHC

Figure 62 shows an example of the non-isothermal curing of EGCHC and DGEBA with IPD and T403. The thermograms of EGCHC indicate a higher reactivity compared to DGEBA, as the starting temperature of the curing enthalpy and the temperature at the peak of the exothermic reaction are lower when using T403 and IPD for curing. This can be explained by the location of the epoxy groups in close proximity to ester groups. The inductive effects make it easier for the oxirane to undergo ring-opening, requiring less energy to start the curing reaction. Comparatively, T403 is perceived as less reactive than IPD, due to the steric hindrance posed by the methyl groups in α position to the amine [185].

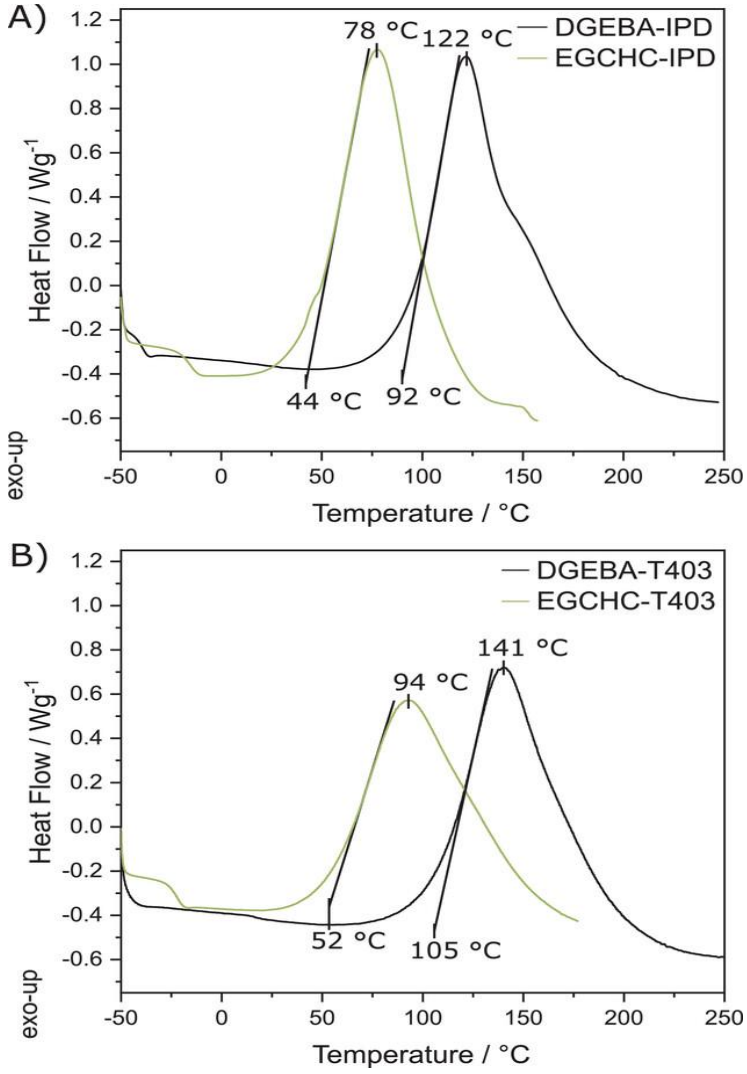

Figure 62: DSC scans of EGCHC/DGEBA-IPD A) and EGCHC/DGEBA-T403 B) with the onset temperature of the curing enthalpy and the temperature of the maximum of the exothermic peak. From: [53]

The curing conditions for EGCHC-based samples (Tab. 14) were chosen according to the results of the non-isothermal DSC measurement (Tab. A- 6). The starting temperature of the curing enthalpy was designated as the curing temperature. The post-curing temperature was selected to be higher than the temperature at the peak of the exothermic reaction. Curing procedures comparable to those outlined in the literature were used to cure the DGEBA samples [186,187].

Tab. 14: Curing conditions for the EGCHC and DGEBA-based samples. Adapted from: [53]

Sample	Curing time + temperature	Post-curing time + temperature
EGCHC-IPD	30 min at 45 °C	30 min at 120 °C
EGCHC-T403	2 h at 60 °C	2 h at 100 °C

Sample	Curing time + temperature	Post-curing time + temperature
DGEBA-IPD	2 h at 60 °C	2 h at 160 °C
DGEBA-T403	3 h at 80 °C	2 h at 120 °C

The curing conditions applied (Tab. 14) allowed the creation of a highly crosslinked material as cured samples were subjected to DSC measurements with a heating ramp (10 K min^{-1}) from -20 to 180 °C and didn't show any residual curing. The curing conditions applied were also justified with the elevated Soxhlet gel contents obtained for EGCHC samples (Tab. 15). ATR-IR measurements also confirm the completion of the curing reaction as no residual IR-bands of the C–O epoxide vibration at a wavelength of 820 cm^{-1} were visible (Fig.A- 28).

Tab. 15: Gel-contents of the cured samples determined by Soxhlet-extraction with acetone as solvent. Extraction time: 24h. From: [53]**.**

Sample	Gel-content in %
EGCHC-IPD	97.90 ± 0.95
EGCHC-T403	97.59 ± 0.15

6.4 Mechanical properties

Fig.A- 29 shows an example of an EGCHC specimen under tensile testing. The results obtained from the tensile testing are really promising and are depicted in Figure 63 and Figure 64.

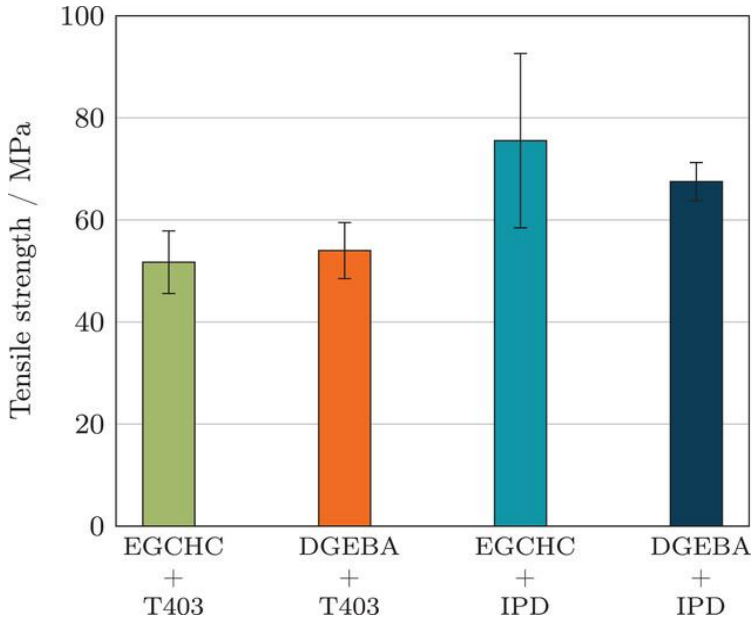

Figure 63: Tensile strength of EGCHC-IPD, EGCHC-T403, DGEBA-IPD, and DGEBA-T403. From: [53].

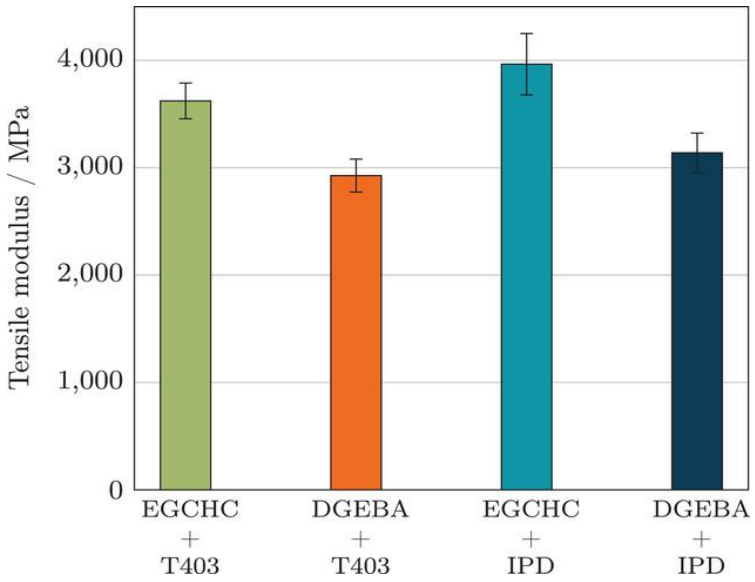

Figure 64: Tensile modulus of EGCHC-IPD, EGCHC-T403, DGEBA-IPD, and DGEBA-T403. From: [53].

EGCHC systems exhibited high tensile strength (Figure 63). The highest tensile strength was obtained for EGCHC cured with IPD, as an impressive average tensile strength of 76 MPa could be obtained. A high standard deviation is also observed on the tensile strength of EGCHC-IPD. Due to the rapid setting of EGCHC-IPD within minutes at room temperature, the mixture underwent degassing for only 30 seconds, leaving air inclusions in the material. The presence of voids in the material after curing significantly impacts the tensile strength. Nevertheless, the average tensile strength of EGCHC-IPD remains higher than that of DGEBA-IPD. EGCHC-T403 exhibits comparable tensile

strength to DGEBA-T403. It is also important to highlight that the tensile strength observed in the DGEBA specimens closely aligns with values documented in the literature [187].

EGCHC systems exhibit greater stiffness compared to DGEBA-based epoxies, and samples cured with IPD are also characterized by increased stiffness in comparison to those cured with T403 (Figure 64). The cycloaliphatic structure of IPD (Fig.A- 30) enables the formation of a more rigid network. A maximum average tensile modulus of 3965 MPa was found for EGCHC-IPD. DGEBA stands out as one of the most used epoxy resins worldwide with applications spanning diverse domains. The elevated E-modulus achieved with EGCHC underscores its capability to meet the necessary stiffness standards for high-performance applications. For instance, SIKA's Biresin CR80 is a DGEBA-based epoxy system tailored for high-performance applications such as the fabrication of fiber-reinforced composite parts in marine, wind turbine, and general industrial composite domains. This system achieves a tensile modulus of 2900–3000 MPa after curing [77].

In general, tensile testing showed that EGCHC can rival the mechanical properties of DGEBA.

6.5 Thermo-mechanical properties

DMA serves as an outstanding technique for determining the Tg of epoxy materials due to its high sensitivity [91]. Additionally, the stiffness of various materials at different temperatures can be compared. Figure 65 illustrates the variation in stiffness across temperature and the tan δ curves for both EGCHC and DGEBA cured with IPD and T403. In line with the tensile modulus outcomes, samples cured with IPD exhibit greater stiffness compared to those cured with T403 as the cycloaliphatic structure of IPD facilitates the establishment of a more rigid network. This more rigid network obtained for the samples cured with IPD also results in a higher Tg.

Tab. 16: Tg obtained from DMA for the EGCHC and DGEBA-based samples. Adapted from: [53]**.**

Sample	Tg in °C
EGCHC-IPD	129.8 ± 6.2
EGCHC-T403	56.5 ± 1.3
DGEBA-IPD	161.7 ± 0.4
DGEBA-T403	82.0 ± 1.2

In the temperature range spanning from -20 °C to around 38 °C, EGCHC-T403 exhibits greater stiffness than DGEBA-T403. Similarly, EGCHC-IPD demonstrates higher stiffness than DGEBA-IPD within the temperature range from -20 °C to approximately 100 °C. The abundant presence of oxirane rings in EGCHC's structure imparts the capability to form a denser crosslinked structure compared to DGEBA. Nevertheless, the Tg of EGCHC-based systems is inferior to that of their DGEBA equivalents (Tab. 16). This can be attributed to the structural disparities between the resins. DGEBA, unlike EGCHC, possesses aromatic substructures that can establish relatively strong intermolecular π–π interactions. Consequently, the glassy region for EGCHC systems concludes at lower temperatures compared to DGEBA systems, resulting in a prompt decline in stiffness at lower temperatures.

Due to the higher stiffness and Tg observed with EGCHC-IPD in comparison with EGCHC-T403, the curing agent IPD is more suitable than T403 for applications that demand high stiffness at elevated temperatures. Although an average Tg of 130 °C was achieved for EGCHC-IPD, the thermoset is not suitable for applications that require high stiffness at temperatures exceeding 100 °C, as EGCHC-IPD experiences a significant loss of stiffness above 100 °C as can be seen from Figure 65A.

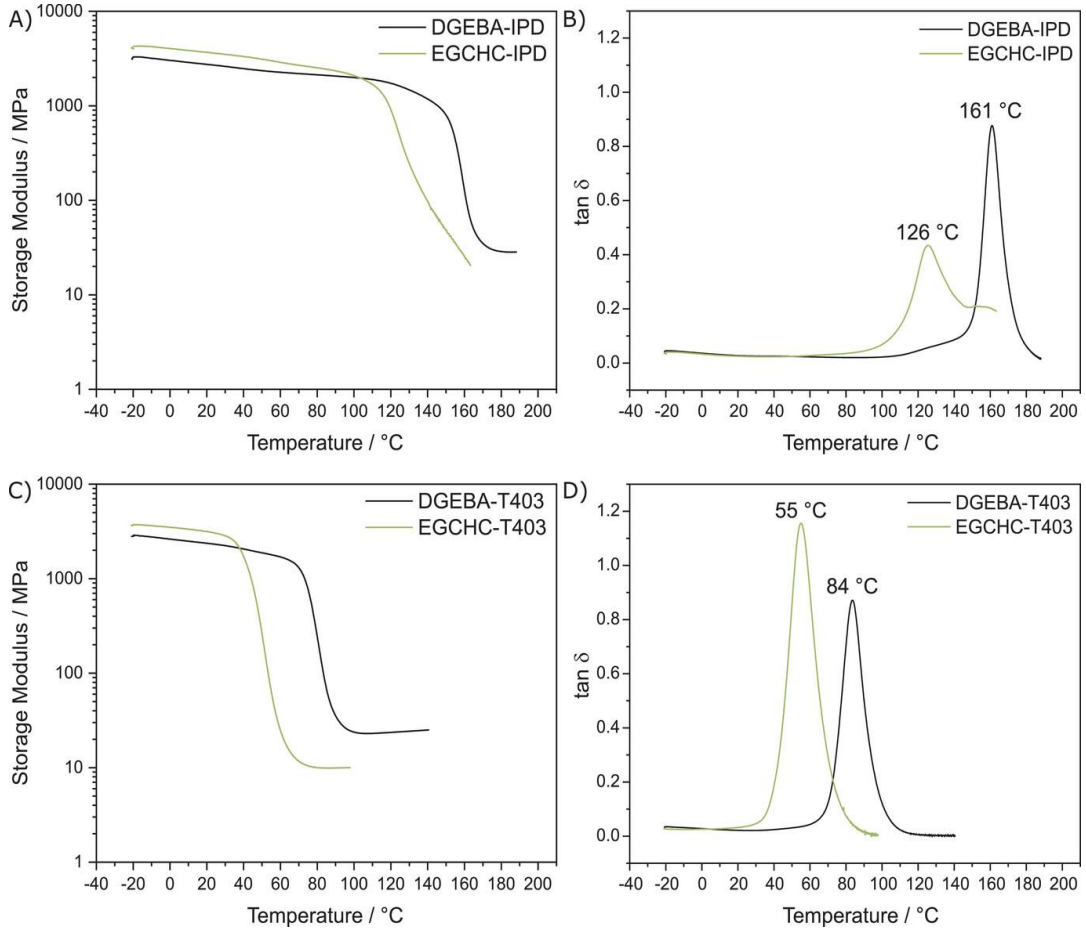

Figure 65: A) Storage modulus and B) tan δ of DGEBA/EGCHC cured with IPD, C) Storage modulus and D) tan δ of DGEBA/EGCHC cured with T403. Determined by DMA. From: [53]**.**

6.6 Thermal stability

The thermal stabilities under nitrogen of EGCHC and DGEBA were analyzed using thermogravimetric analysis (TGA). The thermal degradation of EGCHC samples begins at temperatures of 203 °C when cured with IPD and 222 °C when cured with T403 (Figure 66). While the thermal stability ($T_{5\%}$) of EGCHC is lower than that of DGEBA (approximately 340 °C), the thermal resistance of both EGCHC-IPD and EGCHC-T403 is sufficient to prevent material degradation under standard usage conditions. The reduced thermal stability of EGCHC samples can be attributed to the higher susceptibility of ester bonds to pyrolysis, especially when compared to the more thermally robust ether bonds present in DGEBA. Additionally, the absence of aromatic substructures in EGCHC contributes to its comparatively lower resistance to elevated temperatures.

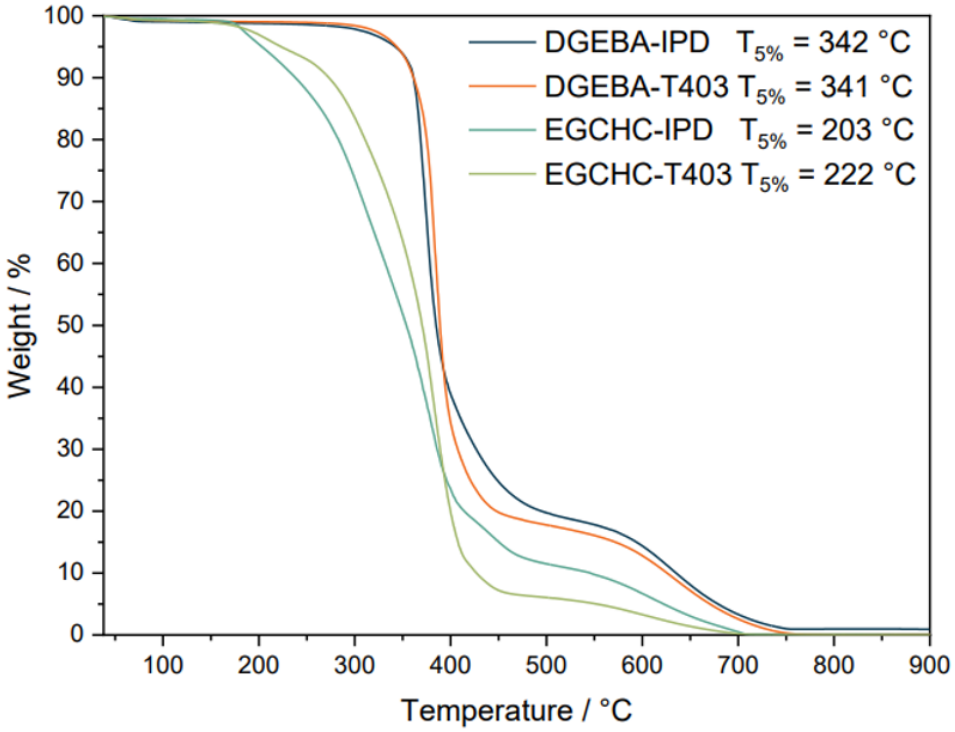

Figure 66: TG curves of EGCHC-IPD, EGCHC-T403 and DGEBA-IPD, DGEBA-T403 for comparison. From: [53]**.**

6.7 Water absorption

The water uptake of EGCHC cured with IPD and T403 is shown in Figure 67. From the graphic, it can be seen that EGCHC has the ability of absorbing a high amount of water. Furthermore, the samples didn't reach equilibrium after 72 h of immersion in water, suggesting elevated water uptake with prolonged immersion. As already highlighted in 4.6, standard epoxy structures (DGEBA-based) are known to have a moderate water uptake capability. The high-water absorption capability of EGCHC can be explained with the high polarity of the molecule due to the presence of ester groups and the high functionality of EGCHC that leads to the creation of multiple hydroxyl groups after curing with an amine hardener. Especially the high amount of hydroxy groups in the cured EGCHC structures is expected to be responsible for the high water absorption of the EGCHC samples [188].

T403 is a curing agent composed of repeating oxypropylene units in its backbone (Fig.A-30) and creates larger gaps than IPD in the cured EGCHC structure. These larger gaps explain the higher water absorption of EGCHC-T403 than EGCHC-IPD.

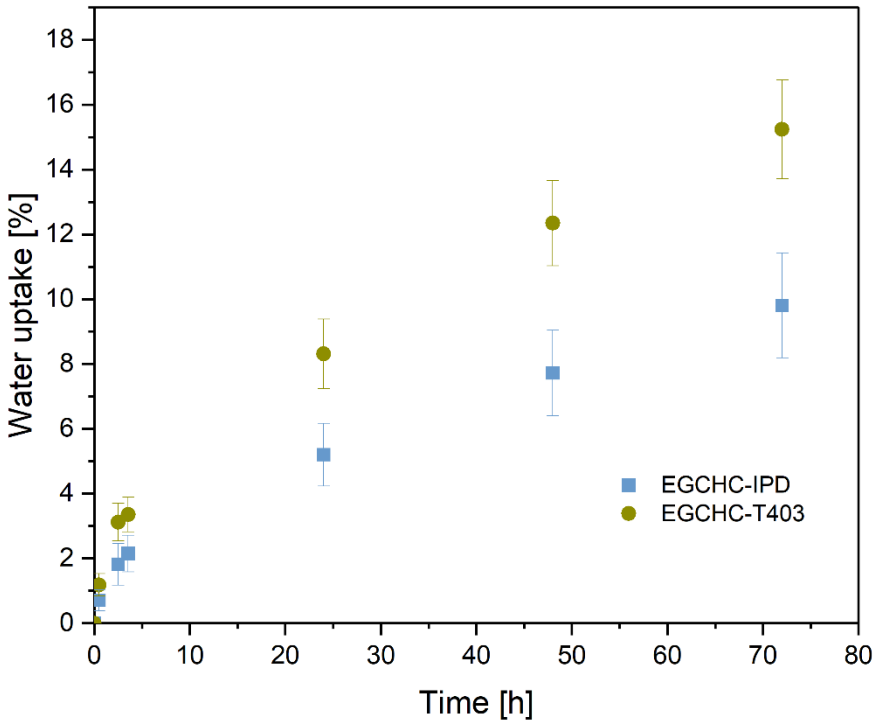

Figure 67: Water uptake of EGCHC-IPD and EGCHC-T403

6.8 Recycling of EGCHC

6.8.1 Mechanical recycling

Tab. 17: Conditions applied for the mechanical recycling of EGCHC.

Sample	Hot-pressing time + temperature
EGCHC-IPD	1 h at 110 °C
EGCHC-T403	1 h at 130 °C

Just like TA/ELO, the existence of ester bonds and the hydroxyl groups generated post-curing grant EGCHC the ability to undergo recycling through transesterification reaction. The ability of EGCHC to be mechanically recycled was confirmed, as recycled samples could be manufactured. Broken EGCHC samples, after tensile testing in chapter 6.4, were grinded into a fine powder through ball milling and hot-pressed with a pressure of 50 bar in an aluminum form under the conditions depicted in Tab. 17. EGCHC-IPD samples were extremely brittle after hot-pressing at 130 °C and could not be taken out of the form. Therefore, a lower hot-pressing temperature of 110 °C was chosen for

EGCHC-IPD. After the recycling process, the EGCHC samples exhibited a yellowish color (Fig.A- 31 and Fig.A- 32).

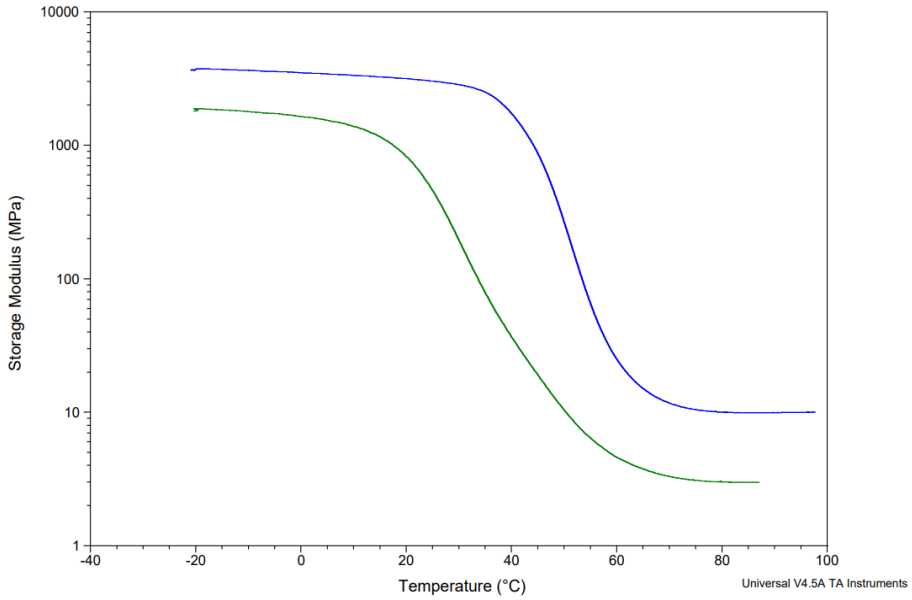

Figure 68: Storage modulus of EGCHC-T403 virgin (blue) and after recycling (green).

A clear decrease of the storage modulus, and hence stiffness, is observed for the recycled samples. Moreover, the recycled samples experienced a rapid loss of stiffness at lower temperatures compared to the virgin samples (Figure 68 and Fig.A- 33). When examining Fig.A- 31 and Fig.A- 32, it can be seen that the recycled samples showcase some coarse particles, suggesting poor powder compaction and a heterogeneous material. This can explain the broad and poorly defined Tg obtained for the recycled samples (Fig.A- 34 and Figure 69).

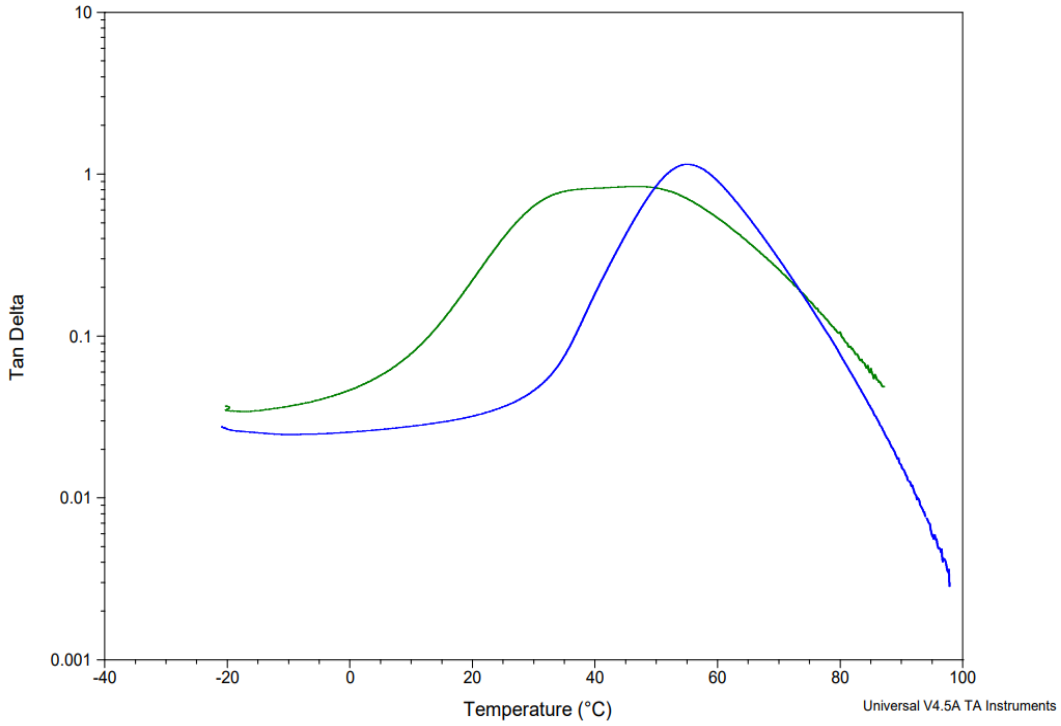

Figure 69: Tan delta of EGCHC-T403 virgin (blue) and after recycling (green).

6.8.2 Solvolysis

As already mentioned in chapter 4.7.2, the presence of multiple ester bonds in the thermoset favors solvolysis as the ester moieties can undergo basic hydrolysis under mild conditions. EGCHC samples cured with IPD and T403 were placed in a NaOH solution and the degradation was evaluated for different temperatures. At 80 °C, both EGCHC-IPD and EGCHC-T403 completely dissolved within 30 min. At room temperature, the EGCHC-T403 sample underwent complete decomposition within 17 h. In contrast, the EGCHC-IPD sample exhibited greater resilience, experiencing only a 17 % reduction in its initial weight, and full decomposition took approximately 4 days. A slight temperature increase notably shortens the decomposition time for EGCHC-IPD, as illustrated in Figure 70.

The distinct behavior observed can be attributed to the density of the 3D network. Jeffamine T403 is composed of repeating oxypropylene units in its backbone (Fig.A- 30), creating larger gaps in the cured structure. As a result, the solvent can penetrate more deeply, facilitating the attack on the ester bonds. In contrast, the network formed by curing with IPD is more densely packed, offering fewer degrees of freedom and impeding the solvent's diffusion into the thermoset.

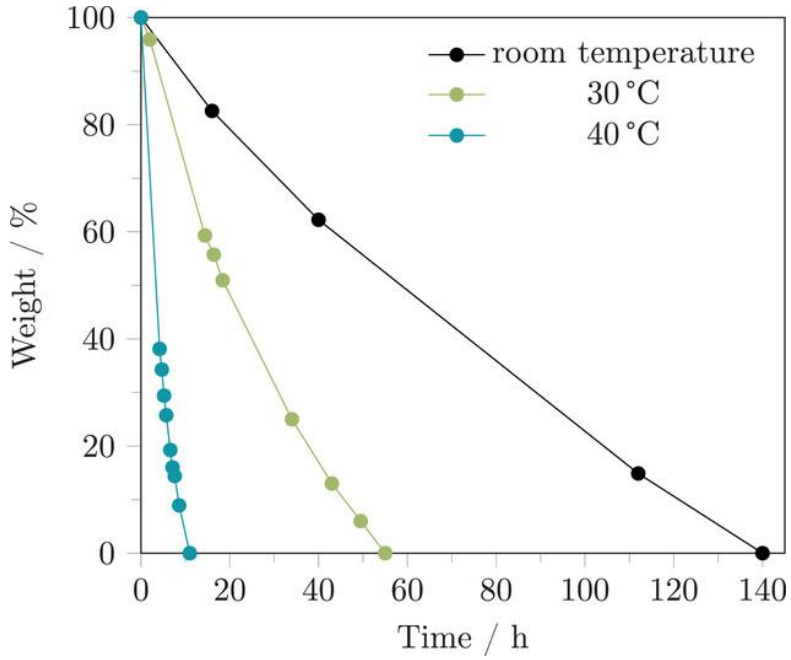

Figure 70: Decomposition of EGCHC-IPD in NaOH (1 mol/L) at room temperature, 30 and 40 °C. From: [53].

6.9 Ecological assessment

The evaluation of the ecological impact of the entire reaction synthesis involves assessing the bio-based fraction of the product. This entails analyzing each component in terms of the bio-based content of substances available on an industrial scale. Various scenarios are presented to illustrate the evolution of the bio-based content using established routes to synthesize different starting materials with renewable resources. Consequently, both a conservative approach and an optimistic outlook on the availability of renewable chemicals are considered for epoxy EGCHC. Additionally, a comparison is made with the industry standard DGEBA, both in its pure form and when cured with conventional curing agents. Bio-based fractions are computed based on the structural information of the molecules and their transformations throughout the reaction, as outlined in standard DIN EN 16785-1 [189]. This method meticulously determines the bio-based fraction through radiocarbon and elemental analysis, considering the total content of bio-originating H, C, O, and N atoms. The bio-based content (w_{bb}) represents the mass fraction of the bio-based mass m_{HCON} (total H, C, O, N mass) in relation to the total sample mass m. Furthermore, the bio-based carbon content is reported in accordance with the ASTM D6866 standard [190].

6.9.1 Synthesis route

As mentioned earlier, allyl alcohol is accessible in a bio-available form as it can be derived from glycerol [180]. Allyl sorbate, derived from the synthesis of sorbic acid and allyl alcohol, is determined to possess a bio-based fraction of $w_{bb} = 0.753$. While sorbic

acid could theoretically be sourced from natural rowan berries [179] the predominant industrial method involves the condensation of malonic acid (fossil-based) and crotonaldehyde (100 % bio-based), as outlined by Doebner [191]. Consequently, a conservative estimate of $w_{bb} = 0.667$ is assigned to sorbic acid. In the subsequent reaction step, where allyl sorbate reacts with maleic anhydride, the bio-based content of the intermediate is reduced to 45.8 %. Maleic anhydride, primarily obtained through butane oxidation in significant quantities is a key building block in the chemical industry [192,193]. Despite the increasing publication of environmentally friendly synthesis routes for maleic anhydride [181,182], none have been implemented on an industrial scale to date.

The formation of TACHC, achieved by the addition and condensation of two allyl alcohol molecules, raises the bio-based fraction once more to $w_{bb} = 0.630$. For the final epoxidation step, the reaction pathway utilizing *m*CPBA is selected as the fundamental synthesis route. *m*CPBA is a commercially available oxidizing agent and its industrial production relies on fossil resources [194]. Consequently, three oxygen atoms are introduced into TACHC, resulting in the final product EGCHC with a bio-based content of $w_{bb} = 0.532$. Utilizing the ASTM D6866 standard methodology, which tracks only carbon atoms, yields a bio-based fraction of 68.4 % [190]. The potential substitution of some conventionally produced chemical components with bio-based alternatives could further augment the overall bio-based content.

6.9.2 Comparison of EGCHC and DGEBA

Figure 71 depicts the conservative assessment of EGCHC's bio-based content, utilizing currently available green chemicals and contrasts it with the standard epoxy DGEBA. The calculation is performed using both of the aforementioned standards, revealing varying bio-based fractions depending on the norm applied.

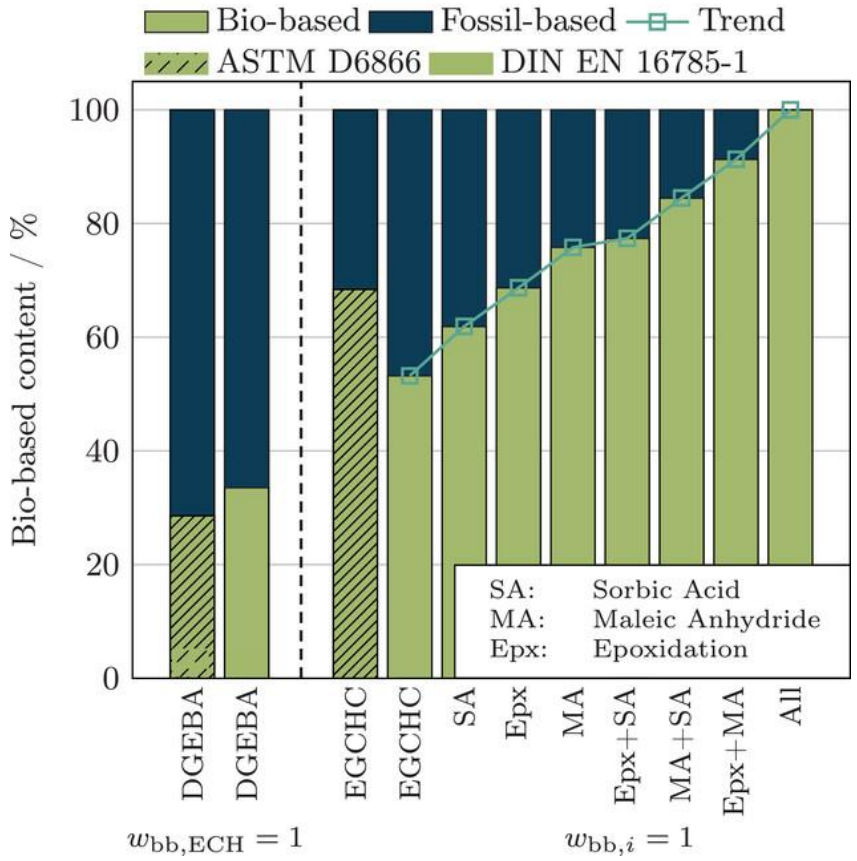

Figure 71: Bio-based content of EGCHC in comparison with DGEBA calculated using the standard DIN EN 16785-1 and ASTM D6866. Development of the bio-based content with substitution of fossil-based components for EGCHC. Bio-based content of DGEBA sytems from assumed 100 % green epichlorohydrine. From: [53].

The bio-based fractions can vary based on the specific norm used, and in this regard, EGCHC demonstrates significantly enhanced bio-based contents compared to DGEBA. In the case of DGEBA, the best-case scenario is considered, assuming a synthesis involving BPA and 100 % green epichlorohydrin. However, due to its small molecular weight, the bio-based content of DGEBA can only be increased to $w_{bb} = 0.335$. Additionally, challenges related to the toxicity of the utilized chemicals, as outlined in the introductory section, persist.

6.9.3 Scenarios for increasing bio-based fraction of EGCHC

Figure 71 also presents various scenarios illustrating the progression of the bio-based fraction through the utilization of environmentally friendly alternatives in the proposed production of EGCHC. Clearly, a significant enhancement in sustainability can be attained without altering the synthesis route. Viable methods for producing bio-based sorbic acid and maleic anhydride are documented in the literature, although they are often impeded by the more economically efficient conventional processes. However, with the growing demand for bio-based products, this dynamic could shift in the near

future. Consequently, bio-based fractions of 61.9, 75.8, and 84.5 % can be readily achieved in scenarios involving 100 % bio-based sorbic acid, maleic anhydride, or both, respectively.

Replacing the epoxidation step poses a greater challenge, given the absence, to our knowledge, of reported routes for bio-based *m*CPBA. Consequently, the logical course of action would be to consider an alternative epoxidation method. Other green alternatives to *m*CPBA include hydrogen peroxide combined with various catalysts such as polyoxometalates [195], Pt [196], methyltrioxorhenium [197], or enzymes [198,199]. Opting for an alternative route involving bio-based starting materials, such as enzymes, could elevate the overall bio-based content by 15.5 %, reaching 68.7 % based on the initial value of $w_{bb} = 0.532$. It is essential to note that, for ASTM D6866, the epoxidation step does not impact the bio-based fraction, as oxygen atoms are not considered in the determination.

6.9.4 Curing of EGCHC and DGEBA

The epoxy EGCHC, cured with both IPD and T403, is compared with the industrially relevant competitor DGEBA. Figure 72 illustrates the achievable bio-based contents for the four resin systems calculated using the standard ASTM D6866. For IPD, two cases are considered: using conventional fossil-based IPD or the readily available green IPD (VESTAMIN IPD eCO), which has a 90 % bio-based carbon content [200]. Due to different required mixing ratios, the influence of the epoxy is more or less pronounced. However, in all studied samples, an increased bio-based fraction is observed.

Substituting IPD with IPD eCO results in the highest bio-based contents. Considering a current standard system of DGEBA cured with IPD, the maximum bio-based carbon amount can be achieved by using both green ECH ($w_{bb} = 1$) in combination with ECO IPD ($w_{bb} = 0.9$). This results in an epoxy resin with a total bio-based carbon content of 40.9 %, which still relies on the use of BPA. In contrast, a resin produced with EGCHC and IPD eCO can reach a total $w_{bb} = 0.747$.

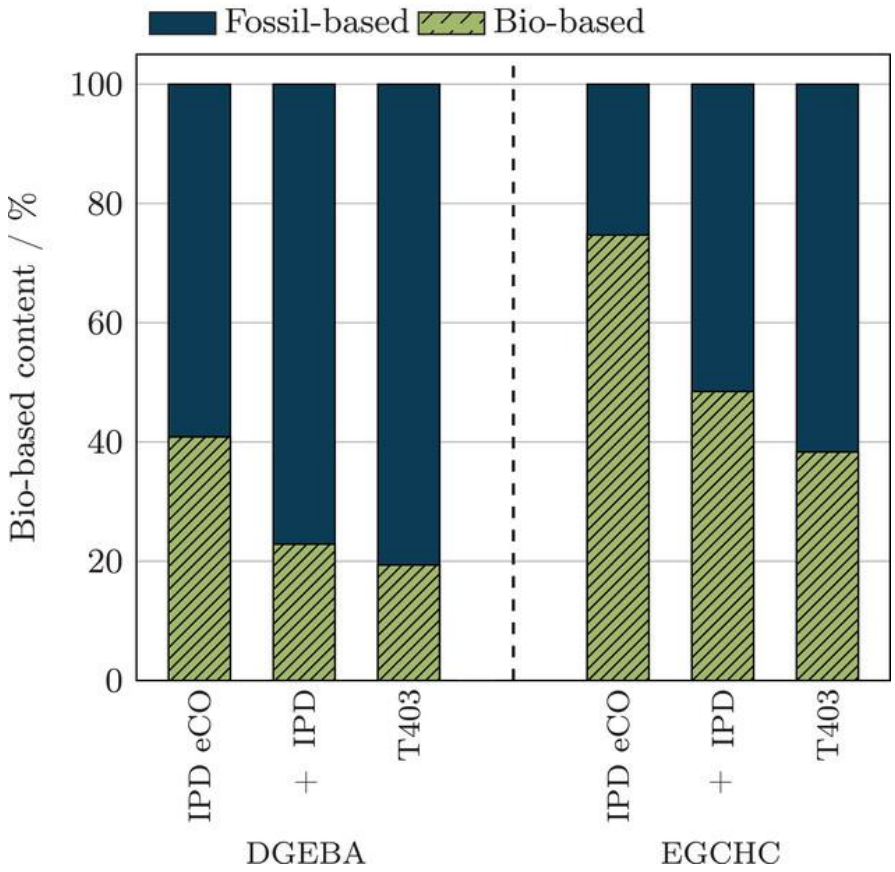

Figure 72: Bio-based content of resins cured with IPD eCO, IPD and T403 of EGCHC in comparison with DGEBA calculated using the standard ASTM D6866. Bio-based content of DGEBA stems from assumed 100 % green epichlorohydrine. From: [53].

6.10 Conclusion of chapter 6

In order to find a bio-based substitute to DGEBA, research has focused on bio-compounds such as vanillin or eugenol, exhibiting a structural resemblance to BPA and featuring aromatic groups that contribute to high mechanical and thermal properties. The novel epoxy monomer EGCHC that readily yields a bio-based fraction of 68.4 % and that necessitates available chemicals for its synthesis, lacks aromatic groups, yet it demonstrates the potential to rival DGEBA in terms of stiffness and strength. The abundance of oxirane rings in EGCHC's structure facilitates the formation of a denser crosslinked structure compared to DGEBA. However, the absence of aromatic substructures accounts for its lower Tg compared to DGEBA.

The curing temperatures applied in this chapter for EGCHC are quite moderate, and curing times are low (especially for EGCHC-IPD) when comparing with their DGEBA counterparts, offering energy-saving benefits. Another notable characteristic of the EGCHC compound is the presence of ester groups, enabling transesterification when cured with amine hardeners and, consequently, mechanical recycling. Also, solvolysis can also be applied with mild conditions, which is a great feature to allow the easy

recovery of the fibers. However, it is crucial to acknowledge the high-water absorption capacity of EGCHC, which strongly limits its usage in outdoor applications. Additionally, the thermal stability may limit its suitability for high-temperature applications, as degradation occurs at temperatures approaching 200 °C. Generally, EGCHC-IPD exhibited superior mechanical and thermal properties. An average Tg of 130 °C was noted. However, it's important to highlight that a significant decline in stiffness occurs rapidly beyond 100 °C. This characteristic renders EGCHC-IPD unsuitable for applications demanding high stiffness at temperatures surpassing 100 °C.

Lastly, further investigation into the properties of EGCHC reinforced with fibers is necessary to determine if EGCHC can serve as a high-performance matrix for composite applications.

7 Conclusion of the thesis

Various bio-based resources have been employed in this study to develop epoxy thermosets, contributing to the expansion of knowledge regarding potential bio-based resources for epoxy thermoset production. This effort aims to address the depletion of fossil resources.

Poor mechanical properties are commonly reported in the literature for EVO. Nevertheless, the investigation of TA/ELO showed that high stiffness, moderate strength, and high Tg can be achieved with ELO cured with a bio-based curing agent (TA), by milling TA into a fine powder and facilitating the reaction between the hydroxyl groups of TA and the oxirane groups of ELO by using an excess of hydroxyl groups. This highlights the potential of using ELO and TA as natural resources to produce performant epoxies. Additionally, with the work on EGCHC, it has been shown that competitive mechanical properties to DGEBA systems could be reached with a novel epoxy compound that doesn't possess aromatic groups in its structure with a significant bio-based content (68.4 %) and that can be produced with available chemicals: sorbic acid, allyl alcohol and maleic anhydride.

This thesis demonstrates the possibility of developing bio-based and BPA- and ECH-free epoxy thermosets with strong mechanical and thermal properties, along with recycling ability. Due to the presence of ester groups and hydroxyl-groups in the cured structures, the materials were able to be mechanically recycled through transesterification reaction. Furthermore, the ester moieties enable the cured thermosets to be degraded via solvolysis under mild conditions using a common chemical: NaOH. This feature is particularly interesting for composite materials, as it allows the recovery of clean CF fibers with low technical efforts. To address the growing issue of composite waste in the coming decades, and in general to reduce the environmental impact of composite materials to meet the imposed directives, the use of recyclable epoxies becomes imperative.

In general, the study of EGCHC and TA/ELO showcased the great impact of the molecule structure on the various properties of the epoxy. In order for an epoxy system to be performant and utilized in load-bearing applications, the epoxy must encompass a multitude of attributes which goes beyond high stiffness, high strength and high Tg. Parameters such as low water uptake, easy processability, good impregnation of fibers capability, low curing temperatures and fast curing are also crucial characteristics for industrial viability. Particularly high water absorption capability was found for the EGCHC and TA/ELO thermosets, which strongly limits their use in wet conditions. Additionally, poor compatibility between TA and ELO, slow curing reactivity, and the solid nature of TA were identified as limitations when using TA/ELO as a matrix for CF-composites. If TA/ELO reinforced with CF could achieve a stiffness comparable to DGEBA-based CF composites, the strength of the TA/ELO composites was much lower. This was due

to poorly impregnated fibers during the composite manufacturing processes and the presence of defects such as TA lumps.

Further investigations into milling TA into particles smaller than fibers and on possible catalysts to enhance curing efficiency are needed to increase the performance of TA/ELO CF composites and reduce curing times. To reduce the high-water uptake of the developed structures, hydrophobization of the molecules can be considered. To enhance the performance of mechanically recycled thermosets and composites, transesterification catalysts can be employed to facilitate bond-exchange reactions. Additional research on the properties of EGCHC reinforced with fibers is essential to ascertain its suitability as a high-performance matrix for composite applications. The properties of EGCHC cured with bio-based curing agents also need to be assessed to work towards a solution for the depletion of fossil resources.

The thermosets and composites developed in this thesis embody the principles of green chemistry and support a circular economy by advocating for the utilization of renewable resources and minimizing waste generation. They facilitate a closed-loop system wherein materials can be recycled at the end of their life cycle, thus promoting resource efficiency and waste reduction.

While the literature acknowledges the promise of epoxy production using EVOs owing to their widespread availability, it is crucial to recognize that utilizing edible vegetable oils in the polymer industry may have potential adverse effects on the long-term stability of the food supply chain. The overall practice of cultivating plants specifically for epoxy production inherently competes with the utilization of arable land for food production. Therefore, it becomes imperative to identify plants with self-sustaining harvesting practices or waste products suitable for epoxy production, without compromising essential resources, to safeguard an adequate global food supply.

8 References

[1] Global Epoxy Resin Market Outlook, (n.d.). https://www.expertmarketresearch.com/reports/epoxy-resins-market (accessed July 3, 2023).

[2] G. Chatziparaskeva, I. Papamichael, I. Voukkali, P. Loizia, G. Sourkouni, C. Argirusis, A.A. Zorpas, End-of-Life of Composite Materials in the Framework of the Circular Economy, Microplastics. 1 (2022) 377–392. https://doi.org/10.3390/microplastics1030028.

[3] N. Reinhardt, J.M. Breitsameter, K. Drechsler, B. Rieger, Fully Bio-Based Epoxy Thermoset Based on Epoxidized Linseed Oil and Tannic Acid, Macromol. Mater. Eng. 307 (2022) 1–10. https://doi.org/10.1002/mame.202200455.

[4] Bisphenols, (n.d.). https://echa.europa.eu/hot-topics/bisphenols (accessed July 6, 2023).

[5] N. To, T.H.E. Reader, European Union Summary Risk Assessment Report JOINT, 2003 (2008).

[6] A. HOHMANN, K. ANGERER, Sustainable Composites Opportunities – Challenges – Further Aspects, in: 2022.

[7] GaBi Professional database (version 2021.2), (n.d.).

[8] H. Memon, Y. Wei, C. Zhu, Recyclable and reformable epoxy resins based on dynamic covalent bonds – Present, past, and future, Polym. Test. 105 (2022) 107420. https://doi.org/10.1016/j.polymertesting.2021.107420.

[9] R.A. Witik, R. Teuscher, V. Michaud, C. Ludwig, J.A.E. Månson, Carbon fibre reinforced composite waste: An environmental assessment of recycling, energy recovery and landfilling, Compos. Part A Appl. Sci. Manuf. 49 (2013) 89–99. https://doi.org/10.1016/j.compositesa.2013.02.009.

[10] S.J. Pickering, Recycling technologies for thermoset composite materials-current status, Compos. Part A Appl. Sci. Manuf. 37 (2006) 1206–1215. https://doi.org/10.1016/j.compositesa.2005.05.030.

[11] J. Beauson, End-of-life of wind turbine blades – Value chain, recycling and composite materials, DTU, 2023. https://doi.org/10.11581/dtu.00000221.

[12] Waste Framework Directive, (n.d.). https://environment.ec.europa.eu/topics/waste-and-recycling/landfill-waste_en (accessed July 3, 2023).

[13] H.Y. Tsai, T. Fujita, S. Wang, M. Naito, Environmentally friendly recycling system for epoxy resin with dynamic covalent bonding, Sci. Technol. Adv. Mater. 22 (2021) 532–542. https://doi.org/10.1080/14686996.2021.1897480.

[14] P.S. Löser, Sustainable Synthesis of Bio-based Recyclable Thermosets, Karlsruher Instituts für Technologie (KIT), 2020.

[15] P. Anastas, N. Eghbali, Green Chemistry: Principles and Practice, Chem. Soc. Rev. 39 (2010) 301–312. https://doi.org/10.1039/b918763b.

[16] A.P. Mouritz, ed., 1 - Introduction to aerospace materials, in: Introd. to Aerosp. Mater., Woodhead Publishing, 2012: pp. 1–14. https://doi.org/https://doi.org/10.1533/9780857095152.1.

[17] J. Choi, H. Kang, J.H. Lee, S.H. Kwon, S.G. Lee, Predicting the Properties of High-Performance Epoxy Resin by Machine Learning Using Molecular Dynamics Simulations., Nanomater. (Basel, Switzerland). 12 (2022). https://doi.org/10.3390/nano12142353.

[18] G. Gibson, Chapter 27 - Epoxy Resins, in: M. Gilbert (Ed.), Brydson's Plast. Mater. (Eighth Ed., Eighth Edi, Butterworth-Heinemann, 2017: pp. 773–797. https://doi.org/https://doi.org/10.1016/B978-0-323-35824-8.00027-X.

[19] N. Karak, Overview of Epoxies and Their Thermosets, ACS Symp. Ser. 1385 (2021) 1–36. https://doi.org/10.1021/bk-2021-1385.ch001.

[20] H. Abdellaoui, M. Raji, R. Bouhfid, A. el kacem Qaiss, 2 - Investigation of the deformation behavior of epoxy-based composite materials, in: M. Jawaid, M. Thariq, N. Saba (Eds.), Fail. Anal. Biocomposites, Fibre-Reinforced Compos. Hybrid Compos., Woodhead Publishing, 2019: pp. 29–49. https://doi.org/https://doi.org/10.1016/B978-0-08-102293-1.00002-4.

[21] S. Kumar, K.K. Singh, Tribological behaviour of fibre-reinforced thermoset polymer composites: A review, Proc. Inst. Mech. Eng. Part L J. Mater. Des. Appl. 234 (2020) 1439–1449. https://doi.org/10.1177/1464420720941554.

[22] Thermosets Market - Forecast(2023 - 2028), (n.d.). https://www.industryarc.com/Report/16296/thermosets-market.html.

[23] H. Memon, Y. Wei, C. Zhu, Recyclable and reformable epoxy resins based on dynamic covalent bonds – Present, past, and future, Polym. Test. 105 (2022) 107420. https://doi.org/https://doi.org/10.1016/j.polymertesting.2021.107420.

[24] G.Y. Romero-Zúñiga, D. Navarro-Rodríguez, M.E. Treviño-Martínez, Enhanced mechanical performance of a DGEBA epoxy resin-based shape memory polymer by introducing graphene oxide via covalent linking, J. Appl. Polym. Sci. 139 (2022) 1–14. https://doi.org/10.1002/app.51467.

[25] L. Yue, A. Maiorana, A. Patel, R. Gross, I. Manas-Zloczower, A sustainable alternative to current epoxy resin matrices for vacuum infusion molding, Compos. Part A Appl. Sci. Manuf. 100 (2017) 269–274. https://doi.org/10.1016/j.compositesa.2017.05.024.

[26] H. Sukanto, W.W. Raharjo, D. Ariawan, J. Triyono, M. Kaavesina, Epoxy resins thermosetting for mechanical engineering, Open Eng. 11 (2021) 797–814. https://doi.org/10.1515/eng-2021-0078.

[27] Y.I. Li, F. Xiao, K.S. Moon, C.P. Wong, Novel curing agent for lead-free electronics: Amino acid, J. Polym. Sci. Part A Polym. Chem. 44 (2006) 1020–1027. https://doi.org/10.1002/pola.21239.

[28] E.A. Baroncini, S. Kumar Yadav, G.R. Palmese, J.F. Stanzione, Recent advances in bio-based epoxy resins and bio-based epoxy curing agents, J. Appl. Polym. Sci. 133 (2016) 1–19. https://doi.org/10.1002/app.44103.

[29] J. Woidasky, C. Klinke, S. Jeanvré, Materials stock of the civilian aircraft fleet,

Recycling. 2 (2017) 1–8. https://doi.org/10.3390/recycling2040021.

[30] I. Julian, A. García-Jiménez, A. Aguado, C. Arenal, A. Calero, V. Campos, G. Escobar, A.M. López-Buendía, D. Romero, E. Verdejo, N. García-Polanco, Advances in the circularity of end-of-life fibre-reinforced polymers by microwave intensification, Chem. Eng. Process. - Process Intensif. 178 (2022). https://doi.org/10.1016/j.cep.2022.109015.

[31] S. Dattilo, G. Cicala, P.M. Riccobene, C. Puglisi, L. Saitta, Full Recycling and Re-Use of Bio-Based Epoxy Thermosets: Chemical and Thermomechanical Characterization of the Recycled Matrices, Polymers (Basel). 14 (2022). https://doi.org/10.3390/polym14224828.

[32] Y. Yang, R. Boom, B. Irion, D.J. van Heerden, P. Kuiper, H. de Wit, Recycling of composite materials, Chem. Eng. Process. Process Intensif. 51 (2012) 53–68. https://doi.org/10.1016/j.cep.2011.09.007.

[33] K. Korniejenko, B. Kozub, A. Bąk, P. Balamurugan, M. Uthayakumar, G. Furtos, Tackling the circular economy challenges—composites recycling: Used tyres, wind turbine blades, and solar panels, J. Compos. Sci. 5 (2021) 1–18. https://doi.org/10.3390/JCS5090243.

[34] S. Karuppannan Gopalraj, T. Kärki, A review on the recycling of waste carbon fibre/glass fibre-reinforced composites: fibre recovery, properties and life-cycle analysis, SN Appl. Sci. 2 (2020) 433. https://doi.org/10.1007/s42452-020-2195-4.

[35] A.E. Krauklis, C.W. Karl, A.I. Gagani, J.K. Jørgensen, Composite material recycling technology—state-of-the-art and sustainable development for the 2020s, J. Compos. Sci. 5 (2021). https://doi.org/10.3390/jcs5010028.

[36] Directive 2000/53/EC of the European Parliament and of the Council of 18 September 2000 on end-of life vehicles, (n.d.). https://eur-lex.europa.eu/legal-content/EN/TXT/?uri=celex%3A32000L0053.

[37] Landfill waste, (n.d.). https://environment.ec.europa.eu/topics/waste-and-recycling/landfill-waste_en (accessed August 29, 2023).

[38] S. Pimenta, S.T. Pinho, Recycling carbon fibre reinforced polymers for structural applications: Technology review and market outlook, Waste Manag. 31 (2011) 378–392. https://doi.org/https://doi.org/10.1016/j.wasman.2010.09.019.

[39] D. Borjan, Ž. Knez, M. Knez, Recycling of Carbon Fiber-Reinforced Composites-Difficulties and Future Perspectives., Mater. (Basel, Switzerland). 14 (2021). https://doi.org/10.3390/ma14154191.

[40] E. Shehab, A. Meiirbekov, A. Amantayeva, A. Suleimen, S. Tokbolat, S. Sarfraz, A Cost Modelling System for Recycling Carbon Fiber-Reinforced Composites, Polymers (Basel). 13 (2021). https://doi.org/10.3390/polym13234208.

[41] M.Y. Khalid, Z.U. Arif, W. Ahmed, H. Arshad, Recent trends in recycling and reusing techniques of different plastic polymers and their composite materials, Sustain. Mater. Technol. 31 (2022) e00382. https://doi.org/https://doi.org/10.1016/j.susmat.2021.e00382.

[42] J. Beauson, B. Madsen, C. Toncelli, P. Brøndsted, J. Ilsted Bech, Recycling of

shredded composites from wind turbine blades in new thermoset polymer composites, Compos. Part A Appl. Sci. Manuf. 90 (2016) 390–399. https://doi.org/10.1016/j.compositesa.2016.07.009.

[43] S. Pimenta, S.T. Pinho, The effect of recycling on the mechanical response of carbon fibres and their composites, Compos. Struct. 94 (2012) 3669–3684. https://doi.org/10.1016/j.compstruct.2012.05.024.

[44] J. Smoleń, P. Olesik, J. Jała, A. Adamcio, K. Kurtyka, M. Godzierz, R. Kozera, M. Kozioł, A. Boczkowska, The Use of Carbon Fibers Recovered by Pyrolysis from End-of-Life Wind Turbine Blades in Epoxy-Based Composite Panels., Polymers (Basel). 14 (2022). https://doi.org/10.3390/polym14142925.

[45] S.R. Naqvi, H.M. Prabhakara, E.A. Bramer, W. Dierkes, R. Akkerman, G. Brem, A critical review on recycling of end-of-life carbon fibre/glass fibre reinforced composites waste using pyrolysis towards a circular economy, Resour. Conserv. Recycl. 136 (2018) 118–129. https://doi.org/https://doi.org/10.1016/j.resconrec.2018.04.013.

[46] R. Abdallah, A. Juaidi, M.A. Savaş, H. Çamur, A. Albatayneh, S. Abdala, F. Manzano-Agugliaro, A Critical Review on Recycling Composite Waste Using Pyrolysis for Sustainable Development, Energies. 14 (2021). https://doi.org/10.3390/en14185748.

[47] G. Oliveux, L.O. Dandy, G.A. Leeke, Current status of recycling of fibre reinforced polymers: Review of technologies, reuse and resulting properties, Prog. Mater. Sci. 72 (2015) 61–99. https://doi.org/https://doi.org/10.1016/j.pmatsci.2015.01.004.

[48] W. Ballout, N. Sallem-Idrissi, M. Sclavons, C. Doneux, C. Bailly, T. Pardoen, P. Van Velthem, High performance recycled CFRP composites based on reused carbon fabrics through sustainable mild solvolysis route, Sci. Rep. 12 (2022) 1–15. https://doi.org/10.1038/s41598-022-09932-0.

[49] A. Isa, N. Nosbi, M. Che Ismail, H. Md Akil, W.F.F. Wan Ali, M.F. Omar, A Review on Recycling of Carbon Fibres: Methods to Reinforce and Expected Fibre Composite Degradations., Mater. (Basel, Switzerland). 15 (2022). https://doi.org/10.3390/ma15144991.

[50] H.-J. Endres, M. Shamsuyeva, Composites-Recycling-Studie, 2023.

[51] K. Kooduvalli, J. Unser, S. Ozcan, U.K. Vaidya, Embodied Energy in Pyrolysis and Solvolysis Approaches to Recycling for Carbon Fiber-Epoxy Reinforced Composite Waste Streams, Recycling. 7 (2022). https://doi.org/10.3390/recycling7010006.

[52] J.S. Terry, A.C. Taylor, The properties and suitability of commercial bio-based epoxies for use in fiber-reinforced composites, J. Appl. Polym. Sci. 138 (2021) 50417. https://doi.org/https://doi.org/10.1002/app.50417.

[53] J.M. Breitsameter, N. Reinhardt, M. Feigel, O. Hinrichsen, K. Drechsler, B. Rieger, Synthesis of a Sustainable and Bisphenol A-Free Epoxy Resin Based on Sorbic Acid and Characterization of the Cured Thermoset, Macromol. Mater. Eng. n/a (n.d.) 2300068.

https://doi.org/https://doi.org/10.1002/mame.202300068.

[54] GreenPoxy, (n.d.). https://greenpoxy.org/technologies/ (accessed November 24, 2023).

[55] Z. Yu, S. Ma, Y. Liu, Y. Su, H. Feng, P. Li, Y. Dong, Z. Tang, K. Zhang, J. Zhu, Facile synthesis of bio-based latent curing agent and its high-Tg epoxy network, Eur. Polym. J. 164 (2022) 110965. https://doi.org/https://doi.org/10.1016/j.eurpolymj.2021.110965.

[56] X. Su, Z. Zhou, J. Liu, J. Luo, R. Liu, A recyclable vanillin-based epoxy resin with high-performance that can compete with DGEBA, Eur. Polym. J. 140 (2020) 110053. https://doi.org/10.1016/j.eurpolymj.2020.110053.

[57] A.S. Amarasekara, R. Garcia-Obergon, A.K. Thompson, Vanillin-based polymers: IV. Hydrovanilloin epoxy resins, J. Appl. Polym. Sci. 136 (2019) 47000. https://doi.org/https://doi.org/10.1002/app.47000.

[58] S. Caillol, B. Boutevin, R. Auvergne, Eugenol, a developing asset in biobased epoxy resins, Polymer (Guildf). 223 (2021) 123663. https://doi.org/https://doi.org/10.1016/j.polymer.2021.123663.

[59] I. Faye, M. Decostanzi, Y. Ecochard, S. Caillol, Eugenol bio-based epoxy thermosets: from cloves to applied materials, Green Chem. 19 (2017) 5236–5242. https://doi.org/10.1039/C7GC02322G.

[60] C. Gioia, M. Colonna, A. Tagami, L. Medina, O. Sevastyanova, L.A. Berglund, M. Lawoko, Lignin-Based Epoxy Resins: Unravelling the Relationship between Structure and Material Properties, Biomacromolecules. 21 (2020) 1920–1928. https://doi.org/10.1021/acs.biomac.0c00057.

[61] S. Kumar, S.K. Samal, S. Mohanty, S.K. Nayak, Recent Development of Biobased Epoxy Resins: A Review, Polym. Plast. Technol. Eng. 57 (2018) 133–155. https://doi.org/10.1080/03602559.2016.1253742.

[62] D. Matykiewicz, K. Skórczewska, Characteristics and Application of Eugenol in the Production of Epoxy and Thermosetting Resin Composites: A Review, Materials (Basel). 15 (2022). https://doi.org/10.3390/ma15144824.

[63] H. Nabipour, H. Niu, X. Wang, S. Batool, Y. Hu, Fully bio-based epoxy resin derived from vanillin with flame retardancy and degradability, React. Funct. Polym. 168 (2021) 105034. https://doi.org/https://doi.org/10.1016/j.reactfunctpolym.2021.105034.

[64] S. Nikafshar, O. Zabihi, S. Hamidi, Y. Moradi, S. Barzegar, M. Ahmadi, M. Naebe, A renewable bio-based epoxy resin with improved mechanical performance that can compete with DGEBA, RSC Adv. 7 (2017) 8694–8701. https://doi.org/10.1039/C6RA27283E.

[65] Z. Wang, P. Gnanasekar, S. Sudhakaran Nair, R. Farnood, S. Yi, N. Yan, Biobased Epoxy Synthesized from a Vanillin Derivative and Its Reinforcement Using Lignin-Containing Cellulose Nanofibrils, ACS Sustain. Chem. Eng. 8 (2020) 11215–11223. https://doi.org/10.1021/acssuschemeng.0c02559.

[66] J. Breitsameter, Innovative Synthesis of Carbon Fiber Precursors and Epoxy Thermosets : Advances Towards Sustainable Fiber Composite Materials, (2023).

[67] K. Zuo, H. Li, J. Chen, Q. Ran, M. Huang, X. Cui, L. He, J. Liu, Z. Jiang, Effective Biotransformation of Variety of Guaiacyl Lignin Monomers Into Vanillin by Bacillus pumilus, Front. Microbiol. 13 (2022) 1–9. https://doi.org/10.3389/fmicb.2022.901690.

[68] A. Hohmann, J. Frank, ENVIRONMENTAL FRIENDLY FIBER REINFORCED PLASTICS (FRP) FOR HIGH PERFORMANCE APPLICATIONS Assessment of the global warming potential (GWP) and related levers, (2021).

[69] A.K. Giri, Genetic toxicology of epichlorohydrin: A review, Mutat. Res. - Rev. Mutat. Res. 386 (1997) 25–38. https://doi.org/10.1016/S1383-5742(96)00042-7.

[70] M.A. Rashid, M.N. Hasan, M.A.R. Dayan, M.S. Ibna Jamal, M.K. Patoary, A Critical Review of Sustainable Vanillin-modified Vitrimers: Synthesis, Challenge and Prospects, Reactions. 4 (2023) 66–91. https://doi.org/10.3390/reactions4010003.

[71] X. Dupain, D.J. Costa, C.J. Schaverien, M. Makkee, J.A. Moulijn, Cracking of a rapeseed vegetable oil under realistic FCC conditions, Appl. Catal. B Environ. 72 (2007) 44–61. https://doi.org/10.1016/j.apcatb.2006.10.005.

[72] I. BALDE, C. KANE, A.K.D. DIME, S. BALDE, K. NDIAYE, Vegetable Oils Epoxidation Mechanisms, World J. Anal. Chem. Vol. 7, 2022, Pages 1-6. 7 (2022) 1–6. https://doi.org/10.12691/wjac-7-1-1.

[73] K.L. Chong, J.C. Lai, R.A. Rahman, N. Adrus, Z.H. Al-Saffar, A. Hassan, T.H. Lim, M.U. Wahit, A review on recent approaches to sustainable bio-based epoxy vitrimer from epoxidized vegetable oils, Ind. Crops Prod. 189 (2022) 115857. https://doi.org/https://doi.org/10.1016/j.indcrop.2022.115857.

[74] Q. Ma, X. Liu, R. Zhang, J. Zhu, Y. Jiang, Synthesis and properties of full bio-based thermosetting resins from rosin acid and soybean oil: the role of rosin acid derivatives, Green Chem. 15 (2013) 1300–1310. https://doi.org/10.1039/C3GC00095H.

[75] E. Ramon, C. Sguazzo, P.M.G.P. Moreira, A Review of Recent Research on Bio-Based Epoxy Systems for Engineering Applications and Potentialities in the Aviation Sector, Aerospace. 5 (2018). https://doi.org/10.3390/aerospace5040110.

[76] R. Wang, Manufacturing of vegetable oils-based epoxy and composites for structural applications, Missouri Univ. Sci. Technol. (2014) 5–10.

[77] PRODUKTDATENBLATT SikaBiresin® CR80, (n.d.). https://industry.sika.com/dam/dms/deaddconst01/a/sikabiresin-cr80.pdf (accessed November 22, 2023).

[78] A. Kadam, M. Pawar, O. Yemul, V. Thamke, K. Kodam, Biodegradable biobased epoxy resin from karanja oil, Polymer (Guildf). 72 (2015) 82–92. https://doi.org/https://doi.org/10.1016/j.polymer.2015.07.002.

[79] A. Anusic, Y. Blößl, G. Oreski, K. Resch-Fauster, High-performance thermoset with 100 % bio-based carbon content, Polym. Degrad. Stab. 181 (2020) 1–9. https://doi.org/10.1016/j.polymdegradstab.2020.109284.

[80] C. Ding, P.S. Shuttleworth, S. Makin, J.H. Clark, A.S. Matharu, New insights into

the curing of epoxidized linseed oil with dicarboxylic acids, Green Chem. 17 (2015) 4000–4008. https://doi.org/10.1039/c5gc00912j.

[81] T. Takahashi, K. Hirayama, N. Teramoto, M. Shibata, Biocomposites composed of epoxidized soybean oil cured with terpene-based acid anhydride and cellulose fibers, J. Appl. Polym. Sci. 108 (2008) 1596–1602. https://doi.org/https://doi.org/10.1002/app.27866.

[82] J.M. España, L. Sánchez-Nacher, T. Boronat, V. Fombuena, R. Balart, Properties of Biobased Epoxy Resins from Epoxidized Soybean Oil (ESBO) Cured with Maleic Anhydride (MA), J. Am. Oil Chem. Soc. 89 (2012) 2067–2075. https://doi.org/10.1007/s11746-012-2102-2.

[83] M.D. Samper, V. Fombuena, T. Boronat, D. García-Sanoguera, R. Balart, Thermal and mechanical characterization of epoxy resins (ELO and ESO) cured with anhydrides, JAOCS, J. Am. Oil Chem. Soc. 89 (2012) 1521–1528. https://doi.org/10.1007/s11746-012-2041-y.

[84] M.D. Samper, J.M. Ferri, A. Carbonell-Verdu, R. Balart, O. Fenollar, Properties of biobased epoxy resins from epoxidized linseed oil (ELO) crosslinked with a mixture of cyclic anhydride and maleinized linseed oil, Express Polym. Lett. 13 (2019) 407–418. https://doi.org/10.3144/expresspolymlett.2019.34.

[85] M. Schwaiger, K. Resch-Fauster, Mechanical flexible epoxy resins with 100% bio-based carbon content based on epoxidized vegetable oils, J. Appl. Polym. Sci. 139 (2022) e53233. https://doi.org/https://doi.org/10.1002/app.53233.

[86] A.P. Gupta, S. Ahmad, A. Dev, Modification of novel bio-based resin-epoxidized soybean oil by conventional epoxy resin, Polym. Eng. Sci. 51 (2011) 1087–1091. https://doi.org/https://doi.org/10.1002/pen.21791.

[87] R. Wang, T.P. Schuman, Vegetable oil-derived epoxy monomers and polymer blends: A comparative study with review, Express Polym. Lett. 7 (2012) 272–292. https://doi.org/10.3144/expresspolymlett.2013.25.

[88] M.I. Necolau, C.M. Damian, E. Olaret, H. Iovu, B. Balanuca, Comparative Thermo-Mechanical Properties of Sustainable Epoxy Polymer Networks Derived from Linseed Oil, Polymers (Basel). 14 (2022). https://doi.org/10.3390/polym14194212.

[89] J.M. Pin, N. Sbirrazzuoli, A. Mija, From epoxidized linseed oil to bioresin: An overall approach of epoxy/anhydride cross-linking, ChemSusChem. 8 (2015) 1232–1243. https://doi.org/10.1002/cssc.201403262.

[90] A. Todorovic, K. Resch-Fauster, A.R. Mahendran, G. Oreski, W. Kern, Curing of epoxidized linseed oil: Investigation of the curing reaction with different hardener types, J. Appl. Polym. Sci. 138 (2021) 1–13. https://doi.org/10.1002/app.50239.

[91] S. Ebnesajjad, Chapter 4 - Surface and Material Characterization Techniques, in: S. Ebnesajjad (Ed.), Surf. Treat. Mater. Adhes. Bond. (Second Ed., Second Edi, William Andrew Publishing, Oxford, 2014: pp. 39–75. https://doi.org/https://doi.org/10.1016/B978-0-323-26435-8.00004-6.

[92] S. Mayer, M. Tallawi, I. De Luca, A. Calarco, N. Reinhardt, L.A. Gray, K.

Drechsler, A. Moeini, N. Germann, Antimicrobial and physicochemical characterization of 2,3-dialdehyde cellulose-based wound dressings systems., Carbohydr. Polym. 272 (2021) 118506. https://doi.org/10.1016/j.carbpol.2021.118506.

[93] F.C. Fernandes, K. Kirwan, P.R. Wilson, S.R. Coles, Optimisation of waste vegetable oil-based thermoset polymers, Green Mater. 6 (2018) 38–46. https://doi.org/10.1680/jgrma.17.00036.

[94] A. Campanella, M. Zhan, P. Watt, A.T. Grous, C. Shen, R.P. Wool, Triglyceride-based thermosetting resins with different reactive diluents and fiber reinforced composite applications, Compos. Part A Appl. Sci. Manuf. 72 (2015) 192–199. https://doi.org/10.1016/j.compositesa.2015.02.009.

[95] M.R.M. Hafiezal, A. Khalina, Z.A. Zurina, M.D.M. Azaman, Z.M. Hanafee, Thermal and flammability characteristics of blended jatropha bio-epoxy as matrix in carbon fiber–reinforced polymer, J. Compos. Sci. 3 (2019). https://doi.org/10.3390/jcs3010006.

[96] A. Murawski, R.L. Quirino, Bio-Based Composites with Enhanced Matrix-Reinforcement Interactions from the Polymerization of α-Eleostearic Acid, Coatings. 9 (2019). https://doi.org/10.3390/coatings9070447.

[97] F.C. Fernandes, K. Kirwan, D. Lehane, S.R. Coles, Epoxy resin blends and composites from waste vegetable oil, Eur. Polym. J. 89 (2017) 449–460. https://doi.org/https://doi.org/10.1016/j.eurpolymj.2017.02.005.

[98] F.-L. Jin, S.-J. Park, Thermomechanical behavior of epoxy resins modified with epoxidized vegetable oils, Polym. Int. 57 (2008) 577–583. https://doi.org/https://doi.org/10.1002/pi.2280.

[99] Y.-N. Jin, H.-C. Yang, H. Huang, Z.-K. Xu, Underwater superoleophobic coatings fabricated from tannic acid-decorated carbon nanotubes, RSC Adv. 5 (2015) 16112–16115. https://doi.org/10.1039/C4RA16074F.

[100] R. Mustapha, A.R. Rahmat, R. Abdul Majid, S.N.H. Mustapha, Vegetable oil-based epoxy resins and their composites with bio-based hardener: a short review, Polym. Technol. Mater. 58 (2019) 1311–1326. https://doi.org/10.1080/25740881.2018.1563119.

[101] M. Korey, G.P. Mendis, J.P. Youngblood, J.A. Howarter, Tannic acid: A sustainable crosslinking agent for high glass transition epoxy materials, J. Polym. Sci. Part A Polym. Chem. 56 (2018) 1468–1480. https://doi.org/10.1002/pola.29028.

[102] C. Ding, A.S. Matharu, Recent developments on biobased curing agents: A review of their preparation and use, ACS Sustain. Chem. Eng. 2 (2014) 2217–2236. https://doi.org/10.1021/sc500478f.

[103] M. Korey, Tannic Acid: A Key To Reducing Environmental Impacts of Epoxy., Purdue University Graduate School, 2020.

[104] Y.O. Kim, J. Cho, H. Yeo, B.W. Lee, B.J. Moon, Y.M. Ha, Y.R. Jo, Y.C. Jung, Flame Retardant Epoxy Derived from Tannic Acid as Biobased Hardener, ACS Sustain. Chem. Eng. 7 (2019) 3858–3865.

https://doi.org/10.1021/acssuschemeng.8b04851.

[105] X. Feng, J. Fan, A. Li, G. Li, Biobased Tannic Acid Cross-Linked Epoxy Thermosets with Hierarchical Molecular Structure and Tunable Properties: Damping, Shape Memory, and Recyclability, ACS Sustain. Chem. Eng. 8 (2020) 874–883. https://doi.org/10.1021/acssuschemeng.9b05198.

[106] M. Qi, Y.J. Xu, W.H. Rao, X. Luo, L. Chen, Y.Z. Wang, Epoxidized soybean oil cured with tannic acid for fully bio-based epoxy resin, RSC Adv. 8 (2018) 26948–26958. https://doi.org/10.1039/c8ra03874k.

[107] M. Shibata, N. Teramoto, K. Makino, Preparation and properties of biocomposites composed of epoxidized soybean oil, tannic acid, and microfibrillated cellulose, J. Appl. Polym. Sci. 120 (2011) 273–278. https://doi.org/https://doi.org/10.1002/app.33082.

[108] M.R. Loos, L.A.F. Coelho, S.H. Pezzin, S.C. Amico, The effect of acetone addition on the properties of epoxy, Polimeros. 18 (2008) 76–80. https://doi.org/10.1590/S0104-14282008000100015.

[109] C. Yi, P. Rostron, N. Vahdati, E. Gunister, A. Alfantazi, Curing kinetics and mechanical properties of epoxy based coatings: The influence of added solvent, Prog. Org. Coatings. 124 (2018) 165–174. https://doi.org/10.1016/j.porgcoat.2018.08.009.

[110] V. Schenk, K. Labastie, M. Destarac, P. Olivier, M. Guerre, Vitrimer composites: current status and future challenges, Mater. Adv. 3 (2022) 8012–8029. https://doi.org/10.1039/d2ma00654e.

[111] W. Alabiso, S. Schlögl, The impact of vitrimers on the industry of the future: Chemistry, properties and sustainable forward-looking applications, Polymers (Basel). 12 (2020). https://doi.org/10.3390/POLYM12081660.

[112] J. Zheng, Z.M. Png, S.H. Ng, G.X. Tham, E. Ye, S.S. Goh, X.J. Loh, Z. Li, Vitrimers: Current research trends and their emerging applications, Mater. Today. 51 (2021) 586–625. https://doi.org/10.1016/j.mattod.2021.07.003.

[113] M.A. Lucherelli, A. Duval, L. Avérous, Biobased vitrimers: Towards sustainable and adaptable performing polymer materials, Prog. Polym. Sci. 127 (2022) 101515. https://doi.org/https://doi.org/10.1016/j.progpolymsci.2022.101515.

[114] A. Trejo-Machin, L. Puchot, P. Verge, A cardanol-based polybenzoxazine vitrimer: Recycling, reshaping and reversible adhesion, Polym. Chem. 11 (2020) 7026–7034. https://doi.org/10.1039/d0py01239d.

[115] H. Sharma, S. Rana, P. Singh, M. Hayashi, W.H. Binder, E. Rossegger, A. Kumar, S. Schlögl, Self-healable fiber-reinforced vitrimer composites: overview and future prospects, RSC Adv. 12 (2022) 32569–32582. https://doi.org/10.1039/d2ra05103f.

[116] D. Montarnal, M. Capelot, F. Tournilhac, L. Leibler, Silica-like malleable materials from permanent organic networks, Science (80-.). 334 (2011) 965–968. https://doi.org/10.1126/science.1212648.

[117] M. Hayashi, Rheological Characteristics of Cross-Linked Materials with Associative Bond Exchange Mechanisms, Nihon Reoroji Gakkaishi. 50 (2022)

15–20. https://doi.org/10.1678/rheology.50.15.

[118] M. Chen, L. Zhou, Y. Wu, X. Zhao, Y. Zhang, Rapid Stress Relaxation and Moderate Temperature of Malleability Enabled by the Synergy of Disulfide Metathesis and Carboxylate Transesterification in Epoxy Vitrimers, ACS Macro Lett. 8 (2019) 255–260. https://doi.org/10.1021/acsmacrolett.9b00015.

[119] W. Denissen, J.M. Winne, F.E. Du Prez, Vitrimers: Permanent organic networks with glass-like fluidity, Chem. Sci. 7 (2016) 30–38. https://doi.org/10.1039/c5sc02223a.

[120] A. Breuillac, A. Kassalias, R. Nicolaÿ, Polybutadiene Vitrimers Based on Dioxaborolane Chemistry and Dual Networks with Static and Dynamic Cross-links, Macromolecules. 52 (2019) 7102–7113. https://doi.org/10.1021/acs.macromol.9b01288.

[121] T. Liu, C. Hao, S. Zhang, X. Yang, L. Wang, J. Han, Y. Li, J. Xin, J. Zhang, A Self-Healable High Glass Transition Temperature Bioepoxy Material Based on Vitrimer Chemistry, Macromolecules. 51 (2018) 5577–5585. https://doi.org/10.1021/acs.macromol.8b01010.

[122] K. Yu, P. Taynton, W. Zhang, M.L. Dunn, H.J. Qi, Reprocessing and recycling of thermosetting polymers based on bond exchange reactions, RSC Adv. 4 (2014) 10108–10117. https://doi.org/10.1039/c3ra47438k.

[123] H. Zhang, J. Cui, G. Hu, B. Zhang, Recycling strategies for vitrimers, Int. J. Smart Nano Mater. 13 (2022) 367–390. https://doi.org/10.1080/19475411.2022.2087785.

[124] Z. Zhou, S. Kim, C.C. Bowland, B. Li, N. Ghezawi, E. Lara-Curzio, A. Hassen, A.K. Naskar, M.A. Rahman, T. Saito, Unraveling a path for multi-cycle recycling of tailored fiber-reinforced vitrimer composites, Cell Reports Phys. Sci. 3 (2022) 101036. https://doi.org/10.1016/j.xcrp.2022.101036.

[125] P. Taynton, Development of Polyimine-Based Dynamic Covalent Networks: From Malleable Polymers to High-Performance Composites, University of Colorado, 2015.

[126] C. Di Mauro, A. Genua, A. Mija, Fully bio-based reprocessable thermosetting resins based on epoxidized vegetable oils cured with itaconic acid, Ind. Crops Prod. 185 (2022) 115116. https://doi.org/https://doi.org/10.1016/j.indcrop.2022.115116.

[127] Y. Zhang, E. Yukiko, I. Tadahisa, Bio-based vitrimers from divanillic acid and epoxidized soybean oil, RSC Sustain. 1 (2023) 543–553. https://doi.org/10.1039/D2SU00140C.

[128] J. Li, S. Zhang, B. Ju, Soft, fully bio-based poly-hydroxyl thermosets based on catalyst-free transesterification with decent re-processability, J. Appl. Polym. Sci. 139 (2022) e52676. https://doi.org/https://doi.org/10.1002/app.52676.

[129] Y. Zhang, M. Zhai, L. Shi, Q. Lei, S. Zhang, L. Zhang, B. Lyu, S. Zhao, J. Ma, V.K. Thakur, Sustainable castor oil-based vitrimers: Towards new materials with reprocessability, self-healing, degradable and UV-blocking characteristics, Ind. Crops Prod. 193 (2023) 116210.

https://doi.org/https://doi.org/10.1016/j.indcrop.2022.116210.

[130] J. Wu, X. Yu, H. Zhang, J. Guo, J. Hu, M.-H. Li, Fully Biobased Vitrimers from Glycyrrhizic Acid and Soybean Oil for Self-Healing, Shape Memory, Weldable, and Recyclable Materials, ACS Sustain. Chem. Eng. 8 (2020) 6479–6487. https://doi.org/10.1021/acssuschemeng.0c01047.

[131] X. Yang, L. Guo, X. Xu, S. Shang, H. Liu, A fully bio-based epoxy vitrimer: Self-healing, triple-shape memory and reprocessing triggered by dynamic covalent bond exchange, Mater. Des. 186 (2020) 108248. https://doi.org/https://doi.org/10.1016/j.matdes.2019.108248.

[132] S. Mu, Y. Zhang, J. Zhou, B. Wang, Z. Wang, Recyclable and Mechanically Robust Palm Oil-Derived Epoxy Resins with Reconfigurable Shape-Memory Properties, ACS Sustain. Chem. Eng. 8 (2020) 5296–5304. https://doi.org/10.1021/acssuschemeng.0c00443.

[133] W. Zhang, J. Wu, L. Gao, B. Zhang, J. Jiang, J. Hu, Recyclable{,} reprocessable{,} self-adhered and repairable carbon fiber reinforced polymers using full biobased matrices from camphoric acid and epoxidized soybean oil, Green Chem. 23 (2021) 2763–2772. https://doi.org/10.1039/D1GC00648G.

[134] L. Lu, J. Pan, G. Li, Recyclable high-performance epoxy based on transesterification reaction, J. Mater. Chem. A. 5 (2017) 21505–21513. https://doi.org/10.1039/C7TA06397K.

[135] Q. Chang, W. Li, L. Xiao, K. Zhang, J. Huang, Y. Wang, X. Nie, J. Chen, Catalyst-Free, Self-Healing, and Recyclable Tung Oil-Based Epoxy Vitrimers with Dynamic Ester Bonds, Macromol. Chem. Phys. 224 (2023) 2300272. https://doi.org/https://doi.org/10.1002/macp.202300272.

[136] A. Ruiz De Luzuriaga, R. Martin, N. Markaide, A. Rekondo, G. Cabañero, J. Rodríguez, I. Odriozola, Epoxy resin with exchangeable disulfide crosslinks to obtain reprocessable, repairable and recyclable fiber-reinforced thermoset composites, Mater. Horizons. 3 (2016) 241–247. https://doi.org/10.1039/c6mh00029k.

[137] S. Guggari, F. Magliozzi, S. Malburet, A. Graillot, M. Destarac, M. Guerre, Vanillin-Based Epoxy Vitrimers: Looking at the Cystamine Hardener from a Different Perspective, ACS Sustain. Chem. Eng. 11 (2023) 6021–6031. https://doi.org/10.1021/acssuschemeng.3c00379.

[138] T. Liu, C. Hao, L. Shao, W. Kuang, L. Cosimbescu, K.L. Simmons, J. Zhang, Carbon Fiber Reinforced Epoxy Vitrimer: Robust Mechanical Performance and Facile Hydrothermal Decomposition in Pure Water, Macromol. Rapid Commun. 42 (2021) 2000458. https://doi.org/https://doi.org/10.1002/marc.202000458.

[139] H. Si, L. Zhou, Y. Wu, L. Song, M. Kang, X. Zhao, M. Chen, Rapidly reprocessable, degradable epoxy vitrimer and recyclable carbon fiber reinforced thermoset composites relied on high contents of exchangeable aromatic disulfide crosslinks, Compos. Part B Eng. 199 (2020) 108278. https://doi.org/10.1016/j.compositesb.2020.108278.

[140] Y.Y. Liu, G.L. Liu, Y.D. Li, Y. Weng, J.B. Zeng, Biobased High-Performance

Epoxy Vitrimer with UV Shielding for Recyclable Carbon Fiber Reinforced Composites, ACS Sustain. Chem. Eng. 9 (2021) 4638–4647. https://doi.org/10.1021/acssuschemeng.1c00231.

[141] H.T.T. Tran, R. Radjef, M. Nikzad, R. Bjekovic, B. Fox, A vanillin-based vitrimer matrix for recyclable and sustainable carbon fibre-reinforced composites, J. Clean. Prod. 483 (2024) 144289. https://doi.org/https://doi.org/10.1016/j.jclepro.2024.144289.

[142] F.I. Altuna, V. Pettarin, R.J.J. Williams, Self-healable polymer networks based on the cross-linking of epoxidised soybean oil by an aqueous citric acid solution, Green Chem. 15 (2013) 3360–3366. https://doi.org/10.1039/C3GC41384E.

[143] Y.-Y. Liu, J. He, Y.-D. Li, X.-L. Zhao, J.-B. Zeng, Biobased, reprocessable and weldable epoxy vitrimers from epoxidized soybean oil, Ind. Crops Prod. 153 (2020) 112576. https://doi.org/https://doi.org/10.1016/j.indcrop.2020.112576.

[144] B. Wang, S. Ma, Q. Li, H. Zhang, J. Liu, R. Wang, Z. Chen, X. Xu, S. Wang, N. Lu, Y. Liu, S. Yan, J. Zhu, Facile synthesis of “digestible”{,} rigid-and-flexible{,} bio-based building block for high-performance degradable thermosetting plastics, Green Chem. 22 (2020) 1275–1290. https://doi.org/10.1039/C9GC04020J.

[145] M. Sauer, D. Schüppel, MARKET REPORT 2021 - The global Market for Carbon Fibers and Carbon Composites, 2022. https://composites-united.com/wp-content/uploads/2022/05/CU-Marktbericht-2021_ENG_Kurz_final.pdf.

[146] X. Huang, Fabrication and properties of carbon fibers, Materials (Basel). 2 (2009) 2369–2403. https://doi.org/10.3390/ma2042369.

[147] H. Bisheh, Y. Abdin, Carbon Fibers: From PAN to Asphaltene Precursors; A State-of-Art Review, C-Journal Carbon Res. 9 (2023). https://doi.org/10.3390/c9010019.

[148] The Japan Carbon Fiber Manufacturers Association, (n.d.). https://www.carbonfiber.gr.jp/english/material/type.html.

[149] N.M. Nurazzi, M.R.M. Asyraf, A. Khalina, N. Abdullah, H.A. Aisyah, S.A. Rafiqah, F.A. Sabaruddin, S.H. Kamarudin, M.N.F. Norrrahim, R.A. Ilyas, S.M. Sapuan, A Review on Natural Fiber Reinforced Polymer Composite for Bullet Proof and Ballistic Applications., Polymers (Basel). 13 (2021). https://doi.org/10.3390/polym13040646.

[150] S.-J. Park, Carbon Fibers, Springer Singapore, 2018. https://doi.org/https://doi.org/10.1007/978-981-13-0538-2.

[151] R. Shokrani Havigh, H. Mahmoudi Chenari, A comprehensive study on the effect of carbonization temperature on the physical and chemical properties of carbon fibers, Sci. Rep. 12 (2022) 10704. https://doi.org/10.1038/s41598-022-15085-x.

[152] Y. Matsuhisa, A.R. Bunsell, 16 - Tensile failure of carbon fibers, in: A.R. Bunsell (Ed.), Handb. Tensile Prop. Text. Tech. Fibres, Woodhead Publishing, 2009: pp. 574–602. https://doi.org/https://doi.org/10.1533/9781845696801.2.575.

[153] Anelia Milbrandt; Samuel Booth, Carbon Fiber from Biomass, 2016. https://www.nrel.gov/docs/fy16osti/66386.pdf.

[154] Econitrile, (n.d.). https://www.econitrile.com/ (accessed November 15, 2023).

[155] A. Todorovic, Y. Blößl, G. Oreski, K. Resch-Fauster, High-performance composite with 100% bio-based carbon content produced from epoxidized linseed oil, citric acid and flax fiber reinforcement, Compos. Part A Appl. Sci. Manuf. 152 (2022) 106666. https://doi.org/https://doi.org/10.1016/j.compositesa.2021.106666.

[156] Linseed Oil Production Technology, (n.d.). https://www.bestoilmillplant.com/linseed-oil-production-technology.html (accessed January 17, 2024).

[157] Tannic acid, (n.d.). https://www.ebi.ac.uk/chebi/searchId.do?chebiId=CHEBI:75211#:~:text=Commercial tannic acid is usually,sumac leaves (Rhus coriaria). (accessed January 17, 2024).

[158] Your supplier of tannic Acid, (n.d.). https://www.natural-specialities.com/our-ingredients/tannic-acid.html (accessed January 17, 2024).

[159] Tannic acid, (n.d.). https://www.chemicalbook.com/ChemicalProductProperty_EN_CB3116328.htm#:~:text=Tannic acid%2C C14H,C (410°F). (accessed November 20, 2023).

[160] L. Shechter, J. Wynstra, Glycidyl Ether Reactions with Alcohols, Phenols, Carboxylic Acids, and Acid Anhydrides, Ind. Eng. Chem. 48 (1956) 86–93. https://doi.org/10.1021/ie50553a028.

[161] Y.-O. Kim, J. Cho, H. Yeo, B.W. Lee, B.J. Moon, Y.-M. Ha, Y.R. Jo, Y.C. Jung, Flame Retardant Epoxy Derived from Tannic Acid as Biobased Hardener, ACS Sustain. Chem. Eng. 7 (2019) 3858–3865. https://doi.org/10.1021/acssuschemeng.8b04851.

[162] D. Lascano, L. Quiles-Carrillo, S. Torres-Giner, T. Boronat, N. Montanes, Optimization of the Curing and Post-Curing Conditions for the Manufacturing of Partially Bio-Based Epoxy Resins with Improved Toughness, Polymers (Basel). 11 (2019). https://doi.org/10.3390/polym11081354.

[163] J. Lange, N. Altmann, C.T. Kelly, P.J. Halley, Understanding vitrification during cure of epoxy resins using dynamic scanning calorimetry and rheological techniques, Polymer (Guildf). 41 (2000) 5949–5955. https://doi.org/https://doi.org/10.1016/S0032-3861(99)00758-2.

[164] A. Shefer, M. Gottlieb, Effect of crosslinks on the glass transition temperature of end-linked elastomers, Macromolecules. 25 (1992) 4036–4042. https://doi.org/10.1021/ma00041a028.

[165] A. Hale, C.W. Macosko, H.E. Bair, Glass transition temperature as a function of conversion in thermosetting polymers, Macromolecules. 24 (1991) 2610–2621. https://doi.org/10.1021/ma00009a072.

[166] A. Shrivastava, 1 - Introduction to Plastics Engineering, in: A. Shrivastava (Ed.), Introd. to Plast. Eng., William Andrew Publishing, 2018: pp. 1–16. https://doi.org/https://doi.org/10.1016/B978-0-323-39500-7.00001-0.

[167] M. Li, L. Wu, C. Zhang, W. Chen, C. Liu, Hydrophilic and antifouling

modification of PVDF membranes by one-step assembly of tannic acid and polyvinylpyrrolidone, Appl. Surf. Sci. 483 (2019) 967–978. https://doi.org/https://doi.org/10.1016/j.apsusc.2019.04.057.

[168] A.F. Abdelkader, J.R. White, Water absorption in epoxy resins: The effects of the crosslinking agent and curing temperature, J. Appl. Polym. Sci. 98 (2005) 2544–2549. https://doi.org/https://doi.org/10.1002/app.22400.

[169] HexFlow® RTM 6 Product Data, (n.d.). https://www.imatec.it/wp-content/uploads/2016/05/RTM6_global.pdf (accessed January 18, 2024).

[170] C. Ji, H. He, Y. Yang, Moisture absorption process of epoxy resin and mechanical properties of its fiber composites, Mater. Test. 61 (2019) 23–26. https://doi.org/doi:10.3139/120.111276.

[171] G. Quino, V.L. Tagarielli, N. Petrinic, Effects of water absorption on the mechanical properties of GFRPs, Compos. Sci. Technol. 199 (2020) 108316. https://doi.org/https://doi.org/10.1016/j.compscitech.2020.108316.

[172] M. Capelot, M.M. Unterlass, F. Tournilhac, L. Leibler, Catalytic Control of the Vitrimer Glass Transition., ACS Macro Lett. 1 (2012) 789–792. https://doi.org/10.1021/mz300239f.

[173] M. Capelot, D. Montarnal, F. Tournilhac, L. Leibler, Metal-Catalyzed Transesterification for Healing and Assembling of Thermosets, J. Am. Chem. Soc. 134 (2012) 7664–7667. https://doi.org/10.1021/ja302894k.

[174] T.H.T. Myren, T.A. Stinson, Z.J. Mast, C.G. Huntzinger, O.R. Luca, Chemical and Electrochemical Recycling of End-Use Poly(ethylene terephthalate) (PET) Plastics in Batch, Microwave and Electrochemical Reactors., Molecules. 25 (2020). https://doi.org/10.3390/molecules25122742.

[175] Sodium Hydroxide, (n.d.). https://www.chemicalsafetyfacts.org/chemicals/sodium-hydroxide/ (accessed November 28, 2023).

[176] L. Liu, H. Shi, H. Yu, R. Zhou, J. Yin, S. Luan, One-step hydrophobization of tannic acid for antibacterial coating on catheters to prevent catheter-associated infections, Biomater. Sci. 7 (2019) 5035–5043. https://doi.org/10.1039/C9BM01223K.

[177] J.D. Piper, P.W. Piper, Benzoate and Sorbate Salts: A Systematic Review of the Potential Hazards of These Invaluable Preservatives and the Expanding Spectrum of Clinical Uses for Sodium Benzoate, Compr. Rev. Food Sci. Food Saf. 16 (2017) 868–880. https://doi.org/https://doi.org/10.1111/1541-4337.12284.

[178] EFSA Panel on Food Additives and Flavourings (FAF), M. Younes, G. Aquilina, L. Castle, K.-H. Engel, P. Fowler, M.J. Frutos Fernandez, P. Fürst, R. Gürtler, U. Gundert-Remy, T. Husøy, W. Mennes, P. Moldeus, A. Oskarsson, R. Shah, D. Wölfle, C. Lambré, A. Christodoulidou, I. Waalkens-Berendsen, Opinion on the follow-up of the re-evaluation of sorbic acid (E200) and potassium sorbate (E202) as food additives, EFSA J. 17 (2019) e05625. https://doi.org/https://doi.org/10.2903/j.efsa.2019.5625.

[179] A.W. Hofmann, Neue flüchtige Säure der Vogelbeeren, Justus Liebigs Ann.

Chem. 110 (1859) 129–140. https://doi.org/https://doi.org/10.1002/jlac.18591100202.

[180] V. Canale, L. Tonucci, M. Bressan, N. d'Alessandro, Deoxydehydration of glycerol to allyl alcohol catalyzed by rhenium derivatives, Catal. Sci. Technol. 4 (2014) 3697–3704. https://doi.org/10.1039/C4CY00631C.

[181] H. Guo, G. Yin, Catalytic Aerobic Oxidation of Renewable Furfural with Phosphomolybdic Acid Catalyst: an Alternative Route to Maleic Acid, J. Phys. Chem. C. 115 (2011) 17516–17522. https://doi.org/10.1021/jp2054712.

[182] Z. Du, J. Ma, F. Wang, J. Liu, J. Xu, Oxidation of 5-hydroxymethylfurfural to maleic anhydride with molecular oxygen, Green Chem. 13 (2011) 554–557. https://doi.org/10.1039/C0GC00837K.

[183] Essential Building Blocks, (n.d.). https://www.huntsman.com/docs/Documents/Essential Building Blocks for Coatings%2C Adhesives %26 Sealants and Composites Applications.pdf (accessed March 15, 2024).

[184] Vestamin, (n.d.). https://composites.evonik.com/en/products-services/coatings/VESTAMIN (accessed August 6, 2024).

[185] E. Darroman, N. Durand, B. Boutevin, S. Caillol, Improved cardanol derived epoxy coatings, Prog. Org. Coatings. 91 (2016) 9–16. https://doi.org/https://doi.org/10.1016/j.porgcoat.2015.11.012.

[186] E. Ernault, Thermo-oxydation de réseaux époxy/amine, L'École Nationale Supérieure d'Arts et Métiers, 2016. https://pastel.hal.science/tel-01563168.

[187] H. Cai, P. Li, G. Sui, Y. Yu, G. Li, X. Yang, S. Ryu, Curing kinetics study of epoxy resin/flexible amine toughness systems by dynamic and isothermal DSC, Thermochim. Acta. 473 (2008) 101–105. https://doi.org/https://doi.org/10.1016/j.tca.2008.04.012.

[188] P. Gilormini, J. Verdu, On the role of hydrogen bonding on water absorption in polymers, Polymer (Guildf). 142 (2018) 164–169. https://doi.org/https://doi.org/10.1016/j.polymer.2018.03.033.

[189] DIN EN 16785-1:2016-03. Bio-based products - Bio-based content - Part 1: Determination of the bio-based content using the radiocarbon analysis and elemental analysis., 2016. https://doi.org/https://dx.doi.org/10.31030/2325059.

[190] ASTM D6866-22 Standard Test Methods for Determining the Biobased Content of Solid, Liquid, and Gaseous Samples Using Radiocarbon Analysis, (2022). https://doi.org/10.1520/D6866-22.

[191] O. Doebner, Synthese der Sorbinsäure, Berichte Der Dtsch. Chem. Gesellschaft. 33 (1900) 2140–2142. https://doi.org/https://doi.org/10.1002/cber.190003302121.

[192] G. Centi, G. Fornasari, F. Trifirò, On the mechanism of n-butane oxidation to maleic anhydride: Oxidation in oxygen-stoichiometry-controlled conditions, J. Catal. 89 (1984) 44–51. https://doi.org/https://doi.org/10.1016/0021-9517(84)90278-1.

[193] M. Müller, Improved Kinetics of n-Butane Oxidation to Maleic Anhydride: The Role of By-products, Clausthal University of Technology, 2021.

[194] H. Hussain, A. Al-Harrasi, I.R. Green, I. Ahmed, G. Abbas, N.U. Rehman, meta-Chloroperbenzoic acid (mCPBA): a versatile reagent in organic synthesis, RSC Adv. 4 (2014) 12882–12917. https://doi.org/10.1039/C3RA45702H.

[195] N. Mizuno, K. Yamaguchi, Polyoxometalate catalysts: toward the development of green H2O2-based epoxidation systems, Chem. Rec. 6 (2006) 12–22. https://doi.org/https://doi.org/10.1002/tcr.20067.

[196] M. Colladon, A. Scarso, P. Sgarbossa, R.A. Michelin, G. Strukul, Regioselectivity and Diasteroselectivity in Pt(II)-Mediated "Green" Catalytic Epoxidation of Terminal Alkenes with Hydrogen Peroxide: Mechanistic Insight into a Peculiar Substrate Selectivity, J. Am. Chem. Soc. 129 (2007) 7680–7689. https://doi.org/10.1021/ja071142x.

[197] W.A. Herrmann, R.M. Kratzer, R.W. Fischer, Alkylrhenium Oxides from Perrhenates: A New, Economical Access to Organometallic Oxide Catalysts, Angew. Chemie Int. Ed. English. 36 (1997) 2652–2654. https://doi.org/https://doi.org/10.1002/anie.199726521.

[198] E. Abdulmalek, M. Arumugam, H.N. Mizan, M.B. Abdul Rahman, M. Basri, A.B. Salleh, Chemoenzymatic Epoxidation of Alkenes and Reusability Study of the Phenylacetic Acid, Sci. World J. 2014 (2014) 756418. https://doi.org/10.1155/2014/756418.

[199] C. Aouf, E. Durand, J. Lecomte, M.-C. Figueroa-Espinoza, E. Dubreucq, H. Fulcrand, P. Villeneuve, The use of lipases as biocatalysts for the epoxidation of fatty acids and phenolic compounds, Green Chem. 16 (2014) 1740–1754. https://doi.org/10.1039/C3GC42143K.

[200] EVONIK THE ECO PORTFOLIO: PERFORMANCE MEETS SUSTAINABILITY, (n.d.). https://crosslinkers.evonik.com/en/products/eco-grades (accessed December 29, 2023).

A Appendix

a Additional figures

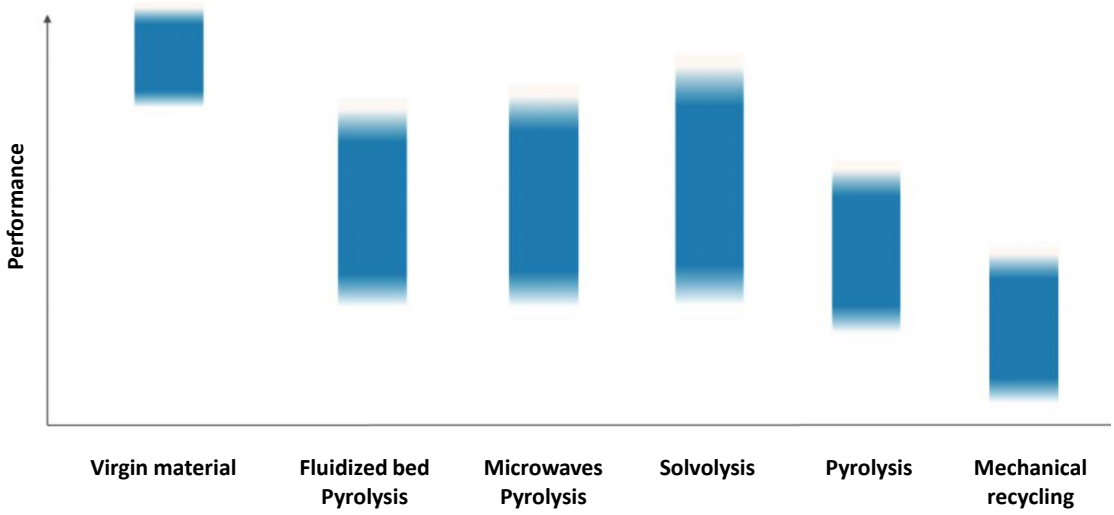

Fig.A- 1: **Performance of fibers in composites in terms of fiber length, sizing, and fiber orientation. The size of the bars is indicative and varies depending on process parameters and fiber type. Adapted from:** [50].

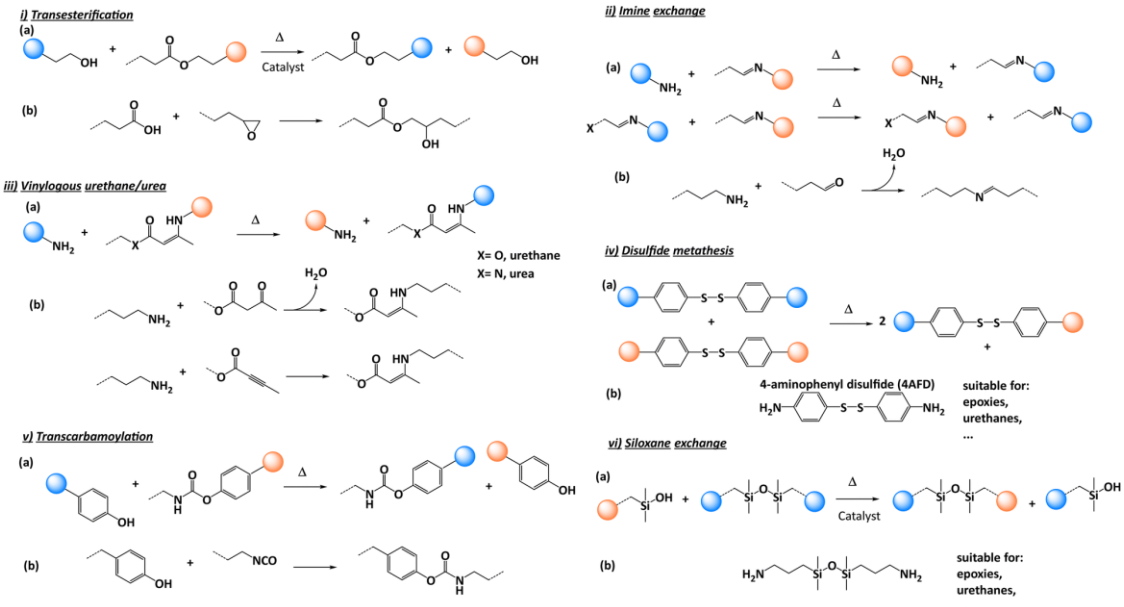

Fig.A- 2: **Exchange reactions for the obtention of vitrimers. From: [110].**

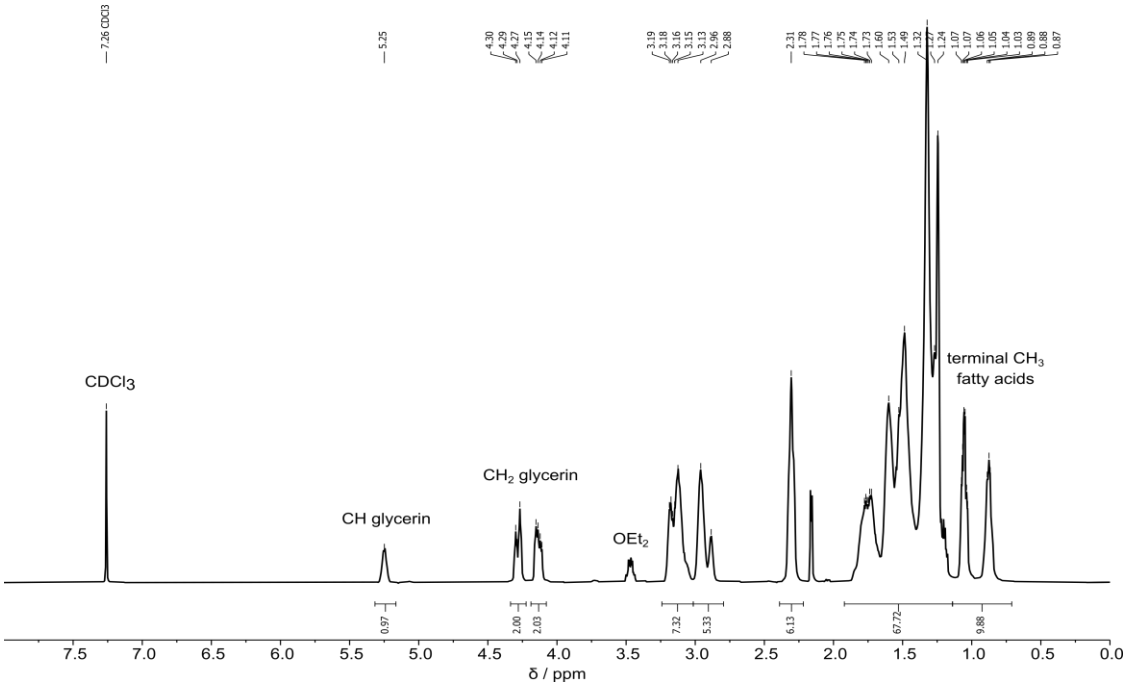

Fig.A- 3: ^{1}H-NMR of epoxidized linseed oil. From: [3].

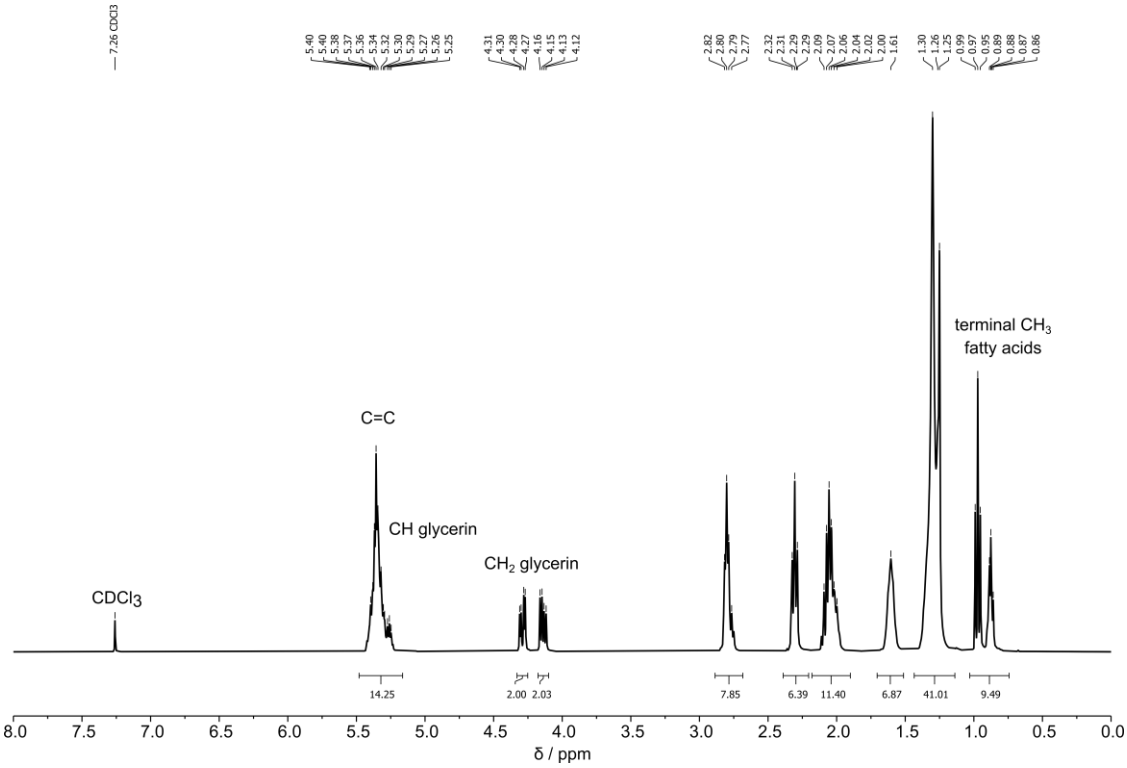

Fig.A- 4: ^{1}H-NMR of linseed oil as bought. From: [3].

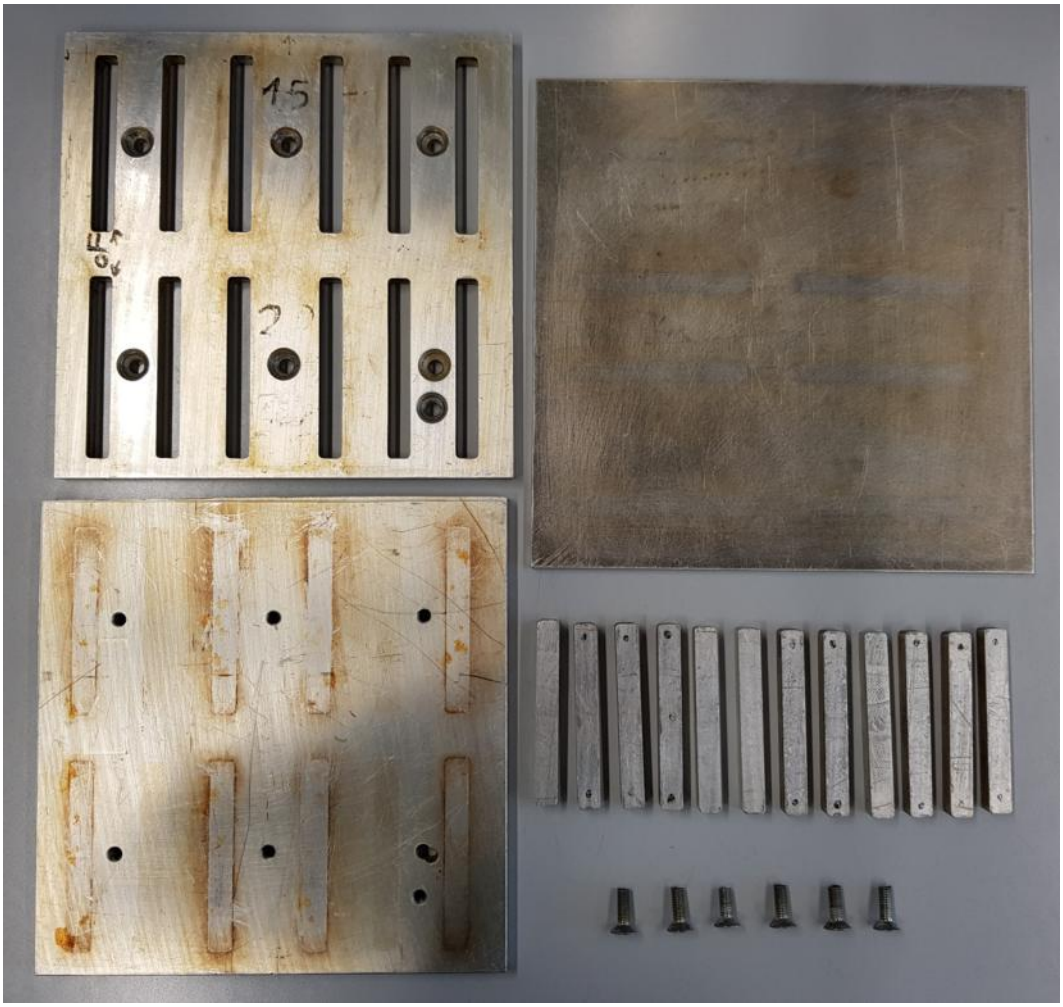

Fig.A- 5: Stamp-die system used for hot-pressing recycled TA/ELO and TA/ELO composites samples. This system was produced in [S15].

Fig.A- 6: TA agglomerates on the sponge roller during lamination

Fig.A- 7: UD Twill 3/1 fabric

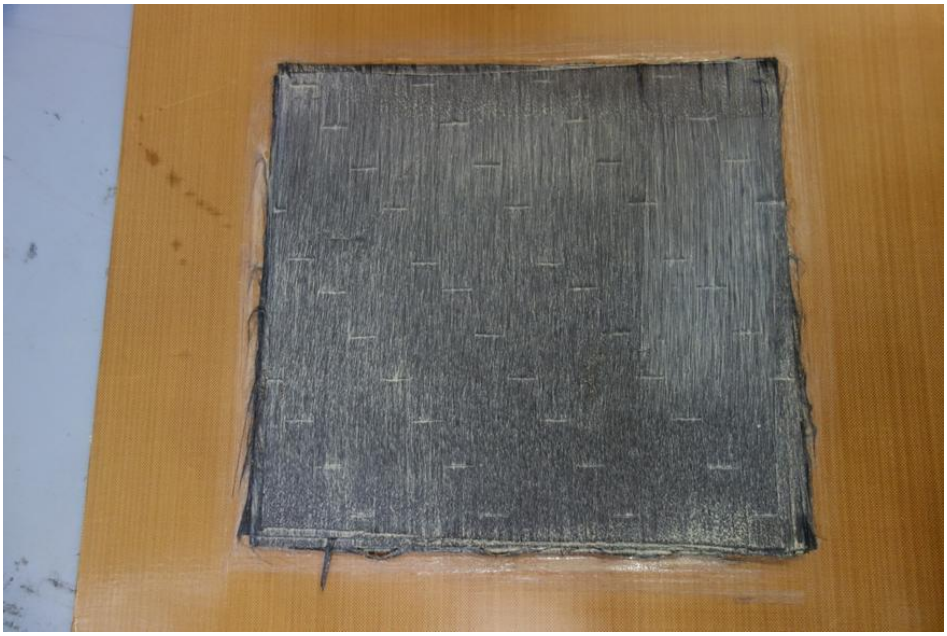

Fig.A- 8: 3/1 twill UD CF fabrics stacked on each other after being hand-laminated.

Fig.A- 9: Oily surface on TA/ELO CF composites plates after hot-pressing.

Fig.A- 10: UD SGL fabric

Fig.A- 11: Inhomogeneous TA/ELO sample after curing at 120 °C

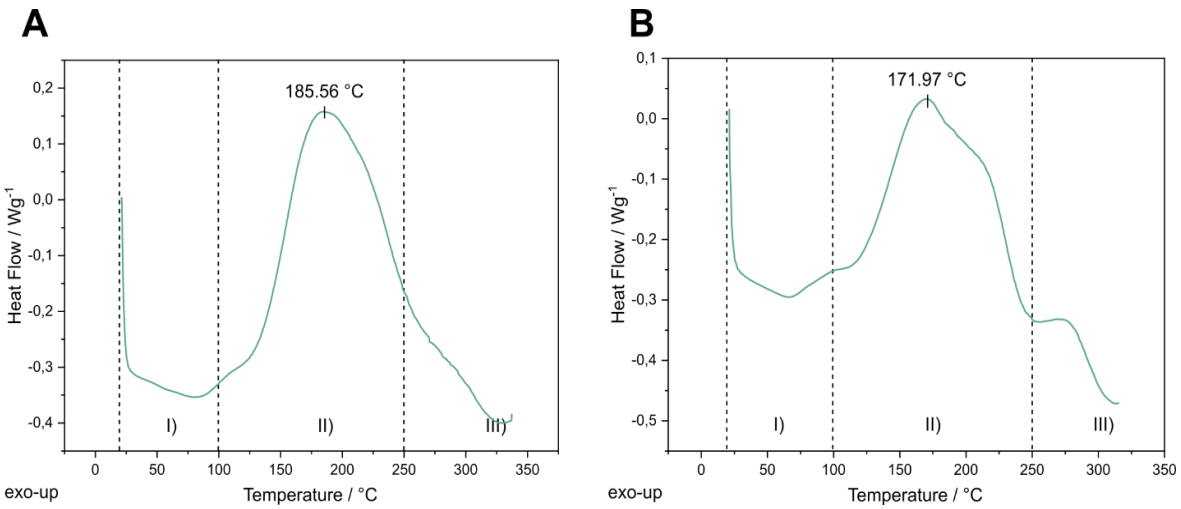

Fig.A- 12: **A) DSC scan of the sample TA/ELO 1.0, B) DSC scan of the sample TA/ELO 2.0. From: [3].**

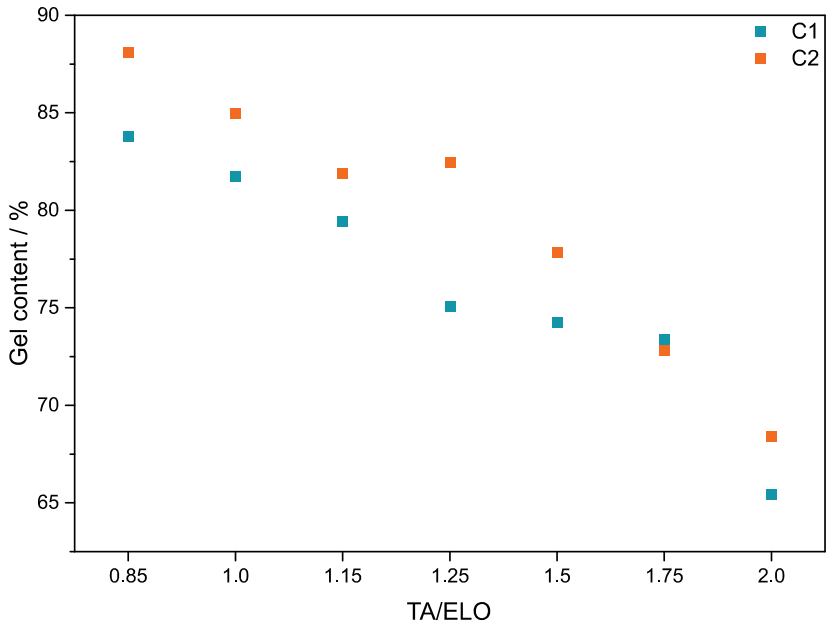

Fig.A- 13: **Gel content measurements of TA/ELO samples cured under condition C1 and C2. From: [3].**

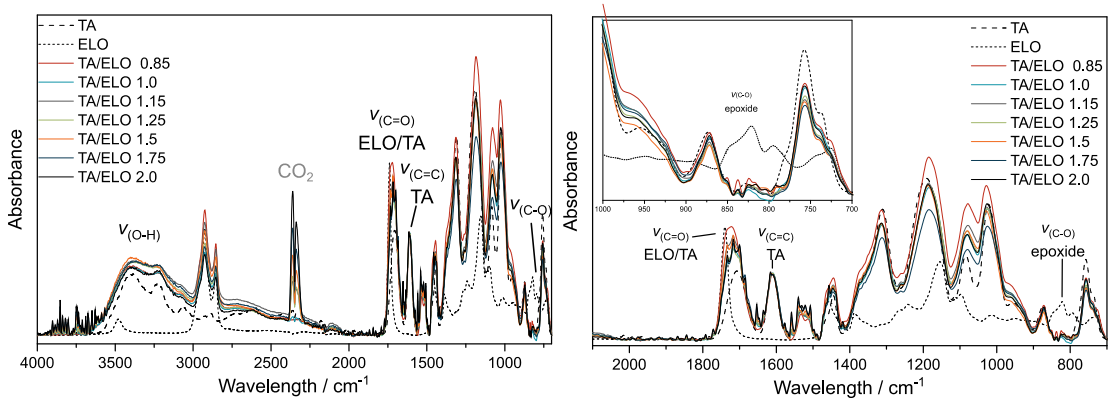

Fig.A- 14: ATR-FTIR spectroscopy of the ELO/TA-samples cured with C1. Left: full spectrum, right: zoom in to the relevant region. Signals normalized to the C=C vibration of TA (1610 cm^{-1}). Signal of the C—O epoxide vibration at 820 cm^{-1}. From: [3].

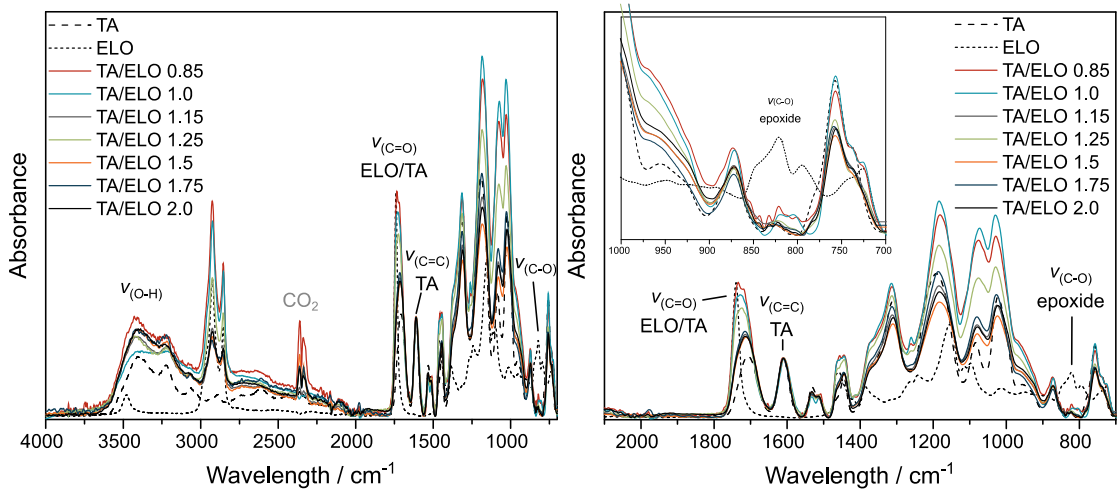

Fig.A- 15: ATR-FTIR spectroscopy of the ELO/TA-samples cured with C2. Left: full spectrum, right: zoom in to the relevant region. Signals normalized to the C=C vibration of TA (1610 cm^{-1}). Signal of the C—O epoxide vibration at 820 cm^{-1}. From: [3].

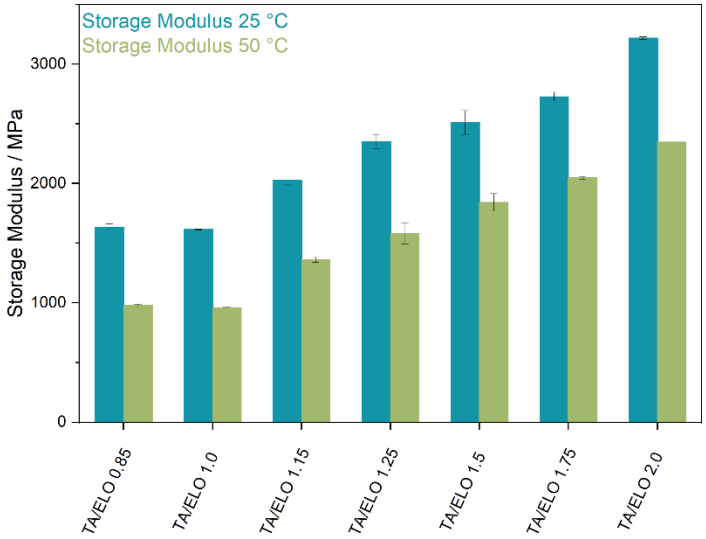

Fig.A- 16: Storage moduli at 25 and 50 °C of the different TA/ELO samples cured with C2. From: [3].

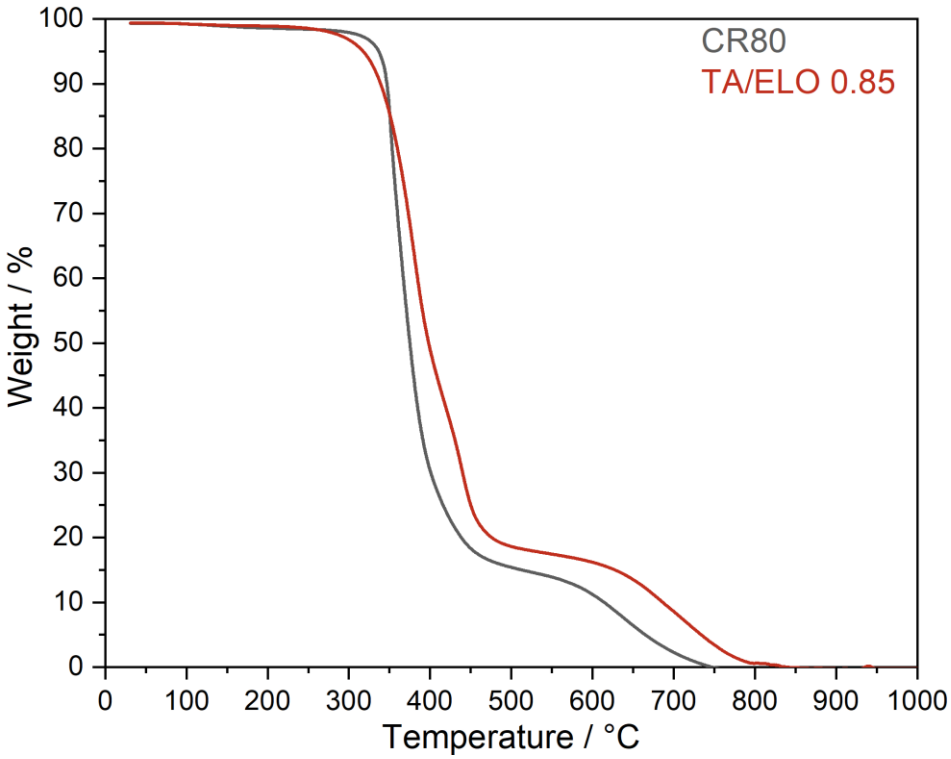

Fig.A- 17: TG curves of high-performance epoxy CR80 from SIKA and TA/ELO 0.85 cured with C2. From: [3].

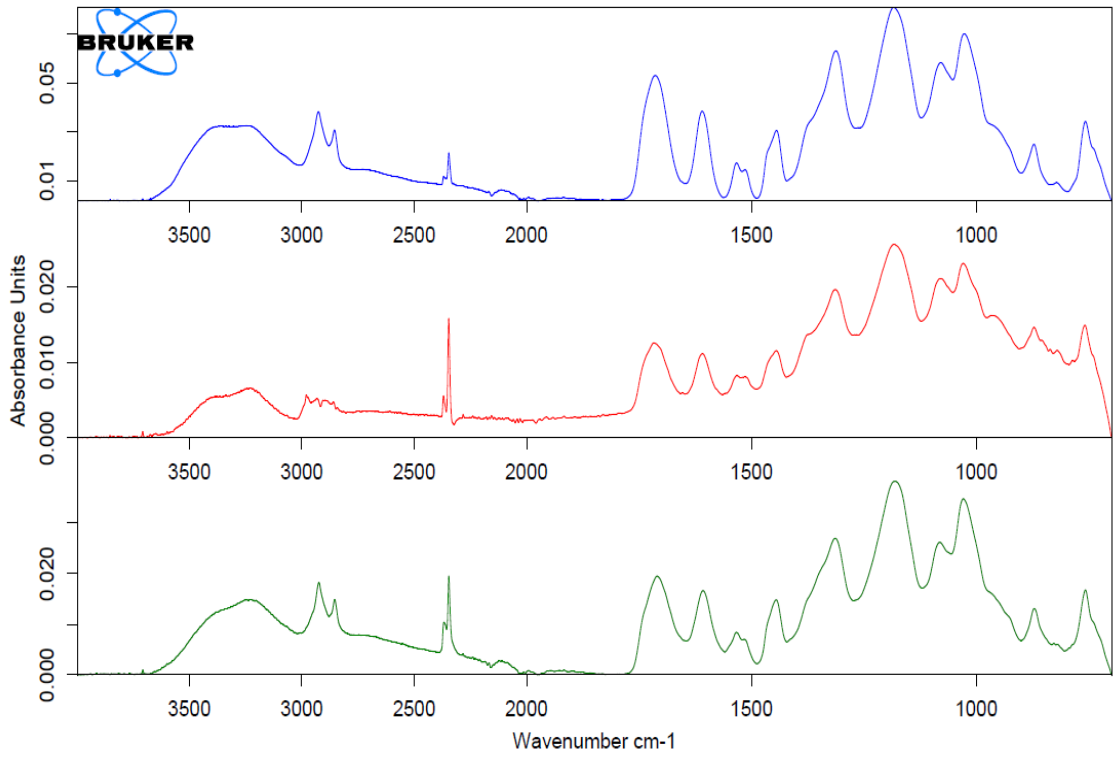

Fig.A- 18: **FTIR spectra of TA/ELO 1.75 cured (blue), TA/ELO 1.75 powder after ball-milling the cured sample (red) and recycled TA/ELO 1.75 after hot-pressing the powder (green).**

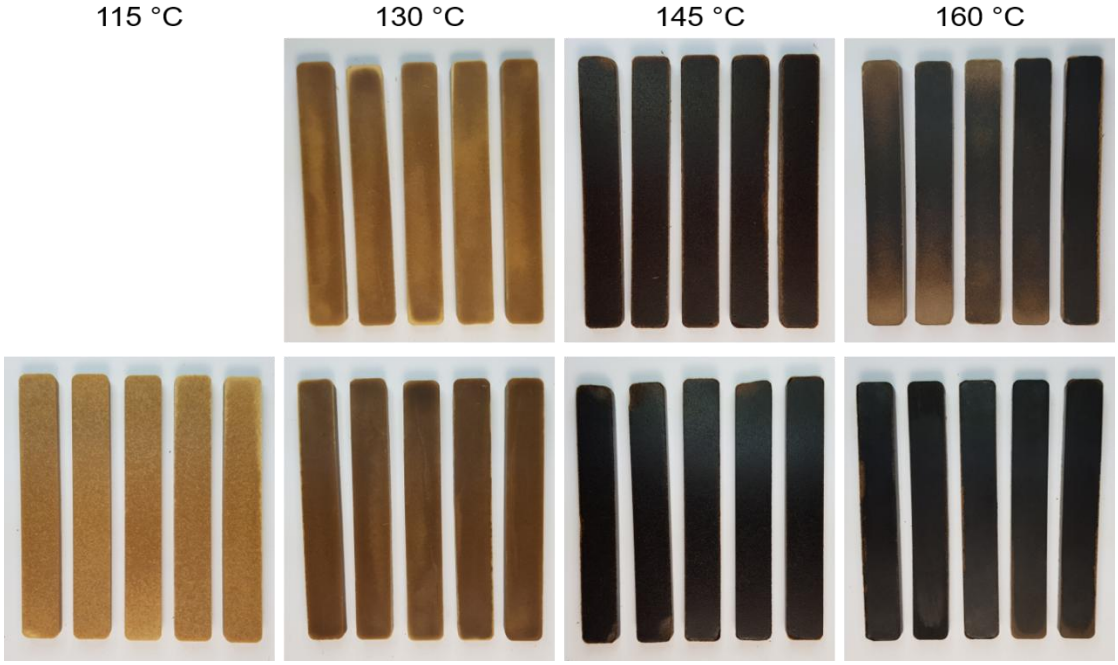

Fig.A- 19: **Change of color of recycled TA/ELO 1.5 with hot-pressing temperature and time applied (up: samples hot-pressed for 1 h, down: samples hot-pressed for 2 h).**

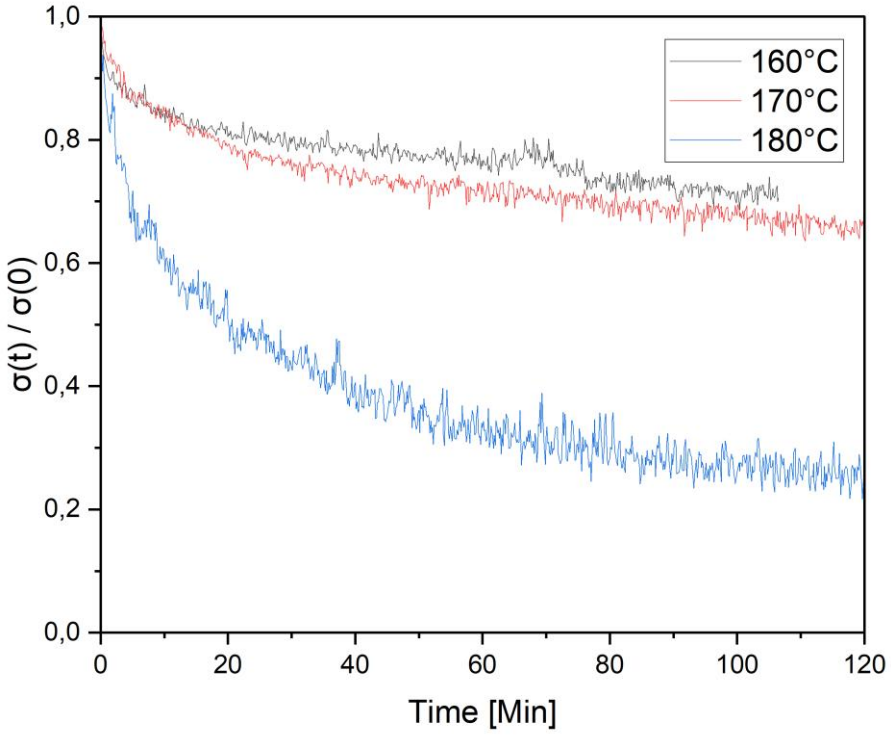

Fig.A- 20: Normalized stress relaxation curves for TA/ELO 1.5 at 160, 170 and 180 °C

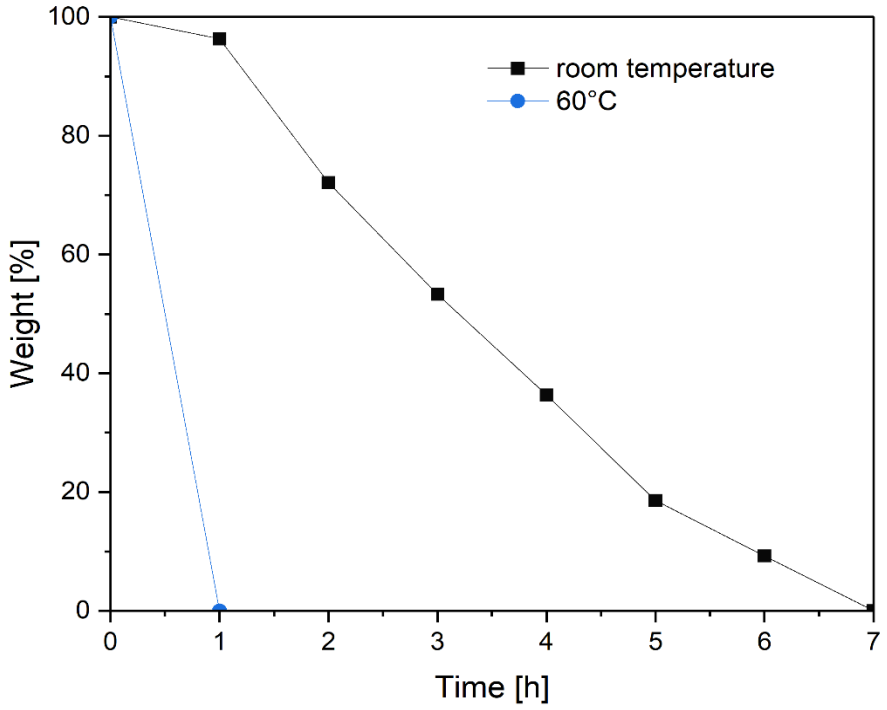

Fig.A- 21: Decomposition of TA/ELO 2.0 in NaOH (1 mol/L) at room temperature and 60 °C.

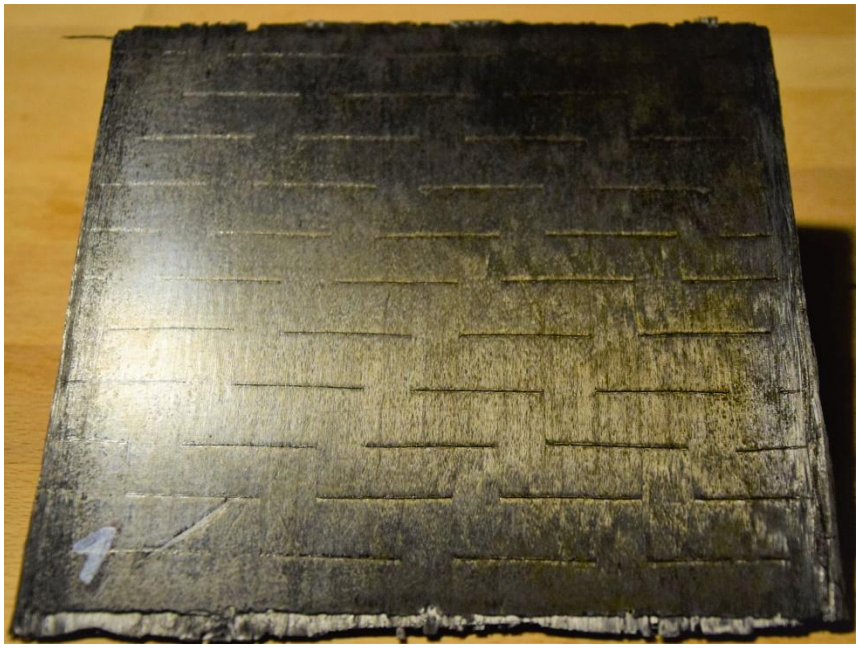

Fig.A- 22: TA/ELO 1.5 CF composite plate manufactured with hot-pressing

Fig.A- 23: TA/ELO 1.5 CF composite plate manufactured with UD SGL fabric and vacuum bagging

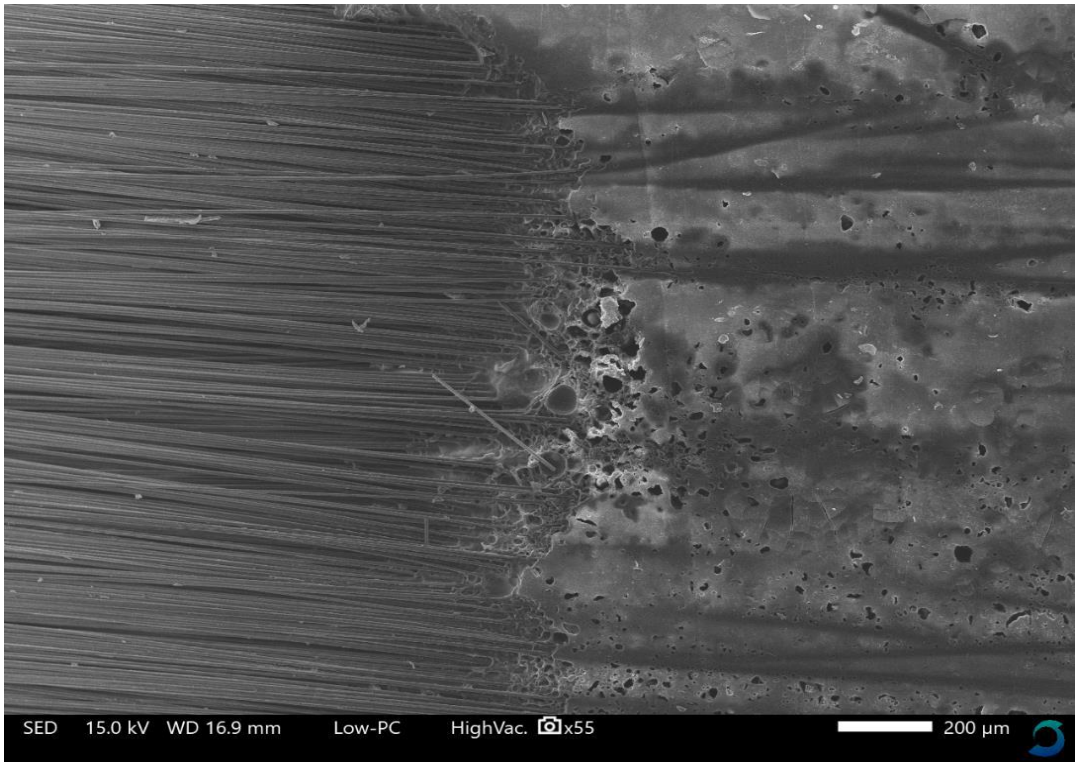

Fig.A- 24: SEM picture showing the interface between immersed TA/ELO composite in NaOH solution (left) and non-immersed TA/ELO composite (right).

Fig.A- 25: TA/ELO composite with stitched UD-CF fabric after immersion in NaOH solution, washing in water and drying. Recovery of the CF.

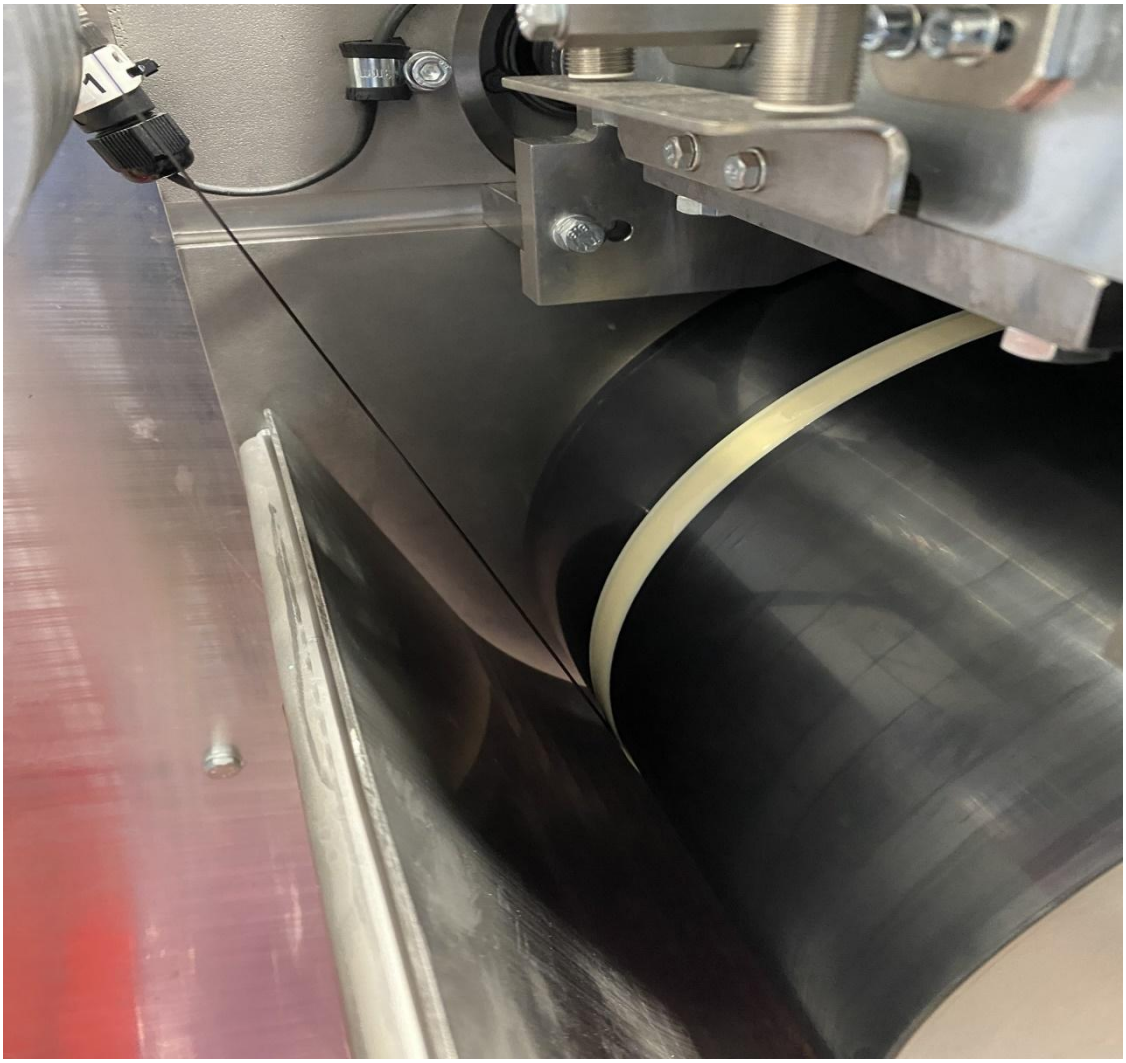

Fig.A- 26: Impregnation of CF tows with TA/ELO 1.5.

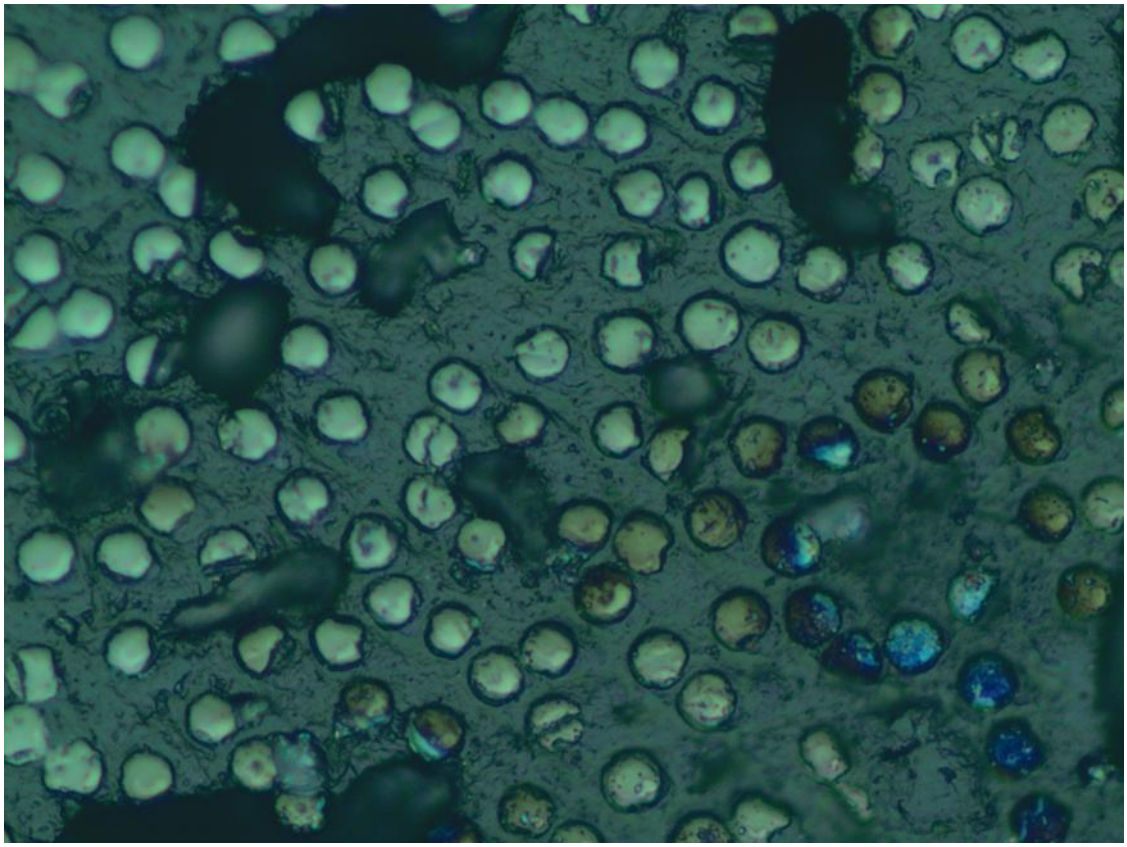

Fig.A- 27. Microscopic image (x50) of the TA/ELO CF pipe.

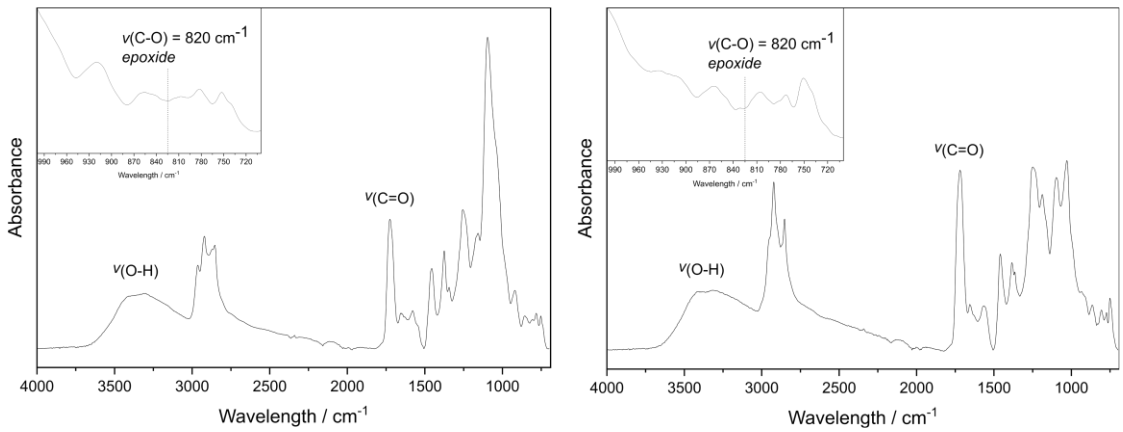

Fig.A- 28: ATR-IR spectra of the cured EGCHC-T403 and EGCHC-IPD samples. Zoom into the relevant region of C—O epoxide vibration at 820 cm^{-1}. From: [53].

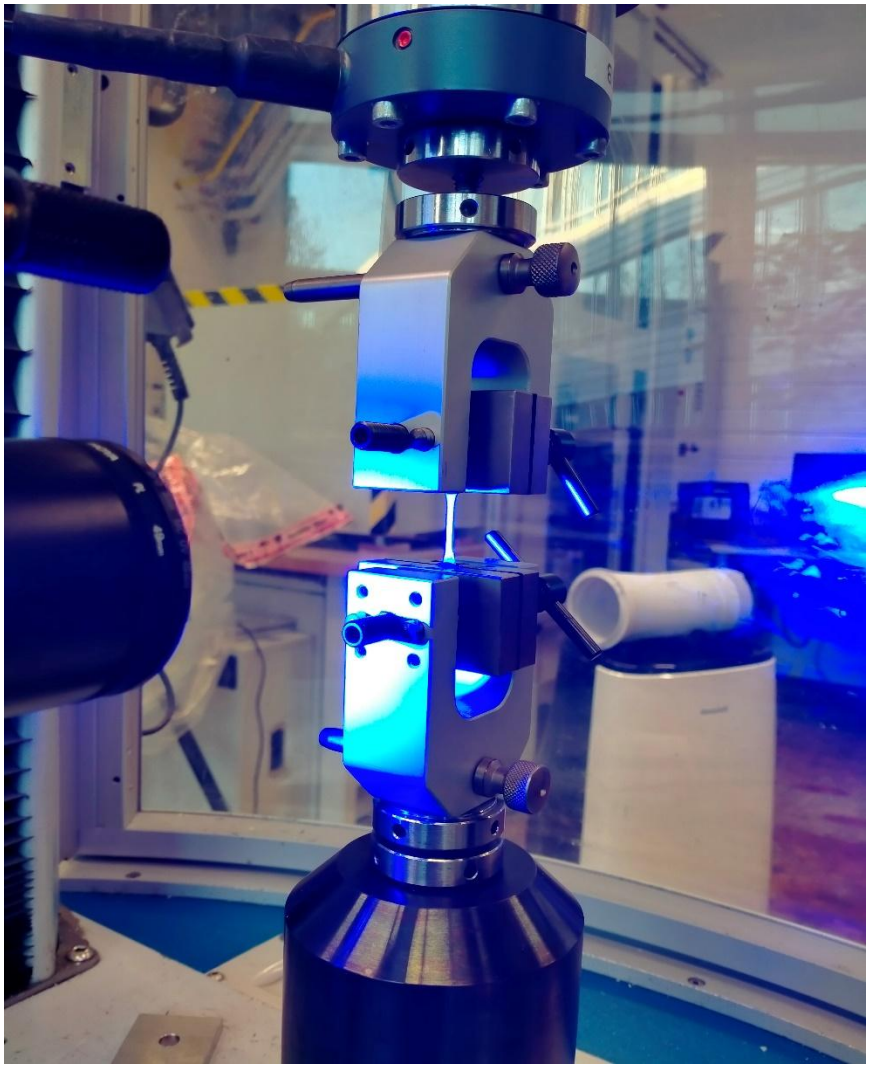

Fig.A- 29: Tensile testing of EGCHC samples

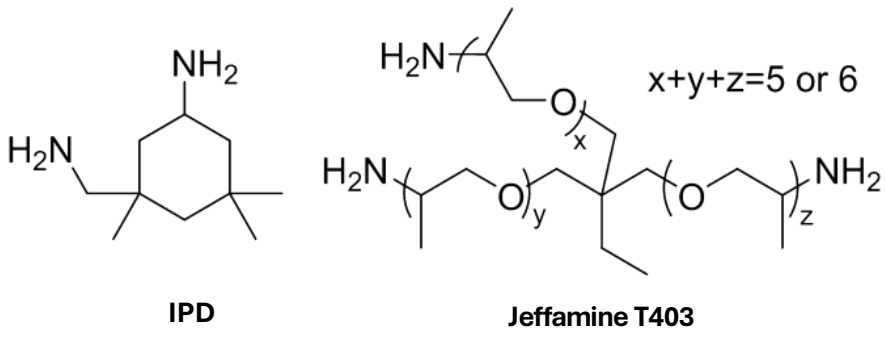

Fig.A- 30: Chemical structures of Jeffamine T403 and IPD

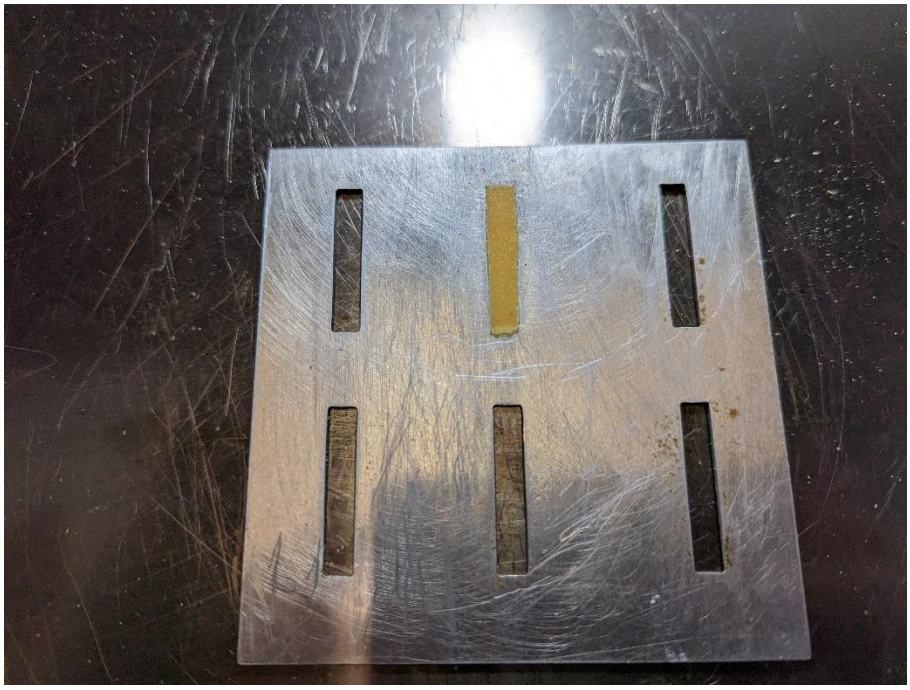

Fig.A- 31: Recycled EGCHC-T403 after hot-pressing at 130 °C for 1 h.

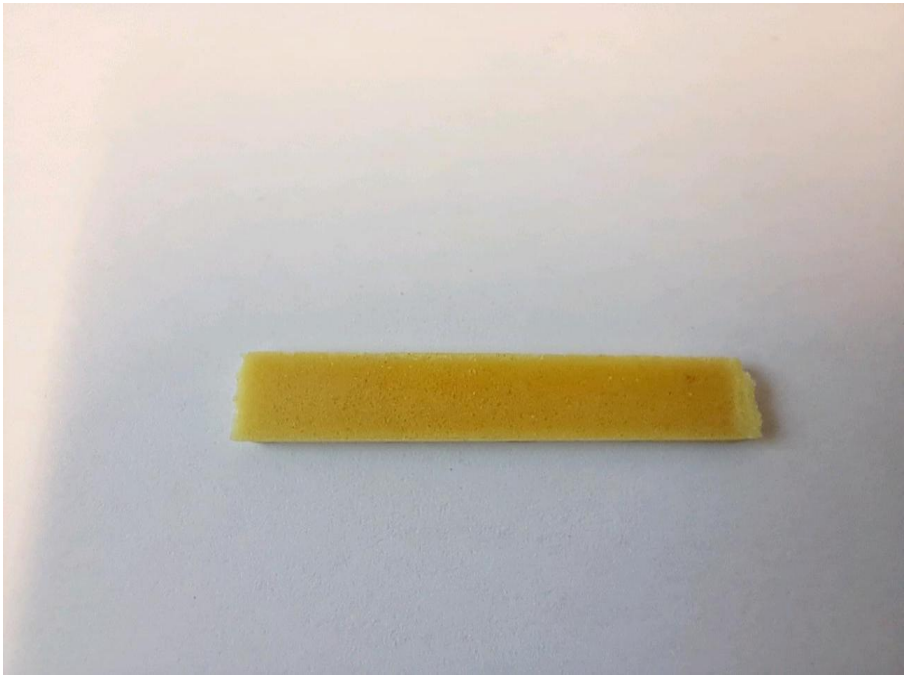

Fig.A- 32: Recycled EGCHC-IPD after hot-pressing at 110 °C for 1 h.

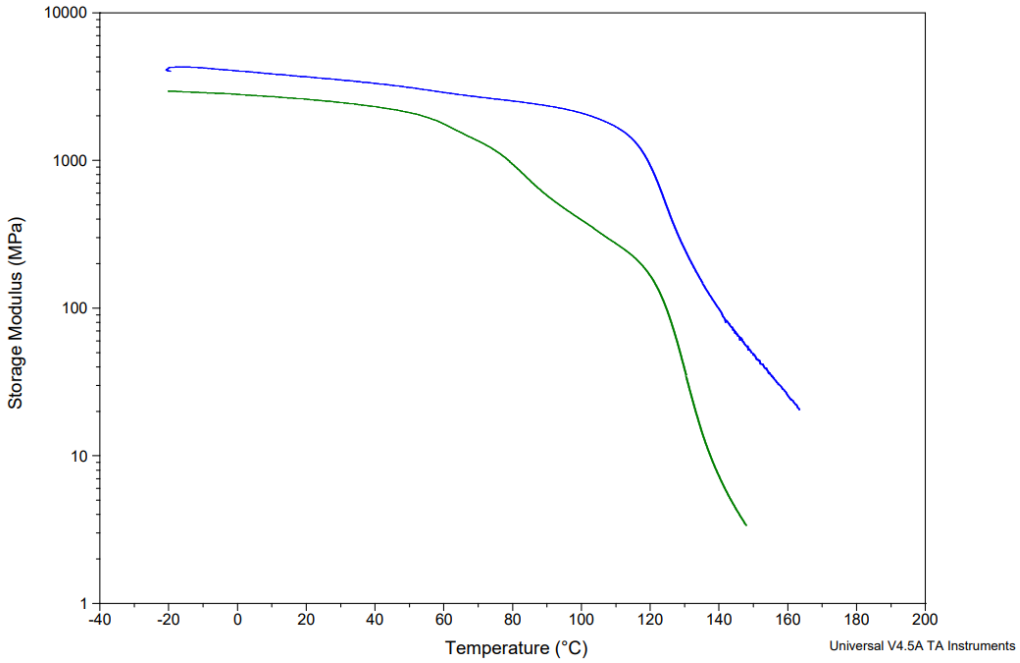

Fig.A- 33: Storage modulus of EGCHC-IPD virgin (blue) and EGCHC-IPD after recycling (green).

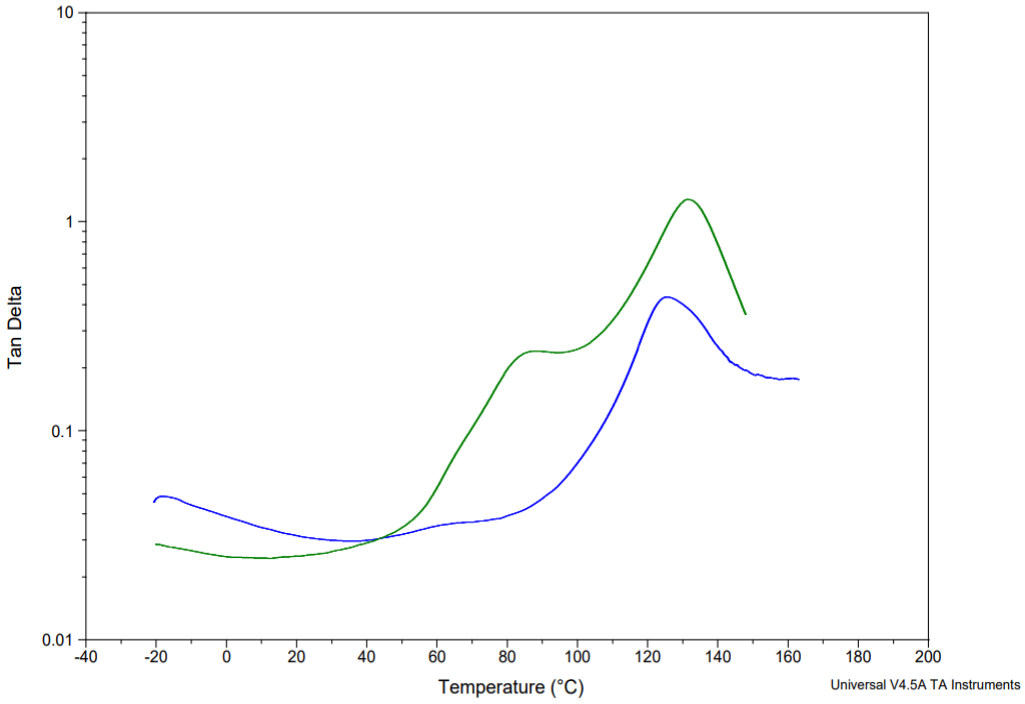

Fig.A- 34: tan δ of EGCHC-IPD virgin (blue) and EGCHC-IPD after recycling (green).

b Additional tables

Tab. A- 1: Amount of CF layers used for the production of the composite plates and V_f obtained.

Resin used	CF fabric used	Number of CF layers	Manufacturing method	V_f (%)
TA/ELO 1.5	UD Twill 3/1	9	Hot-pressing	64.7
TA/ELO 1.75	UD Twill 3/1	8	Hot-pressing	62.2
CR80	UD Twill 3/1	8	Hot-pressing	56.2
CR80	UD Twill 3/1	9	Hot-pressing	67.3
CR80	SGL Tow	3	Hot-pressing	33.2
TA/ELO 1.5	Towpregs	5	Vacuum bagging 400 mbar	23.6
TA/ELO 1.5	Towpregs	5	Vacuum bagging 600 mbar	24.4
TA/ELO 1.5	UD SGL	7	Vacuum bagging 400 mbar	33.2
TA/ELO 1.5	UD SGL	7	Vacuum bagging 600 mbar	32.9
TA/ELO 1.75	UD SGL	6	Vacuum bagging 400 mbar	30.9
TA/ELO 1.75	UD SGL	7	Vacuum bagging 600 mbar	31

Tab. A- 2: Comparison of the mechanical properties with a pre-curing temperature of 120 and 140 °C for TA/ELO 1.25. From: [3]**.**

	Flexural Modulus (MPa)		Flexural Strength (MPa)		Elongation at break (%)	
Sample ↓ / Curing →	16 h 120 °C + 3 h 140 °C	16 h 140 °C	16 h 120 °C + 3 h 140 °C	16 h 140 °C	16 h 120 °C + 3 h 140 °C	16 h 140 °C
TA/ELO 1.25	1991 ± 27	2241 ± 78	65 ± 1	35 ± 3	4.2 ± 0.5	1.5 ± 0.1

Tab. A- 3: Flexural moduli obtained for recycled TA/ELO 2.0 and recycled TA/ELO 2.0 CF composites.

Material	Recycled at 130 °C for 2 h [MPa]	Recycled at 160 °C for 2 h [MPa]
TA/ELO 2.0	2922 ± 94	2464 ± 233
TA/ELO 2.0 + 5 wt.% CF	2652 ± 47	3613 ± 257
TA/ELO 2.0 + 10 wt.% CF	3707 ± 148	4265 ± 180

Tab. A- 4: Flexural strengths obtained for recycled TA/ELO 2.0 and recycled TA/ELO 2.0 CF composites.

Material	Recycled at 130 °C for 2 h [MPa]	Recycled at 160 °C for 2 h [MPa]
TA/ELO 2.0	31.5 ± 1.1	8.9 ± 1.5
TA/ELO 2.0 + 5 wt.% CF	21.5 ± 0.5	21.0 ± 1.2
TA/ELO 2.0 + 10 wt.% CF	28.9 ± 1.3	17.9 ± 1.7

Tab. A- 5: Mixing ratios for the EGCHC and DGEBA samples with IPD and Jeffamine T403 as hardeners. Molar ratio of epoxy compound and hardener = 1.0. Adapted from: [53]**.**

Sample	curing agent per 2 g resin / g
EGCHC-IPD	0.842
EGCHC-T403	1.571

Sample	curing agent per 2 g resin / g
DGEBA-IPD	0.499
DGEBA-T403	0.950

Tab. A- 6: Onset temperature of the curing enthalpy and temperature at the maximum of the exothermic peak. Adapted from: [53].

Sample	Onset temperature in °C	Maximum of the exothermic peak in °C
EGCHC-IPD	43 ± 3	78 ± 1
EGCHC-T403	53 ± 3	94 ± 2
DGEBA-IPD	87 ± 3	121 ± 1
DGEBA-T403	103 ± 1	140 ± 1

B Publications

Scientific journal papers

[P1] N. Reinhardt, J. M. Breitsameter, K. Drechsler, B. Rieger, Fully Bio-Based Epoxy Thermoset Based on Epoxidized Linseed Oil and Tannic Acid. *Macromol. Mater. Eng.* 2022, 307, 2200455. https://doi.org/10.1002/mame.202200455

[P2] J. M. Breitsameter, N. Reinhardt, M. Feigel, O. Hinrichsen, K. Drechsler, B. Rieger, Synthesis of a Sustainable and Bisphenol A-Free Epoxy Resin Based on Sorbic Acid and Characterization of the Cured Thermoset. *Macromol. Mater. Eng.* 2023, 308, 2300068. https://doi.org/10.1002/mame.202300068

[P3] Mayer S, Tallawi M, De Luca I, Calarco A, Reinhardt N, Gray LA, Drechsler K, Moeini A, Germann N. Antimicrobial and physicochemical characterization of 2,3-dialdehyde cellulose-based wound dressings systems. Carbohydr Polym. 2021 Nov 15;272:118506. doi: 10.1016/j.carbpol.2021.118506. Epub 2021 Aug 4. PMID: 34420752.

C Supervised student works

During my employment at the Chair of Carbon Composites of the Technical University of Munich (TUM-LCC), I supervised the following student theses:

[S1] C. Wetzel, “Entwicklung eines neuen materialeffizienten Fertigungsprozesses, um Bio-basierte Kunststoffprobekörper herzustellen”, Bachelor's Thesis, Chair of Carbon Composites, TUM, 2021.

[S2] N. Eker, “Development of a New Test Method to Determine the Bending Characteristics of New Bio-based Thermoset Materials”, Bachelor's Thesis, Chair of Carbon Composites, TUM, 2021.

[S3] A. Linder, “Untersuchung des Einflusses von Wasser und Feuchtigkeit auf die Eigenschaften eines neuen biobasierten Epoxid-Materials für high-performance Anwendungen”, Bachelor's Thesis, Chair of Carbon Composites, TUM, 2022.

[S4] H. Zhang, “Development of new 100% bio-based epoxies”, Master's Thesis, Chair of Carbon Composites, TUM, 2022.

[S5] J. Bendala de Orbe, “ Investigation and characterization of new bio-based epoxy materials from vegetable oils” Term Project (Semesterarbeit), Chair of Carbon Composites, TUM, 2022.

[S6] R.G. Neumeyer, “Entwicklung von biobasierten Carbon Composites”, Master's Thesis, Chair of Carbon Composites, TUM, 2022.

[S7] R. Frehland, “Herstellung und Charakterisierung neuer biobasierter Carbon Composites”, Bachelor's Thesis, Chair of Carbon Composites, TUM, 2023.

[S8] H. Silbermann, “Untersuchung der Recyclingfahigkeit eines neuen biobasierten Epoxid-Materials”, Term Project (Semesterarbeit), Chair of Carbon Composites, TUM, 2023.

[S9] M. Herold, “Untersuchung der Recyclingfähigkeit eines neuen biobasierten Epoxid-Materials aus Pflanzenöl”, Term Project (Semesterarbeit), Chair of Carbon Composites, TUM, 2023.

[S10] T. Eichinger, “Herstellung von biobasierten carbonfaserverstärkten Composite Bauteilen aus rezykliertem Material und Untersuchung der Eigenschaften”, Bachelor's Thesis, Chair of Carbon Composites, TUM, 2023.

[S11] D. Donatiello, “Recycling eines neuen biobasierten Epoxidharzes auf Pflanzenölbasis und Untersuchung der Eigenschaften”, Bachelor's Thesis, Chair of Carbon Composites, TUM, 2023.

[S12] L. Buchwieser, “Untersuchung der Biegeeigenschaften eines neuen biobasierten carbonfaserverstärkten Epoxidharzes”, Bachelor's Thesis, Chair of Carbon Composites, TUM, 2023.

[S13] Y. Liang, “Untersuchung der Zugeigenschaften eines neuen biobasierten carbonfaserverstärkten Epoxidharzes”, Term Project (Semesterarbeit), Chair of Carbon Composites, TUM, 2023.

[S14] M. Nowak, “Ermittlung von Randfaserspannungen mittels Dehnungsmessstreifen an Hochleistungsfußprothesen zur Validierung des Simulationsmodells”, Master's Thesis in cooperation with Steptics GmbH, Chair of Carbon Composites, TUM, 2023.

[S15] F. Gehringer, “Mechanisches Recycling eines neuartigen und biobasierten Carbonfaser-Epoxid-Composites und Optimierung des Prozesses sowie der mechanischen Eigenschaften”, Master's Thesis, Chair of Carbon Composites, TUM, 2024

Parts of the above listed theses contributed to the underlying doctoral thesis: [S3], [S6], [S7], [S9], [S12], [S15].

[S4] and [S5] helped pave the way for the production of TA/ELO samples. [S8], [S10] and [S11] helped pave the way for understanding the recycling ability of TA/ELO.